



National Aeronautics and Space Administration

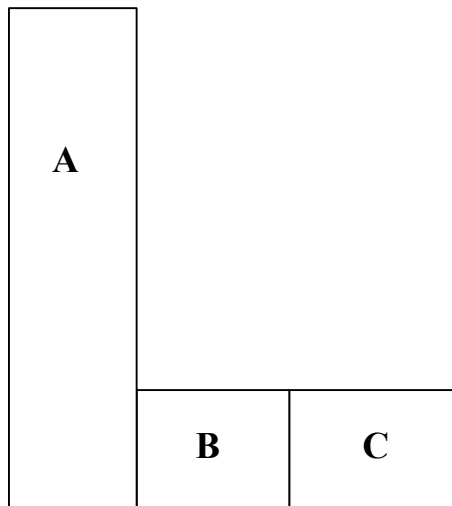
Study to Determine the Feasibility of Extending the Search for Near-Earth Objects to Smaller Limiting Diameters

Report of the
Near-Earth Object Science Definition Team

August 22, 2003

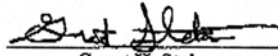
Prepared at the Request of
National Aeronautics and Space Administration
Office of Space Science
Solar System Exploration Division

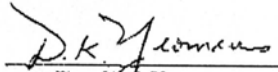


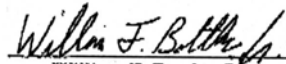


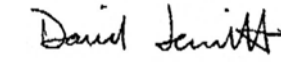
- A. The abundance of impact craters on the Moon demonstrates that Earth too has been subjected to an influx of near-Earth objects. However, erosion processes have erased all but the youngest of Earth's craters. Clementine colorized image showing the full Earth over the Moon's north pole. The angular distance between the Earth and the Moon has been reduced for illustration purposes. This image was taken by the UV/visible camera at the end of mapping orbit 102 on 13 March 1994. The 109 km diameter crater Plaskett is in the foreground at 82 N, 174 E.
- B. Many tons of rocky material rain down upon the Earth daily. Much of it is in the form of dust and sand-sized particles that strike the Earth's atmosphere at high velocity and cause visible meteors. John Pane took this photo during the Leonids meteor storm on Sunday, November 18, 2001, from Laurel Mountain State Park near Ligonier, PA, USA. The photo was taken with an ordinary 35mm SLR camera mounted on a tripod, with a "normal" 50mm f/1.4 lens. Copyright © 2001 John Pane. All rights reserved. <http://leonids.johnpane.com>
- C. An aerial view of Meteor Crater, Arizona, one of the Earth's youngest impact craters. Just over one kilometer in diameter and 200 meters deep, this crater was formed about 50,000 years ago when an iron mass about 60 meters in diameter struck the Earth's surface releasing more than 10 megatons of equivalent energy. From the Smithsonian Scientific Series (1929), taken by the U.S. Army Air Service. Public domain.

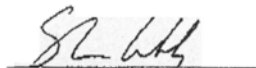
Signature Page

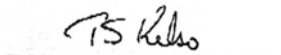

Grant H. Stokes


Donald K. Yeomans

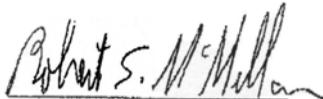

William F. Bottke, Jr.

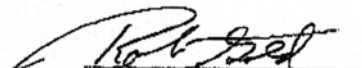

David Jewitt


Steven R. Chesley

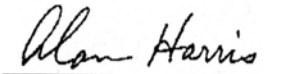

TS Kelso

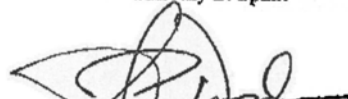

Jenifer B. Evans


Robert S. McMillan


Robert E. Gold


Timothy B. Spahr


Alan W. Harris


S. Peter Worden

EXECUTIVE SUMMARY

A Study to Determine the Feasibility of Extending the Search for Near-Earth Objects to Smaller Limiting Diameters

In recent years, there has been an increasing appreciation for the hazards posed by near-Earth objects (NEOs), those asteroids and periodic comets (both active and inactive) whose motions can bring them into the Earth's neighborhood. In August of 2002, NASA chartered a Science Definition Team to study the feasibility of extending the search for near-Earth objects to smaller limiting diameters. The formation of the team was motivated by the good progress being made toward achieving the so-called Spaceguard goal of discovering 90% of all near-Earth objects (NEOs) with diameters greater than 1 km by the end of 2008. This raised the question of what, if anything, should be done with respect to the much more numerous smaller, but still potentially dangerous, objects. The team was tasked with providing recommendations to NASA as well as the answers to the following 7 specific questions:

1. What are the smallest objects for which the search should be optimized?
2. Should comets be included in any way in the survey?
3. What is technically possible?
4. How would the expanded search be done?
5. What would it cost?
6. How long would the search take?
7. Is there a transition size above which one catalogs all the objects, and below which the design is simply to provide warning?

Team Membership

The Science Definition Team membership was composed of experts in the fields of asteroid and comet search, including the Principal Investigators of two major asteroid search efforts, experts in orbital dynamics, NEO population estimation, ground-based and space-based astronomical optical systems and the manager of the NASA NEO Program Office. In addition, the Department of Defense (DoD) community provided members to explore potential synergy with military technology or applications.

Analysis Process

The Team approached the task using a cost/benefit methodology whereby the following analysis processes were completed:

Population estimation – An estimate of the population of near-Earth objects (NEOs), including their sizes, albedos and orbit distributions, was generated using the best methods in the current literature. We estimate a population of about 1100 near-Earth objects larger than 1 km, leading to an impact frequency of about one in half a million years. To the lower limit of an object's atmospheric penetration (between 50 and 100 m diameter), we estimate about half a million NEOs, with an impact frequency of about one in a thousand years.

Collision hazard – The damage and casualties resulting from a collision with members of the hazardous population were estimated, including direct damage from land impact, as well as the amplification of damage caused by tsunami and global effects. The capture cross-section of the Earth was then used to estimate a collision rate and thus a yearly average hazard from NEO collisions as a function of their diameter. We find that damage from smaller land impacts below the threshold for global climatic effects is peaked at sizes on the scale of the Tunguska air blast event of 1908 (50-100 m diameter). For the local damage due to ocean impacts (and the associated tsunami), the damage reaches a maximum for impacts from objects at about 200 m in diameter; smaller ones do not reach the surface at cosmic speed and energy.

Search technology – Broad ranges of technology and search systems were evaluated to determine their effectiveness when used to search large areas of the sky for hazardous objects. These systems include ground-based and space-based optical and infrared systems across the currently credible range of optics and detector sizes. Telescope apertures of 1, 2, 4, and 8 meters were considered for ground-based search systems along with space-based telescopes of 0.5, 1, and 2 meter apertures. Various geographic placements of ground-based systems were studied as were space-based telescopes in low-Earth orbit (LEO) and in solar orbits at the Lagrange point beyond Earth and at a point that trailed the planet Venus.

Search simulation – A detailed simulation was conducted for each candidate search system, and for combinations of search systems working together, to determine the effectiveness of the various approaches in cataloging members of the hazardous object population. The simulations were accomplished by using a NEO survey simulator derived from a heritage within the DoD, which takes into account a broad range of “real-world” effects that affect the productivity of search systems, such as weather, sky brightness, zodiacal background, etc.

Search system cost - The cost of building and operating the search systems described herein was estimated by a cost team from SAIC. The cost team employed existing and accepted NASA models to develop the costs for space-based systems. They developed the ground-based system cost estimates by analogy with existing systems.

Cost/benefit analysis – The cost of constructing and operating potential survey systems was compared with the benefit of reducing the risk of an unanticipated object collision by generating a catalog of potentially hazardous objects (PHOs). PHOs, a subset of the near-Earth objects, closely approach Earth’s orbit to within 0.05 AU (7.5 million kilometers). PHO collisions capable of causing damage occur infrequently, but the threat is large enough that, when averaged over time, the anticipated yearly average of impact-produced damage is significant. Thus, while developing a catalog of all the potentially hazardous objects does not actually eliminate the hazard of impact, it does provide a clear risk reduction benefit by providing awareness of potential short- and long-term threats. The nominal yearly average remaining, or residual, risk in 2008 associated with PHO impact is estimated by the Team to be approximately 300 casualties worldwide, plus the attendant property damage and destruction. About 17% of the risk is attributed to regional damage from smaller land impacts, 53% to water impacts and the ensuing tsunamis, and 30% to the risk of global climatic disruption caused by large impacts, i.e. the risk that is expected to remain after the completion of the current Spaceguard effort in 2008. For land impacts and all impacts causing global effects, the consequences are in terms of casualties,

whereas for sub-kilometer PHOs causing tsunamis, the “casualties” are a proxy for property damage. According to the cost/benefit assessment done for this report, the benefits associated with eliminating these risks justify substantial investment in PHO search systems.

PHO Search Goals and Feasibility

The Team evaluated the capability and performance of a large number of ground-based and space-based sensor systems in the context of the cost/benefit analysis. Based on this analysis, the Team recommends that the next generation search system be constructed to eliminate 90% of the risk posed by collisions with sub-kilometer diameter PHOs. Such a system would also eliminate essentially all of the global risk remaining after the Spaceguard efforts are complete in 2008. The implementation of this recommendation will result in a substantial reduction in risk to a total of less than 30 casualties per year plus attendant property damage and destruction. A number of search system approaches identified by the Team could be employed to reach this recommended goal, all of which have highly favorable cost/benefit characteristics. The final choice of sensors will depend on factors such as the time allotted to accomplish the search and the available investment (see Figures 9.3 and 9.4).

Answers to Questions Stated in Team Charter

What are the smallest objects for which the search should be optimized? The Team recommends that the search system be constructed to produce a catalog that is 90% complete for potentially hazardous objects (PHOs) larger than 140 meters.

Should comets be included in any way in the survey? The Team’s analysis indicates that the frequency with which long-period comets (of any size) closely approach the Earth is roughly one-hundredth the frequency with which asteroids closely approach the Earth and that the fraction of the total risk represented by comets is approximately 1%. The relatively small risk fraction, combined with the difficulty of generating a catalog of comets, leads the Team to the conclusion that, at least for the next generation of NEO surveys, the limited resources available for near-Earth object searches would be better spent on finding and cataloging Earth-threatening near-Earth asteroids and short-period comets. A NEO search system would naturally provide an advance warning of at least months for most threatening long-period comets.

What is technically possible? Current technology offers asteroid detection and cataloging capabilities several orders of magnitude better than the presently operating systems. NEO search performance is generally not driven by technology, but rather resources. This report outlines a variety of search system examples, spanning a factor of about 100 in search discovery rate, all of which are possible using current technology. Some of these systems, when operated over a period of 7-20 years, would generate a catalog that is 90% complete for NEOs larger than 140 meters (see Figure 9-4).

How would the expanded search be done? From a cost/benefit point-of-view, there are a number of attractive options for executing an expanded search that would vastly reduce the risk posed by potentially hazardous object impacts. The Team identified a series of specific ground-based, space-based and mixed ground- and space-based systems that could accomplish the next

generation search. The choice of specific systems will depend on the time allowed for the search and the resources available.

What would it cost? For a search period no longer than 20 years, the Team identified several systems that would eliminate, at varying rates, 90% of the risk for sub-kilometer NEOs, with costs ranging between \$236 million and \$397 million. All of these systems have risk reduction benefits which greatly exceed the costs of system acquisition and operation.

How long would the search take? A period of 7-20 years is sufficient to generate a catalog 90% complete to 140-meter diameter, which will eliminate 90% of the risk for sub-kilometer NEOs. The specific interval depends on the choice of search technology and the investment allocated.

Is there a transition size above which one catalogs all the objects, and below which the design is simply to provide warning? The Team concluded that, given sufficient time and resources, a search system could be constructed to completely catalog hazardous objects with sizes down to the limit where air blasts would be expected (about 50 meters in diameter). Below this limit, there is relatively little direct damage caused by the object. Over the 7-20 year interval (starting in 2008) during which the next generation search would be undertaken, the Team suggests that cataloging is the preferred approach down to approximately the 140-meter diameter level and that the search systems would naturally provide an impact warning of 60-90% for objects as small as those capable of producing significant air blasts.

Science Definition Team Recommendations

The Team makes three specific recommendations to NASA as a result of the analysis effort:

Recommendation 1 – Future goals related to searching for potential Earth-impacting objects should be stated explicitly in terms of the statistical risk eliminated (or characterized) and should be firmly based on cost/benefit analyses.

This recommendation recognizes that searching for potential Earth impacting objects is of interest primarily to eliminate the statistical risk associated with the hazard of impacts. The “average” rate of destruction due to impacts is large enough to be of great concern; however, the event rate is low. Thus, a search to determine if there are potentially hazardous objects (PHOs) likely to impact the Earth within the next few hundred years is prudent. Such a search should be executed in a way that eliminates the maximum amount of statistical risk per dollar of investment.

Recommendation 2 – Develop and operate a NEO search program with the goal of discovering and cataloging the potentially hazardous population sufficiently well to eliminate 90% of the risk due to sub-kilometer objects.

The above goal is sufficient to reduce the average casualty rate from about 300 per year to less than 30 per year. Any such search would find essentially all of the larger objects remaining undiscovered after 2008, thus eliminating the global risk from these larger objects. Over a

period of 7-20 years, there are a number of system approaches that are capable of meeting this search metric with quite good cost/benefit ratios.

Recommendation 3 – Release a NASA Announcement of Opportunity (AO) to allow system implementers to recommend a specific approach to satisfy the goal stated in Recommendation 2.

Based upon our analysis, the Team is convinced that there are a number of credible, current technology/system approaches that can satisfy the goal stated in Recommendation 2. The various approaches will have different characteristics with respect to the expense and time required to meet the goal. The Team relied on engineering judgment and system simulations to assess the expected capabilities of the various systems and approaches considered. While the Team considers the analysis results to be well-grounded by current operational experience, and thus, a reasonable estimate of expected performance, the Team did not conduct analysis at the detailed system design level for any of the systems considered. The next natural step in the process of considering a follow-on to the current Spaceguard program would be to issue a NASA Announcement of Opportunity (AO) as a vehicle for collecting search system estimates of cost, schedule and the most effective approaches for satisfying the recommended goal. The AO should be specific with respect to NASA's position on the trade between cost and time to completion of the goal.

TABLE OF CONTENTS

EXECUTIVE SUMMARY	i
1 INTRODUCTION.....	1
1.1 Background.....	1
1.2 Science Definition Team Formation and Charter	1
1.3 Team Membership	2
1.4 Study Approach	3
2 POPULATION ESTIMATES	7
2.1 Near-Earth Asteroids	7
2.2 Near-Earth Comets.....	8
2.3 Quantitative Modeling of the NEO Population	9
2.4 The Debiased NEO Population.....	10
2.5 Nearly-Isotropic Comets.....	13
2.6 The Relative Importance of Long-Period Comets to the Earth’s Impact Flux	14
2.7 NEA Size-Frequency Distribution.....	17
3 THE IMPACT HAZARD: What Remains After the Spaceguard Survey?	20
3.1 NEO Population, Impact Frequency, and Expected Completeness	20
3.2 Regional Damage from Land Impacts	22
3.3 Tsunami Hazard from Ocean Impacts	27
3.4 Global Impact Risk from Large Impacts	29
3.5 Hazard from Long-Period Comets.....	31
3.6 Summary of the Impact Hazard after Spaceguard	34
4 CANDIDATE TECHNOLOGIES AND SYSTEMS	36
4.1 Ground-Based Systems.....	37
4.1.1 Ground-Based Sensors.....	37
4.1.2 Ground-Based System Performance Estimation.....	40
4.2 Space-Based Systems.....	43
4.2.1 Visible versus Infrared Sensors	43
4.2.2 Space-Based Visible System Design Methodology.....	43
4.2.2.1 Space System Assumptions	46
4.2.2.2 Telescope Payload	47
4.2.2.3 Orbits.....	47
4.2.2.4 Scientific Implications of Orbit Choice	48

4.2.3	Spacecraft System.....	49
5	SEARCH STRATEGY.....	53
5.1	Search Regions.....	53
5.2	Cadence Issues.....	54
5.3	Linkages.....	55
5.4	Astrometric Accuracy and Precision.....	55
5.5	Cadence Requirement for Linkage and Orbits.....	56
5.6	Search Strategies for Warning.....	56
5.7	Conclusions.....	56
6	SIMULATION DESCRIPTION AND RESULTS.....	58
6.1	Simulation Tool.....	58
6.1.1	FROSST Input Parameters and Methodology.....	58
6.1.2	Necessary FROSST Modifications.....	59
6.1.2.1	Heliocentric Propagator.....	59
6.1.2.2	Solar Phase Equation.....	59
6.1.2.3	Sensitivity as Function of Seeing.....	59
6.1.2.4	Sky Brightness Due to the Moon.....	60
6.1.2.5	Losses Due to Galactic Plane.....	60
6.1.2.6	Gegenschein and Zodiacal Light.....	60
6.1.2.7	Seasonal Variations.....	61
6.1.2.8	Losses Due To Observing In Haze and Clouds.....	62
6.1.2.9	Trailing Losses.....	62
6.1.2.10	Probability of Detection.....	62
6.1.3	FROSST Inputs.....	63
6.1.3.1	Input Population.....	63
6.1.3.1.1	Catalog Objects.....	63
6.1.3.1.2	Establishing a Baseline.....	64
6.1.3.2	Warning of Impactors.....	66
6.1.3.3	System Dependent Parameters.....	66
6.1.3.4	Search Patterns.....	67
6.1.3.5	Search Patterns for Ground-Based Systems.....	67
6.1.3.5.1	Automation.....	67
6.1.3.5.2	Cadence.....	68
6.1.3.5.3	Search Pattern Effectiveness Results.....	68
6.1.3.6	Search Patterns for Space-Based Systems.....	70
6.1.4	Outputs.....	71
6.2	Validation and Comparison to LINEAR Data.....	71
6.2.1	Populations Used For Comparison.....	72
6.2.2	Detected Velocity Distribution.....	72
6.2.3	Apparent Magnitude Distribution.....	73
6.2.4	Absolute Magnitude Distribution.....	74

6.2.5	NEOs Detected.....	76
6.3	Results.....	76
6.3.1	Performance Measures.....	76
6.3.1.1	Cataloging.....	76
6.3.1.2	Warning.....	77
6.3.2	Ground-Based Systems.....	78
6.3.2.1	Large Format CCD versus Small Format CCD.....	78
6.3.2.2	Mauna Kea versus Kitt Peak.....	80
6.3.2.3	Dual Systems.....	81
6.3.3	Space-Based Systems.....	83
6.3.3.1	Cataloging.....	83
6.3.3.2	Warning.....	85
6.3.4	Networks.....	87
7	SYSTEM COST ESTIMATION.....	90
7.1	Ground-Based Observatory.....	90
7.1.1	Telescope Development and Construction.....	90
7.1.2	Instrument Design and Development.....	92
7.1.3	Observatory Operations.....	94
7.1.4	Software.....	94
7.1.5	Ground-Based Observatory Cost Roll-up.....	95
7.2	Space-Based Observatory.....	96
7.2.1	Space-Based Instruments.....	97
7.2.2	Spacecraft Bus.....	97
7.2.3	Operations and Ground Tracking.....	98
7.2.4	Space-Based Observatory Cost Roll-up.....	99
7.3	Multiple Ground-Based and Combined Ground-Based and Space-Based Systems... ..	101
7.3.1	Ground-Based Network of Observatories.....	101
7.3.2	Mixed Ground- Based and Space-Based Observatories.....	103
7.4	Summary.....	103
8	COST / BENEFIT CONCLUSIONS.....	104
8.1	Approach.....	104
8.2	Results and Conclusions of Cost Benefit Study.....	110
9	SYSTEM COMPARISONS AND SUMMARY OF STUDY RESULTS.....	112
9.1	Establishing A Realistic Goal.....	112
9.2	Performance Overview For Systems Designed To Meet The Goal.....	114
9.3	Space-Based Systems Verses Ground-Based System Performance.....	115
9.4	Time And Expense Required To Complete The Survey Goal.....	116
10	RESPONSES TO THE CHARTER QUESTIONS.....	118

REFERENCES.....	121
APPENDIX 1 - 1998 Statement before Subcommittee on Space and Aeronautics.....	128
APPENDIX 2 - Study Charter.....	133
APPENDIX 3 - Optimal Search Sensor Design	136
APPENDIX 4 - Some Caveats on Predicting the Frequency of Tunguska-Type Events... 	140
APPENDIX 5 - Cost/Benefit Analysis Cases	143

1 INTRODUCTION

1.1 Background

In a 1992 report to NASA (Morrison, 1992), a coordinated Spaceguard Survey was recommended to discover, verify and provide follow-up observations for Earth-crossing asteroids. This survey was expected to discover 90% of these objects larger than one kilometer within 25 years. Three years later, another NASA report (Shoemaker, 1995) recommended search surveys that would discover 60-70% of short-period, near-Earth objects larger than one kilometer within ten years and obtain 90% completeness within five more years. In 1998, NASA formally embraced the goal of finding and cataloging, by 2008, 90% of all near-Earth objects (NEOs) with diameters of 1 km or larger that could represent a collision risk to Earth (Appendix 1). The 1 km diameter metric was chosen after considerable study indicated that an impact of an object smaller than 1 km could cause significant local or regional damage but is unlikely to cause a worldwide catastrophe (Morrison, 1992). The impact of an object much larger than 1 km diameter could well result in worldwide damage up to, and potentially including, extinction of the human race. The NASA commitment has resulted in the funding of a number of NEO search efforts that are making considerable progress toward the 90% by 2008 goal. At the current epoch, more than 50% of the expected population included in the goal has been discovered and the subject objects continue to be discovered at impressive rates. While the current goal covers the larger objects, which could cause global devastation, it is silent on the much more numerous smaller objects (between 50 meters and 1 km diameter) that could cause local or regional damage in an impact. Given the steeply increasing population of near-Earth objects with decreasing diameter, it is much more likely that civilization will experience the impact of an object smaller than 1 km than experience an impact from a larger one. Indeed, the significance of small impactors is beginning to be appreciated by the broad public and by scientists alike. Current NEO surveys are dedicated to finding the largest objects. They also serendipitously find some that are sub-kilometer, but are not optimized to do so and, consequently, are inefficient in finding these objects.

The vast majority of near-Earth objects (NEOs), and the roughly 20% subset of potentially hazardous objects (PHOs) that can closely approach the Earth's orbit, are near-Earth asteroids. However, a small fraction of the NEOs and PHOs are active and inactive short-period comets. Throughout this report, we will most often refer to NEOs and PHOs, generally meaning the set of near-Earth asteroids and inactive short-period comets and excluding long-period comets. However, near-Earth asteroids (NEAs) and potentially hazardous asteroids (PHAs) will also be used when appropriate. Since it is likely that the numbers of asteroids completely dominates the cometary members of the NEO and PHO groups, the reader can normally assume that the populations of NEOs and NEAs are nearly identical, as are the populations of PHOs and PHAs.

1.2 Science Definition Team Formation and Charter

Given the fact that the existing search programs are making good progress toward meeting the current goal, and the emerging discussion of smaller objects, it is natural to ask what, if any, action should be taken to catalog or warn against potential impacts of objects smaller than 1 km

in diameter. In August of 2002, NASA initiated the formation of a Science Definition Team with a charter to develop an understanding of the threat posed by near-Earth objects smaller than one kilometer and to assess methods of providing warnings of potential impacts. The Team was instructed to provide recommendations to NASA and to outline an executable approach to addressing any recommendations made. Specifically, the team was instructed to address the following questions:

1. What are the smallest objects for which the search should be optimized?
2. Should comets be included in any way in the survey?
3. What is technically possible?
4. How would the expanded search be done?
5. What would it cost?
6. How long would the search take?
7. Is there a transition size above which one catalogs all the objects, and below which the design is simply to provide warning?

The complete formal charter for the Science Definition Team is contained in Appendix 2 of this document.

1.3 Team Membership

The Science Definition Team, henceforth referred to as the “Team”, was chaired by Grant H. Stokes from MIT Lincoln Laboratory. Vice Chair of the team was Donald K. Yeomans from the NASA Jet Propulsion Laboratory. The Team members, carefully chosen to represent the breadth and depth of expertise required to address the questions posed in the charter, are listed in Table 1-1, along with their institutions and technical specialties.

Table 1-1. The Science Definition Team Membership

Name	Institution	Technical Specialty
Dr. Grant H. Stokes	MIT Lincoln Laboratory	Asteroid Search, PI for LINEAR
Dr. Donald K. Yeomans	NASA Jet Propulsion Laboratory	Manager, NASA Near-Earth Object Program Office
Dr. William F. Bottke, Jr.	Southwest Research Institute	Asteroid and comet population models
Dr. Steven R. Chesley	NASA Jet Propulsion Laboratory	Hazard assessments and search strategies
Jenifer B. Evans	MIT Lincoln Laboratory	Search system simulations, Co-I for LINEAR
Dr. Robert E. Gold	Johns Hopkins University Applied Physics Lab	Space-based detector systems
Dr. Alan W. Harris	Space Science Institute	Hazard assessments and search strategies
Dr. David Jewitt	University of Hawaii	Visual detectors and search strategies

Table 1-1 (cont.). The Science Definition Team Membership

Col. T.S. Kelso	USAF/AFSPC	DoD assets
Dr. Robert S. McMillan	Spacewatch, University of Arizona	Ground-based NEO Survey, PI for Spacewatch
Dr. Timothy B. Spahr	Smithsonian Astrophysical Observatory	Small body astrometry and orbit determination
Dr./Brig. Gen. S. Peter Worden	USAF/SMC	Space-based detectors and DoD assets
Ex Officio Members:		
Dr. Tomas H. Morgan	NASA Headquarters	Manager, NASA NEO Program
Lt. Col. Lindley N. Johnson (USAF, ret.)	NASA Headquarters	Surveillance of space and DoD space capabilities
Team Support:		
Don E. Avery	NASA Langley Research Center	Study Lead
Sherry L. Pervan	SAIC	Executive Secretary
Michael S. Copeland	SAIC	Cost Analyst
Dr. Monica M. Doyle	SAIC	Cost Analyst

1.4 Study Approach

Providing authoritative answers to the questions posed for the Team requires an understanding of the relationships between the costs of implementing a search effort for smaller NEOs and the benefits accrued. Thus, the study process was constructed along the lines of a cost/benefit analysis as shown in Figure 1-1.

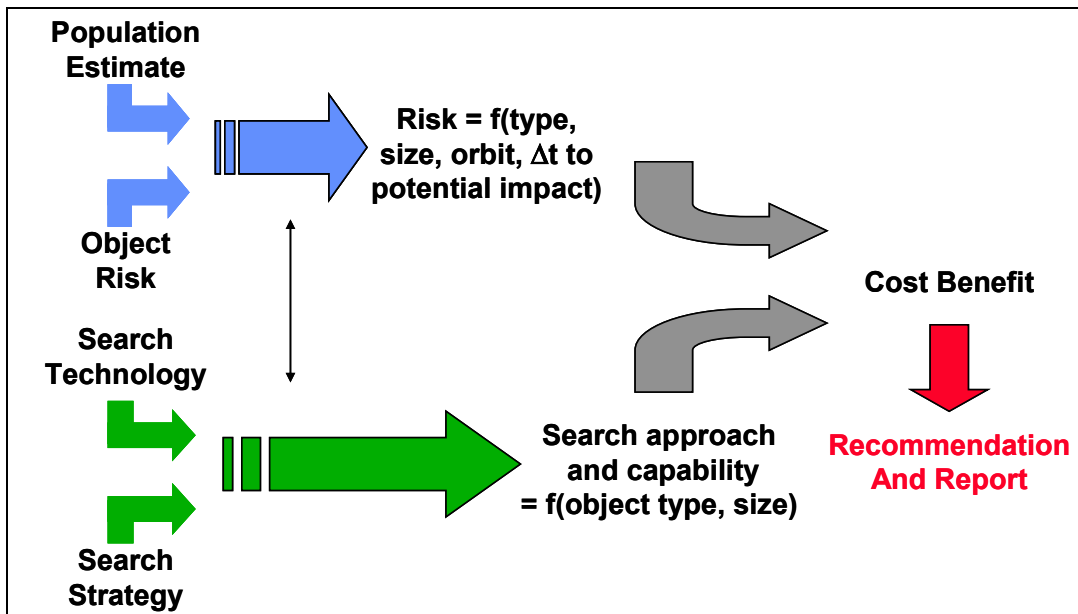


Figure 1-1. Study Process to Develop Cost/benefit Estimate and Recommendations

The five areas that need to be explored to produce the cost/benefit analysis are as follows:

1. The population of asteroids as a function of size, orbital distribution and albedo must be accurately estimated. This will allow an estimate of the collision rate of asteroids with the Earth as a function of size and orbital parameters and will provide the basis for an estimation of the search capabilities of potential systems.
2. The collision damage associated with the impact of an asteroid must be quantified as a function of impactor size. The damage, including effects for both land and water impacts, can be combined with a collision rate to yield an expected damage per year as a function of asteroid size. Assuming that advance warning allows some fraction of the damage and loss of life to be avoided, this represents an estimate or upper bound for the “benefit” that can be accrued in return for the cost of conducting a search.
3. The capabilities of potential search technologies, or combinations of technologies, to execute the search must be assessed as a function of the size, albedo and orbital parameters of the asteroid population. In addition, the costs of developing and operating the search system(s) must be quantified. The funds required to build and operate the search system form the “cost” element of the cost/benefit analysis.
4. The method of operating a particular search system must be defined in order to determine search effectiveness. The capabilities of a search system to find any particular population of asteroids will depend not only on the inherent capabilities of the system, but also on how it is employed with respect to scan pattern, integration time, etc.
5. The benefits, in terms of casualty avoidance and property loss, must be quantified.

The five inputs discussed above provide the basic information required to:

1. Estimate the danger to the Earth from collisions of “smaller” asteroids;
2. Estimate the performance and cost/benefit of a range of search systems intended to provide notification of impending risk.

An assessment of the productivity for an operating search system is complex and requires a realistic accounting for real-world effects that degrade its theoretical performance. These effects include the weather, moonlight, air mass and zodiacal light background. Some of these can be determined by the geometry of the observations (e.g. the effect of the Moon and air mass, which are coupled), while others can be estimated only by statistical methods (e.g., the weather). Most analyses of asteroid search systems to date have either ignored these effects, especially when proposing a specific system for funding, or treated them with some form of estimated correction factor. However, the effects of the real-world degradations to a search are intimately related to the details of the search operation, and will have a large effect on the search productivity. For the purposes of this study, the performance of a search sensor, or a network of sensors, was estimated using a much more detailed simulation process, which “displays” the population of asteroids as a function of time and operates the search sensors in the chosen search modes to see what is found. This allows the geometry-dependent effects to be modeled specifically for each

search area, resulting in a high fidelity performance estimate. In addition, the simulation includes realistic noise from the background and from a comprehensive list of sources. Both ground-based and space-based sensors are modeled, along with backgrounds and noise sources appropriate to each operating environment. Networks consisting of combinations of various sensor types and in various locations may be modeled together to assess their combined performance.

The inputs to the simulation are as follows:

1. The asteroid population - including orbital parameters, size and albedo for each asteroid;
2. The sensor model(s) – including parameters of the sensor(s) such as sensitivity as a function of integration time, step and settle time, site location or ephemeris, and site characteristics;
3. The search pattern(s) for each sensor;
4. The time ranges over which to simulate.

The output of the simulation is a list of detections as a function of time. From these detections, the performance of the search system and strategy may be compared on a realistic basis with the performance of other configurations.

The benefits provided by a given search system need to be measured relative to the system costs. The costs of a given system are governed by the construction and operational expenses, which can be estimated in a relatively straightforward manner, while the benefit side of the equation is much more challenging for several reasons. Most importantly, the benefits provided by a system cannot be described in strictly financial terms due to the potential for casualties and to various political and emotional considerations that are relevant to the problem. Furthermore the benefit depends directly upon estimates of the hazard posed by NEOs, and these estimates are plagued by large uncertainties.

The direct benefit of a search program comes from two sources, cataloging and warning. “Cataloging” refers to the idea that the statistical impact risk is only posed by the undiscovered component of the NEO population. Therefore, by discovering and cataloging NEOs and by verifying that none will impact within the next century, we reduce the potential risk to life and property on Earth. If an object is actually discovered on a threatening trajectory there will presumably be many years, even decades, in which to execute a plan to deflect or disrupt the impactor. Hence the cataloging approach enables the complete mitigation of future impacts, saving both population and infrastructure.

The term “warning” describes a situation where an impactor is first detected and recognized some days to months before the event. This “warning period” would afford civil authorities an opportunity to take actions that would mitigate the impact effects, but there would be insufficient time to avert the collision. In such a scenario the warning benefit is largely comprised of casualties avoided through the evacuation of affected areas. Major infrastructure would not be saved, although, time permitting, some portion of the physical infrastructure could also be removed to a safe distance.

The balance of this report describes the study process in greater detail, answers the seven specific questions posed for the Team, and provides the recommendations along with a rationale for each.

2 POPULATION ESTIMATES

This section discusses the methods for generating a synthetic population of near-Earth objects (NEOs) that is used in the simulation process and described in later sections. The results are based on the best available estimates of the orbital distribution of the near-Earth objects (e.g., Bottke et al. 2002a; Morbidelli et al. 2002a, b).

NEOs are asteroids and comets that, by convention, have perihelion distances $q \leq 1.3$ AU and aphelion distances $Q \geq 0.983$ AU (e.g., Rabinowitz et al. 1994). Sub-categories of the NEO population include the Apollos ($a \geq 1.0$ AU; $q \leq 1.0167$ AU) and Atens ($a < 1.0$ AU; $Q \geq 0.983$ AU), which are on Earth-crossing orbits, and the Amors (1.0167 AU $< q \leq 1.3$ AU) that are on nearly-Earth-crossing orbits and can evolve into Earth-crossers over relatively short timescales. Another group of related objects that are not yet considered part of the “formal” NEO population are the IEOs, or those objects located inside Earth’s orbit ($Q < 0.983$ AU). The combined NEO and IEO populations are comprised of bodies ranging in size from dust-sized fragments to objects tens of km in diameter (Shoemaker 1983).

2.1 Near-Earth Asteroids

The dynamics of bodies in NEO space are strongly influenced by a complicated interplay between close encounters with the planets and resonant dynamics. Encounters provide an impulse velocity to the body's trajectory, causing the semimajor axis, eccentricity, and inclination to change by an amount that depends on both the geometry of the encounter and the mass of the planet. Resonances, on the other hand, keep the semimajor axis constant while changing a body's eccentricity and/or inclination.

Most asteroidal NEOs, or near-Earth asteroids (NEAs), are believed to be collisional fragments that were driven out of the main belt by a combination of Yarkovsky thermal forces (e.g., see Bottke et al. 2002b for a review) and secular/mean motion resonances (e.g., J.G. Williams, see Wetherill 1979; Wisdom 1983). In a scenario favored by many scientists, main belt asteroids with diameter $D < 20$ -30 km slowly spiral inward and outward via the Yarkovsky effect until they are captured by a dynamical resonance capable of increasing their orbital eccentricity enough to reach planet-crossing orbits. Hence, by understanding the populations of asteroids entering and exiting the most important main belt resonances, we can compute the true orbital distribution of the NEAs as a function of semimajor axis a , eccentricity e , and inclination i .

The most powerful main belt resonances that provide NEAs are the ν_6 secular resonance, which marks the inner edge of the main belt, and the 3:1 mean motion resonance with Jupiter at ~ 2.5 AU (e.g., Bottke et al. 2000; 2002a). The ν_6 secular resonance occurs when the precession frequency of the asteroid's longitude of perihelion is equal to the sixth secular frequency of the planetary system. Numerical results show that main belt asteroids entering the ν_6 secular resonance reach Earth-crossing orbits in $\sim 500,000$ years (or ~ 0.5 Myr). The median dynamical lifetime of bodies started in the ν_6 resonance is ~ 2 Myr, with typical end-states being collision with the Sun (80% of the cases) and ejection onto hyperbolic orbit via a close encounter with Jupiter (12%) (Gladman et al. 1997). The 3:1 mean motion resonance with Jupiter occurs where

the orbital period of the asteroid is one third of that of the giant planet. For a population initially uniformly distributed inside the resonance, the median time required to cross the orbit of the Earth is ~ 1 Myr, while their median dynamical lifetime is ~ 2 Myr. Typical end-states for test bodies include colliding with the Sun (70%) and being ejected onto hyperbolic orbits (28%) (Gladman et al., 1997). Only a small fraction of objects from either resonance strike the Earth.

NEAs also come from hundreds of tiny resonances that crisscross the main belt. These resonances are produced by high order mean motion resonances with Jupiter (where the orbital frequencies are in a ratio of large integer numbers), three-body resonances with Jupiter and Saturn (where an integer combination of the orbital frequencies of the asteroid, Jupiter and Saturn is equal to zero; Nesvorny et al. 2002), and mean motion resonances with Mars (Morbidelli and Nesvorny 1999). The typical width of each of these resonances is on the order of a few 10^{-4} - 10^{-3} AU. Because of these resonances, many, if not most, main belt asteroids are chaotic (e.g., Nesvorny et al. 2002). The effect of this chaotic behavior is very weak, with an asteroid's eccentricity and inclination slowly changing in a secular fashion over time. The time required to reach a planet-crossing orbit ranges from several 10^7 years to billions of years, depending on the resonances and the starting eccentricity. It has been shown that the population of asteroids solely on Mars-crossing orbits, which is roughly 4 times the size of the NEO population, is predominately resupplied by diffusive resonances in the main belt (Migliorini et al. 1998; Morbidelli and Nesvorny 1999; Michel et al. 2000; Bottke et al. 2002a). To become NEAs, Mars-crossing asteroids random walk in semimajor axis under the effect of Martian encounters until they enter a resonance that is strong enough to decrease their perihelion distance below 1.3 AU.

2.2 Near-Earth Comets

Comets also contribute to the NEO population. Comets can be divided into two groups: those coming from the Transneptunian region (the Kuiper belt or, more likely, the scattered disk; Levison and Duncan 1994; Levison and Duncan 1997; Duncan and Levison 1997) and those coming from the Oort cloud (e.g., Weissman et al. 2002). Some NEOs with comet-like properties may come from the Trojan population as well, though it is believed their contribution is small compared to those coming from the Transneptunian region and Oort cloud (Levison and Duncan 1997). The Tisserand parameter T , the pseudo-energy of the Jacobi integral that must be conserved in the restricted circular three-body problem, has been used in the past to classify different comet populations (e.g., Carusi et al. 1987). Writing T with respect to Jupiter, the Tisserand parameter becomes (Kresak 1979):

$$T = (a_{\text{JUP}} / a) + 2 \cos(i) ((a / a_{\text{JUP}})(1 - e^2))^{1/2}$$

where a_{JUP} is the semimajor axis of Jupiter. Adopting the nomenclature provided by Levison (1996), we refer to $T > 2$ bodies as ecliptic comets, since they tend to have small inclinations, and $T < 2$ bodies as nearly-isotropic comets, since they tend to have high inclinations.

Numerical simulations suggest that comets residing in particular parts of the Transneptunian region are dynamically unstable over the lifetime of the solar system (e.g., Levison and Duncan

1997; Duncan and Levison 1997). Those ecliptic comets that fall under the gravitational sway of Jupiter ($2 < T < 3$) are called Jupiter-family comets (JFCs). These bodies frequently experience low-velocity encounters with Jupiter. Though most model-JFCs are readily thrown out of the inner solar system via a close encounter with Jupiter (i.e., over a timescale of ~ 0.1 Myr), a small component of this population achieves NEO status (Levison and Duncan 1997). The orbital distribution of the ecliptic comets has been well characterized using numerical integrations by Levison and Duncan (1997), who find that most JFCs are confined to a region above $a = 2.5$ AU. Comets that are gravitationally decoupled from Jupiter ($T > 3$), like 2P/Encke, are thought to be rare. It is believed that comets reach these orbits via a combination of non-gravitational forces and close encounters with the terrestrial planets.

Nearly-isotropic comets, comprised of the long-period comets and the Halley-type comets, come from the Oort cloud (Weissman et al. 2002) and possibly the Transneptunian region (Levison and Duncan 1997; Duncan and Levison 1997). Numerical work has shown that nearly-isotropic comets can be thrown into the inner solar system by a combination of stellar and galactic perturbations (Duncan et al. 1987). At this time, however, a complete understanding of their dynamical source region (e.g., Levison et al. 2001) is lacking.

To understand the population of ecliptic comets and nearly-isotropic comets, an understanding of more than cometary dynamics is needed. Comets undergo physical evolution as they orbit close to the Sun. In some cases, active comets evolve into dormant, asteroidal-appearing objects, with their icy surfaces covered by a lag deposit of non-volatile dust grains, organics, and/or radiation processed material that prevents volatiles from sputtering away (e.g., Weissman et al. 2002). Accordingly, if a $T < 3$ object shows no signs of cometary activity, it is often assumed to be a dormant, or possibly extinct, comet. In other cases, comets self-destruct and totally disintegrate (e.g., comet C/1999 S4 (LINEAR)). The fraction of comets that become dormant or disintegrate among the ecliptic and nearly-isotropic comet populations must be understood to gauge the absolute impact hazard to the Earth.

2.3 Quantitative Modeling of the NEO Population

Although there is currently a good working understanding of NEO dynamics, it is still challenging to deduce the true orbital distribution of the NEOs. There are two main reasons for this: (i) it is not obvious which source regions provide the greatest contributions to the steady state NEO population, and (ii) the observed orbital distribution of the NEOs, which could be used to constrain the contribution from each NEO source, is biased against the discovery of objects on some types of orbits. Given the pointing history of a NEO survey, however, the observational bias for a body with a given orbit and absolute magnitude can be computed as the probability of being in the field of view of the survey with an apparent magnitude brighter than the limit of detection (Jedicke 1996; Jedicke and Metcalfe 1998, see review in Jedicke et al. 2002). Assuming random angular orbital elements of NEOs, the bias is a function $B(a, e, i, H)$, dependent on semimajor axis, eccentricity, inclination and the absolute magnitude H . Each NEO survey has its own bias. Once the bias is known, in principle the real number of objects N can be estimated as:

$$N(a,e,i,H) = n(a,e,i,H) / B(a,e,i,H)$$

where n is the number of objects detected by the survey. The problem, however, is that there are rarely enough observations to obtain more than a coarse understanding of the debiased NEO population (i.e., the number of bins in a 4-dimensional orbital-magnitude space can grow quite large), though such modeling efforts can lead to useful insights (Rabinowitz 1994; Rabinowitz et al. 1994; Stuart 2001).

An alternative way to construct a model of the real distribution of NEOs relies on dynamics (Bottke et al. 2000; 2002a). Using numerical integration results, it is possible to estimate the steady state orbital distribution of NEOs coming from each of the main source regions defined above. The method used by Bottke et al. (2002a) is described below. First, a statistically significant number of particles, initially placed in each source region, is tracked across a network of (a,e,i) cells in NEO space until they are dynamically eliminated. The mean time spent by these particles in those cells, called their residence time, is then computed. The resultant residence time distribution shows where the bodies from the source statistically spend their time in the NEO region. As it is well known in statistical mechanics, in a steady state scenario, the residence time distribution is equal to the relative orbital distribution of the NEOs that originated from the source. This allowed Bottke et al. (2002a) to obtain steady state orbital distributions for NEOs coming from all the prominent NEO sources: the v_6 resonance, the 3:1 resonance, the population coming from numerous diffusive resonances in the main belt, and the Jupiter family comets. The overall NEO orbital distribution was then constructed as a linear combination of these distributions, with the contribution of each source dependent on a weighting function. (Note that the nearly isotropic comet population was excluded in this model, but its contribution is discussed in Section 2.5).

The NEO magnitude distribution, assumed to be source-independent, was constructed so its shape could be manipulated using an additional parameter. Combining the resulting NEO orbital-magnitude distribution with the observational biases associated with the Spacewatch survey (Jedicke 1996), Bottke et al. (2002a) obtained a model distribution that could be fit to the orbits and magnitudes of the NEOs discovered or accidentally re-discovered by Spacewatch. A visual comparison showed that the best-fit model adequately matched the orbital-magnitude distribution of the observed NEOs. The resulting best-fit model nicely matches the distribution of the NEOs observed by Spacewatch (see Figure 10 of Bottke et al. 2002a).

Once the values of the parameters of the model are computed by fitting the observations of *one* survey, the steady state orbital-magnitude distribution of the *entire* NEO population is determined. This distribution is also valid in regions of orbital space that have never been sampled by any survey because of extreme observational biases. This underlines the power of the dynamical approach for debiasing the NEO population.

2.4 The Debiased NEO Population

The model results indicate that $37 \pm 8\%$ of the NEOs come from the v_6 resonance, $23 \pm 9\%$ from the 3:1 resonance, $33 \pm 3\%$ from the numerous diffusive resonances stretched across the main

belt, and $6 \pm 4\%$ come from the Jupiter-family comet region. The model results were constrained in the JFC region by several objects that are almost certainly dormant comets. For this reason, factors that have complicated the discussions of previous JFC population estimates (e.g., issues of converting cometary magnitude to nucleus diameters, etc.) are avoided. Note, however, that the Bottke et al. (2002a) model does not account for the contribution of comets of Oort cloud origin. This issue will be discussed in Sections 2.5 and 2.6.

Figure 2-1 displays the debiased (a,e,i) NEO population as a residence time probability distribution plot. To display as much of the full (a,e,i) distribution as possible in two dimensions, the i bins were summed before plotting the distribution in (a,e) , while the e bins were summed before plotting the distribution in (a,i) . The color scale depicts the expected density of NEOs in a scenario of steady state replenishment from the main belt and transneptunian region. Red colors indicate where NEOs are statistically most likely to spend their time. Bins whose centers have perihelia $q > 1.3$ AU are not used and are colored white. The gold curved lines that meet at 1 AU divide the NEO region into Amor ($1.0167 \text{ AU} < q < 1.3 \text{ AU}$), Apollo ($a > 1.0 \text{ AU}; q < 1.0167 \text{ AU}$) and Aten ($a < 1.0 \text{ AU}; Q > 0.983 \text{ AU}$) components. IEOs ($Q < 0.983 \text{ AU}$) are inside Earth's orbit. The Jupiter-family comet region is defined using two lines of constant Tisserand parameter $2 < T < 3$. The curves in the upper right show where $T=2$ and $T=3$ for $i=0$ deg.

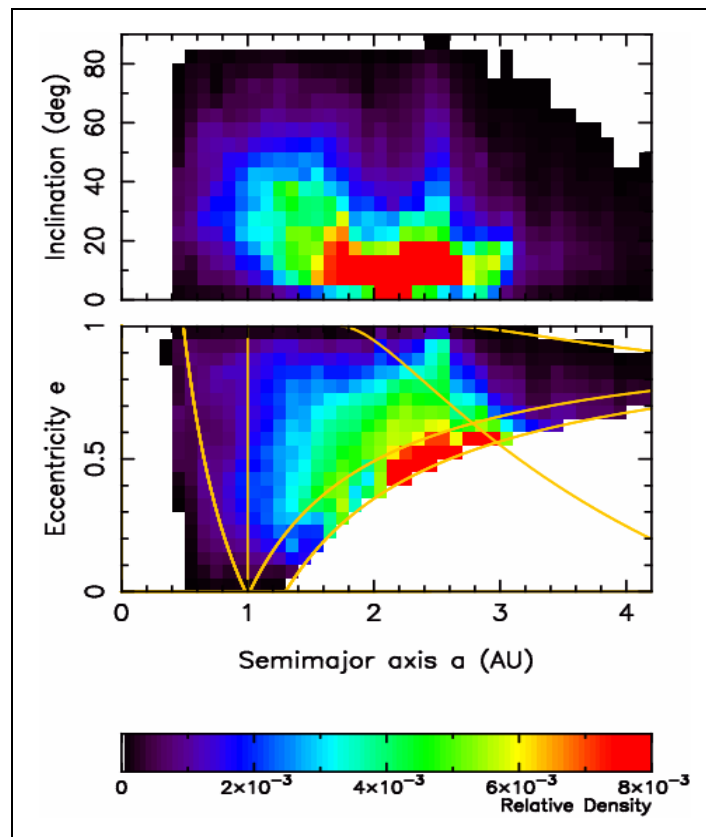


Figure 2-1. A representation of the probability distribution of residence time for the debiased near-Earth object (NEO) population.

Figure 2-2 displays the debiased distribution of the NEOs with absolute magnitude $H < 18$ as a series of three one-dimensional plots (see Bottke et al. 2002a for other representations of these data). For comparison, the figure also reports the distribution of the objects discovered up to $H < 18$, all surveys combined, as of 2003. For objects with an absolute magnitude brighter than about 18, the object's diameter would be expected to be larger than one kilometer.

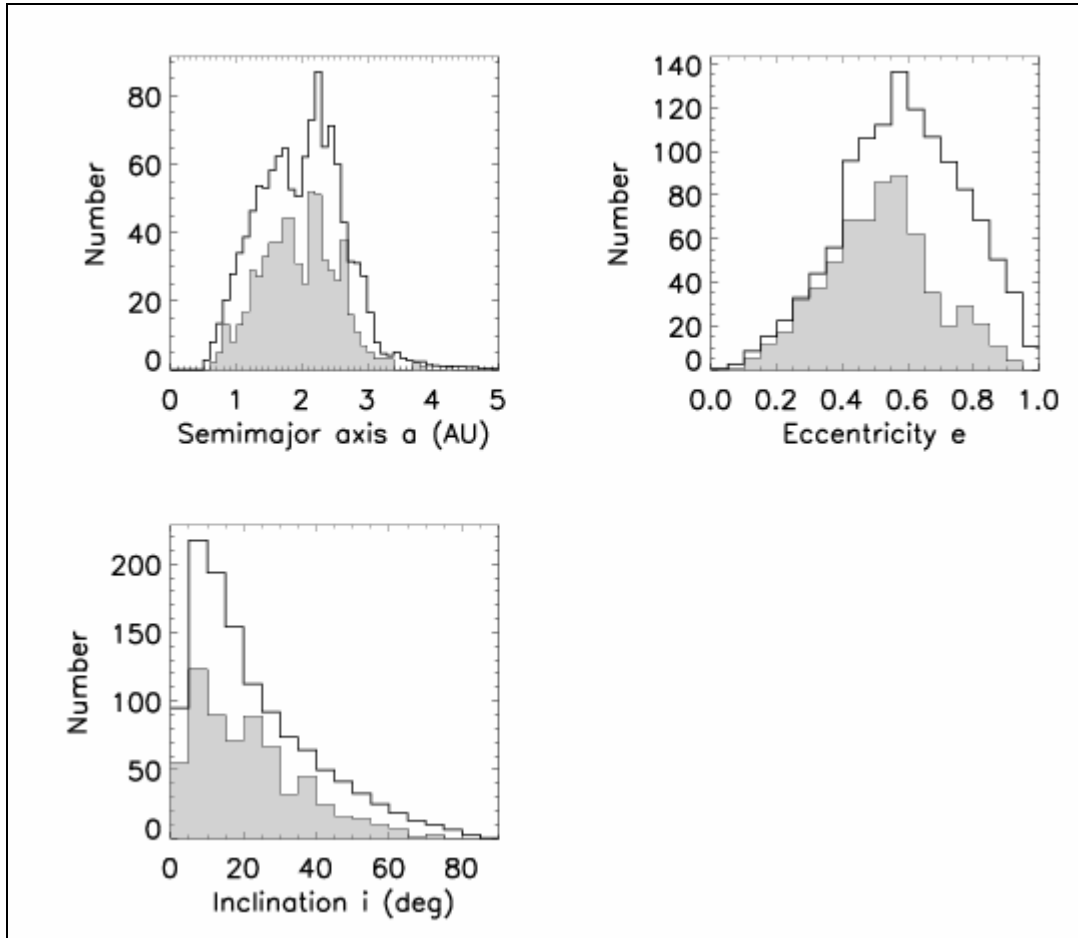


Figure 2-2. The debiased orbital distribution for NEOs with absolute magnitude $H < 18$. The predicted NEO distribution (dark solid line) is normalized to 1200 NEOs. It is compared with the 645 known NEOs (as of April 2003) from all surveys (shaded histogram).

The absolute magnitude and size-frequency distributions of the NEO population are discussed in Section 2.7. Most of the NEOs that are still undiscovered have H larger than 16, e larger than 0.4, a in the range 1-3 AU and i between 5-40 degrees. The populations with $i > 40^\circ$, $a < 1$ AU or $a > 3$ AU have a larger relative incompleteness, but contain a much more limited number of undiscovered bodies. Of the total NEOs, $32 \pm 1\%$ are Amors, $62 \pm 1\%$ are Apollos, and $6 \pm 1\%$ are Atens. Some $49 \pm 4\%$ of the NEOs should be in the evolved region ($a < 2$ AU), where the dynamical lifetime is strongly enhanced. As far as the objects inside Earth's orbit, or IEOs, the ratio between the IEO and the NEO populations is about 2%. Thus, there are only about 20 IEOs with $H < 18$.

With this orbital distribution, and assuming random values for the argument of perihelion and the longitude of node, about 21% of the NEOs turn out to have a Minimal Orbital Intersection Distance (MOID) with the Earth smaller than 0.05 AU. The MOID is defined as the closest possible approach distance between the osculating orbits of two objects. NEOs with MOID < 0.05 AU are herein defined as Potentially Hazardous Objects (PHOs), and their accurate orbital determination is considered top priority. About 1% of the NEOs have a MOID smaller than the Moon's distance from the Earth; the probability of having a MOID smaller than the Earth's radius is 0.025%. This result does not necessarily imply that a collision with Earth is imminent since both the Earth and the NEO still need to rendezvous at the same location, which is unlikely.

2.5 Nearly-Isotropic Comets

We now address the issue of the contribution of nearly-isotropic comets (NICs) to the NEO population (and the terrestrial impact hazard). Dynamical explorations of the orbital distribution of the nearly-isotropic comets (Wiegert and Tremaine 1999; Levison et al. 2001) indicate that, in order to explain the orbital distribution of the observed population, nearly-isotropic comets (NIC) need to rapidly “fade” (i.e., become essentially unobservable). In other words, physical processes are needed to hide some fraction of the returning NICs from view. One possible solution to this so-called “fading problem” would be to turn bright active comets into dormant, asteroidal-appearing objects with low albedos. If most NICs become dormant, the potential hazard from these objects could be significant. An alternative solution would be for cometary splitting events to break comets into smaller (and harder-to-see) components. If most returning NICs disrupt, the hazard to the Earth from the NIC population would almost certainly be smaller than that from the NEA population.

To explore this issue, Levison et al. (2002) took several established comet dynamical evolution models of the NIC population (Wiegert and Tremaine 1999; Levison et al. 2001), created fake populations of dormant NICs from these models, and ran these fake objects through a NEO survey simulator that accurately mimics the performance of various NEO surveys (e.g., LINEAR, NEAT) over a time period stretching from 1996-2001 (Jedicke et al. 2003). Levison et al. (2002) then compared their model results to the observed population of dormant comets found over the same time period. For example, the survey simulator discovered 1 out of every 22,000 dormant NICs with orbital periods > 200 years, $H < 18$, and perihelion $q < 3$ AU. This result, combined with the fact that only 2 dormant objects with comparable parameters had been discovered between 1996-2001, led them to predict that there are a total of $44,000 \pm 31,000$ dormant nearly-isotropic comets with orbital periods $P > 200$ years, $H < 18$, and perihelion $q < 3$ AU.

Levison et al. (2002) then used these values to address the fading problem by comparing the total number of fake dormant nearly-isotropic comets discovered between 1996-2001 to the observed number. The results indicated that dynamical models that fail to destroy comets over time produce ~ 100 times more dormant nearly-isotropic comets than can be explained by current NEO survey observations. Hence, to resolve this paradox, Levison et al. (2002) concluded that, as comets evolve inward from the Oort cloud, the vast majority of them must physically disrupt.

Assuming there are 44,000 dormant comets with $P > 200$ years, $H < 18$, and perihelion $q < 3$ AU, Levison et al. (2002) estimated that they should strike the Earth once per 370 Myr. In contrast, the rate that active comets with $P > 200$ years strike the Earth (both new and returning) is roughly once per 32 Myr (Weissman 1990; Morbidelli 2001). For comets with $P < 200$ years, commonly called Halley-type comets (HTCs), Levison et al. (2002) estimate there are 780 ± 260 dormant objects with $H < 18$ and $q < 2.5$ AU. This corresponds to an Earth impact rate of once per 840 Myr. Active HTCs strike even less frequently, with a rate corresponding to once per 3500 Myr (Levison et al. 2001; 2002). Hence, since all of these impact rates are much smaller than that estimated for $H < 18$ NEO's (one impact per 0.5 Myr; Bottke et al. 2002a, Morbidelli et al. 2002a), we conclude that nearly-isotropic comets currently represent a tiny fraction of the total impact hazard.

In summary, the consequences of the results described above are that asteroids rather than comets provide most of the present-day impact hazard. This conclusion is discussed further in the following section.

2.6 The Relative Importance of Long-Period Comets to the Earth's Impact Flux

Long-period comets, defined as those with orbital periods longer than 200 years, are often considered the most difficult group of near-Earth objects (NEOs) to deal with should one happen to be on an Earth-threatening trajectory. The arrival of these objects from the distant Oort cloud cannot be predicted and, as a rule, they are not discovered until inside the orbit of Jupiter. At the distance of Jupiter, an inactive cometary nucleus with a diameter of one kilometer and a geometric albedo equal to 0.04 would have an apparent magnitude fainter than 24 near opposition and, hence, would be well outside the detection capability of current NEO search telescopes. Even if a long-period comet should be discovered at the distance of Jupiter's orbit, it would take only nine months to reach Earth's orbit. Hence, warning times for Earth-threatening long-period comets are measured in months, not years. In addition, the mean Earth impact velocity for a long-period comet (~ 55 km/s) is more than twice that for a typical near-Earth asteroid (~ 23 km/s) and, for equal masses, it would deliver about six times the impact energy. To properly allocate the very limited resources available for NEO discoveries and physical characterization, it is important to understand the relative threat from long-period comets versus the threat posed by near-Earth asteroids (NEAs).

Estimating the impact flux for long-period comets is particularly difficult because this population is not well understood. Because the nuclei of active long-period comets are most often hidden by their gas and dust atmospheres, few reliable measurements are available for their sizes. No direct measurements of any comet's mass or bulk density are available. Indirect mass and bulk density estimates have been made for a number of comets (e.g., Rickman et al., 1987) and these estimates suggest a bulk density less than 1 g/cm^3 . If we assume the bulk densities for a cometary nucleus and an S-type NEA are 0.6 and 2.6 g/cm^3 , respectively, and the mean Earth impact velocities for long-period comets and NEAs are 55 and 23 km/s , respectively, then the average impact energy of a long-period comet impact would be only 30% more than a similarly-sized NEA that impacts the Earth.

The Earth impact probability for a long-period comet is highest for those objects with perihelia near the Earth's orbital distance ($q \sim 1$ AU) and for those objects whose orbital inclinations are low with respect to the Earth's orbit plane (i.e., $i \sim 0$ or 180 degrees). Since the likelihood of a comet's inclination falling within a particular inclination interval is proportional to the sine of the orbital inclination, one would expect to find relatively few low-inclination, long-period comets and those that did have a low inclination would be expected to be discovered with the current NEO discovery surveys that stress observations near opposition and at low ecliptic latitudes (Marsden and Steel, 1994).

An estimate of the impact flux of long-period comets with the Earth has been attempted by a number of techniques, all of which include some assumptions or approximations. Sekanina and Yeomans (1984) plotted the number of actual Earth encounters in history by all comets within a particular minimum separation distance versus the minimum separation distance itself. For a sample time of 700 years (1300 - 2000) and taking into account the northern hemisphere observing bias, the Earth impact rate for all comets was computed to be $2.3 \pm 0.73 \times 10^{-8}$ impacts per year or an average of 43 million years between impacts. Assuming the average Earth impact interval for NEAs with absolute magnitude (H) less than 18 is 0.5 Myr, the relative threat of all comet impacts versus that due to large NEAs is $0.5/43 \sim 1\%$. Over the interval from 1700 to 2000, when telescopes and accurate orbit determinations were available, they found the rate of cometary Earth close approaches remained constant. This suggests that there is a paucity of small active comets since, were this not the case, the improvement in telescopes and search techniques over this interval would have resulted in an increasing discovery rate.

Marsden (1992) employed a straightforward technique to arrive at a similar conclusion. Updating the data used by Marsden, we note that throughout history, until the end of October 2002, there have been 1324 NEAs of all sizes discovered that came to perihelion within 1.05 AU. Their average orbital period is ~ 3 years so that 441 NEAs arrived at perihelion (and crossed the Earth's orbit) each year. During the same interval, 25 short-period comets were discovered (average orbital period ~ 5 years) that had a perihelion distance of less than 1.05 AU so ~ 5 of these short-period comets reached perihelion per year. Again over the same interval, 451 long-period comets have been discovered that came to perihelion within 1.05 AU. Each of these latter objects had a *minimum* orbital period of 200 years, so an upper limit for the number of long-period comets reaching perihelion each year would be 2.3, with the actual rate likely to be far less. Using this technique, the relative threat of long-period comets to the NEAs would be $2.3/441 \leq 0.5\%$.

Weissman (1997) computed an annual Earth impact rate of 10^{-6} for long period comets capable of causing a crater diameter of 10 km (comets for which the absolute total magnitude $H_{10} \leq 16.8$). Unlike the total magnitude for asteroids (H), the cometary absolute magnitude (H_{10}) contains a significant brightness contribution from the comet's atmosphere. Weissman (1997) used Öpik's (1951, 1976) equation to compute the impact probability per return for long-period comets, Everhart's (1967) relationship for the number of long-period comets as a function of their absolute magnitude and his own conversion between absolute magnitude and the mass of the nucleus. By comparing the annual impact rate for long-period comets (10^{-6}) with the rate of NEAs capable of causing a 10 km crater (9.2×10^{-6}), he concluded that the threat of long-period comets is $\sim 11\%$ the threat from NEAs. For this estimate to be correct, some 415 long period

comets with $H_{10} \leq 16.8$ must cross the Earth's orbit each year with 10 of these brighter than $H_{10} = 11$. Since less than four Earth-crossing comets of any absolute magnitude are actually observed each year, some 99% of these objects must then go unobserved, which is unlikely.

An early work by Shoemaker and Wolfe (1982) noted an even higher relative threat of long-period comets but the values provided in this work were meant only to be crude upper bound estimates. For example, they took as an upper bound on the cratering rate of active comets the value of the one standard deviation uncertainty for their asteroid cratering rate. They also concluded that the majority of Earth-crossing asteroids are extinct comets and these were themselves derived from long-period comets. Both of these ideas have since been abandoned in the light of more recent results (Levison et al., 2002; Duncan et al., 1988).

Since the estimate by Weissman (1997) is an order of magnitude larger than those by Sekanina and Yeomans (1984) and the result found using the Marsden (1992) technique, we shall investigate these estimates using actual Earth close approach data as a reality check. For the 11% estimate to be true, one would expect one close Earth approach by a long-period comet to come within a certain Earth distance for every ten NEA close approaches to within that distance. During the interval 1900 – 2002, 155 separate NEAs made Earth close approaches to within 0.1 AU. During the same interval, only two long-period comets have come as close and both of these approaches occurred in 1983 (1983 J1 Sugano-Saigusa-Fujikawa and 1983 H1 IRAS-Iraki-Alcock). This comparison, using actual close approach data, suggests the threat of long-period comets relative to NEAs is 2/155 or ~1%.

The relative constancy of the long-period comet discovery rate over the past 300 years, the results from the Sekanina and Yeomans (1984) analysis, the Marsden (1992) type analysis and the above reality check all suggest that the threat of long-period comets is only about 1% the threat from NEAs. Levison et al. (2002) note that as comets evolve inward from the Oort cloud, the vast majority of them must physically disrupt rather than fade into dormant comets; otherwise, vast numbers of dormant long-period comets would have been discovered by current NEO surveys. This conclusion would strengthen the case against there being a significant number of dormant long-period or Halley-type comets that annually slip past the Earth unnoticed. While Earth impacts by long-period comets are relatively rare when compared to the NEA impact flux, the present number of Earth-crossing asteroids drops very steeply for asteroids larger than 2 kilometers in diameter, more steeply than the flux of cometary nuclei (Weissman and Lowry 2003). Hence, it is possible, perhaps even likely, that long-period comets provide most of the large craters on the Moon (diameter > 60 km) and most of the extinction level large impacts on Earth (Shoemaker et al., 1990).

The conclusion is that, while a newly discovered Earth-threatening, long-period comet would have a relatively short warning time, the impact threat of these objects is only about 1% the threat from NEAs. More generally, the threat from all long-period or short-period comets, whether active or dormant, is about 1% the threat from the NEA population. The limited amount of resources available for near-Earth object searches would be better spent on finding Earth-threatening NEAs with the knowledge that these types of surveys will, in any case, find many of the Earth-crossing, long-period comets as well. Finally, it has been argued that we currently enjoy a relatively low cometary flux into the inner solar system and that some future comet

shower, perhaps due to a passing star in the Oort cloud or a perturbation of our Oort cloud by the material in the galactic plane, could greatly increase this flux. The time scale for an increased cometary flux of this type is far longer than one hundred years so that current NEO searches can afford to concentrate their efforts on the more dangerous NEAs.

2.7 NEA Size-Frequency Distribution

Figure 2-3 summarizes our present knowledge of the population of NEAs. For purposes of defining populations, we include all NEAs, that is, all asteroids with perihelion q less than 1.3 AU. Included in the figure is a plot of the currently discovered population, believed to be essentially complete down to about $H = 15$ or 16. Three main methods have been used to observationally determine the size-frequency distribution of NEAs. Shoemaker (e.g. 1983) was perhaps first to estimate the population based on the cratering record of lunar maria. The most recent attempt to relate the lunar cratering record to the NEA population is by Werner et al. (2002). When they adopt the usual assumed albedo of 0.11 to relate absolute magnitude to diameter and then adjust their curve vertically to match the presently discovered population in the large size range ($H < 15$), they obtain a very low population at smaller sizes, due to the pronounced dip in the slope of their population curve in the range $17 < H < 24$. They suggest that maybe there is a systematic increase in albedo with decreasing size, and plot a second curve shifted to be equivalent to an albedo of 0.25. Thus, they suggest that the dashed curve in the figure might be appropriate for the small size range, smoothly blending into the solid line at larger sizes. This brings their estimated population into closer agreement with other methods to be described next, but still leaves the cratering-derived population estimate well below other methods.

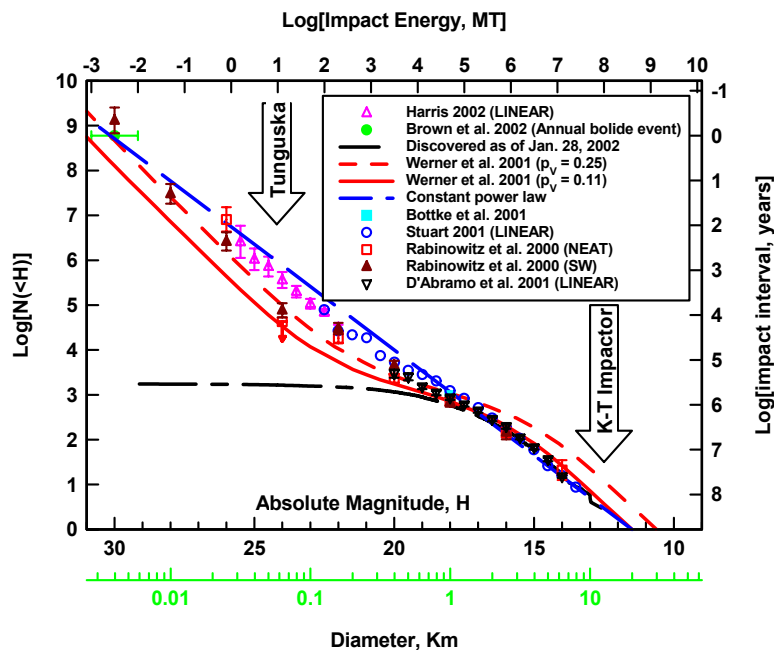


Figure 2-3. The population of near Earth Asteroids

A second method of population estimation is to attempt to estimate what fraction of the population is expected to be discovered by a given controlled survey, then “bias correct” the number detected by that survey to obtain an estimate of the total population. Rabinowitz et al. (2000) employed this method on the small detection samples of Spacewatch and NEAT, using very coarse size bins two magnitudes in H wide. Bottke et al. (2000; 2002a) used a comparable bias-correction method to estimate the NEO absolute magnitude distribution with $13 < H < 22$. This estimate was based on the Spacewatch detections, still a very small sample. Stuart (2001) was the first to use the much larger LINEAR data sample to attempt a population estimate by the bias correction method. He used much smaller size bins, 0.5 magnitude wide, to obtain a detailed size-frequency plot down to $H = 22.5$.

The third method that has been employed is to tabulate the ratio of the number of re-detections of already known objects to the sum of the number of re-detections plus the number of new discoveries by a survey in a limited time interval. This should equal the fraction of completeness of the population in that size range before the start of the controlled time interval. D'Abramo et al. (2001) used this method to estimate the NEA population using LINEAR discoveries in the years 1999-2000. In Figure 2-3, updated population estimates using detections in the years 2000-2001 are plotted.

Recently, Harris (2002) has done a relative bias estimate for the LINEAR survey in the size range $22.0 < H < 25.5$. In this small size range, the fraction discovered is so small that it takes a very large computer simulation to make an absolute estimate of detection efficiency. Harris was able to determine relative detection efficiency in this range with a more limited computer simulation, and by applying those bias factors to the number of LINEAR discoveries in those size bins, obtain estimates of the relative population, i.e. the slope of the population line. He then simply adjusted these vertically to match the Stuart population estimates in his smallest two overlapping size bins, to extend the population estimate from LINEAR down to $H = 25.5$, that is, NEAs only a few tens of meters in diameter and below the size of atmospheric penetration.

One further population estimate is that by Brown et al. (2002), based on infrasound and orbiting infrared sensors detecting bolide entries into the atmosphere. They estimate the largest NEA entering the Earth's atmosphere with an annual frequency is about 4 meters in diameter, with an energy in the range of ~ 5 KT. This size agrees very well with the smallest size estimate by Rabinowitz et al. (2000), and a straight-line extrapolation of the Stuart (2001) and Harris (2002) population estimates.

Considering all of the above estimates, it appears that a single straight line population model (constant power law in diameter units) fits well enough for this study and is likely within realistic estimates of current uncertainty. The straight line in the figure is the following function in logarithmic/magnitude units:

$$\log[N(<H)] = -5.414 + 0.4708H.$$

In units of diameter, taking an equivalence of $H = 18.0$ to be equal to $D = 1$ km, the relation is:

$$N(>D) = 1148D^{-2.354}.$$

This population model lies slightly above the number currently estimated for the population of NEAs larger than 1 km, i.e., 1148 rather than the current “best” estimate of ~1000. However, it is recognized that selection effects tend to work in the direction that population calculations underestimate the real population, so ~1100-1200 is not an unreasonable guess of the true population. Technically, this is the estimated number with $H < 18$. Recently Stuart (2003) has attempted to estimate a bias-corrected mean albedo for the NEA population and arrives at an albedo of about 0.14, implying an equivalence of $H = 17.75$ to $D = 1$ km. Morbidelli et al. (2002a), who independently modeled the NEO albedo distribution by combining dynamical data (Bottke et al. 2002a) with asteroid albedo data from the Sloan Digital Sky Survey (Ivezic et al. 2001), found similar results (i.e., a mean albedo of ~0.13, which leads to an equivalence of $H = 17.85 \pm 0.03$ to $D = 1$ km). For our adopted shift in H to diameter, the estimated population is $N(D > 1\text{km}) = N(H < 17.75) = 1090 \pm 180$. The larger error bar is primarily due to uncertainty in the albedo calibration.

The above population slightly overestimates, but falls within a factor of 2 or so, of the small body NEO populations predicted by different groups. By using this model, impact frequencies may be overestimated somewhat, but this model still lies below earlier population estimates. For example, this population model predicts an impact interval for Tunguska-sized impactors of around 500-1000 years, still quite long compared to some previous estimates (See Appendix 4), and the population of objects larger than one kilometer (1150) is still well below the “traditional” value of ~2000 in use prior to the Rabinowitz et al. (2000) paper.

3 THE IMPACT HAZARD: What Remains After the Spaceguard Survey?

At the time of the Spaceguard Survey Report (Morrison 1992), the lower limit to the size of an impactor that could lead to global environmental consequences was estimated to be around 1.5-2 km. Such events are estimated to occur about once in a million years and could lead to a billion or more deaths. Thus, the annualized risk is on the order of a thousand deaths per year. In defining the “Spaceguard Goal”, the intention was to assure that the first generation survey would discover most near-Earth objects (NEOs) down to 1 km in diameter, thus establishing with certainty whether or not any such global catastrophe could occur in the next century. As a public policy, we believe the first step “Spaceguard Survey” is eminently worth the cost. The purpose of the present study is to assess, in more detail, the benefit to be gained in extending the survey to smaller NEOs, and to higher levels of completeness among large NEOs. To do this, the current estimates of the NEO population and impact rate versus size must be evaluated. The completeness expected of present surveys, over the entire range, from the largest NEOs down to the smallest size that can penetrate the Earth's atmosphere, must also be assessed. The remaining risk posed by the undiscovered fraction of the population can then be defined. The impact risk is broken down into three components: (1) regional damage caused by impacts onto land or, in the smallest size range, air bursts over land; (2) tsunami damage caused by impacts into the sea; and (3) global climatic catastrophes from large impacts, largely independent of where they strike. For each of the three classes of hazard, an attempt is made to assess the uncertainty range of our estimates by assigning minimum, nominal, and maximum values of risk versus impactor size.

3.1 NEO Population, Impact Frequency, and Expected Completeness

Stuart (2003) obtains an estimate of the cumulative population of near-Earth asteroids (NEAs) of absolute magnitude 18.0 or brighter of $N_{\text{NEA}}(H < 18) = 1227_{-90}^{+170}$. Using various bias-corrections to relate magnitude to diameter, he finds that the equivalence of 1 km in diameter lies in the range of absolute magnitude $H = 17.62 - 17.83$. Morbidelli et al. (2002b) obtain a similar result. Henceforth, $H = 17.75$ is taken to be equivalent to $D = 1.00$ km. Note that this represents a change from the Spaceguard Report (Morrison, 1992) and several subsequent works where $H = 18$ was taken to be equivalent to a diameter of one kilometer. For the adopted slope of the population function of -2.354 (slightly different than that obtained by Stuart), the population function becomes:

$$N_{\text{NEA}}(>D) = 942D^{-2.354},$$

where N_{NEA} is the cumulative number of NEAs larger than diameter D in km.

In this study, we concentrate only on the population of potentially hazardous objects (PHOs), which we define as NEAs and extinct short-period comets with a minimum orbit intersection distance ($MOID$) < 0.05 AU from the Earth's orbit. For the NEO orbital distribution defined in the previous section, the ratio of PHOs to NEOs is 0.21 (Bottke et al. 2002). Thus the cumulative population model for PHOs is:

$$N(>D) = 198D^{-2.354}.$$

In order to assess the impact hazard over the entire range of size, we break the population up into size bins. We choose a bin width of a factor of two in mass, or $2^{1/3}$ in diameter. Thus, in a size bin from D_1 to $D_2 = 2^{1/3}D_1$, and midrange $\langle D \rangle = 2^{1/6}D_1$, the number of PHOs in that bin is:

$$n(D_1-D_2) = 82.4D_1^{-2.354} = 141.9 D_2^{-2.354} = 108.1\langle D \rangle^{-2.354}$$

Table 3-1. PHO Population, Impact Frequency, and Projected Completion

D_1-D_2 km	$\langle D \rangle$ km	H_2-H_1	$\langle E \rangle$ MT	$N(>D_1)$	$n(D_1-D_2)$	$f(n)$ yr ⁻¹	(1-C)	(1-C)n
.0279-.0352	.0313	25.0-25.5	1.91e+00	9.00e5	3.78e5	3.17e-3	1.000	3.75e5
.0352-.0443	.0394	24.5-25.0	3.81e+00	5.22e5	2.19e5	1.84e-3	1.000	2.19e5
.0443-.0559	.0496	24.0-24.5	7.63e+00	3.03e5	1.27e5	1.07e-3	1.000	1.27e5
.0559-.0704	.0625	23.5-24.0	1.53e+01	1.76e5	7.38e4	6.19e-4	1.000	7.38e5
.0704-.0887	.0787	23.0-23.5	3.05e+01	1.02e5	4.29e4	3.60e-4	.999	4.29e4
.0887-.1117	.0992	22.5-23.0	6.10e+01	5.93e4	2.49e4	2.09e-4	.996	2.48e4
.1117-.141	.125	22.0-22.5	1.22e+02	3.44e4	1.44e4	1.21e-4	.996	1.43e4
.141-.177	.157	21.5-22.0	2.44e+02	2.00e4	8.38e3	7.03e-5	.984	8250
.177-.223	.198	21.0-21.5	4.88e+02	1.16e4	4.87e3	4.08e-5	.979	4770
.223-.282	.250	20.5-21.0	9.77e+02	6.73e3	2.83e3	2.37e-5	.967	2740
.282-.355	.315	20.0-20.5	1.95e+03	3.91e3	1.64e3	1.38e-5	.931	1530
.355-.447	.397	19.5-20.0	3.91e+03	2.27e3	952	7.99e-6	.902	859
.447-.563	.500	19.0-19.5	7.81e+03	1.32e3	553	4.64e-6	.827	457
.563-.709	.630	18.5-19.0	1.56e+04	765	321	2.69e-6	.744	239
.709-.894	.794	18.0-18.5	3.13e+04	444	186	1.56e-6	.598	111
.894-1.126	1.00	17.5-18.0	6.25e+04	258	108	9.07e-7	.472	51.0
1.126-1.42	1.26	17.0-17.5	1.25e+05	150	62.8	5.26e-7	.342	21.5
1.42-1.79	1.59	16.5-17.0	2.50e+05	86.8	36.4	3.06e-7	.246	8.95
1.79-2.25	2.00	16.0-16.5	5.00e+05	50.4	21.1	1.77e-7	.159	3.35
2.25-2.84	2.52	15.5-16.0	1.00e+06	29.3	12.3	1.03e-7	.048	0.59
2.84-3.58	3.17	15.0-15.5	2.00e+06	17.0	7.12	5.98e-8	.000	0
3.58-4.50	4.00	14.5-15.0	4.00e+06	9.86	4.14	3.47e-8	.000	0
4.50-5.68	5.04	14.0-14.5	8.00e+06	5.72	2.40	2.01e-8	.000	0
5.68-7.15	6.35	13.5-14.0	1.60e+07	3.32	1.39	1.17e-8	.000	0
7.15-9.01	8.00	13.0-13.5	3.20e+07	1.93	.809	6.79e-9	.000	0
>9.01		<13.0	>4.5e+07	1.12	-	-	.000	0

The bin width chosen corresponds to 0.5017 in absolute magnitude, H , of NEOs, assuming constant albedo with size. Thus, the bin width is almost exactly equal to the half-magnitude bin widths used in NEO population estimates (e.g., Stuart 2001, D'Abramo et al. 2001). For convenience, we take $\langle D \rangle = 1.0$ km as the center of one of the bins. The equivalent absolute magnitude associated with that bin center is $\langle H \rangle = 17.75$, and the bin boundaries are $H = 17.50$

and 18.00. Table 3-1 lists the size bins from the smallest NEOs that penetrate the atmosphere up to sizes much larger than any that may remain undiscovered. For each size bin, we tabulate:

1. D_1 - D_2 : the range of diameter;
2. $\langle D \rangle$: mean diameter within the bin;
3. H_2 - H_1 : the range of absolute magnitude H ;
4. $\langle E \rangle$: the impact energy in megatons of TNT for an object of size $\langle D \rangle$, density 2.5 g/cm³ and velocity of 20 km/s;
5. $N(>D_1)$: the total number of NEOs larger than D_1 ;
6. $n(D_1$ - $D_2)$: the number in size range D_1 to D_2 ;
7. $f(n)$: the impact frequency expected from that population.

In a recent analysis of impact frequency, $f(n)$, based on the currently known population of NEOs of $H < 18.0$, Harris (2003) finds a single-object NEO impact frequency of $\sim 1.6 \times 10^{-9} \text{ yr}^{-1}$. Scaled to relate only to the PHO population (130 objects), the rate is $8.4 \times 10^{-9} \text{ yr}^{-1}$. The next column lists the incompleteness, $(1 - C)$, of objects in each size range expected after 5 more years of the current surveys (i.e., what fraction of PHOs remain undiscovered after the Spaceguard Survey), and in the final column, the number of objects in the size range that remain undiscovered, according to that estimate. This estimate of completion is obtained by running the FROSST simulation (as discussed in Section 6.1 of this report) with LINEAR parameters for 5 years starting with the present level of completion. This estimate of completion is lower than some other estimates of expected completion by 2008, perhaps because it ignores the contributions from other surveys and the inevitable improvements over time. However this only affects our assessment of remaining risk from the largest, global events. It can be further noted that this component of the remaining risk will be easily eliminated by even the most modest of the next-generation surveys. In any case, only a baseline case is established here for the simulations and not an attempt at a realistic estimate for the completion levels at the end of 2008.

3.2 Regional Damage from Land Impacts

To assess the hazard from land impacts as a function of impactor size we begin with the estimates of blast damage as a function of impactor size by Hills and Goda (1993). Figure 3-1, from that paper, is their plot of radius of destruction versus impactor radius (note: their scale is radius, not diameter), for hard stone impactors of mean density 3 g/cm³.

According to their calculations, objects up to about 150 m in diameter will deposit most of their energy in the atmosphere rather than hitting the ground at cosmic velocities. Thus, in the range from about 40 - 150 m in diameter, impact events will be air bursts, like the Tunguska event of 1908, rather than cratering events. Recently Bland and Artemieva (2003) used a similar type of analysis to obtain an upper limit of 220 meters for an air blast but, given the uncertainties inherent in these analyses, the Team retained the 150-meter limit established earlier by Hills and Goda (1993). In Table 3-2, we list the mean impactor diameter for each of our size bins, followed by the radius of destruction, R_D , for hard stone impactors which was determined from Figure 3-1, assuming an impact velocity of 20 km/sec. Next, we tabulate the fraction of the Earth's surface, F_D , represented by the area of the radius of destruction in the previous column,

followed by that fraction multiplied by the population of the Earth (6×10^9), which is the estimated average number of fatalities per event, F_1 . The next three columns list our estimates of the minimum, nominal, and maximum number of fatalities per year, F_{yr} , for each size of impactor. The nominal value is the product of impact frequency $f(n)$ times F_1 . Note that in doing this calculation, we do not adjust for the fraction of impacts that occur on land rather than in the ocean. To do so, the frequency $f(n)$ would be reduced by the ratio of land area to the total area of the Earth, but we would also have to increase the average population density of the land area, and hence the fatalities per event, F_1 , by the same factor, so the product, F_{yr} , would be unchanged. Nevertheless, it is worth remembering that the actual frequency of land impacts is about a factor of 3 less than given by $f(n)$ in Table 3-1, and the average number of fatalities per land impact is correspondingly greater than F_1 by the same factor.

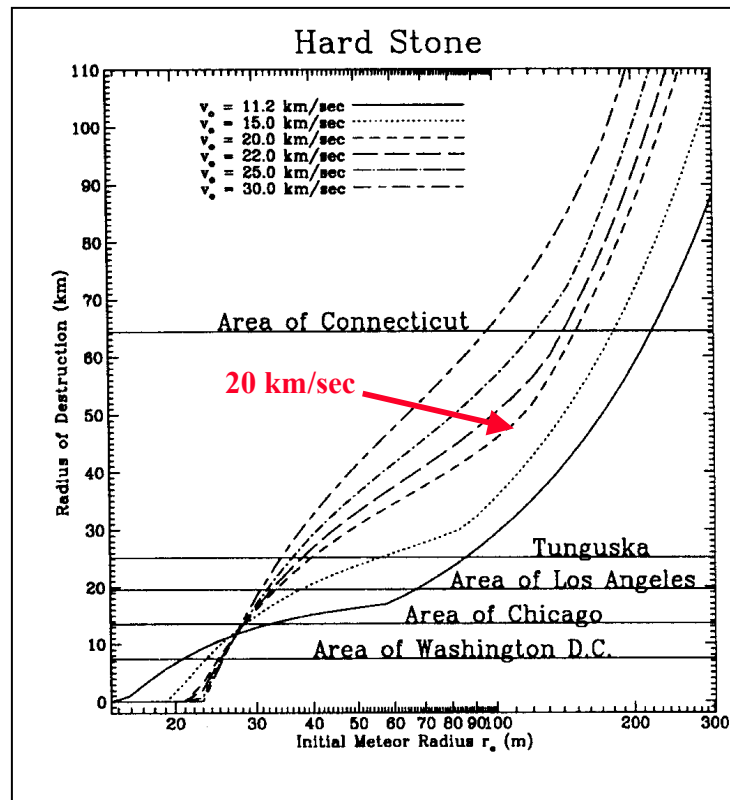


Figure 3-1. Radius of Destruction versus Impactor Radius, From Hills and Goda (1993)

Because the blast damage from land impacts is similar in nature and scale to blast damage from nuclear explosions, which have been well studied, the range of uncertainty is not as large as we will see for tsunami damage or global climatic effects, for which there is no “ground truth”. For minimum and maximum values of blast damage, we assume an uncertainty of a factor of two in energy needed to produce a given radius of destruction and number of fatalities. Thus the minimum and maximum values for F_D and F_1 are simply shifted up and down one size bin from the nominal values tabulated. The two columns of Table 3-2 that list the minimum and maximum estimates of F_{yr} are obtained from the shifted values of F_1 times the impact frequency for each size bin. Finally, the last three columns of the table list the remaining hazard, using the incompleteness $(1-C)$ remaining after 5 more years of the present level survey.

Table 3-2. Expected Damage from Impacts onto Land

$\langle D \rangle$ km	R_D km	F_D	F_1	F_{yr} Min.	F_{yr} Nom.	F_{yr} Max.	$(1-C)F_{yr}$ Min.	$(1-C)F_{yr}$ Nom.	$(1-C)F_{yr}$ Max.
0.031	0.00	0.00E+00	0.00E+00	0.00	0.00	0.00	0.00	0.00	0.00
0.039	0.00	0.00E+00	0.00E+00	0.00	0.00	3.64	0.00	0.00	3.64
0.050	7.30	3.28E-07	1.97E+03	0.00	2.11	11.85	0.00	2.11	11.85
0.062	17.30	1.84E-06	1.10E+04	1.23	6.88	14.03	1.23	6.88	14.03
0.079	24.70	3.75E-06	2.25E+04	3.99	8.14	12.33	3.99	8.14	12.33
0.099	30.40	5.68E-06	3.41E+04	4.73	7.16	9.54	4.72	7.15	9.53
0.125	35.10	7.57E-06	4.54E+04	4.16	5.54	7.09	4.14	5.52	7.06
0.157	39.70	9.69E-06	5.81E+04	3.22	4.11	5.31	3.20	4.10	5.29
0.198	45.10	1.25E-05	7.50E+04	2.39	3.08	4.34	2.35	3.03	4.27
0.250	53.50	1.76E-05	1.06E+05	1.79	2.52	3.97	1.75	2.46	3.89
0.315	67.22	2.78E-05	1.67E+05	1.46	2.31	3.66	1.41	2.23	3.54
0.397	84.69	4.41E-05	2.64E+05	1.34	2.13	3.37	1.25	1.98	3.14
0.500	106.70	7.00E-05	4.20E+05	1.23	1.96	3.11	1.11	1.77	2.80
0.630	134.43	1.11E-04	6.66E+05	1.14	1.80	2.87	0.94	1.49	2.37
0.794	169.38	1.76E-04	1.06E+06	1.05	1.66	2.64	0.78	1.24	1.96
1.000	213.40	2.80E-04	1.68E+06	0.97	1.53	2.43	0.58	0.92	1.45
1.260	268.87	4.44E-04	2.67E+06	0.89	1.41	2.24	0.42	0.67	1.06
1.587	338.75	7.05E-04	4.23E+06	0.82	1.30	2.07	0.28	0.45	0.71
2.000	426.80	1.12E-03	6.72E+06	0.76	1.20	1.90	0.19	0.29	0.47
2.520	537.73	1.78E-03	1.07E+07	0.70	1.10	1.75	0.11	0.18	0.28
3.175	677.50	2.82E-03	1.69E+07	0.64	1.02	1.62	0.03	0.05	0.08
4.000	853.60	4.48E-03	2.69E+07	0.59	0.94	1.49	0.00	0.00	0.00
5.040	1075.47	7.11E-03	4.26E+07	0.54	0.86	1.37	0.00	0.00	0.00
6.350	1355.01	1.13E-02	6.77E+07	0.50	0.80	1.26	0.00	0.00	0.00
8.000	1707.20	1.79E-02	1.07E+08	0.46	0.73	1.17	0.00	0.00	0.00
10.079	2150.94	2.84E-02	1.71E+08	0.43	0.68	1.07	0.00	0.00	0.00
Total all size bins				35.01	60.98	106.13	28.48	50.65	86.12

From Table 3-2, it can be seen that the total fatality rate from land impacts of NEOs below the threshold for global catastrophe is only about 60/year, a tiny fraction of the hazard from larger, globally hazardous events. Figures 3-2 and 3-3 are plots of the total land impact hazard and the fraction remaining after five more years at the current search survey efficiency.

In performing the above calculations, we have, as noted, ignored the uneven distribution of population on the Earth. In addition to the simple fact that people live on the land and not on the sea, the population on land is also very unevenly distributed. As a result, most sub-global events are unlikely to cause any fatalities, and only the extraordinarily rare events over heavily populated areas will result in large numbers of fatalities. To investigate this quantitatively, we obtained a digital population map of the world from data compiled by the National Center for Geographic Information and Analysis (NCGIA, 2003). This map gives the population within each cell of 5 arc minutes of latitude and longitude on the Earth's surface from latitude -57° to $+72^\circ$ (there is essentially no population outside of this range). This works out to about 6.7×10^6 cells covering most of the Earth's surface.

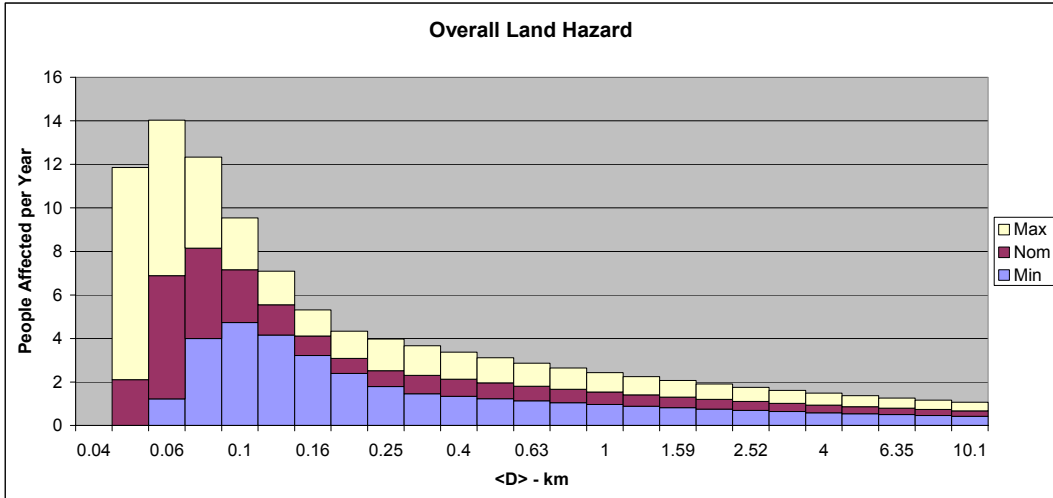


Figure 3-2. Total Land Impact Hazard

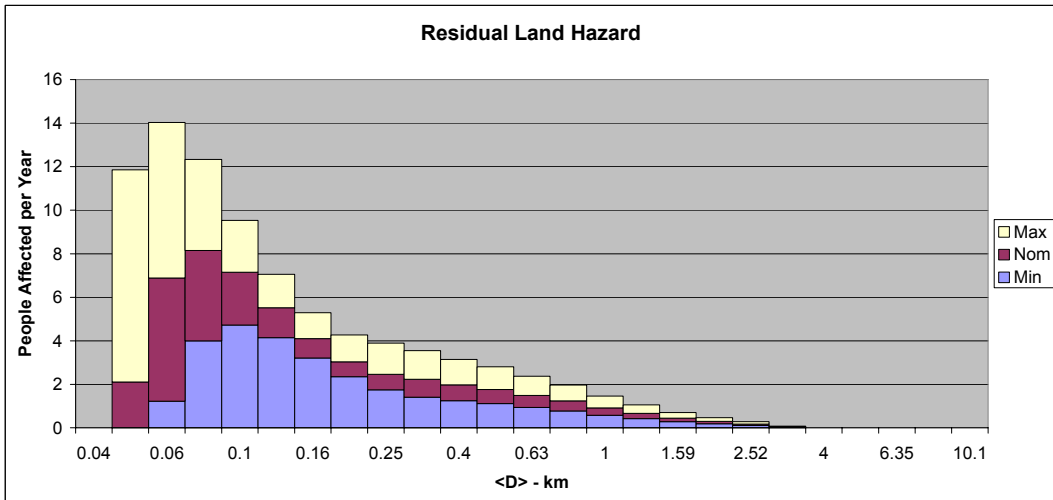


Figure 3-3. Residual Land Impact Hazard

To estimate the number of fatalities expected from events of each size, we extend the 5 arc minute grid over the full latitude range -90° to $+90^\circ$ by inserting zero population in each of the additional cells, and simulate an impact centered on each of the total of 9.3×10^9 cells. At each cell location, we map the fraction of neighboring cells included in a circle of radius equal to the Hills & Goda (1993) radius of destruction for the event size considered, and sum up the total casualties expected from an event at that location. We then sum over all possible events, weighted by the cosine of latitude of each event, since the grid with constant steps in longitude has equal numbers of events at each latitude whereas the actual surface area of the Earth at each latitude decreases as cosine of latitude. We thus tabulate the fraction of events of a given impactor size versus expected fatalities. Table 3-3 lists the results, using the same factor-of-two-in-mass bins as Table 3-1. The first two columns repeat the mean impactor diameter and impact frequency as in Table 3-1. The remaining pairs of columns list the fraction Φ_N of events of that impactor size that result in $>N$ fatalities, and the frequency, $f_N = f(n)\Phi_N$ that such an event is

expected. The three rows at the bottom list, for the sum over all sizes, the frequencies of events with $>N$ fatalities; the inverse of this frequency, which is the mean time between such events; and, finally, the dominant size of impactor responsible for events of that magnitude. A column for $N > 0$ is not included because it does not differ from the $N > 10$ column.

Table 3-3. Distribution of Event Fatalities over Size of Impactor, Land Impacts

$\langle D \rangle$ km	$f(n)$ $10^6 y^{-1}$	Φ_{10}	f_{10} $10^6 y^{-1}$	Φ_{100}	f_{100} $10^6 y^{-1}$	Φ_{1K}	f_{1K} $10^6 y^{-1}$	Φ_{10K}	f_{10K} $10^6 y^{-1}$	Φ_{100K}	f_{100K} $10^6 y^{-1}$	Φ_{1M}	f_{1M} $10^6 y^{-1}$	Φ_{10M}	f_{10M} $10^6 y^{-1}$	Φ_{100M}	f_{100M} $10^6 y^{-1}$
0.050	1070	.24	257	.18	193	.11	118	.06	64	.011	12	-	-	-	-	-	-
0.062	619	.26	161	.25	155	.21	130	.12	74	.036	22	.0023	1.4	1e-6	6e-4	-	-
0.079	360	.27	97	.26	94	.24	86	.16	58	.06	22	.006	2.2	1e-5	.004	-	-
0.099	209	.28	59	.27	56	.25	52	.18	38	.075	16	.012	2.5	5e-5	.01	-	-
0.125	121	.28	34	.28	34	.26	31	.19	23	.085	10	.017	2.1	.0001	.01	-	-
0.157	70.3	.29	20	.28	20	.26	18	.20	14	.10	7	.022	1.5	.0003	.02	-	-
0.198	40.8	.29	12	.29	12	.27	11	.21	9	.12	5	.028	1.1	.0004	.02	-	-
0.250	23.7	.30	7	.30	7	.28	7	.23	5	.13	3	.042	1.0	.0015	.04	-	-
0.315	13.8	.31	4.3	.30	4.1	.29	4.0	.25	3.5	.15	2.1	.059	0.8	.004	.06	-	-
0.397	7.99	.32	2.6	.31	2.5	.30	2.4	.27	2.2	.19	1.5	.079	0.6	.009	.07	-	-
0.500	4.64	.33	1.5	.33	1.5	.32	1.5	.28	1.3	.23	1.1	.10	0.5	.014	.07	-	-
0.630	2.69	.34	0.9	.34	0.9	.33	0.9	.30	0.8	.25	0.7	.13	0.35	.026	.07	-	-
0.794	1.56	.36	0.56	.36	0.56	.35	0.56	.32	0.50	.28	0.44	.16	0.25	.045	.07	-	-
1.000	0.907	.38	0.34	.38	0.34	.37	0.34	.35	0.32	.31	0.28	.19	0.17	.062	.056	-	-
1.260	0.526	.40	0.21	.40	0.21	.40	0.21	.36	0.19	.34	0.18	.23	0.12	.09	0.05	.005	0.003
1.587	0.306	.44	0.13	.43	0.13	.43	0.13	.40	0.12	.37	0.11	.28	0.09	.13	0.04	.012	0.004
2.000	0.177	.46	0.08	.46	0.08	.45	0.08	.45	0.08	.40	0.07	.33	0.06	.17	0.04	.024	0.004
Total	2545	-	658	-	581	-	463	-	294	-	103	-	15	-	0.63	-	0.011
t, yrs	393	-	1,500	-	1,700	-	2,200	-	3,400	-	9,700	-	70K	-	1.6M	-	90M
D	-	-	50m	-	60m	-	60m	-	70m	-	70m	-	100m	-	600m	-	1.5km

The total frequency for all events with $N > 0$, that is, the frequency of any land impact event causing even a single fatality, is about one per 1,500 years. Note that only about 1/4 of all events result in even a single fatality, but this is expected since that is about the fraction that are not over water or polar regions with no population. It is noteworthy that the average frequency of events does not fall off much with increasing fatalities up to about 10,000 per event. This again is not surprising because there are not many highly isolated settlements of fewer than 10,000 individuals. So although the interval between events causing even one fatality is around 1,500 years, an event causing 10,000 fatalities or more is half as frequent. It is perhaps surprising that the majority of these highly lethal events are expected from small impactors, in the size range ~ 70 -200m in diameter, rather than from the local effects of the larger but less frequent impacts by km-sized objects. This shifts dramatically in the $N > 10$ and $N > 100$ million fatality events, where the largest impactors are indeed the predominant, or even only, source of such events. However, the frequency of such events is even less than the expected frequency of events causing global climatic catastrophe, and the size range of objects causing such events is in the range of NEOs already being well cataloged by the present surveys. Thus we see that below the size range of global catastrophe, the next most important size range for land damage is at the far lower end of the size range that can only just make it through the atmosphere.

3.3 Tsunami Hazard from Ocean Impacts

Analogous to the above analysis for land impacts, Chesley and Ward (2003) have produced an analysis of the risk from impact-generated tsunamis as a function of impactor size and including estimates of model uncertainties. They followed the models of wave size and coastal runup and penetration of Ward and Asphaug (2000), coupled with a model of coastal population derived from Small et al. (2000). Following Ward and Asphaug (2000), they used a single power law model of NEO population, but about a factor of 5 less frequent impacts at a given size than assumed by Ward and Asphaug. This reduction in frequency is consistent with the population derived in Section 2.7 of this report and used in the land impact risk analysis in Section 3.2. The frequency adopted corresponds to one impact per 500,000 years of an asteroid 1 km in diameter or larger.

In doing their analysis, Chesley and Ward evaluated a number of uncertainties in the analysis. These include the minimum practical elevation above sea level of population settlement, due to other natural variations like diurnal tides and frequent storm waves, and “harbor protection”; that is, much of the world’s population that lives very near sea level occupies land inside of estuaries and other protected areas. Melosh (2003) has argued, based on the report of Van Dorn et al. (1968), that short wavelength tsunami waves from small impactors would break upon passing over continental shelves, thus substantially reducing the coastal run-up of impact generated tsunami waves. In their paper Chesley and Ward assign lower and upper bounds for all of these uncertainties and more, to obtain overall limits on the tsunami risk as a function of impactor size.

The results are summarized in Table 3-4. As in Table 3-2 we tabulate the range of the risk for the total hazard, F_{yr} , and the fraction, $(1-C)F_{yr}$, estimated to remain undiscovered after five more years of a LINEAR-like survey. In each category, the numbers are estimates of the annualized inundation rate of population, that is the number of people who live close enough to the shoreline and at low enough elevation to be affected by impact tsunamis, in each impactor size bin.

Chesley and Ward find that the highest risk comes from small (but more frequent) events. Thus the image of a “killer tsunami” of tens of meters height and moving at tens of km/hr is not likely. Instead the main risk is from waves of only a few meters height and penetrating only a km or less inland. We expect that many people affected by such relatively small tsunami will successfully evacuate. Therefore the numbers (F_{yr} Tsunami) should be taken as a measure of property damage rather than expected fatalities. One can suppose, based on historical fatality rates from earthquake tsunami, that actual fatalities might be only 10% or so of the number of people within an inundation zone.

Figures 3-4 and 3-5 are histograms of the estimated “lives at risk” (property damage) per year from impact-generated tsunami, as a function of impactor size. Figure 3-4 is for the total NEO population and Figure 3-5 is the risk from the estimated fraction remaining undiscovered. Clearly the current NEO discovery efforts will not significantly address the hazards due to impact-generated tsunami.

Table 3-4. Expected Tsunami Damage from Impacts into the Sea

$\langle D \rangle$ km	F_{yr}			$(1-C)F_{yr}$		
	Min	Nom	Max	Min	Nom	Max
0.062	0.00	0.00	0.00	0.00	0.00	0.00
0.079	0.12	0.37	0.77	0.12	0.37	0.77
0.099	0.74	2.29	4.77	0.74	2.29	4.75
0.125	2.43	7.51	15.59	2.42	7.48	15.53
0.157	5.42	16.78	34.84	5.33	16.51	34.29
0.198	7.79	24.12	50.09	7.63	23.61	49.03
0.250	8.24	25.51	52.97	7.97	24.66	51.23
0.315	7.94	24.59	51.07	7.40	22.89	47.55
0.397	7.10	21.96	45.62	6.40	19.81	41.15
0.500	6.07	18.79	39.03	5.02	15.54	32.28
0.630	4.74	14.68	30.50	3.53	10.92	22.69
0.794	3.31	10.25	21.29	1.98	6.13	12.73
1.000	2.14	6.64	13.78	1.01	3.13	6.51
1.260	1.33	4.11	8.55	0.45	1.41	2.92
1.587	0.78	2.40	4.99	0.19	0.59	1.23
2.000	0.40	1.24	2.58	0.06	0.20	0.41
2.520	0.20	0.62	1.29	0.01	0.03	0.06
3.175	0.10	0.31	0.65	0.00	0.00	0.00
4.000	0.05	0.15	0.32	0.00	0.00	0.00
5.040	0.02	0.07	0.15	0.00	0.00	0.00
6.350	0.01	0.03	0.07	0.00	0.00	0.00
8.000	0.00	0.02	0.03	0.00	0.00	0.00
10.079	0.00	0.01	0.02	0.00	0.00	0.00
Total	58.95	182.46	378.96	50.26	155.57	323.11

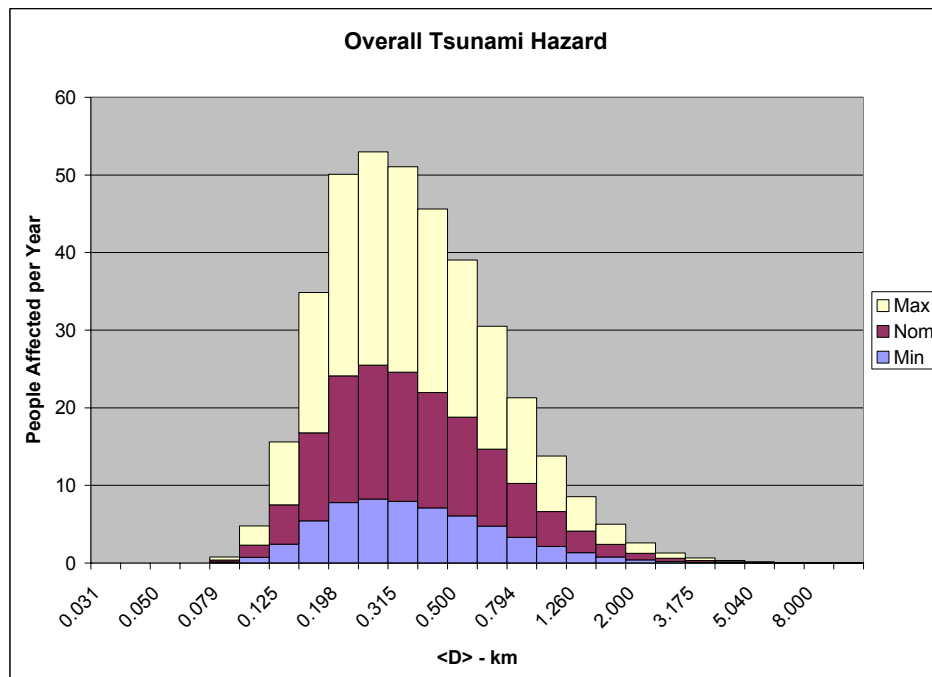


Figure 3-4. Tsunami Risk from Total Impactor Population

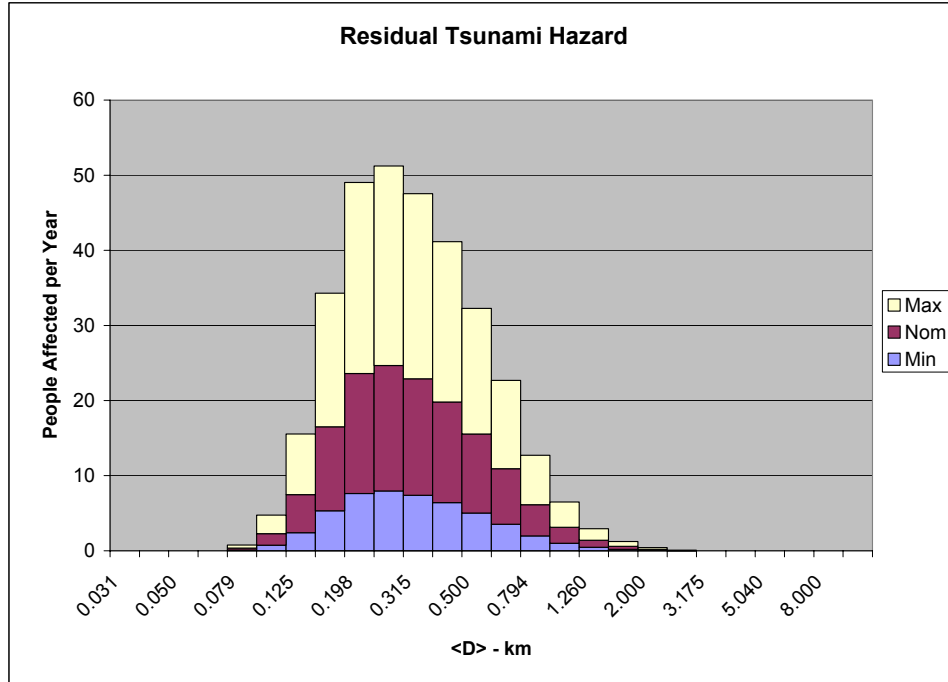


Figure 3-5. Remaining Tsunami Risk from Undiscovered Impactor Population

3.4 Global Impact Risk from Large Impacts

The risk of a global environmental catastrophe resulting from the impact of an asteroid larger than 1 km in diameter is what motivated the original Spaceguard Survey. The risk associated with such an event is so large that the residual risk from even the small fraction of the population that will remain undiscovered by the present surveys is substantial. The uncertainty in this category is dominated by (a) what fraction of the remaining impactor population will remain undiscovered, and (b) the threshold size of impact that can cause a global climatic catastrophe. The coupling between these two uncertainties exacerbates the range of uncertainty, because the fraction of undiscovered NEOs increases rapidly with decreasing size.

In Table 3-5 we attempt to quantify the global hazard and the risk that remains following the present survey. Toon et al. (1997) estimate that an impact energy of $\sim 10^5$ MT is the lower limit for global environmental effects. From Table 3-1, this energy relates to an impactor slightly larger than 1 km in diameter. They further estimate that at an energy as great as 10^6 MT ($\langle D \rangle = 2.5$ km), global effects would be major, placing a substantial fraction of the world's population at risk, and by 10^7 MT ($\langle D \rangle = 5$ km), most of the world's population would be at risk.

A final touch point is the impact that led to the extinction of the dinosaurs, which is estimated to have been an object about 10 km in diameter (10^8 MT). By this size, most of the world's population would almost certainly perish. To attempt to capture these large impactor fatality rate estimates quantitatively, and assign an uncertainty range, we adopt as the “nominal” level a fatality rate ($\%F$) of zero in size bins below $\langle D \rangle = 1.587$ km, 10% in that size bin, advancing to

20%, 30%, etc. in successive larger size bins. This leads to 90% in the largest size bin for $\langle D \rangle = 10.079$ km. It appears from the various graphs and tables in the Toon et al. (1997) paper that there is an uncertainty of about half an order of magnitude between energy of impact and the resulting environmental effects. Therefore, we establish the minimum and maximum effect levels by shifting our percentage “kill curves” up and down by two size bins, or a factor of 4 in impact energy. This results in an absolute lower bound of *global effects* falling in the $\langle D \rangle = 1.00$ km bin, or for minimum effect, in the $\langle D \rangle = 2.52$ km bin. This range reasonably captures the uncertainty range given by Toon et al. (1997).

Table 3-5. Expected Damage from Global Environmental Effects of Large Impacts

$\langle D \rangle$ km	Minimum			Nominal			Maximum		
	%F	F_{yr}	$(1-C)F_{yr}$	%F	F_{yr}	$(1-C)F_{yr}$	%F	F_{yr}	$(1-C)F_{yr}$
0.794	0	0	0	0	0.00	0.00	0	0.00	0.00
1.000	0	0	0	0	0.00	0.00	10	547.61	258.47
1.260	0	0	0	0	0.00	0.00	20	635.76	217.43
1.587	0	0	0	10	184.53	45.39	30	553.58	136.18
2.000	0	0	0	20	214.23	34.06	40	428.46	68.12
2.520	10	62.18	2.98	30	186.54	8.95	50	310.89	14.92
3.175	20	72.19	0	40	144.37	0.00	60	216.56	0.00
4.000	30	62.86	0	50	104.76	0.00	70	146.66	0.00
5.040	40	48.65	0	60	72.97	0.00	80	97.30	0.00
6.350	50	35.30	0	70	49.42	0.00	90	63.54	0.00
8.000	60	24.59	0	80	32.79	0.00	100	40.98	0.00
10.079	70	16.65	0	90	21.41	0.00	100	23.79	0.00
Total	-	322.41	2.98	-	1011.01	88.41	-	3065.13	695.13

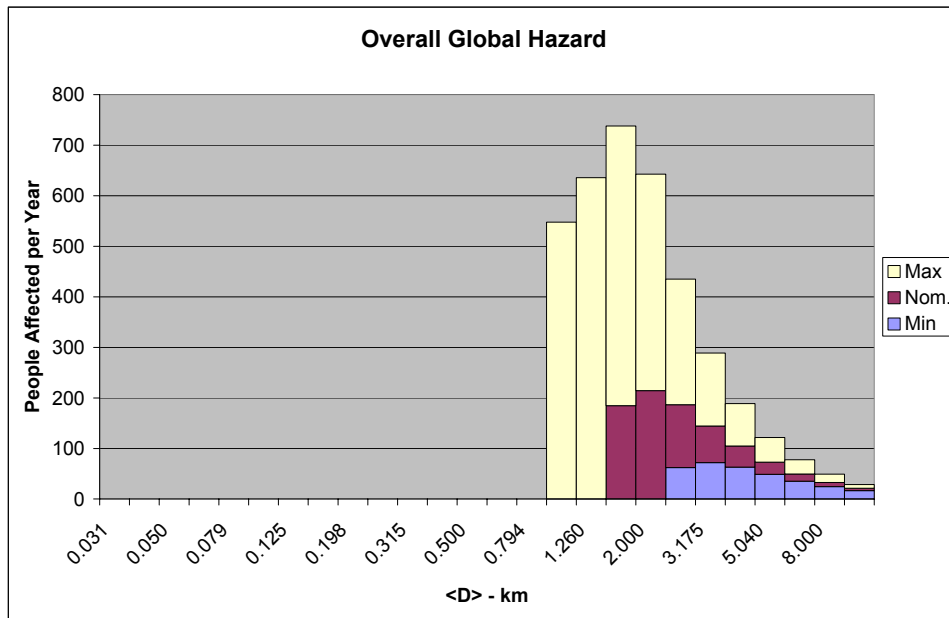


Figure 3-6. Risk from Global Environmental Effects of Large Impacts, Total Impactor Population

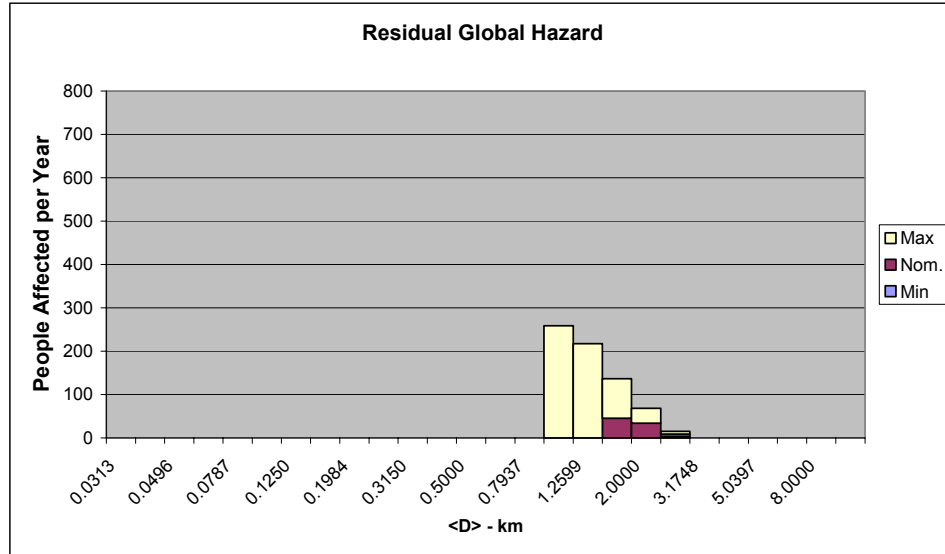


Figure 3-7. Risk from Global Environmental Effects of Large Impacts, Residual Undiscovered Impactor Population

The uncertainties we have assigned result in a full order of magnitude range in the estimated hazard from global impacts. Even greater is the range of residual risk, $(1-C)F_{yr}$, since the population of undiscovered PHOs is even steeper than the full population. Figures 3-6 and 3-7 are histograms plotting the people affected per year versus impactor size for the total global risk and for the residual risk from undiscovered PHOs.

3.5 Hazard from Long-Period Comets

The impact hazard from long-period comets is perhaps the most difficult to assess quantitatively, but a reasonable estimate appears to place the risk at such a low level ($< 1\%$ that of NEOs of comparable size) that further quantification at this time seems unnecessary (see Section 2.6). The flux of long-period comets in parabolic orbits is essentially isotropic in direction, so calculating the impact probability per object passing closer than 1 AU from the Sun is straightforward, and yields an impact probability of 2.2×10^{-9} per perihelion passage (Weissman, 1997). Weissman (1997) further indicates that the frequency of observed long-period comet passages closer than 1.05 AU from the Sun is ~ 2.4 per year. We have confirmed this, finding that there were 22 (non-SOHO) long-period comets with perihelia less than 1.05 AU discovered in the past decade (1993-2002). One can imagine that a few comets may escape discovery, so we adopt a total number of 3/year. It is generally agreed that the size-frequency distribution of long-period comets is much shallower than the asteroid distribution, with the power law exponent in the range of -1.3 to -2.0, rather than the NEA value of -2.354. Lamy, et al. (2003) claims a slope of only -1.23 down to a diameter of 4 km, and further notes that the population of small nuclei ($D < 3.2$ km) appears to be seriously depleted. Finally, we note that the frequency of “great comets”, with nuclei estimated to be ~ 9 km in diameter or larger, passing closer than 1 AU from the Sun, is very roughly once per decade. From these constraints, we infer a flux of Earth-crossing long-period comets of:

$$N_C(>D) = 5.6D^{-1.83}, \quad D > 1.4 \text{ km};$$

$$N_C(>D) = 3.0, \quad D < 1.4 \text{ km}.$$

This flux can now be broken up into the same size bins used for asteroids. Using the impact rate per perihelion passage, we can calculate an impact flux for each size bin. Long-period comets have a mean impact velocity on the Earth somewhat more than twice that of NEOs, but the nuclei are expected to be perhaps five times less dense, so overall the impact energy of a comet nucleus of a given size is only perhaps 30% greater than the same size asteroid, a difference well below the accuracy of the calculations we are making. Thus, we will simply take the impact consequences to be equal. In Table 3-6, we list for each diameter the long-period comet flux, $N_C(>D_1)$, and the corresponding impact frequency, f_C , in impacts per year, along with fatality estimates following the algorithm we employed for global effects from large NEO impacts. We compute only a “nominal” curve, although one could impose similar maximum and minimum estimates by shifting the “kill curve” up or down by two size bins.

Figures 3-8 and 3-9 illustrate the long-period comet impact hazard. In Figure 3-8, we plot the comet hazard by itself, since it is dwarfed by other components of the impact hazard. In Figure 3-9, we place it in perspective along with the various NEO impact hazards (land, tsunami, and global). Here we display only the residual hazard levels projected for the end of the ten-year Spaceguard Survey. We plot only the nominal values of hazard, not the maximum and minimum ranges.

Table 3-6. Expected damage from global environmental effects of long-period comet impacts

$\langle D \rangle$ km	$N_C(>D_1)$	$n_C(D_1-D_2)$	f_C	%F	F_{yr}
1.260	3.00	0	0.00E+0	0	0.00
1.587	3.00	1.04	2.29E-09	10	1.37
2.000	1.96	0.68	1.49E-09	20	1.79
2.520	1.28	0.44	9.76E-10	30	1.76
3.175	0.84	0.29	6.38E-10	40	1.53
4.000	0.55	0.19	4.17E-10	50	1.25
5.040	0.36	0.12	2.73E-10	60	0.98
6.350	0.23	0.08	1.78E-10	70	0.75
8.000	0.15	0.05	1.17E-10	80	0.56
10.079	0.10	0.03	7.62E-11	90	0.41
Total		3.00	6.60E-09	-	10.41

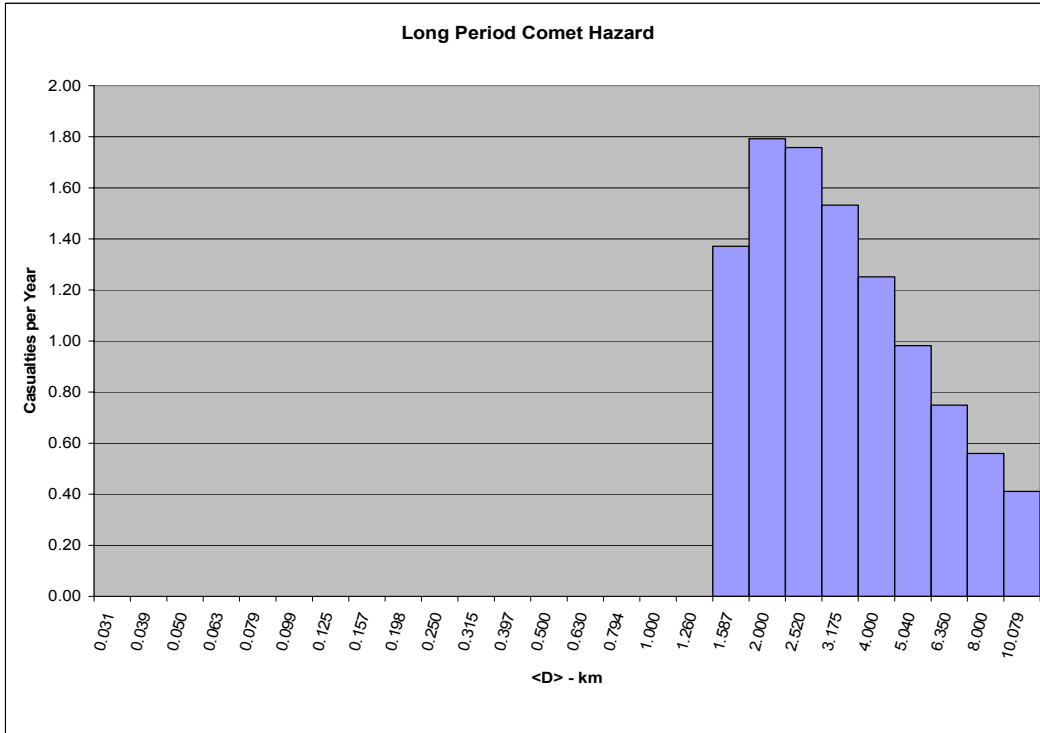


Figure 3-8. LP comet impact hazard

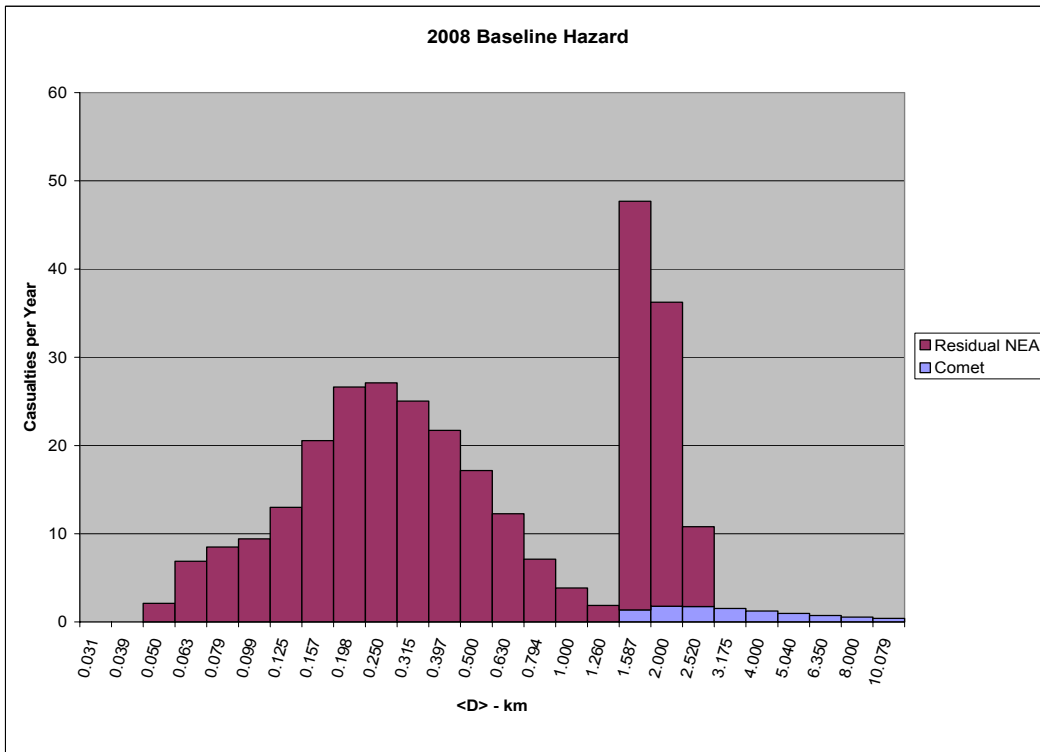


Figure 3-9. Residual impact hazard from all sources, including LP comets.

3.6 Summary of the Impact Hazard after Spaceguard

In the previous sections, we have attempted to quantify the impact hazard due to local damage by land impacts, tsunami damage from impacts into the sea, and from global environmental effects from the largest impacts into either land or sea. We also considered the frequency of large comet impacts and conclude that they constitute only a tiny fraction of the impact hazard, even after the completion of a first generation Spaceguard Survey. For each of these hazards, we estimate the total hazard and the remaining hazard from undiscovered objects after five more years of the current surveys. Figures 3-10 and 3-11 are summary plots of the overall hazard, before any surveys, and after five more years of the current surveys. Table 3-7 summarizes the residual impact hazard from all sources, assuming the completeness we infer after five more years of the present survey. It should be remembered that the largest component of the residual hazard, from the undiscovered large PHOs, is overestimated due to our conservative estimate of completeness to be achieved by current surveys. The residual hazard from large PHOs may in fact be a factor of 2 or 3 times less, but in any event will be easily retired by even a modest augmentation to existing surveys. The estimated hazard from smaller impactors is essentially independent of our estimate of completion from present surveys because completion is very low, and thus most of the hazard remains. Finally, it should be noted that in combining all three categories of impacts in units of “people affected”, we have glossed over the fact that the different categories of impact “affect” people differently. In the case of local blast damage from small land impacts, both property and lives are lost, so “people affected” is a measure of fatalities and property loss. For global environmental catastrophe from the largest impacts, our estimates are of lives lost, and property destroyed may be minimal outside the blast area. In the case of impact tsunamis (dominant in the mid-range from 200 m to 1 km diameter), we expect most affected individuals will escape by evacuation, so the number of “people affected” should be taken as a proxy for property damage. Actual lives lost could be a small fraction of that number, perhaps 10%.

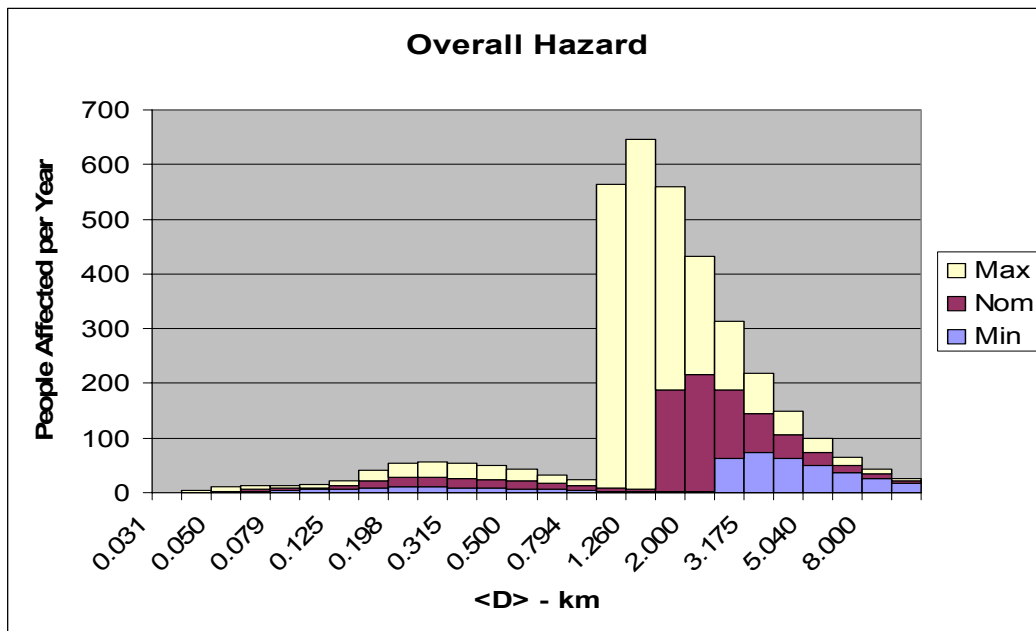


Figure 3-10. Summary of Overall Impact Hazard

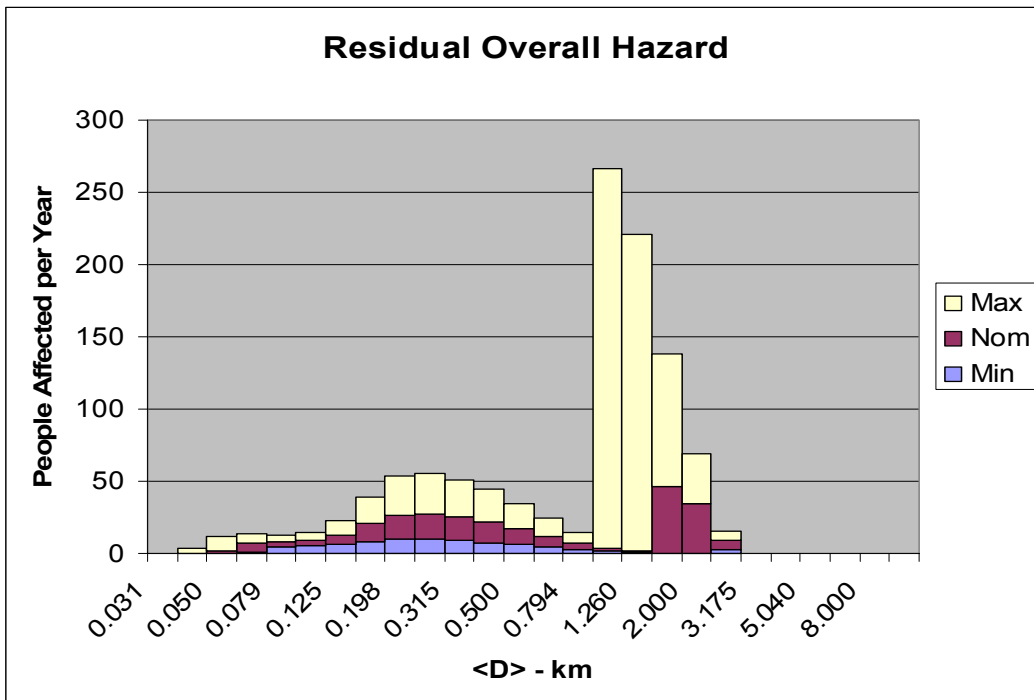


Figure 3-11. Residual Hazard after Five More Years of Current Surveys

Table 3-7. Summary of Residual Impact Hazard

Case	Residual hazard casualties/year	Source		
		Land	Tsunami	Global
Minimum	81	34%	62%	4%
Nominal	293	17%	53%	30%
Maximum	1105	8%	29%	63%

4 CANDIDATE TECHNOLOGIES AND SYSTEMS

In order to estimate the performance achievable by an asteroid search system based on current technology, the Team chose to implement a detailed search simulation. The simulation, described in detail in Section 6, takes as input estimates of the asteroid population of interest (i.e., size, orbital parameters, albedo), and “observes” this population over a simulation time of years with a variety of search sensors. A critical input to the simulation is the set of characteristics of the search sensors. This section describes the methodology behind the selection of potential sensors and the estimation of each sensor’s performance.

The primary objectives of the sensor complement are: (1) the initial discovery of previously unknown, potentially hazardous asteroids and (2) acquisition of sufficiently accurate astrometric measurements of the asteroid’s angular position and velocity to enable timely orbit determination and eventual cataloging of the objects discovered.

The sensor technologies initially chosen for evaluation include:

1. Ground-based visible band search telescopes, which have provided the vast majority of discoveries and observations to date.
2. Space-based visible band search telescopes, which have potential advantages with respect to search duty cycle and timely access to a larger portion of the sky (3π solid angle) than is achievable from the ground. In addition, the seeing and background noise are favorable due to the lack of an atmosphere. These advantages, however, typically come at the expense of the higher costs associated with fabricating, launching and operating space systems.
3. Space-based infrared (IR) search telescopes, which have the advantages associated with space-based visible band systems, along with potential detection sensitivity advantages, for a portion of the PHO population. In addition, the background clutter (i.e., stars) is much less in the far IR band, leading to potential advantages in the asteroid detection process. The advantage of IR comes at the additional cost of system complexity associated with cooling the telescope and focal plane. In addition, the maturity of IR focal plane array technology considerably lags that of visible focal planes. IR detection from ground-based systems was not considered feasible due to the interference of the atmosphere.

Other technologies, especially active methods such as radars or lidars, were considered by the Team to be unsuitable due to their relatively small search volume achievable compared to passive optical search techniques.

In order to map the cost/benefit potential of each search technology, a series of technically realizable search systems were defined by the Team. Driven largely by the diameter of the primary optics, these systems covered the range of capability considered reasonable by the Team. For purposes of specifying candidate systems, 1 degree per day sky-plane motion was selected as the maximum target rate-of-motion. Objects moving faster than this will be trailed

given the expected exposure times. While trailed images are generally easier for a human observer to detect, they represent more of a difficulty for standard detection software. Additional problems arise in that once trailing has set in, the peak pixel no longer receives the increased signal-to-noise benefit one usually enjoys with successively longer exposures. In fact, very rapidly moving objects will have lower signal-to-noise ratios than untrailed objects. To test the limitation inherent in this target rate selection, simulations were run using the NEO population discussed previously, and results were tabulated using both the expected V magnitude and the V magnitude after correction for trailing losses. At an apparent motion rate of 1 deg/day, ~25% of objects at any given time would be affected by trailing losses, and all of these objects are at $H > 21.8$, or diameter < 200 meters. Thus greater than 70% of even the smallest objects will be unaffected by trailing loss at any given time. This includes objects down to even 30 to 50 meter sizes. The design methodology for each of the systems, and their expected performance with respect to search rate and detection sensitivity, are described below.

4.1 Ground-Based Systems

4.1.1 Ground-Based Sensors

Two series of ground-based systems were defined for analysis. Their apertures cover the range between 1 and 8 meters primary optics. Unlike typical astronomical telescopes, those defined here are wide field systems designed to achieve the maximum practical product of [collection area (A)] x [field of view (Ω)]. Maximizing $A\Omega$ provides the most search capability (see Appendix 3).

The first group of candidate sensors uses a CCD detector array that was designed for near optimum performance following the prescription contained in Appendix 3. A second group uses a smaller CCD detector array that would provide good performance, but would be easier to fabricate and hence a lower cost. Practical telescopes were specified for each of the two CCD arrays. The optics are aggressive but thought to be realizable within the current state of the art for telescope optics fabrication. Especially for the large format CCD arrays, the pixel scale is considerably smaller than the seeing as prescribed by Appendix 3.

A search sensor should have a detector array with a large number of pixels covering a focal plane area that is large enough not to require an unreasonably low focal ratio (f-number) for a telescope with an adequate aperture. The focal planes are designed to be fabricated from existing CCD technology and be consistent with the following constraints:

1. Physical pixels between 10 and 24 micrometers (current limits of CCD fabrication technology)
2. Site seeing of 0.6 arc seconds (a very good site)
3. NEO apparent motion of 1 deg/day or slower (defines the onset of trailing loss as integration time increases)

The parameters of the CCD focal planes resulting from this design process are given in Table 4-1. The LINEAR CCD, in use since 1996, is also shown for reference as imager number 3 in Table 4-1.

Table 4-1. CCD Camera Characteristics

Imager	1	2	3
Pixel width (microns)	10	10	24
# pixels	36k x 24k	18k x 12k	2560 x 1960
Basis CCD	CCID-34	CCID-34	CCID-16
Basis CCD pixel #	6k x 3k	6k x 3k	2560 x 1960
Basis CCD FP area (mm)	60 x 30	60 x 30	61.4 x 47.0
# basis CCDs for tiling	48	12	1
FP area (mm)	360 x 240	180 x 120	61.4 x 47.0
Average solar quantum efficiency	0.66	0.66	0.66
QE variation (% rms)	0.3	0.3	0.3
Dark current (e/pixel/s)	5	5	10.5
Dark current variation (% rms)	2	2	2
Data rate (MHz)	2	2	2
Readout noise (e/pixel rms)	5	5	12.7
Well capacity (e/pixel)	200k	200k	200k
# ports/basis CCD	4	4	8
Total # ports	192	48	8
Readout time (s)	1.5	1.5	0.6
Shutter needed?	Y	Y	N (frame-transfer)

Table 4-2 indicates characteristics of four ground-based sensors using the large CCD array (column 1 in Table 4-1). While these sensor choices are near “optimum” for detection purposes, the focal planes have very large pixel counts and physical sizes, and thus will be expensive to fabricate. Furthermore, it will be costly to provide the large number of high-speed camera channels required to service them.

The cost/benefit justification for putting such a large focal plane into small optics (i.e., 1 meter) is arguable. In these tables, FP, FOV, $f\#$, and FWHM denote the focal plane, the field of view, the focal ratio, and the full width at half maximum. The “straddle factor” is the average fraction of detected energy that falls in one CCD pixel.

A second series of ground-based systems was defined, following a process of engineering judgment, to balance the cost/benefit of the focal plane combined with the optics. These systems, described in Table 4-3, use the CCD array from Column 2 of Table 4-1. The second series of focal plane options covers the range of primary optics diameter between 1 and 4 meters. The 8-meter optics system is clearly costly enough to justify the optimal focal plane. Each of the 7 systems was analyzed for performance and achievable cost/benefit.

Table 4-2. Characteristics of Ground-Based Sensors with 24k x 36k Pixel CCD Camera

System	1	2	3	4
Telescope aperture (m)	1	2	4	8
f #	5	4	2	1.25
Telescope effective aperture (m ²)	0.46	1.8	7.4	29
FOV (diagonal deg)	4.9	3.1	3.1	2.5
FOV (H x V deg)	4.1 x 2.7	2.6 x 1.7	2.6 x 1.7	2.1 x 1.4
FOV (square deg)	11.3	4.4	4.4	2.9
CCD imager (# from Table 4-1)	1	1	1	1
Pixel width (arc s)	0.41	0.26	0.26	0.21
1 deg/day pixel traverse time (s)	9.8	6.2	6.2	5
0.6 arc s FWHM seeing disk traverse time (s)	14.4	14.4	14.4	14.4
Straddle factor	0.28	0.14	0.14	0.094
Improvement with spatial filter (factor)	1.43	1.98	1.98	2.38
Effective straddle factor	0.41	0.28	0.28	0.22
Figures of merit:				
(Eff. Aperture m ²)(FOV deg ²) /(seeing arc s) ²	14.4	22	90.4	234
(# pixels)(Eff. aperture m ²)	4.0+8	1.6+9	6.4+9	2.5+10

Table 4-3. Characteristics of Ground-Based Sensors with 18k x 12k Pixel CCD Camera

System	1	2	3
Telescope aperture (m)	1	2	4
f #	2.5	2	1
Telescope effective aperture (m ²)	0.46	1.8	7.4
FOV (diagonal deg)	4.9	3.1	3.1
FOV (H x V deg)	4.1 x 2.7	2.6 x 1.7	2.6 x 1.7
FOV (square deg)	11.3	4.4	4.4
CCD imager (# from Table 4-1)	2	2	2
Pixel width (arc s)	0.83	0.52	0.52
1 deg/day pixel traverse time (s)	19.8	12.5	12.5
0.6 arc s FWHM seeing disk traverse time (s)	14.4	14.4	14.4
Straddle factor	0.57	0.38	0.38
Improvement with spatial filter (factor)	1.17	1.32	1.32
Effective straddle factor	0.67	0.5	0.5
Figures of merit:			
(Eff. Aperture m ²)(FOV deg ²) /(seeing arc s) ²	14.4	22	90.4
(# pixels)(Eff. aperture m ²)	1.0+8	4.0+8	1.6+9

For comparison purposes, Table 4-4 contains the parameters associated with the LINEAR system, which has contributed more than 50% of the currently known population of PHOs. All of the systems described above are considerably more capable than the current LINEAR system.

Table 4-4. Characteristics of LINEAR Sensor

System	LINEAR
Telescope aperture (m)	1
f #	2.15
Telescope effective aperture (m ²)	0.46
FOV (diagonal deg)	2.05
FOV (H x V deg)	1.6x1.2
FOV (square deg)	2
CCD imager (# from Table 4-1)	3
Pixel width (arc s)	2.27
1 deg/day pixel traverse time (s)	53.3
2.5 arc s FWHM seeing disk traverse time (s)	60
Straddle factor	0.4
Improvement with spatial filter (factor)	not used
Effective straddle factor	0.4
Figures of merit:	
(Eff. Aperture m ²)(FOV deg ²)/(seeing arc s) ²	0.15
(# pixels)(Eff. aperture m ²)	2.3+6

4.1.2 Ground-Based System Performance Estimation

The detection performance of each of the ground-based systems described above was assessed using a set of tools developed for the DoD space surveillance applications by Lincoln Laboratory. The details of the performance estimation process are described in Section 6. The intent of the performance estimation is to realistically capture all of the sensor and site dependent parameters, which define the sensitivity achieved by the sensor as a function of the time spent integrating. The sensor model does not include the pointing-dependent or time-dependent effects (i.e., air mass, Moon, etc.) that will be accounted for in the simulation process.

Curves that display the limiting magnitude achieved by systems with the large CCD array as a function of integration time are shown in Figure 4-1. All of the curves are for signal-to-noise ratio (SNR) equal to 6. The SNR=6 metric has been chosen based on the experience of the LINEAR system and represents a high threshold of detection.

Figure 4-2 shows similar performance curves for the “engineering optimized” set of sensors in bold lines, with the original curves maintained as thin lines for comparison. With matched filter detection, the limiting magnitude of the 1, 2, and 4m engineering optimized systems is the same as or within about 0.1 magnitude for the same aperture systems with the larger CCDs. While the performance of the smaller CCD systems is expected to be lower due to fewer pixels in the focal

plane, and thus the larger angular extent of each pixel, it is not significantly different. As previously mentioned, the engineering optimized systems in Figure 4-2 have lower cost due to their less complex focal planes.

The overall capability of each of these systems may be estimated by considering the search rate achieved by the system as a function of limiting magnitude. This analysis is conducted under a set of standard conditions, which account for the step and settle time for each telescope but does not account for any variation in background or other pointing and time-dependent effects. The results of these analyses are shown in Figure 4-3 for the complete set of ground-based systems. As expected, if large search rates are desired at faint limiting magnitudes, large optics are required.

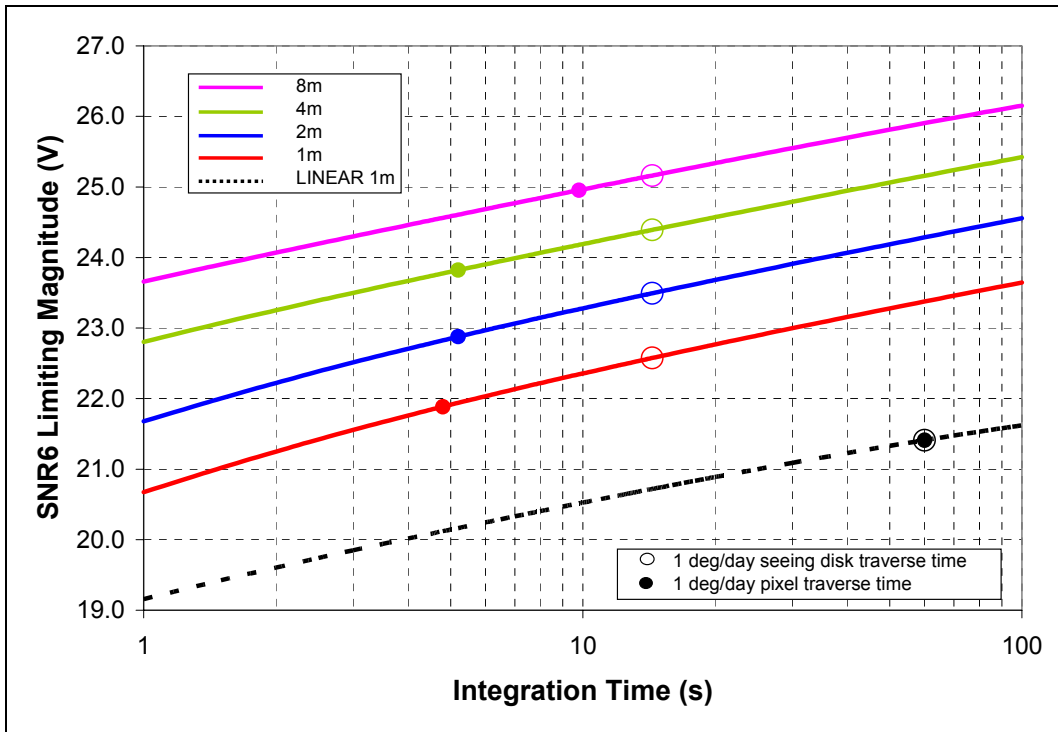


Figure 4-1. Limiting Magnitude of Ground-Based Sensors with 36k x 24k Pixel CCD Camera and LINEAR Sensor for Comparison

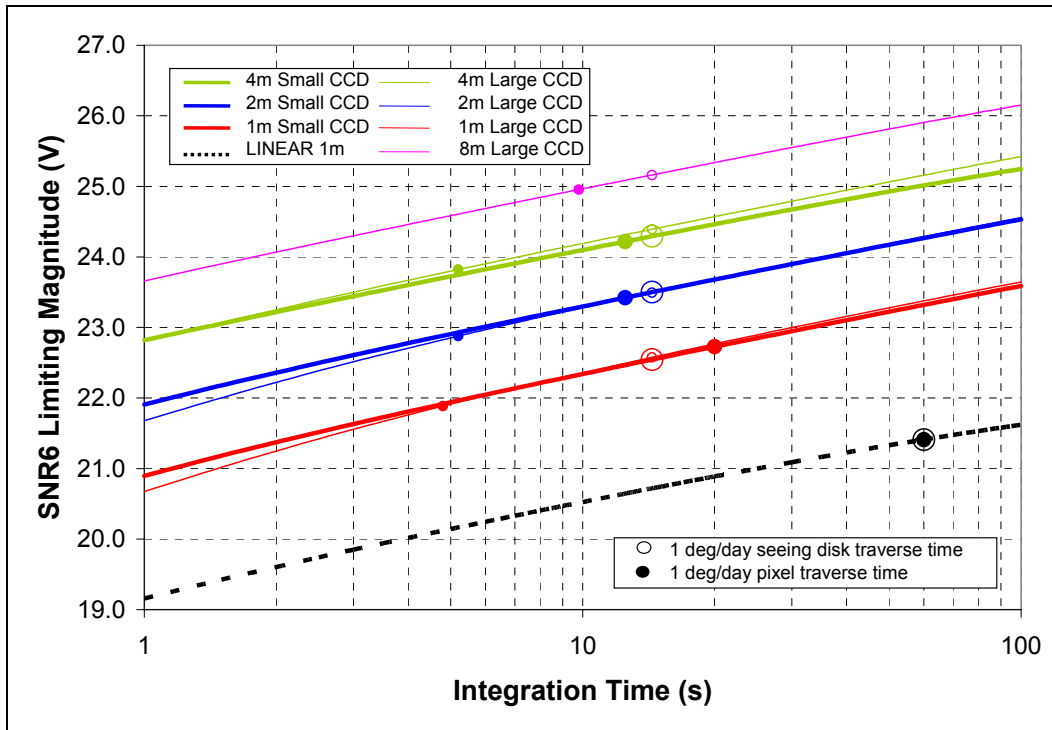


Figure 4-2. Limiting Magnitude of Ground-Based Sensors and LINEAR Sensor for Comparison

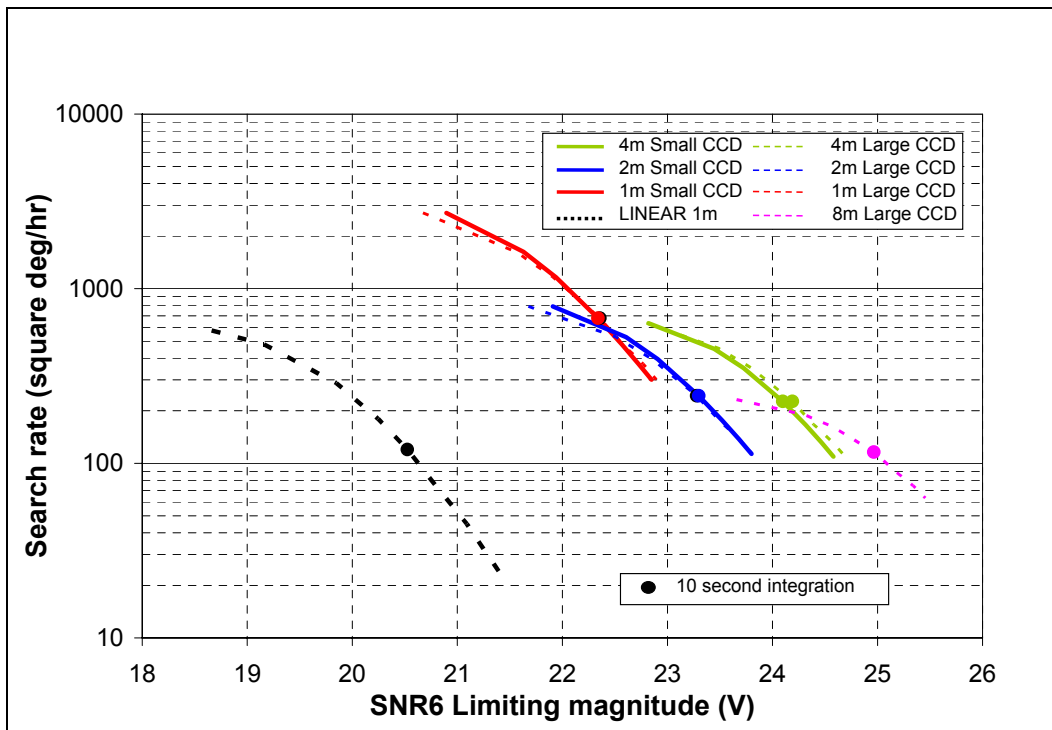


Figure 4-3. Ground-Based Sensor Search Rate versus Limiting Magnitude

4.2 Space-Based Systems

4.2.1 Visible versus Infrared Sensors

Studies of the observability of NEOs have shown that objects with low albedo that are close to the Sun may be brighter in the long-wave infrared than in visible light. However, a visible light system has been chosen for several reasons primarily traceable to component availability, but also based on the mass and power implications of these components. Long-wave infrared (LWIR) focal planes need to be operated at very low temperatures of ~ 40 K or ~ 10 K, depending on the detector technology that is chosen. The telescope optics must also be cooled to ~ 50 K to limit their contribution to the detector background. These temperatures require either a large amount of cryogen, such as the solid hydrogen used by the Spirit III instrument on the Mid-course Space Experiment mission, or an active cryocooler. Cryogenics require a very large spacecraft and have limited lifetimes. Cryocoolers for these temperature ranges are under development, but space-qualified devices are not available at this time. The existing designs work down to about 77 K and their cooling capacity falls off rapidly below that range. When appropriate cryocoolers are available, they will necessitate a significant spacecraft power system to deliver the several hundred additional watts they will require.

Cooling the optics can be accomplished by a mix of passive radiators and active cooling. This would help limit the power burden for the coolers, but it would also require large radiator surfaces that do not see the Sun, regardless of spacecraft pointing direction. This may be feasible, but it would significantly complicate the spacecraft and possibly interfere with the size constraints of the Delta II launch vehicle fairing.

The LWIR focal plane detectors may also be a concern. LWIR detectors exist but focal-plane arrays with a sufficient number of pixels do not. With the pace of detector developments, this limitation may be overcome relatively soon.

Since this study is predicated on achieving an operating observing system inside this decade with a presumed start in 2005, almost all of the required components should be available as space-qualified items at the time of the new start. Therefore, despite the fact that a LWIR telescope of a given size may be more sensitive than a visible system, the latter has been chosen as the focus of this study because almost all of the required components are available today.

4.2.2 Space-Based Visible System Design Methodology

Following a methodology similar to that of the ground-based sensors discussed in Section 4.1.1, a series of space-based visible sensor systems was defined to cover the range of performance and affordability. Again, the systems were designed with a view toward optimizing $A\Omega$ and were populated with as many pixels as were thought achievable and compatible with processors that could be launched in the next 5 years. The parameters defining the three space-based visible systems considered, with apertures of 0.5, 1, and 2 meters, are included in Table 4-5. These systems use the smaller CCD array shown in Column 2 of Table 4-1, with correspondingly lower f-number optics, since it is difficult to put such a large array in a space-based sensor, and the

performance advantage of systems with the larger array were calculated to be only about 0.1 magnitude with matched filter detection.

Table 4-5. Characteristics of Space-Based Sensors with 18k x 12k Pixel CCD Camera

System	1	2	3
Telescope aperture (m)	0.5	1	2
f #	2	2	1.5
Telescope effective aperture (m ²)	0.11	0.46	1.8
FOV (diagonal deg)	12.3	6.2	4.1
FOV (H x V deg)	10.2 x 6.8	5.1 x 3.4	3.4 x 2.3
FOV (square deg)	69.8	17.7	7.9
CCD imager (# from Table 4-1)	2	2	2
Pixel width (arc s)	2	1	0.69
1 deg/day pixel traverse time (s)	48	24	16.5
Seeing disk (arc s FWHM)	1	0.5	0.5
Seeing disk traverse time (s)	24	12	12
Straddle factor	0.69	0.69	0.57
Improvement with spatial filter (factor)	1.15	1.15	1.18
Effective straddle factor	0.79	0.79	0.67
Figures of merit:			
(Eff. Aperture m ²)(FOV deg ²)/(seeing arc s) ²	7.7	32.6	56.9
(# pixels)(Eff. aperture m ²)	2.4+7	1.0+8	4.0+9

There are several differences between space- and ground-based systems that need to be considered, as follows:

1. Seeing – The seeing of a ground-based telescope is determined by the atmosphere. The “seeing” of a space-based system is determined by either the diffraction limit of the optical aperture (the best case) or the ability of the satellite system to maintain stable pointing over the integration interval (the more likely case for a search system with a fast step and settle time).
2. Background and Extinction – Space systems do not suffer degradations due to atmospheric background or extinction.
3. Duty cycle – The observational duty cycle of a ground-based system is limited by daylight and weather. Space systems are not fundamentally limited by these effects and thus have a potential duty cycle advantage of a factor of 4-5.
4. Access – A ground-based system has access to a bit less than ½ of the total sky (4π steradian) at any time, and much of that sky is at zenith angles unfavorable due to atmospheric effects. Over the period of a winter night, a bit more than 2π steradian of the sky is accessible. A space-based system, on the other hand, can have access to more than 3π of solid angle (depending on the Sun exclusion zone of the sensor). Thus, for searches requiring observations inside the orbit of the Earth or short lifetime access to any particular area in the sky, a space-based system is advantageous.

5. Cost – Space-based systems generally have a higher cost-to-aperture ratio, higher operations costs, and shorter useful lifetimes than ground-based systems.
6. Upgrades – In general, space system hardware cannot be upgraded on a cost effective basis after launch. Thus, once launched, a space system is not able to take advantage of advances in focal plane or processing technology. Furthermore, the hardware is typically “frozen” well before launch so the system is likely a generation behind the state-of-the-art at the launch epoch. Finally, the capability of “launch qualified” processors typically considerably lags the commercial state-of-the-art employable in ground-based systems.

These effects are included in the sensor design, the performance analysis, and the simulation process in order to provide a realistic cost/benefit comparison between space- and ground-based sensor systems, and to show the efficiency of operating networks composed of both types of systems.

The sensitivity achievable by each space-based system considered is shown in Figure 4-4 and the search rate as a function of limiting magnitude is provided in Figure 4-5.

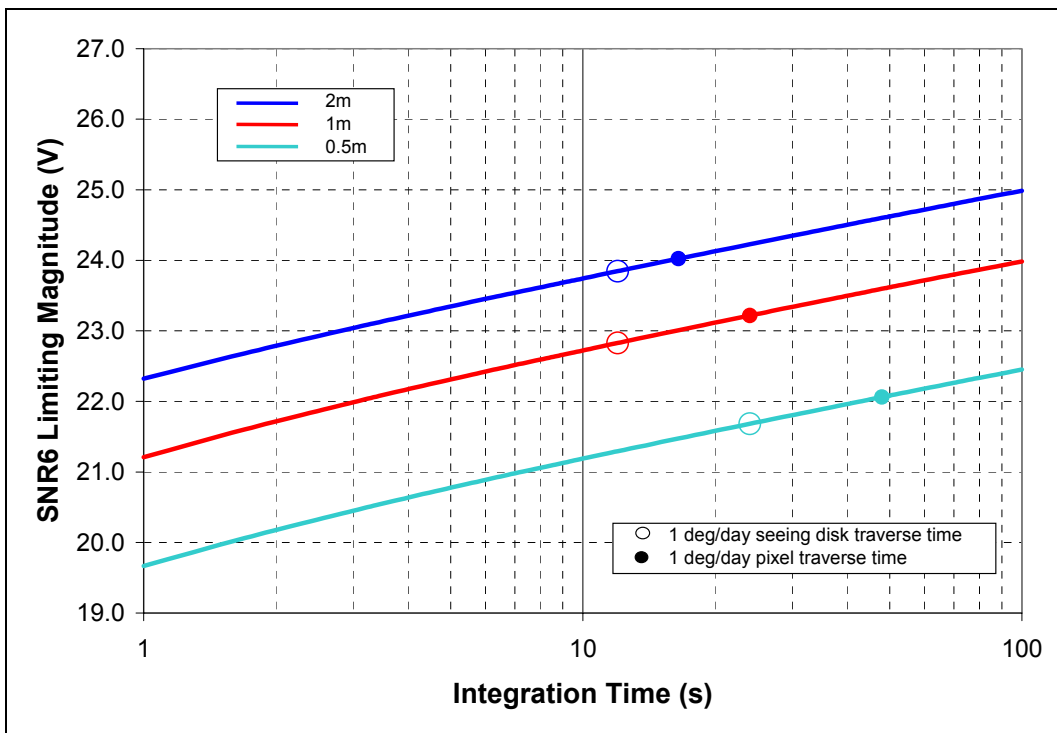


Figure 4-4. Limiting Magnitude of Space-Based Sensors with 18k x 12k Pixel CCD Camera

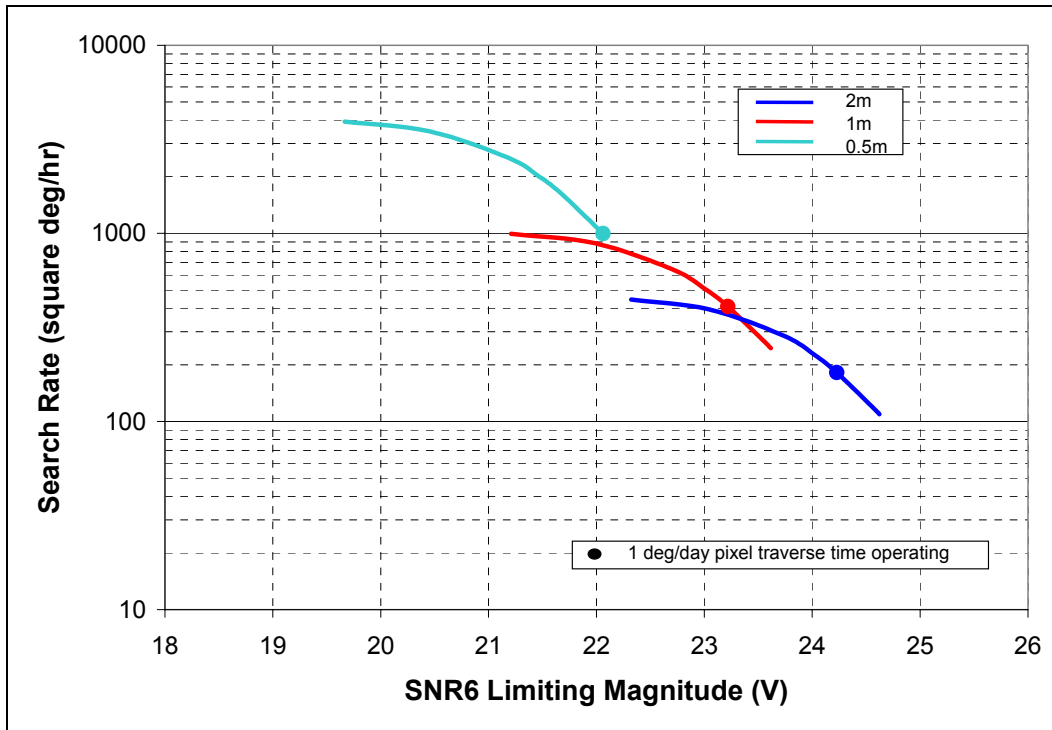


Figure 4-5. Space-Based Sensor Search Rate versus Limiting Magnitude

The Team has looked at several mission options to catalog and provide early warning of NEOs. Both system architectures and possible orbits were examined to evaluate their relative strengths, weaknesses, and cost implications. These characteristics provide a basis for trade studies. Even though this is only a preliminary study, many of the tradeoff options were clearly identified by this comparison.

Examining these options in some detail led to the cost model inputs for the final cost/benefit analysis. Many of the scientific and engineering implications of each option also feed into the cost/benefit analysis. As a measure of cost comparison, all of the studied options for a visible wavelength search mission fit within the cost cap of the NASA Discovery program for low-cost planetary missions.

4.2.2.1 Space System Assumptions

There are a number of assumptions in the development of these candidate space missions. First, the selected mission should fly within this decade, perhaps as a FY '05 new start with a launch in 2008. It should be designed for a minimum 3- to 5-year mission, but nothing should preclude a 10-year mission lifetime. To accomplish this, the strawman spacecraft design has fully redundant electronics and other redundancies, to the extent possible, similar to Discovery-class planetary missions.

The baseline for the study assumed a 1m telescope. Designs with 0.5 m and 2.0 m telescopes were also considered and the differences between these and the 1m design were assessed for both engineering and cost implications.

A Delta II launch vehicle with a 10-ft fairing was assumed because the various Delta II models can meet all of the required propulsion needs and the costs are well known.

The data from the telescope images are assumed to be processed on board to reduce the raw images to only the streaks resulting from objects that are moving relative to the fixed star background. Star matching against a reference catalog and the generation of astrometric data can be done onboard the spacecraft. Other characteristics of the observing system lead to additional requirements for many of the spacecraft subsystems. These will be discussed in the individual sections describing the subsystems.

4.2.2.2 Telescope Payload

The important requirements that affect the spacecraft design are the mass, required pointing stability, and the “step-and-settle” time. The mass of a 1m telescope and its associated focal plane and processing electronics are assumed to be 340 kg. This mass is the geometric mean of the estimates from instrument builders that ranged from 260 to 500 kg.

The various payload descriptions have pixels as small as 1 or 2 arc seconds (5 or 10 microradians). Thus the overall system must be able to hold pointing jitter to significantly less than 5 μ rad for the duration of the longest exposure time. To minimize the overall cost, both the pointing stability and settling time improvement are assumed to be controlled by an auxiliary, high-speed focal plane detector that actively adjusts the telescope secondary mirror position to stabilize the image. The readout frequency of this auxiliary detector is about 10 to 20 Hz to maintain a loop bandwidth higher than 2 Hz. With an angular correction dynamic range greater than 200 μ rad, the auxiliary detector has sufficient range to compensate for spacecraft motions and minimize the settling time. The reaction wheels in the guidance and control system need to be large enough to limit the step-and-settle time to within 15 seconds to ensure a high rate of sky coverage.

4.2.2.3 Orbits

Three potential orbits for a NEO spacecraft were studied. The options are low-Earth orbit (LEO), an Earth-Sun Lagrange point (L_2), and a 0.7 AU heliocentric orbit. Each orbital choice has strong scientific and engineering benefits. The tradeoff among them must balance the scientific advantages of each mission with the required launch vehicle performance, on-board propulsion, guidance and control system component choice, communications system, and the required on-board processing power to accommodate the available downlink.

The Delta II launch vehicle has medium and high-lift models. These come from two-stage and three-stage rockets with 3, 4, or 9 strap-on boosters. The appropriate Delta II was chosen for each mission.

Onboard propulsion may be needed for achieving final orbit and unloading the momentum wheels. The low-Earth orbit mission may not need onboard propulsion and may use magnetic torque rods for unloading its momentum wheels. The Lagrange-point orbits need a monopropellant system to inject into their final orbit and perform periodic orbital corrections. The 0.7-AU mission could use a Venus flyby to circularize its orbit. Otherwise the spacecraft and mission requirements are similar to the Lagrange-point orbits. If a Venus flyby were not used, it would require a much more capable propulsion system for injection into the final orbit and momentum wheel unloading. This enhanced propulsion requirement could be accomplished with a dual-mode, bi-propellant and monopropellant system that would use nitrogen tetroxide and hydrazine bi-propellant for the large delta-V burns, and monopropellant hydrazine for small maneuvers and momentum wheel unloading. The assumption in this report is that a Venus flyby would be used along with the simpler propulsion system.

The orbit chosen drives the guidance and control system component choices. The low-Earth orbit spacecraft would use Earth horizon sensors, while the deep space missions would use star cameras. Communications system choices of operating frequency band, RF transmitter power, and antenna type and size vary with each mission.

4.2.2.4 Scientific Implications of Orbit Choice

Sun-synchronous low-Earth orbits at about 800 km altitude have ~ 100 minute orbital periods, and the spacecraft may view any patch of sky within about π steradians at any time. However, it must view in opposite hemispheres during each half orbit. It must avoid viewing within ~ 40 degrees of the Sun to prevent a high photon background. The solar exclusion angle would need to be even greater if the telescope does not have a very high quality baffle. The telescope must also avoid pointing too close to the sunlit atmosphere and Earth.

Sun-Earth Lagrange point orbits are actually quasi-stable halos about the unstable equilibrium points. The external Lagrange point L_2 has the advantage that the Sun and Earth are close to each other in one direction and therefore the spacecraft can view nearly the full sky except for the approximately 40 degree half-angle cone centered on the Sun. Spacecraft in Lagrange-point orbits can view the Earth orbital prograde and retrograde directions at all times, which is vital if the goal of the mission is early warning.

A spacecraft at the interior Lagrange point L_1 (between the Sun and Earth) cannot view as much of the sky as one at the exterior Lagrange point L_2 because the Earth is in front of the spacecraft and the Sun is behind so there are two pointing exclusion zones. However, L_1 is an excellent position for a warning spacecraft because all Earth-approaching bodies may be viewed repeatedly and with good phase angles for maximum visibility (see Section 5). Since the cataloging of PHOs was the primary goal, the Team considered only the L_2 case in the cost/benefit analyses (Section 8).

A spacecraft in a heliocentric orbit at about 0.7 AU probably has the best orbit for discovering the full population of near-Earth objects. It may view them with a fuller phase near opposition all the time and it is the only orbital choice that can efficiently discover the Atens that spend almost all of their time inside 1 AU. In addition, the short orbital period (0.62 years) of a spacecraft in this orbit ensures nearly constant monitoring of the Earth's neighborhood and makes it difficult for objects to pass near the Earth undetected.

The low-Earth orbit mission is the lowest cost option since it does not need on-board propulsion to get into or maintain its orbit. It also enables high downlink data rates with simple, low-power communications hardware. The Lagrange-point orbits are more costly because of the need for a more capable launch vehicle, onboard propulsion to make orbital correction maneuvers every six months, and large Deep Space Network antennas for tracking and data downlink. The most costly mission is the heliocentric 0.7 AU orbit since it requires the largest launch vehicle, the most powerful communications hardware, a large onboard antenna, a more capable processor, and the use of the Deep Space Network.

4.2.3 Spacecraft System

A 10-year mission life requires a high-reliability spacecraft design with redundant systems wherever possible. Figure 4-6 shows a strawman block diagram of the spacecraft based on the MESSENGER mission to Mercury. Although the details of the architecture may vary depending on the actual spacecraft manufacturer, the key items are fully redundant avionics and communication systems. This design is based on the redundant Mil-Standard 1553 bus. Besides redundancy, this bus has automatic retries to replace missing messages and an automatic transfer to the redundant bus in the case of a hardware failure. All potential spacecraft suppliers must accommodate these features in one form or another.

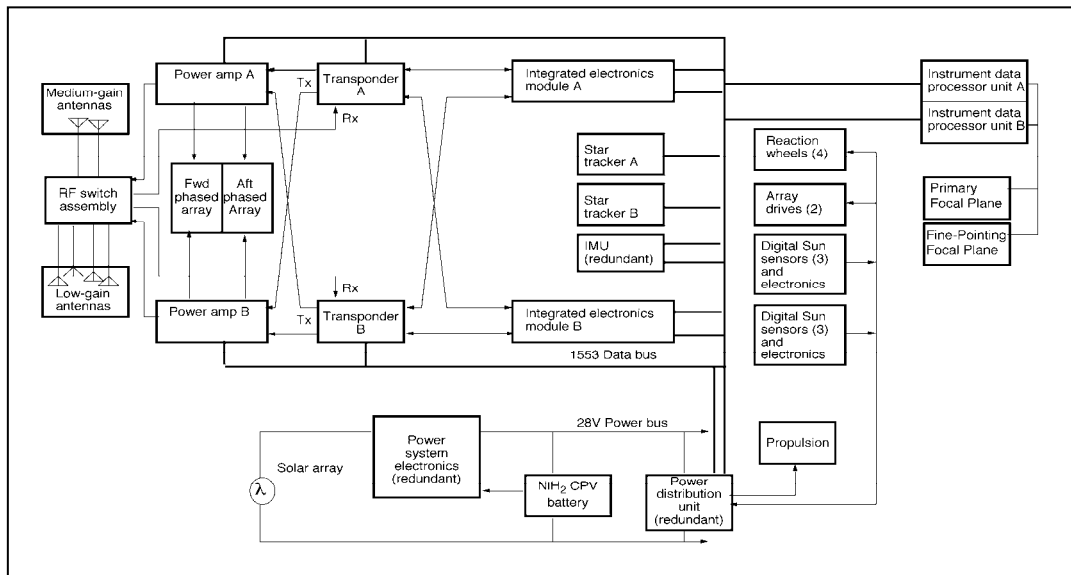


Figure 4-6. Strawman Spacecraft Architecture for a NEO Observer

As stated above, the three potential orbit choices strongly influence the design parameters of the spacecraft subsystems. Table 4-6 shows the propulsion system; Table 4-7 the guidance and control system; Table 4-8 the telecom system; Table 4-9 the command and data handling system; and Table 4-10 the Power system.

Table 4-6. Propulsion System

	LEO	L₁ or L₂	0.7 AU
Propulsion	None (Torque Rods)	Hydrazine blowdown	Hydrazine blowdown
Estimated Delta-V	None	250 m/s	250 m/s
Fuel Tank	None	1 Fuel tank	1 Fuel tank
Pressurant Tank	None	None	None
Thrusters	None	12 - 4.4 N each	12 - 4.4 N each

Table 4-7. Guidance and Control System Characteristics

	LEO	L₁ or L₂	0.7 AU
Control type	3 axis, Zero momentum	3 axis, Zero momentum	3 axis, Zero momentum
Sensors	Star Trackers, IMU, Coarse Sun sensors, Magnetometer	Star Trackers, IMU, Coarse Sun sensors	Star Trackers, IMU, Coarse Sun sensors, Magnetometer
Actuators	Reaction wheels, Torque Rods	Reaction wheels, N ₂ H ₄ Propulsion	Reaction wheels, N ₂ H ₄ Propulsion

Table 4-8. Telecom System Characteristics

	LEO	L₁ or L₂	0.7 AU
RF Band	X-Band	X-Band	X-Band
Transmitter	5W SSPA (solid-state power amplifier)	18W SSPA	60W TWTA (traveling-wave- tube amplifier)
Antennas	0.1m parabolic, No gimbal	1.5-m-parabolic, Single-axis gimbal	1.8m parabolic, Dual-axis gimbal
Downlink Rate	5 Mbps	360 Kbps	191 kbps
	HGA/ 2 LGA	HGA/2 LGA	HGA/2 LGA/1 MGA
Ground Station	3 passes/day	DSN 4.2 hrs/day	DSN 8.0 hrs/day
	10m antenna	34m antenna	34m antenna

Table 4-9. Command and Data Handling System

	LEO	L₁ or L₂	0.7 AU
Computers	2-Rad750/133 MHz	2-Rad750/133 MHz	2-Rad750/133 MHz
	80 and 8MB RAM	80 and 8MB RAM	80 and 8MB RAM
	8MB EEPROM	8MB EEPROM	8MB EEPROM
Recorder	16 Gbit	16 Gbit	16 Gbit
	Solid-state	Solid-state	Solid-state

Table 4-10. Power System Characteristics

	LEO	L₁ or L₂	0.7 AU
Solar Array	600 W	600 W	650 W
	InGaP/GaAs/Ge	InGaP/GaAs/Ge	InGaP/GaAs/Ge
	3.5 m ²	3.5 m ²	3.9 m ²
	1-axis gimbal	1-axis gimbal	1-axis gimbal
Battery	10 AH Li-Ion	10 AH Li-Ion	10 AH Li-ion
Electronics	Direct Energy Transfer	Direct Energy Transfer	Direct Energy Transfer
	Regulated bus	Regulated bus	Regulated bus
	28 ± 2V	28 ± 2V	28 ± 2V

These subsystem characteristics lead directly to system mass values that determine the launch mass required for each of the strawman missions. Table 4-11 is a rolled up mass list for each of the potential missions.

Table 4-11. Spacecraft Estimated Mass List

Mass (kg)	LEO	L₁ or L₂	0.7 AU
Propulsion System (Dry)	0	26	26
Bus Electronics (Integrated avionics)	43	43	43
Power System (Solar arrays, Battery, Electronics)	44	44	48
RF/Comm. (Amps, Switches, Antennas)	12	22	33
Guidance & Control Devices	24	22	22
Thermal	12	12	12
Harness	24	26	26
Payload (1m telescope and focal-plane electronics)	340	340	340
Fuel	0	60	60
Structure (@10% of wet mass)	49.9	59.5	61
Total	548.9	654.5	671

From these launch masses and the required C_3 (launch vehicle performance measured in km^2/s^2 at infinity), the launch vehicle can be determined. Table 4-12 shows the appropriate Delta II launch vehicle model number and the maximum launch mass that the corresponding launch vehicle can put into the corresponding orbit for each of the three potential missions.

Table 4-12. Launch Vehicle Performance

	LEO	L₁ or L₂	0.7 AU
Max Launch Mass	1610 kg	790 kg	850 kg
Delta II Model No.	7320-10	7425-10	7926-10

The Delta II model numbers can be decoded as follows: the second digit (3, 4, or 9) represents the number of strap-on booster rockets attached to the exterior of the first stage of the vehicle, and the fourth digit (0, 5, 6) represents whether there is a third stage and its size (0=none, 6=smaller version, 5=larger version). The suffix (-10) means that there is a 10-ft. diameter fairing to hold the spacecraft. The launch vehicle costs for these Delta II models range from about \$56M to \$69M.

An important consideration in the mission development is whether the spacecraft will fit within the available space in the launch vehicle fairing. Figure 4-7 shows the outline of the envelope of the fairing and a preliminary analysis shows that the spacecraft can be accommodated within the fairing.

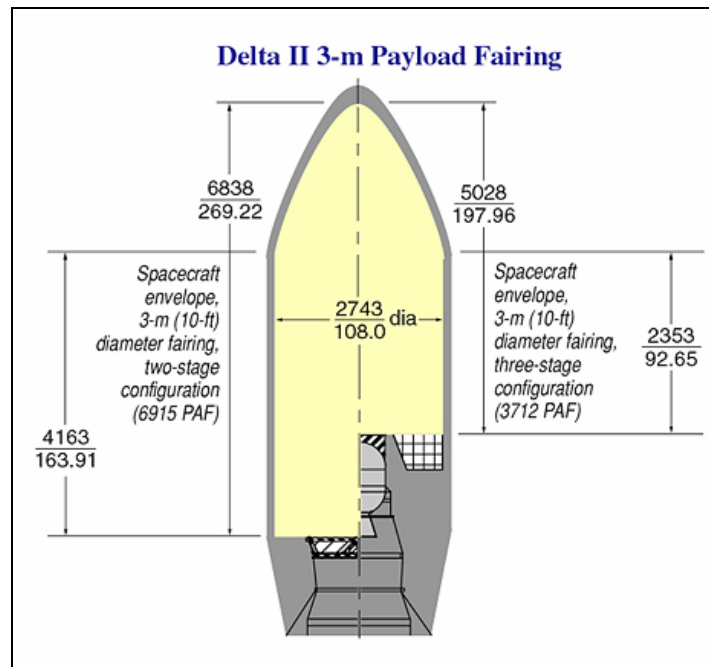


Figure 4-7. Allowable volume for the spacecraft in a Delta II 10-ft. fairing. The left half of the figure applies to two-stage vehicles as in the LEO case; the right half applies to three-stage vehicles as used for the Lagrange-point and 0.7 AU orbits.

5 SEARCH STRATEGY

In recent years, much attention has been given to studying search strategies for detecting and cataloging NEOs. With any new survey system, this topic must be revisited and investigated to find the particular nuances and operational modes that allow this system to run in a near-optimal fashion. In attempting to catalog objects smaller than 1 kilometer in size, the goal is to provide a search mode that results in as many detections as possible and also provides the astrometry necessary for well-determined orbits. These strategies and operational modes are discussed below, paying particular attention to search locations and observational cadences. Note that, in this section, the distinction between space-based and ground-based searches is largely ignored.

5.1 Search Regions

Historically, the opposition region has proved to be the most profitable area of the sky to search for NEOs for numerous reasons. Objects are characteristically bright here since they approach their fullest phases, or smallest phase angles. Discriminating NEOs from other asteroids based on their motion is also easiest near opposition (Jedicke 1996). Moreover, astrometric observations are most powerful near opposition due to small geocentric distances and the easily observable diurnal parallax.

It has been known for some time that, for certain classes of NEOs, surveying far from opposition (i.e., near the Sun in the sky), is also very profitable (Jedicke 1996). The most hazardous objects are those with small inclinations and perihelia or aphelia near 1 AU (Whiteley and Tholen 1998; Chesley and Spahr 2003). Chesley and Spahr (2003) compute the fraction of dangerous objects detected in near-Sun and opposition-based surveys, and find the near-Sun surveys can achieve completeness for larger objects on 10 year time scales. They also conclude that any survey with a short-term goal of eliminating the hazard from large NEOs must survey these near-Sun regions, since some of these objects have aphelia very near 1 AU and thus rarely pass through the opposition region. The survey area is much smaller here and there are fewer observable main belt objects that might confuse the orbit linking process. This latter process involves the linking of an orbit using recent observations of a newly discovered object with a previously determined orbit, for the same object, that is based upon earlier observations. A new orbit over the entire (longer) data interval generally secures the object's motion for a lengthy interval of time. On the downside, orbit determination using near-Sun data may be more difficult since, at small solar elongations, multiple viable solutions may exist instead of the unique solution near opposition. Additionally, discriminating NEOs from main-belt objects on the basis of their motion is more difficult than in the near-opposition regions.

Because the near-Sun regions of sky are difficult to observe due to their low elevations, it may be important to have two or more ground-based telescopes widely spaced in latitude. Near-Sun regions could be observed at their highest points in the sky from each hemisphere, thus reducing the losses due to poor seeing and atmospheric extinction. Space-based telescopes do not suffer from such severe limitations on either observing location or observing time, nor do they suffer as much from sky brightness issues when compared to their ground-based counterparts. Thus they are far superior to ground-based telescopes for near-Sun surveying.

From the ground, the near-Sun regions are only available for a small fraction of the night, thus, opposition-based surveys will only be marginally affected by devoting a few hours per night to this region. Chesley and Spahr (2003) have shown that for the largest hazardous objects, near-Sun searching is best, while for the smaller objects, concentrating near opposition with good coverage in latitude and achieving very faint limiting magnitudes is necessary for rapid completeness. Wide latitude coverage is most important for an opposition-based survey, and extreme positive and negative ecliptic latitude areas should be observed. Less important are the so-called stationary points near the ecliptic longitude ranges 60 ± 15 degrees from opposition where asteroids and comets are reversing their motions in the sky due to purely geometric effects. Because of phase effects, objects in this region will be fainter than at other areas of the sky closer to opposition.

Large-area surveys are essential, not only for reducing the NEO threat, but also for reducing the smaller threat from long-period comets and cataloging the main-belt asteroid population. Any new large-scale survey for solar system objects will require an excellent main-belt asteroid orbit catalog to aid in the identification of subsequent object detections. The identification of NEOs from their distinctive motion vectors is also critically dependent on the main-belt asteroid orbit catalog. In addition, a good orbit catalog provides a wealth of scientific information on the formation and history of the solar system.

If all designs under consideration (either ground-based or space-based) can cover the entire observable sky multiple times per month, then designing more complex observing strategies may not be necessary. A good initial strategy would be to produce coverage similar to that achieved by LINEAR, but with more frequent revisits for cataloging purposes. The strategy of all-sky coverage and multiple revisits results in the best payoff in all aspects of this problem. No objects can “hide” and remain undiscovered in certain uncovered areas of accessible sky. Comets, main-belt asteroids, and PHOs are all detected routinely, and most objects will be frequently redetected serendipitously over several months, thus providing the astrometric data required to secure their orbits. The robustness and effectiveness of all-sky surveying has been a driver for some of the ambitious telescope and CCD designs presented in this report.

5.2 Cadence Issues

Selecting the observational cadence for the nightly number and spacing of images, together with the frequency and interval of repeat visits, is of paramount importance. Rapidly moving objects can traverse CCD frames or slip off the edges of frames in a few hours, and the slowest objects may not cross a single pixel within the integration time intervals. Objects very close to the Earth may have large diurnal parallax, thus a long interval between frames will result in distinctly nonlinear apparent motion. This may present difficulties for software that expects nearly linear motion. Our analyses have assumed a LINEAR-like observational cadence, with 5 images over a 1-2 hour interval. Given the smaller pixel sizes assumed in Section 4 (1/4 of the LINEAR pixel size), perhaps a 0.5-1 hour total interval may be chosen for a ground-based system. Assuming a faint limit of about $V = 24$, only the smallest objects ($H > 22$) have any chance of being lost (see

Section 4) due to trailing losses; anything larger will be very bright at close approach distances and will be easily detected even at very high rates of motion.

Each observed field must be revisited on subsequent nights in order to confirm detections and provide the data necessary for computing preliminary orbits. In addition, the entire sky is refreshed with new NEOs that climb just above the faint limit of any system on the timescale of a few weeks. Thus, repeat visits of each field on more or less weekly intervals, is required. With only two nights of data, a longer interval on one night, exploiting the diurnal parallax may help the orbit determination process; observing at a different time of the night may also help. To reliably compute an orbit usually requires more than 3 nights of data. The orbit determination process can be improved by a somewhat uneven distribution of data, rather than an even interval of observations over a few nights. For the majority of objects detected within a survey, potential impacts will be ruled out immediately on the basis of three individual nights of data. It is expected that advances in the orbit determination and linking process will be made in the next few years, and that these advances may soon allow fewer observations to achieve the current orbit linkage and orbit determination efficiency.

5.3 Linkages

Any of the new search systems described in this report would almost immediately become the foremost discovery system for solar system objects. The ability to link, from night-to-night, the myriad detections with high confidence and reliability then becomes critical. Future search surveys will demand and deliver high astrometric accuracy and precision, and this will dramatically improve our ability to link orbits and identify the objects observed. With high-quality astrometry also comes the ability to lengthen the interval between revisits, thus allowing larger regions of sky to be covered before a revisit. Orbit quality will be substantially improved for the sparsely observed, short-arc NEOs and this will improve detections of future potential impacts.

From a set of search fields with the CFHT for Transneptunian Objects, E. Magnier and D. Jewitt (2003) recently presented an estimate of a few hundred main-belt asteroids per square degree at opposition for objects down to visual magnitude 23.5 – 24.0. Given a sky-plane density of 10 times this value (~3000 objects per square degree) and an astrometry precision of 0.2 arcseconds, G. V. Williams and T. B. Spahr (2003) tested various simplistic linking routines currently in place at the Minor Planet Center. These linking routines resulted in a better than 99% linkage rate with an interval of only one night between pairs of observations; the pairs themselves are spaced by around 1 hour. Increasing the interval between nights resulted in somewhat more confusion at around night four. These results are also confirmed by E. Bowell (2003) using similar data-sets and observation distributions.

5.4 Astrometric Accuracy and Precision

Implicit in the above discussions on linkages, identifications, and orbit determination is the assumption that astrometric accuracy and precision will improve in the near future. Present NEO

surveys have rather large pixels (1 to 2.5 arcsec), and even the best large-scale stellar reference catalogs have rms position uncertainty values of 0.2-0.4 arcsec. Nyquist sampling the point-spread function for smaller-pixel designs will immediately result in a much better-determined image centroid. A few new and dense star catalogs are in the works and should provide complete star catalogs with rms position uncertainties of near 0.1 arcsec or even 0.05 arcsec. These key improvements will result in dramatic improvements for NEO identification, orbital linkage, orbit improvement and hazard evaluation. Astrometric observations accurate to about 0.1 arcsec represent a 5-fold increase on average over several reference star catalogs that are in use today. These improvements may well verify that most new discoveries, even those with the shortest arcs, are not hazardous objects.

5.5 Cadence Requirement for Linkage and Orbits

Sections 5.2-5.4 provide fairly solid requirements on the search strategy. Observations of individual objects must be spaced closely enough to link their orbits in the first place and also closely enough that linkages will be fairly easy from a computational standpoint. These requirements, coupled with a NEO refresh rate of a few weeks, provide sky coverage and repeat visit requirements. For the analysis conducted by the Team, the assumption was made that each object must be observed over a total arc of at least 21 nights, and two nights must be spaced by less than 7 nights in order to be placed in the catalog. A pair of nights is necessary for linkage purposes, and the third night (before or after the pair) is needed for computing the unique general solution for the orbital elements. The resulting demand on the sky coverage also places requirements on the design specifications of the telescope and spacecraft; systems incapable of covering the entire observable sky 4-5 times per month may not be competitive.

5.6 Search Strategies for Warning

In the above discussion, special attention was paid to locating and cataloging objects in order to eliminate the hazard from each individual object on a case-by-case basis. There could, however, be objects that are detected that pose an immediate threat to the Earth on timescales from days to months. Unfortunately, objects on their final approach to the Earth can come from any direction of the sky. Preferentially, some may approach from morning or evening twilight, while others will come from the day-time sky and be almost undetectable until just a few days before impact. In order to provide an adequate warning system, the entire observable sky should be surveyed at least a few times per month, with special attention paid to areas around 90 degrees from the Sun. Fortunately, this search strategy for warning differs little from our initial search strategy for cataloging all PHOs.

5.7 Conclusions

The systems and strategies discussed in this report represent a dramatic improvement over existing NEO search technology and capability. More frequent sky coverage to greater limiting magnitudes, multiple search systems, and fusing near-Sun and opposition-based surveys will

enable much improved NEO discovery rates. Improvements in astrometric accuracy and precision will allow much more precise orbit determinations and more efficient orbital linkage and identification work. Hazard evaluation can then be undertaken for most objects once three separate nights of data are obtained. Frequent visits of the sky will allow a very thorough and complete inventory of hazardous objects, from those whose orbits lie mostly interior to the Earth's, to those that only rarely enter the Earth's neighborhood. This type of complete sky coverage even provides a significant possibility of warning for objects that pose a more immediate risk to the Earth.

6 SIMULATION DESCRIPTION AND RESULTS

6.1 Simulation Tool

Overall system performance analysis for ground-based, space-based, and networked (combined) systems requires a robust, flexible simulation tool. Such a tool has been developed for the Department of Defense to assess the performance of proposed space surveillance networks. The Fast Resident Object Surveillance Simulation Tool, FROSST, takes as an input the catalog of satellites and space debris, and a network of sensors, and, based on an operations concept defined by the user, generates an output list of detections. Input sensor types include ground-based optical, ground-based radar, space-based visible, space-based infrared, and space-based radar. FROSST is written in C++, and can accept a broad range of operations concepts, new sensors, new sensor models, and is easily adapted for enhanced detection models. FROSST was adopted as the Team's baseline simulation tool for assessing system performance for asteroid detection and cataloging. Modifications to FROSST that were implemented for this study are described in Section 6.1.2.

6.1.1 FROSST Input Parameters and Methodology

The original FROSST inputs include number, location, and types of sensors, and a catalog of targets.

The ground-based optical sensor parameters include a search elevation limit, limiting magnitude for a given integration time, integration time, step-and-settle time, read time, field of view, pixel field of view, good weather percentage, and operational limits (e.g., only operate after astronomical twilight). A general search pattern is also input in the original FROSST, although the pattern is static night-to-night.

The space-based visible sensor parameters include the sensor's orbital element set, the exclusion angles for the Sun, Moon, and Earth in addition to the relevant optical sensor parameters.

The original FROSST output is a list of detections including the target's location and velocity, the sensor making the detection, and the time of detection. The basic processing loop for the original FROSST simulations is described below:

- For each sensor in the network, determine pointing.
- Propagate all objects to the time of interest.
- Determine which objects fall within the field of view.
- Compute apparent magnitude of object.
- Degrade apparent magnitude for object motion (e.g., trailing loss)
- Compute sensor sensitivity.
- Degrade sensitivity for airmass, extinction, Moon brightness, etc.
- Compare apparent magnitude and sensor sensitivity.
- Output detections.

6.1.2 Necessary FROSST Modifications

FROSST is a very capable tool, but some modifications were necessary to make it appropriate for assessing the detection of asteroids. Some modifications were made to adapt to the different inputs and desired outputs, and others were made to improve the fidelity of the simulation. The following sections are provided to give an understanding of the fidelity sought with this simulation tool. Many of the modifications rely on statistics, and for the most part, these statistics were determined from LINEAR's experience and its database that includes millions of observations and detections. However, nowhere in FROSST are actual LINEAR algorithms, search fields, or operational variables used. The pertinent modifications and enhancements to FROSST are described in the following sections.

6.1.2.1 Heliocentric Propagator

The existing simulation did not include a heliocentric object propagator. A two-body propagator was added and tests showed this was sufficient, even for analyzing potential impactors and warning efficiency.

6.1.2.2 Solar Phase Equation

The apparent visual magnitude for an object is determined from the solar phase equation. For solar elongations larger than 60 degrees, the standard solar phase equation is used (Bowell et al. 1989):

$$V = H + 5 \log r\Delta - 2.5 \log[(1 - G)\Phi_1 + G\Phi_2]$$

with

$$\Phi_1 = \exp[-3.33(\tan \frac{\alpha}{2})^{0.63}], \quad \Phi_2 = \exp[-1.87(\tan \frac{\alpha}{2})^{1.22}]$$

where $G = 0.15$, H is absolute magnitude, α is solar phase angle, r is the distance from Sun to the target, and Δ is the distance from the observer to the target. For solar elongations less than 60 degrees, a modified solar phase equation is used:

$$V = H + 5 \log r\Delta + 5.03 - 10.373 \log(\pi - \alpha).$$

6.1.2.3 Sensitivity as Function of Seeing

The sensor sensitivity is degraded as a function of seeing and the seeing degrades away from the zenith according to $0.1 \cdot \text{airmass}$. The degradation is dependent on the individual sensor's pixel field of view and the full-width, half-max (FWHM) of the system.

6.1.2.4 Sky Brightness Due to the Moon

The sensor sensitivity is degraded by the sky brightness due to the Moon. This degradation is a function of the sensor pointing, the position and phase of the Moon, and the sensor's characteristics including pixel size, integration time, and system noises (Lambour et al. 2003). Typical losses are less than 1.5 visual magnitudes, although losses of 3-5 visual magnitudes are not unusual when the search pattern brings the pointing within a few degrees of the full Moon.

6.1.2.5 Losses Due to Galactic Plane

Losses due to the galactic plane were estimated from the LINEAR experience. The losses are computed as a function of distance from the galactic equator, and coarsely as a function from the galactic center. The losses vary from 2.0 visual magnitudes at the galactic equator, near the galactic center, down to 0.5 visual magnitudes away from the center. The losses drop to 0 when the center of the field of view is more than 7 degrees from the galactic equator.

6.1.2.6 Gegenschein and Zodiacal Light

The sky background due to the zodiacal light and the gegenschein affects a space-based sensor's sensitivity. The gegenschein is an enhanced brightness of the zodiacal dust cloud at opposition (i.e., zero phase angle). For ground-based sensors, the sky background is assumed to be a constant and the sensor sensitivity losses are due primarily to the atmosphere (e.g., extinction, degradation in seeing, and weather). Actual variation in the sky background is negligible compared to all of the other losses. However, in space, the variation in the sky background is the primary loss in sensitivity, especially given the ability of the space-based sensors to point within 45 degrees of the Sun. The sky background in space has been tabulated in Roach and Gordon (1973) and is the basis for the FROSST sensor sensitivity look-up table.

The loss in sensitivity due to the zodiacal light and gegenschein varies from system to system and is dependent on the aperture, pixel field of view, and other system parameters. Figure 6-1 shows how the limiting magnitude of a candidate sensor varies with solar elongation and distance from the ecliptic plane.

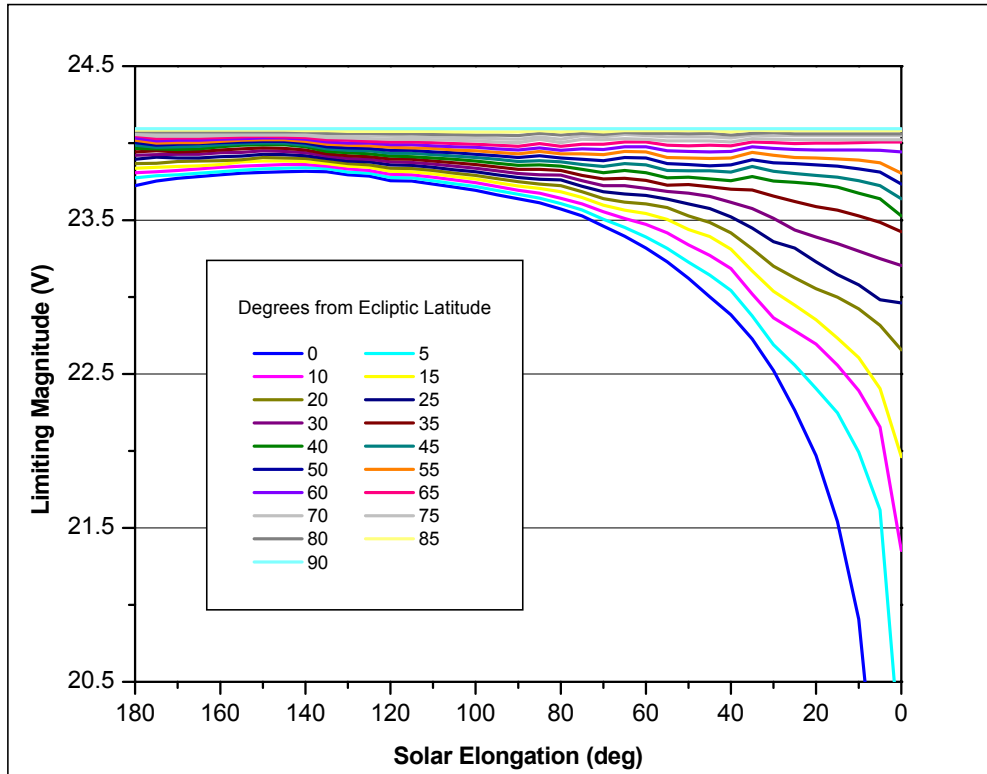


Figure 6-1. The effect of zodiacal light and the gegenschein on the limiting magnitude of a 2m space-based system. Each curve follows an ecliptic latitude as a function of solar elongation.

6.1.2.7 Seasonal Variations

The seasonal weather patterns affect the availability of sensors, ranging from as low as 50% availability in the U.S. Southwest during the summer, to 80% availability in the same area during the fall. Four numbers corresponding to the average good-weather number for each of the seasons has been added. For the desert Southwest, the numbers were estimated from the LINEAR experience over the past 3 years: 80% spring, 50% summer, 80% fall, 77% winter. For Mauna Kea, a single value of 75% is used for all four seasons. Note that while the total detections and availability of the system may not be noticeably affected by the original implementation of a single average for a site, the ability to catalog objects can be significantly aided or hampered by such an assumption.

For sensors located off the equator, seasonal variations also affect the number of search hours available between astronomical twilight and daybreak. The LINEAR experience has been to adjust the integration time of the sensor seasonally in an attempt to balance sky coverage and depth of search. The ability to mimic this strategy by seasonally varying the minimum integration time has been added to FROSST.

6.1.2.8 Losses Due To Observing In Haze and Clouds

The majority of calculations made to characterize a system assume optimal surveying conditions (e.g., clear, moonless night, looking at zenith). Reality dictates that observations take place under less than optimal conditions, including hazy and partially cloudy nights. A comparison of LINEAR observers' comments, recorded observing conditions, and field-by-field sensitivity measurements, gives average seasonal losses due primarily to haze and clouds. The ability to include these losses by way of a random number (uniform distribution) times the loss was added to FROSST. For the desert Southwest, the maximum losses are 0.6, 0.5, 0.4, and 0.5 magnitudes for spring, summer, fall, and winter, respectively. For Mauna Kea, the maximum losses are 0.3 magnitudes for all four seasons.

6.1.2.9 Trailing Losses

Loss in sensitivity due to the apparent motions of the asteroids is accounted for by computing the trailing loss for each object. Matched filtering is assumed.

$$\Delta V = 2.5 \log((\text{pixel speed})(\text{pixel size}) / \text{PSF})$$

where PSF is the point spread function.

6.1.2.10 Probability of Detection

The probability of detection curve, added to FROSST's capability, was generated from LINEAR survey data. Previous analysis of LINEAR data included nightly comparisons of objects detected versus objects predicted to be in the LINEAR field of view, the estimated visual magnitude of those objects, and knowledge of LINEAR's field-by-field SNR6 values and sensitivity (SNR6 defined in Section 4.1.2). This analysis resulted in a curve defining probability of detection as a function of the SNR6 value and the estimated visual magnitude of the objects.

This probability of detection curve is applied to the difference between the apparent magnitude of the object and the sensor sensitivity, after all degradations have been applied. Objects for which the sensor sensitivity is sufficiently in excess of the apparent magnitude of the object, there is a probability of detection of 1. Objects for which the sensor sensitivity is sufficiently less than the apparent magnitude, there is a probability of detection of 0. For all other objects where the sensor sensitivity and apparent magnitude are within a few tenths of each other, the detection is determined by the probability of detection curve and a random number generator.

The optimal number of nightly revisits is widely debated in the asteroid survey community. Consistent with the conservative estimates used throughout this study, and mimicking the LINEAR experience, five revisits and the LINEAR-like probability of detection curve are used for all of the ground-based systems in this study.

6.1.3 FROSST Inputs

6.1.3.1 Input Population

The inputs to FROSST have been expanded to provide increased fidelity for our simulations. The areas expanded or modified with the enhanced version of FROSST are the system dependent parameters and the search pattern. The remaining major input is the input population, which did not require FROSST modifications, but did require study and justification.

6.1.3.1.1 Catalog Objects

Determining the appropriate input population for FROSST is key to generating a useful output. Early runs of FROSST used a modeled PHO population described in Section 2. The population had approximately 25,000 NEOs of absolute magnitude $H < 22.0$, and 2.3 million with $H < 25.0$. While most asteroid survey studies have focused on NEOs, it was determined that this study should only focus on Potentially Hazardous Asteroids (PHOs). The output of the early simulations quickly showed that small number statistics were troublesome for the larger PHOs, and that large quantities of processing time were being spent on the numerous, very small PHOs. The detection of a single object in some bins could be the difference between 50% and 100% completion in that bin. The data bins most adversely affected by the small number statistics and the detection or non-detection of a single object, are the bins with the largest objects (i.e., the bins that correspond to the majority of the impact risk due to the possibility of global effects).

To avoid the statistics of small numbers problem and simultaneously reduce the processing required for small objects, a statistical representation of the PHO population was developed. One thousand objects were put in 20 different bins, each bin spanning 0.5 magnitude with the objects uniformly distributed across H within each bin, and the orbits chosen at random from our set of 470,000 PHO orbits. The effect of switching from a model of all PHOs to running a uniform, statistical model is to reduce the number of objects per simulation from 470,000 to 20,000 objects, making it feasible to more fully explore the system parameter space and run approximately 100 simulations of different systems and networks of systems for 10-20 years each. More importantly, it also eliminated the small number statistics issues for large objects. For example, while it is likely that there are only 11 PHOs ranging from $15.5 < H < 16.0$, and there are currently 10 of these PHOs known, this uniform, statistical distribution allows the completion in this range to move gradually from 90.9% (10/11) to 100% over ten years. Rather than jumping from 90.9% to 100% with the simulated detection of a single simulated object, the percent completion certainty moves gradually with the simulated detection of 91 simulated objects.

Figure 6-2 shows the bin-by-bin performance of a 4m ground-based system against a full PHO population model, and against a uniform statistical model. There are 3 sets of curves corresponding to 1, 5, and 10 years of search. The ordinate shows the percent completion within each bin. As expected, the curve generated with the uniform, statistical model is smoother and does not have sporadic significant dips due to small number statistics for large objects.

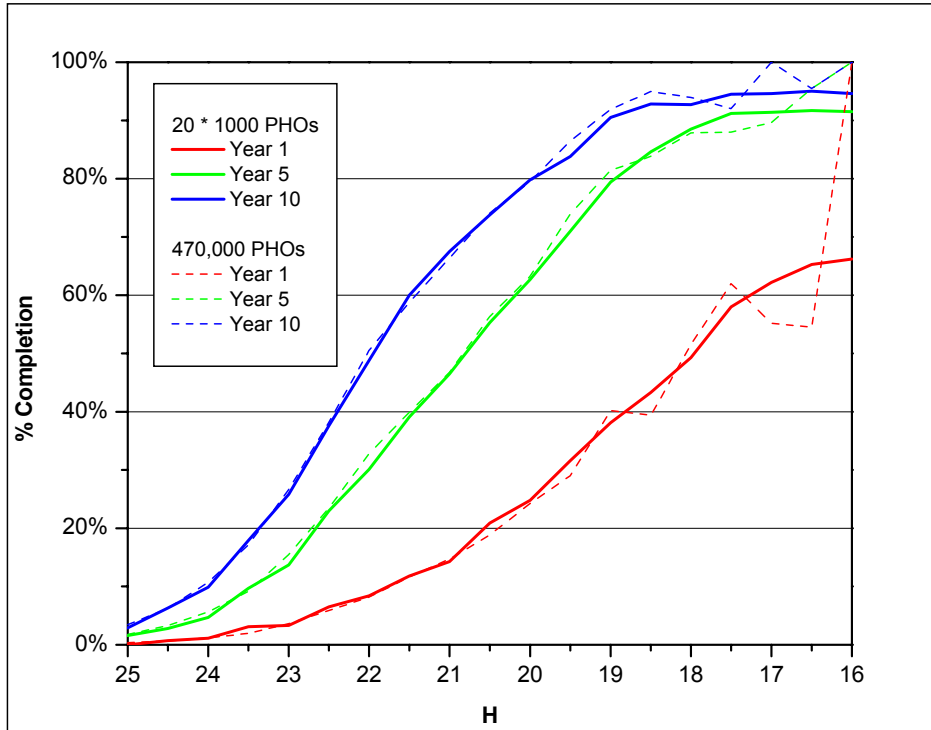
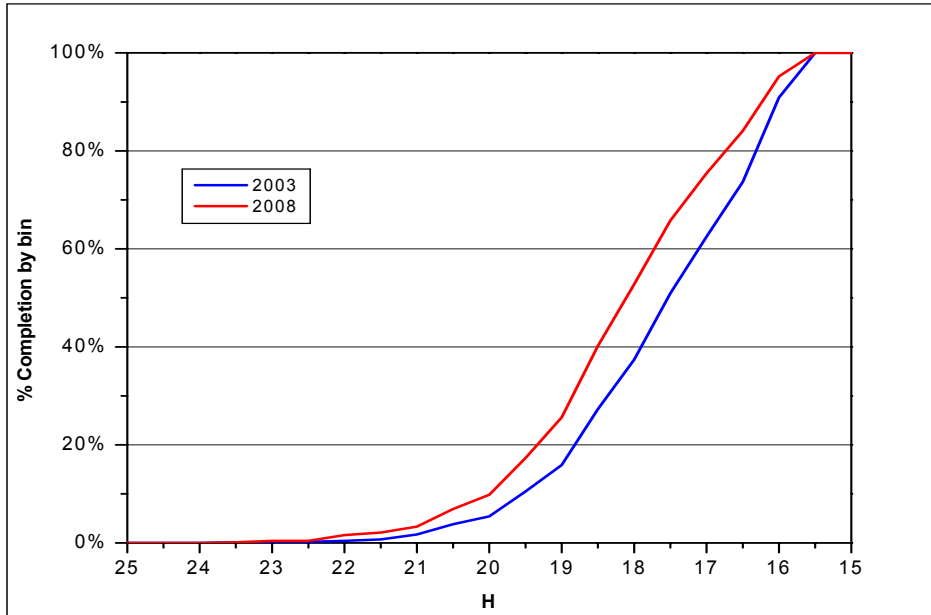


Figure 6-2. Comparison of uniform, statistical distribution population of 20,000 PHOs versus a complete model of 470,000 PHOs.

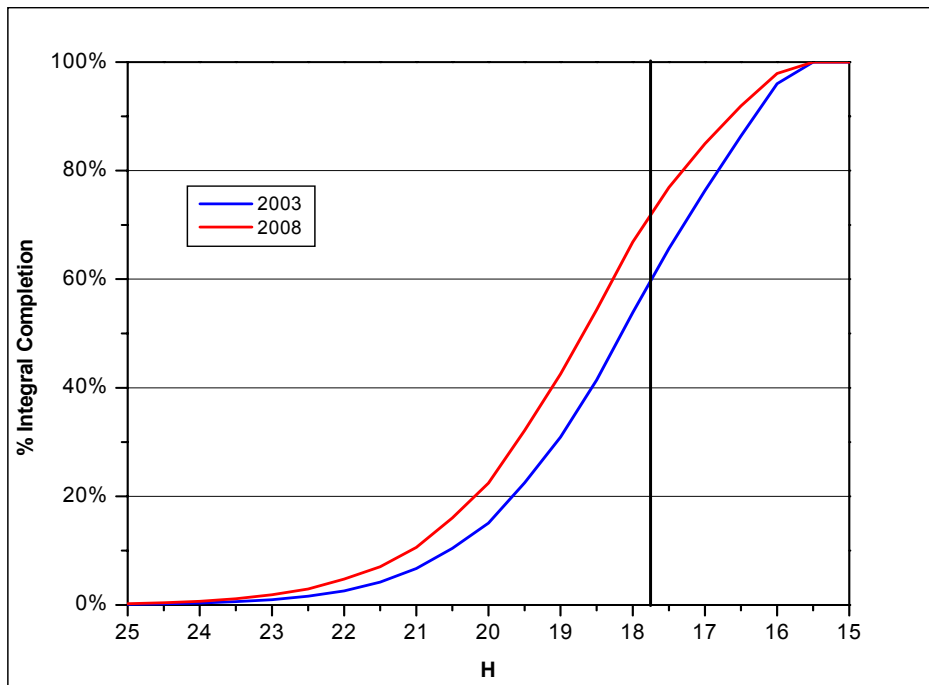
6.1.3.1.2 Establishing a Baseline

Switching to a uniform, statistical model as the input population is, in general, beneficial to the simulation. However, it makes establishing a baseline population more challenging. To assess the performance of each of the systems under consideration, it is necessary to assess the ability of each system to add to the current catalog of known PHOs. That requires establishing a set of PHOs that represents the currently known catalog, and a set of undiscovered PHOs.

To establish the catalog, the first step was to estimate the current completion rate for each data bin based on our population estimates and the known catalog (JPL, 2003). Figure 6-3(a) shows the estimate for the bin-by-bin percent catalog completion as of January 2003. Figure 6-3(b) shows the same information converted to integral completion. The conversion to integral completion puts the performance measure in the same terms as the Spaceguard goal that was stated as the discovery of 90% of NEOs with diameters larger than 1 km in 10 years. Assuming $H = 17.75$ corresponds to a diameter of 1 km, this plot estimates that we are currently at 60% completion for PHOs with diameters larger than 1 km.



(a) Bin by Bin Completion



(b) Integral Completion

Figure 6-3. Baseline catalog as of 2003, and estimated for 2008. Shown with (a) bin-by-bin completion and (b) integral completion with Spaceguard goal indicated.

To establish a simulated catalog for 2003, a LINEAR-like system, with a LINEAR-like search pattern, was simulated in FROSST and run for 20 years. The first n objects detected with the LINEAR-like system in each bin were determined to be the n objects making up the simulated

catalog. For example, with the $15.5 < H < 16.0$ bin, the first 909 objects detected by the simulation make up the baseline catalog, and the remaining 91 objects represent the undiscovered PHOs. The effect is that objects in the simulated baseline catalog were, in general, the easiest to detect and those with higher inclinations, larger eccentricities, or inner-Earth orbits are more likely to remain undetected.

If a decision were made in 2003 to implement a next generation asteroid search system, the acquisition process would take approximately 5 years. During the acquisition period, the existing search systems would continue to operate. Rather than use the 2003 simulated catalog as a baseline for system performance assessment, and thereby give the proposed systems credit for reducing impact risks that would have been handled by the existing systems, the baseline for the performance assessment was moved to 2008. The 2008 baseline was determined by extending the simulation of the LINEAR-like system for 5 additional years. It is acknowledged that there are likely to be search systems developed or enhanced over the next 5 years that will be able to achieve more than LINEAR's current capability. However, details of those systems are not known at this time and hence our simulations assume that only the current surveys will continue as is. The resulting 2008 baseline is also shown in Figures 6-3(a) and (b).

6.1.3.2 Warning of Impactors

Any model representing the actual PHO population does not contain enough potential impactors to accurately assess the capability of a system to warn against them. To reasonably assess a system's warning efficiency, a population of 990 impactors was used (Chesley and Spahr, 2003). All of the simulated impactors in this population had impact dates spread across a one year period. To assess the warning efficiency of the systems, the orbital elements for these objects were combined with a uniform distribution of absolute magnitudes for each 0.5 magnitude bin. The same 990 orbital elements are used in each bin, with only the absolute magnitudes varying bin-to-bin.

6.1.3.3 System Dependent Parameters

Many of the system dependent parameters added to FROSST, such as seeing degradation, were discussed in Section 6.1.2 as part of the algorithmic enhancements. Other new system dependent parameters are primarily associated with the sensor and camera and are necessary to accurately model the sensor sensitivity and effect of the sky brightness due to the Moon. For each system, the parameters were expanded to include the quantum efficiency, quantum efficiency variation, straddle factor, zenith sky brightness with airglow, dark current, dark current variation, system noise, and point spread function, to name a few.

6.1.3.4 Search Patterns

To model asteroid search systems over 10 years, it's necessary to automate the search pattern. Ground-based systems require the flexibility to adapt to weather outages, weather patterns, and seasonal variations in the search time available. Space-based systems need not adapt to weather and season, but the search patterns must account for the moving observation platform. Both types of systems need to be optimized for balance between depth of search and sky coverage.

In addition, search systems must have an observational cadence to support cataloging without depending on other systems to provide the necessary follow-up observations. It was decided that a reasonable criteria for cataloging is detection of an object two times in a seven-day period, and three times in a twenty-one day period (see Section 5.5).

6.1.3.5 Search Patterns for Ground-Based Systems

The automated search pattern generator must be flexible enough to incorporate the basic ideas presented in Section 5. The search pattern generator must be able to cover the ecliptic region, the near-Sun regions (while avoiding the Moon), and the full range of accessible latitudes. It must also allow wide longitude excursions from opposition, longitudes near opposition avoiding the stationary spots, or any combination of these regions. The search pattern generator must also be flexible enough to support various observing cadences and allow trade studies of depth and sensitivity for coverage.

6.1.3.5.1 Automation

At the beginning of each simulated observing day, the automated search pattern generator determines the available time for search simulation between astronomical twilight and daybreak. Given the minimum elevation constraint for the system (typically 30 degrees), beginning and ending search times, and a chosen declination, the algorithm determines the minimum and maximum right ascension (RA) accessible, and therefore, the maximum accessible search area for the night. Taking into consideration the step-and-settle time, the read time, and the field of view of the system, the integration time is computed. If the resulting integration time is less than the minimum desirable integration time, the search area for the night is reduced by symmetrically reducing the RA extent. If the resulting integration time is larger than the minimum, then the larger integration time is used, thereby increasing the sensor sensitivity.

To address the near-Sun search regions, the first and/or last hour of the nightly search is dedicated to searching +/- 10° from the ecliptic, as close to the Sun as possible given the location of the ecliptic, minimum elevation angles for the system (typically 25-30 degrees), and astronomical twilight and daybreak. The phase of the Moon determines whether the near-Sun regions are searched near twilight, daybreak, or both. In a typical 28-day lunation, both regions are searched 18 days, twilight-only for 5 days, and daybreak-only for 5 days. The time not spent searching the near-Sun regions is allocated by maximizing the RA extent of the search area given

a minimum integration time. As the minimum integration time is increased, the RA extent of the search is decreased, and it is possible to decrease the RA extent to the point of avoiding the stationary spots as defined in Chapter 5.

6.1.3.5.2 Cadence

If the cataloging of PHOs, not just detecting PHOs, is the primary measure of success, then setting a cadence and revisit rate is just as important as determining the optimal regions of sky to search. Search patterns were developed for this study with the 2 detections in 7 days and 3 detections in 21 days cataloging requirement. Full-sky coverage rates of once every five days, once every three days (only for 1m system with 11 sq deg field of view), and once every 8 days were chosen. The search pattern with a coverage rate of once every 8 days was implemented in a way that allowed cataloging by covering half of the available sky in 4 days, repeating that coverage, then covering the other half of the sky in 4 days, and repeating that coverage.

In general, search patterns with a longer repeat rate, have longer integration times and are therefore more sensitive. Area of sky covered is traded with depth of search by way of integration time. While increased sensitivity increases the total number of unique detections, increased coverage increases the total number of detections. Since cataloging is the primary figure of merit for this study, there are trades to be made to determine a near optimal search pattern for each system.

6.1.3.5.3 Search Pattern Effectiveness Results

For this study a wide variety of search patterns were tested. After initial tests, the search strategies were narrowed down to five basic patterns with slight differences for each of the 4 ground-based systems due to the differing step-and-settle times and fields of view. These are shown in Table 6-1. Note that the 8m system has significantly less coverage capability than the other systems due its smaller field of view (2.9 sq deg) and longer step-and-settle time (8 sec). Therefore, it was not feasible to implement all 5 of the strategies for the 8m system.

Table 6-2 shows the effectiveness for each of these basic search patterns for four ground-based systems. The time frame is 10 years and the population is 20,000 objects. The top 4 rows show the area searched with each method. The next 4 rows show the number of detections for each system and method. The next 4 rows show the number of unique detections. The bottom 4 rows show the number of new correlated detections assuming the 2 detections in 7 days and 3 detections in 21 days cataloging requirement, and not counting asteroids already in the baseline catalog.

Table 6-2 illustrates the importance of a well-tuned, well-planned search strategy. Some strategies significantly outperform others. However, the top performing search strategies only differ by 1.5% or less for all systems when considering the number of unique asteroids and the number of newly cataloged asteroids. While it is certain that none of these search strategies provide the ultimate, optimal strategy that is attainable only by additional time and layers of

fidelity, these strategies are certainly reasonable and have been tuned to a point of diminishing returns. For the remainder of the study, the best performing search strategy determined for each system is the basis for all comparisons.

Table 6-1. Search Strategies

	PATTERN NAME	ATTRIBUTES
A	All-sky, short integration time	Integration time ~5-7 seconds Centered on opposition. As large an RA extent possible given system constraints Results in 5 day repeat (3-day for 1m)
B	All-sky, long integration time	Integration time ~10-12 seconds Centered on opposition. As large an RA extent possible given system constraints Results in 8 day repeat (5-day for 1m)
C	Near-Sun, short integration time	Morning/evening, low solar elongation, ecliptic 1-hour search Remaining time like all-sky short integration time 5-day repeat for all-sky aspect (3-day for 1m) Reduced RA extent due to near-Sun time
D	Near-Sun, long integration time	Morning/evening, low solar elongation, ecliptic 1-hour search Remaining time like all-sky long integration 8-day repeat for all-sky aspect (5-day for 1m) Reduced RA extent due to near-Sun time
E	Near-Sun, no stationary points	Morning/evening, low solar elongation, ecliptic 1-hour search Remaining time similar to all-sky long integration 5-day repeat for all-sky aspect (3-day for 1m) Significantly reduced RA extent due to near-Sun time and 5-day repeat

Table 6-2. Search Pattern Effectiveness

System	FOV	A	B	C	D	E
<i>Area Searched (sq deg)</i>						
1m	11.1 sq deg	17,161,607	10,200,045	15,610,175	9,841,211	11,604,386
2m	4.4 sq deg	9,358,703	5,895,009	8,653,066	6,018,969	6,768,708
4m	4.4 sq deg	8,367,428	5,660,280	7,678,610	5,756,198	6,170,076
8m	2.9 sq deg	2,949,719	2,766,002	2,871,631	2,736,779	--
<i>Total Detections</i>						
1m	11.1 sq deg	886,780	609,013	916,878	696,980	734,838
2m	4.4 sq deg	587,317	460,354	695,377	607,438	597,418
4m	4.4 sq deg	654,585	549,139	811,188	737,840	715,552
8m	2.9 sq deg	285,655	289,920	479,974	481,841	--
<i>Unique Asteroids</i>						
1m	11.1 sq deg	12,908	12,765	12,762	12,618	12,492
2m	4.4 sq deg	13,427	13,477	13,415	13,433	13,294
4m	4.4 sq deg	14,504	14,828	14,643	14,779	14,586
8m	2.9 sq deg	14,270	14,375	15,106	15,125	--
<i>New Cataloged Asteroids</i>						
1m	11.1 sq deg	6,282	5,190	6,194	5,361	5,979
2m	4.4 sq deg	5,692	4,245	6,030	5,274	5,940
4m	4.4 sq deg	6,828	5,474	7,169	6,373	7,180
8m	2.9 sq deg	6,712	5,171	7,390	6,460	--

6.1.3.6 Search Patterns for Space-Based Systems

Automating the search patterns for a space-based system is, in general, much simpler than automating the search patterns for a ground-based system. Issues of variable night length and weather outages do not affect space-based systems. Furthermore, the longer settling times of the space-based systems (15 seconds), argue against trading sensitivity for coverage, especially given the already generous coverage available from a system that operates continuously. The optimal operating point for each of the space-based systems was determined to be the integration time at which 1 degree per day trailing losses begins to set in.

The most difficult space-based search pattern is for the Earth-orbiting system. A pattern must be determined that allows for access to all of the sky over a reasonable time period, yet avoids pointing at the Earth. The pattern chosen accomplishes this by dividing the satellite's orbit around Earth into four sections. The assumption is that during the first pass through section one of orbit one, the satellite will visit the same piece of sky two times. One satellite orbit later, the same piece of sky will be visited two more times, resulting in 4 revisits of that piece of sky over a two-orbit period. Each of the four sections of the orbit is planned independently.

A single search strategy was used for all space-based cases. For each case the sky was divided into four quadrants centered on opposition. Each quadrant was scheduled independently from the others – this was instrumental to the LEO search and had no effect on the L₂ or Venus-

trailing orbit. The first tile was placed at the apex of the quadrant near opposition, and the size of the tile was determined by the field-of-view of the system. The following tiles were placed as if filling concentric rings centered on opposition until the final tiles were laid in a ring 45 degrees from the Sun. For the 0.5m system, this pattern could be accomplished in 3-4 days. For the 2m systems the pattern took 9-10 days. Thus, to support the cataloging requirement, the first half of the pattern was completed then repeated before proceeding to the second half of the pattern which was then completed and repeated.

The ground-based systems all have a 5 revisit per night assumption, and the above space-based search pattern results in 4 revisits per night. However, part of the incentive behind a 5 revisit per night assumption is that variable atmospheric conditions, reduced seeing conditions adding to resolution difficulties between asteroids and stars, and occasionally less than optimal pointing constraints for some fields results in lost fields. In space, there are no atmospheric conditions, better seeing, and fewer pointing issues like minimum elevations and large air masses. The easier environment, combined with the benefit of parallax due to the orbiting platform, justifies the use of 4 revisits in space for Earth-orbiting systems versus 5 revisits from the ground.

6.1.4 Outputs

The output from FROSST is a list of detections including object number, location, velocity, absolute magnitude, apparent magnitude, sensor that made the detection, and the sensor sensitivity at the time of detection. The detection list is then reduced to a list of cataloged objects with 2 detections within 7 days and 3 detections within 21 days. The cataloged objects are binned according to absolute magnitude. A percent completion is computed for each bin based on the number of objects in the bin versus the number of objects cataloged.

The Spaceguard goal is the discovery of 90% of all near-Earth objects larger than 1 km within 10 years. Given the precedence of defining a goal and assessing performance in terms of “all objects larger than”, an effort has been made to convert the percent completion numbers for each bin into integral completion numbers. In our plots showing the cataloging capability of systems, the curves show the percent integral completeness (i.e., completeness for all objects larger than the given size).

Converting the warning efficiency capability to a similar scale is a moving target since warning only applies to uncataloged objects. As systems approach 100% completion for cataloging objects of a particular size, no warning is required for objects of that size. Since the population for which warning is applicable is not constant, an integral completion is not feasible. All warning efficiency numbers are determined bin-by-bin.

6.2 Validation and Comparison to LINEAR Data

The FROSST simulation was developed to study proposed space surveillance networks. The simulation has been widely used and proven to be robust and reliable. However, before proceeding with the use of the enhanced FROSST simulation, a thorough effort was made to

validate the software. Validating the ground-based system model was the most straightforward. The two LINEAR telescopes were simulated and a comparison was made between the FROSST predictions and the actual LINEAR experience. Since there are currently no space-based asteroid detection systems with which we can do a comparison, the validation of the space-based system model involved extrapolating the ground-based performance to space and employing a piecewise validation.

While the LINEAR observing experience was used to enhance FROSST via statistics, at no time were actual LINEAR detection algorithms, search fields, or operational parameters used in FROSST. The LINEAR system was simulated in the same manner as all the candidate systems. The sensitivity curves that serve as the primary sensor definition in FROSST were derived from first principles. No adjustments were made based on measured LINEAR performance. The time period for which the comparison is made is a 16-month period from late 2001 to early 2003 during which time there were no significant variations in the LINEAR hardware, processing, or operations plan.

6.2.1 Populations Used For Comparison

Comparing the predicted performance of LINEAR with the actual performance is not as straightforward as it might seem. The performance measure for the comparison is the detections of NEOs. However, when LINEAR makes detections, it is not known if the object is an NEO, a main belt asteroid, or something else. The observations are sent to the Minor Planet Center (MPC) where orbit determinations are performed. While the MPC does a remarkable job, there are NEOs that do not have enough observations to determine any orbit, nor enough to differentiate between an NEO and a main belt orbit. Many objects that go on the MPC confirmation page are never confirmed. The net effect is that not as many NEOs are cataloged as NEOs as could be possible. The objects least likely to have sufficient follow-up and confirmation are the small, fast-moving objects. If an object has already been cataloged, the chances of it being recognized as an NEO are greatly enhanced. For this reason, it was decided to use two different populations for validating the FROSST performance. These included the list of already cataloged NEOs, and the modeled NEO population out to $H=22$. The use of the already cataloged NEOs avoids the issue of follow-up and the confirmation of primarily small, fast-moving NEOs. The use of the modeled population shows the degree of agreement with the actual data and supports the use of this population model for all the candidate system simulations.

6.2.2 Detected Velocity Distribution

Figure 6-4 shows the velocity distribution of NEOs detected by LINEAR, and the velocity distributions of the FROSST predicted detections for both of the input populations. The peaks, shapes, and sizes of all three curves agree nicely.

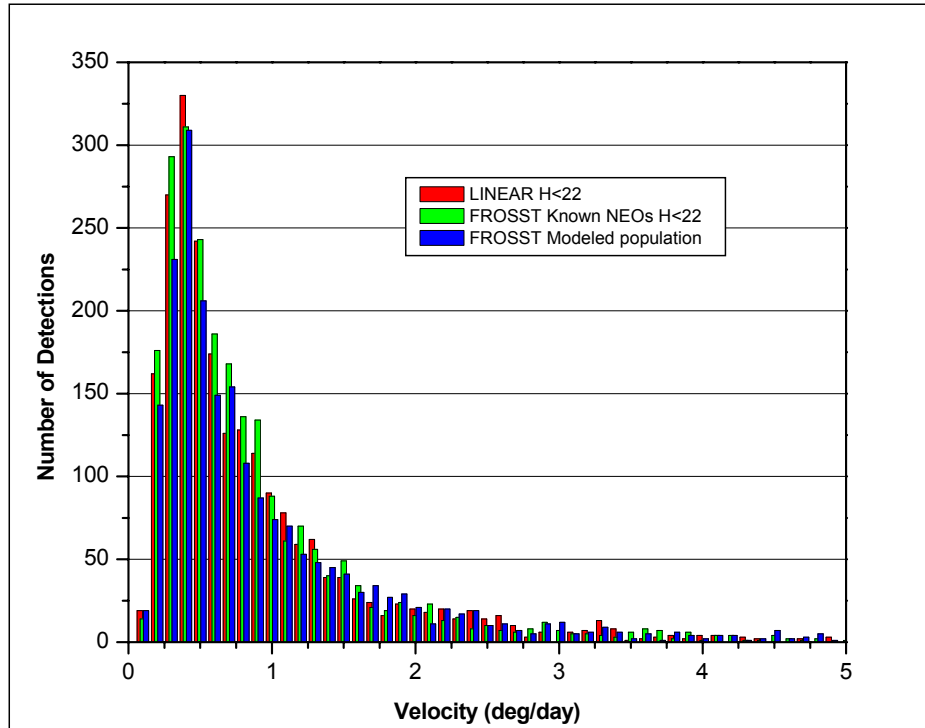


Figure 6-4. The apparent velocity distribution of actual NEO detections made by LINEAR, and simulated detections by FROSST for two different input populations: 2,182 cataloged NEOs and 24,563 modeled NEOs.

6.2.3 Apparent Magnitude Distribution

Figure 6-5 shows the apparent magnitude distribution of NEOs detected by LINEAR, and the apparent magnitude of the FROSST predicted detections for both of the input populations. The double peak in the distribution corresponds to the peaks of the two LINEAR telescopes. While the two telescopes are essentially the same, they are not operated the same and on a given night, rarely have the same limiting magnitude due to the differences in operation.

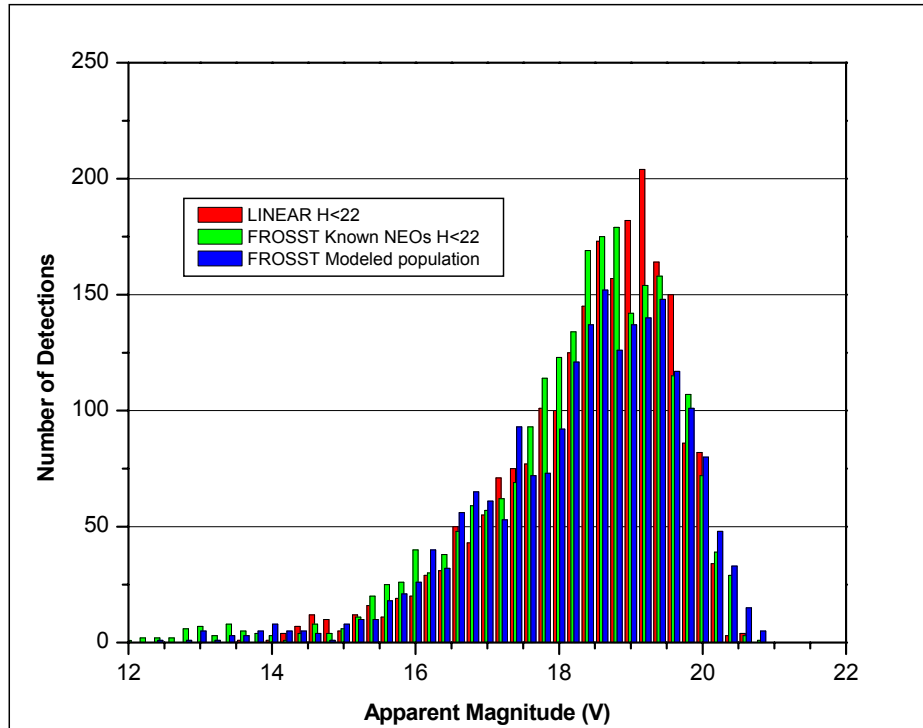
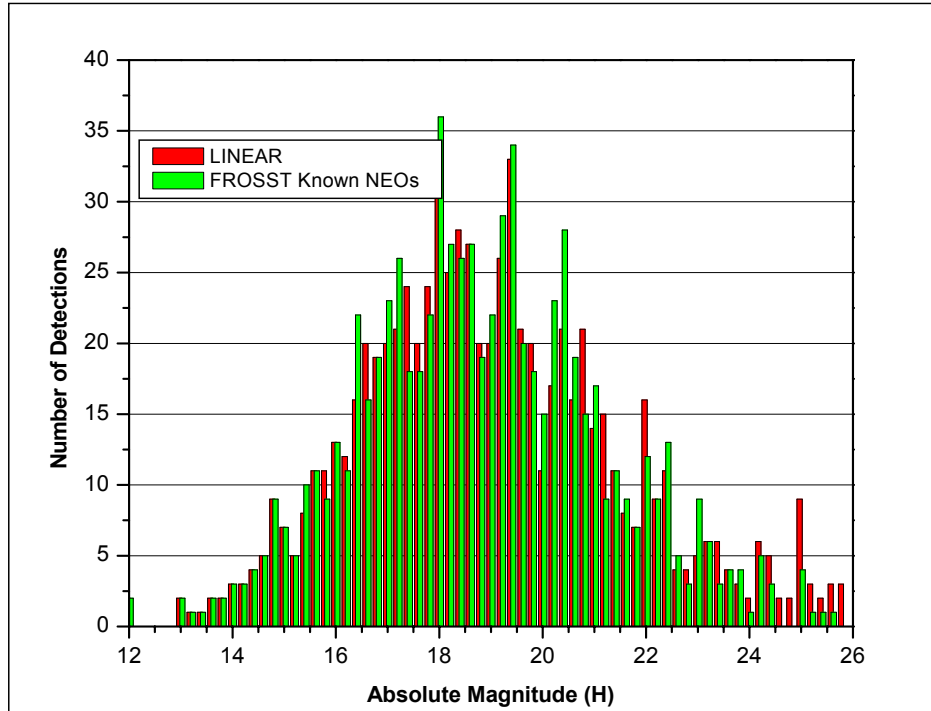


Figure 6-5. *The apparent magnitude distribution of actual NEO detections made by LINEAR, and simulated detections by FROSST for two different input populations: 2,182 cataloged NEOs and 24,563 modeled NEOs.*

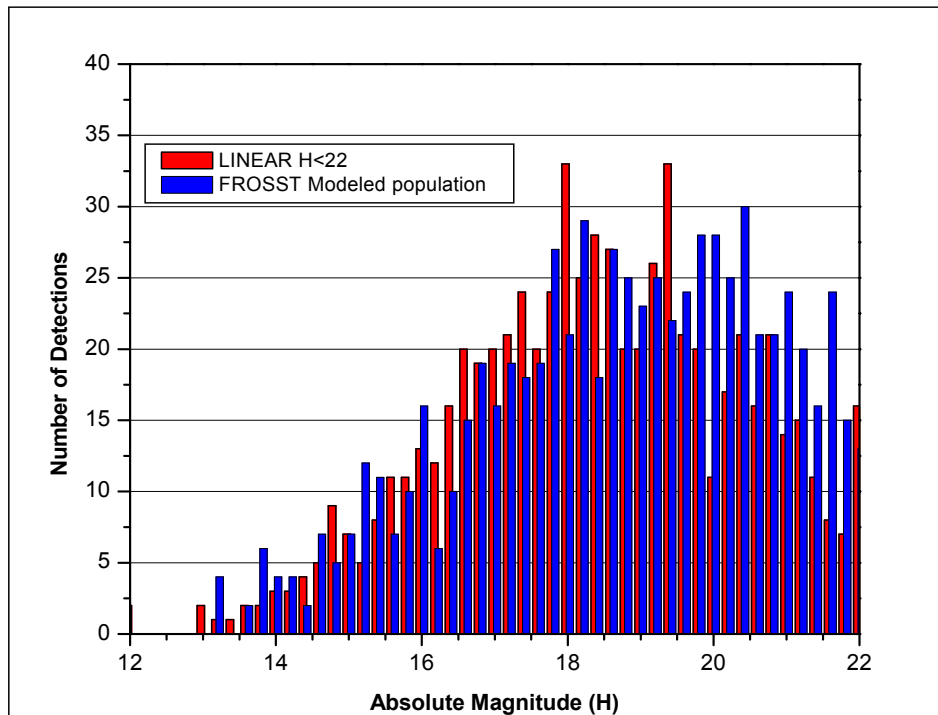
6.2.4 Absolute Magnitude Distribution

Figure 6-6(a) shows the absolute magnitude distribution of NEOs detected by LINEAR and the absolute magnitudes of the FROSST predicted detections. The input population of currently known NEOs was used. Figure 6-6(b) corresponds to the modeled input population. The only significant divergence in these curves occurs as H gets large; FROSST predicts higher detection capabilities than LINEAR realized. This divergence is due to the aforementioned inability to flag all of LINEAR's actual NEO detections, especially those smaller, faster-moving objects.

Note that this issue of follow-up and confirmation is a different issue for LINEAR than is for the candidate systems in this study. The current operations model for LINEAR relies on second party observers to provide follow-up and confirmation for many of the LINEAR discoveries, while the candidate systems are simulated to have a cadence that provides self-follow-up by providing full-sky repeat coverage. Divergence between the simulation and the actual LINEAR experience for small, fast moving objects does not imply that the simulation for the candidate systems will also diverge from reality for such objects.



(a) All LINEAR detections compared to FROSST and known NEO population.



(b) LINEAR detections of $H < 22$ compared to FROSST and modeled population.

Figure 6-6. The absolute magnitude distribution of unique detections of actual NEOs made by LINEAR, and simulated detections by FROSST for two different input populations: a.) 2,182 cataloged NEOs and b.) 24,563 modeled NEOs.

6.2.5 NEOs Detected

Table 6-3 lists the number of NEO detections made by LINEAR along with the number predicted by FROSST given the input population of currently known NEOs, and given our modeled input population. In addition to total detections, the number of unique detections is listed. The simulation comes within 3% agreement with the actual performance when using the cataloged NEOs as the input and within 5% agreement when using the population model described in Section 2 down to $H < 22.0$.

Table 6-3. Comparison of actual detections made by LINEAR and simulated detections by FROSST for two different input populations: a) 2,182 cataloged NEOs and b) 24,563 modeled NEOs

Case	H limits	Detections	Unique Detections
LINEAR detections	None	2406	772
FROSST (cataloged NEOs)	None	2480	761
LINEAR detections	$H < 22$	2259	675
FROSST (modeled population)	$H < 22$	2132	725

Again, note that the actual LINEAR observing experience was not duplicated. A model of the LINEAR system was used along with a statistical weather model. The simulation model did not look at the same parts of the sky on the same nights; therefore it is not possible to do an object-by-object comparison of the detections.

6.3 Results

The following sections present the results across a wide-range of comparisons for single ground-based and space-based systems, and for a number of networked systems. Two types of simulations were done for each case; assessments of the cataloging and the warning capabilities were carried out.

6.3.1 Performance Measures

6.3.1.1 Cataloging

Cataloging requires detection of the same object twice within 7 days and 3 times within 21 days. This requirement was derived after discussions centered on current experience at the MPC and the Jet Propulsion Laboratory NEO Program Office. This cataloging assumption has a significant effect on the overall performance of each system and makes repeat coverage a key parameter for success. In order to achieve full-sky coverage with a cadence that supports the cataloging requirement, the optimal operating points for the systems are generally found by trading some depth of coverage (i.e., sensitivity), for area by shortening the integration time. For each of the systems under consideration, a number of search strategies and operating points were

analyzed by simulation (see Section 6.1.3.5). The best search strategy and operating point for each individual system was chosen for the final comparisons shown in this report.

The cataloging performance measure is determined from the number of new objects added to the catalog each year for 10 years. The baseline catalog was defined earlier in Section 6.1.3.1.1. Figure 6-7 shows how a catalog grows over 10 years for a 4m telescope located on Mauna Kea. Each line in the plot corresponds to the integral completion of the catalog for sizes greater than H for a single year. For example, the Spaceguard goal of detecting 90% of all NEOs greater than 1km is achieved in year 2 on this plot. After 10 years, this survey is 90% complete for all objects larger than $H \leq 19.5$. As expected, the catalog grows rapidly during the first years of operation, and then the growth slows as fewer objects with apparent magnitudes accessible by the system remain uncataloged.

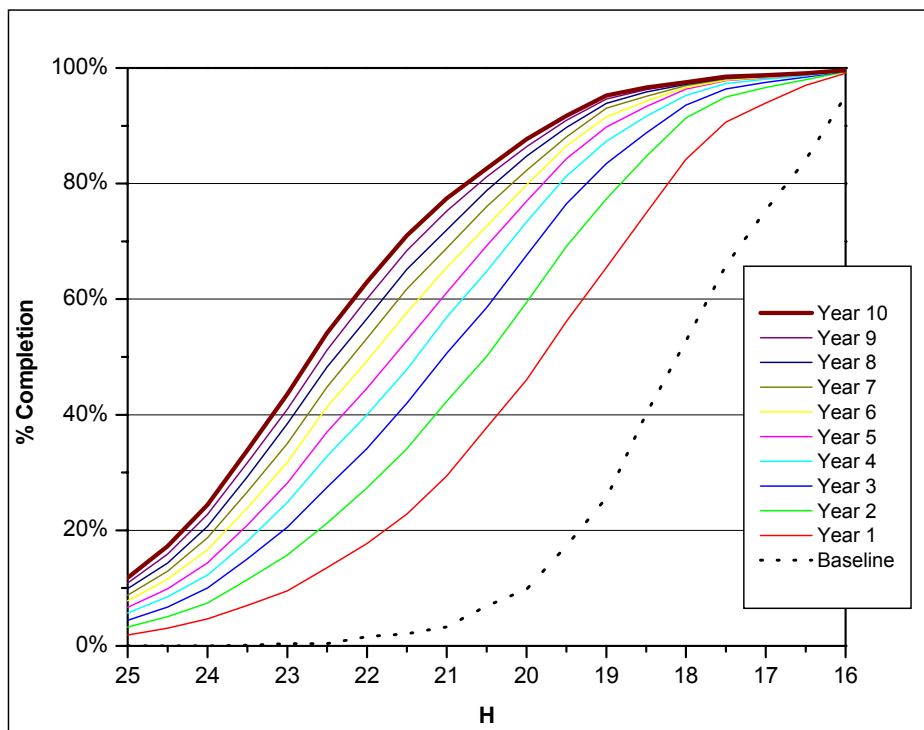


Figure 6-7. Growth of catalog over 10 years with 4m ground-based search system.

6.3.1.2 Warning

Warning is the ability to detect an impactor prior to impact and during its last orbital period. Warning efficiency for a system is defined as the percentage of objects warned against for each bin of data. The population used to assess the warning capability of a system was defined in Section 6.1.3.1.2.

The assumption in this study is that benefits due to warning only accrue for objects not yet cataloged. As the catalog grows, there are fewer objects to warn against. Given that the number

of objects to warn against is continually changing, it is not possible to state the warning efficiency in terms of integral warning, or warning against all objects greater than H. The warning efficiency is defined bin-by-bin.

6.3.2 Ground-Based Systems

6.3.2.1 Large Format CCD versus Small Format CCD

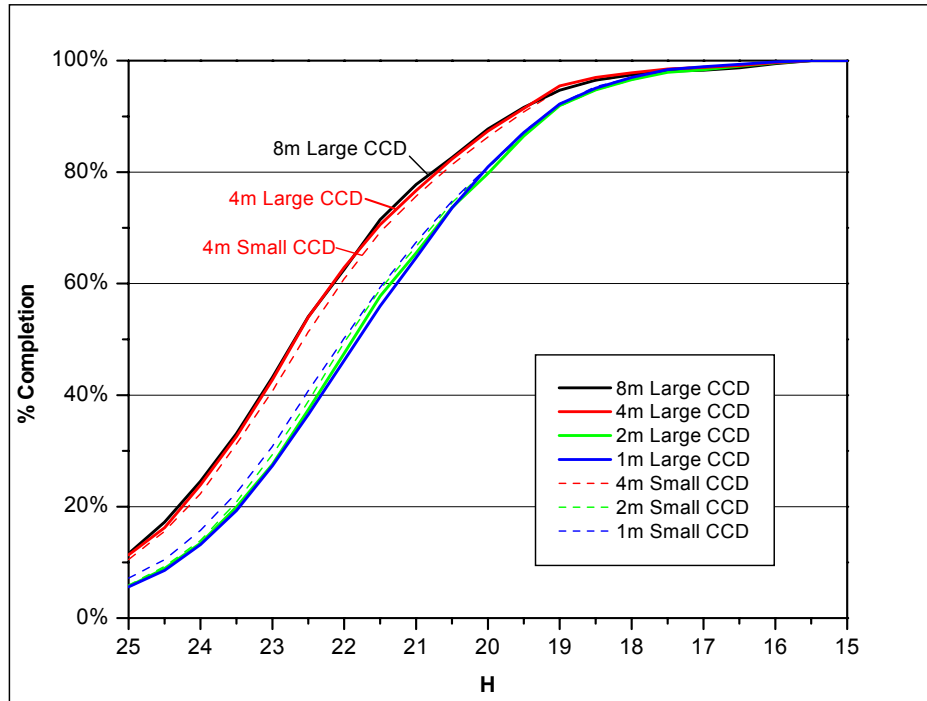
Two different CCD formats were considered for the ground-based systems in this study, as noted in Section 4. The large format CCD has 24K x 36K pixels covering the same focal surface as the small format CCD with 12K x 18K pixels. The large format CCD with smaller pixels is more optimally sampled and provides increased sensitivity compared to the small format CCD with larger pixels. However, the objects being imaged by this system are PHOs, which are frequently fast-moving objects. This occasionally puts the large format CCD with smaller pixels at a disadvantage due to trailing losses. Additionally, the four-fold increase in pixels also translates to increased costs due to increased manufacturing and data processing effort. Hence, both large and small format CCDs were considered.

The sensitivity advantage and trailing loss disadvantage for large format CCDs can be seen in Table 6-4. The total detections for the large format CCD systems exceed the total detections for the equivalent small format CCD systems. However, for some of the systems, the advantage disappears for unique detections and cataloged objects.

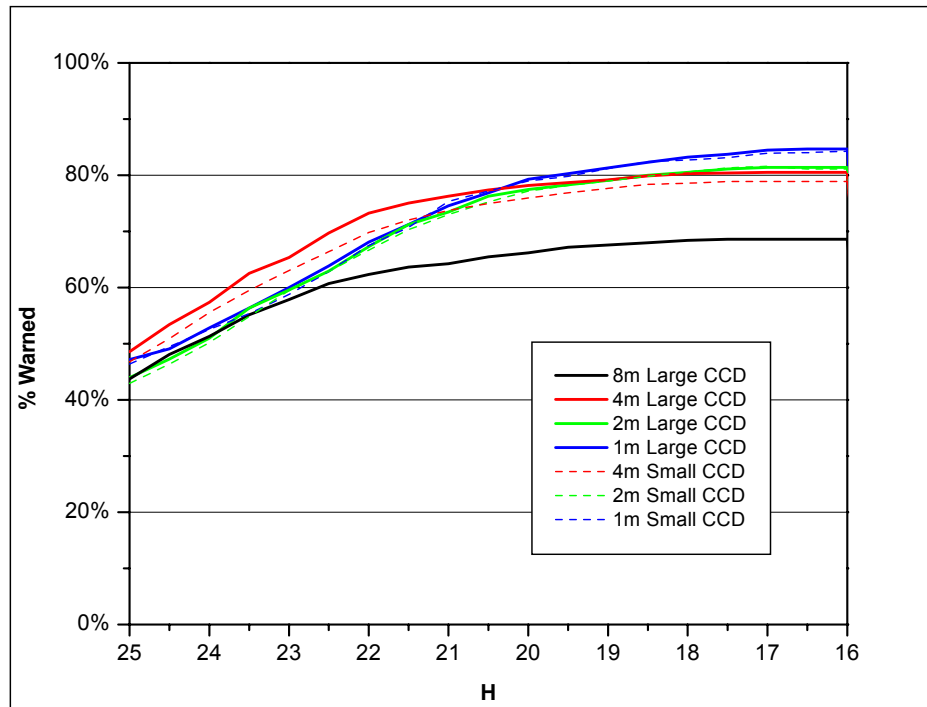
Table 6-4. Comparison of detections and correlations for same telescope with different focal planes.

Aperture	CCD	Detections	Unique Detections	Newly Cataloged PHOs
1m	24K x 36K CCD	918,550	12,312	5,883
1m	12K x 18K CCD	916,878	12,762	6,194
2m	24K x 36K CCD	699,530	13,188	5,902
2m	12K x 18K CCD	695,377	13,415	6,030
4m	24K x 36K CCD	867,625	14,650	7,355
4m	12K x 18K CCD	811,188	14,643	7,169

Figure 6-8(a) shows the 10-year overall cataloging capability for the 1m, 2m, 4m, and 8m large format CCD, and the 1m, 2m, and 4m small format CCD. Figure 6-8(b) shows the warning efficiency for the small format CCDs on telescopes with apertures of 1m, 2m, 4m, and 8m. There is no distinct difference between the 1m and 2m systems. This is due to the fact that the 1m has more than twice the field of view of the 2m system (11.1 versus 4.4 sq deg) and is only slightly less sensitive ($V_{lim} = 22.0$ versus 22.9 for a 7 second integration). While the 8m system has the best sensitivity, its smaller field of view (2.9 sq deg) and longer step-and-settle time (8 seconds) puts it at a disadvantage. For both cataloging and warning, the best performing system is the 4m with large format CCD followed closely by the 4m with the small format CCD.



(a) Cataloging capability.



(b) Warning capability

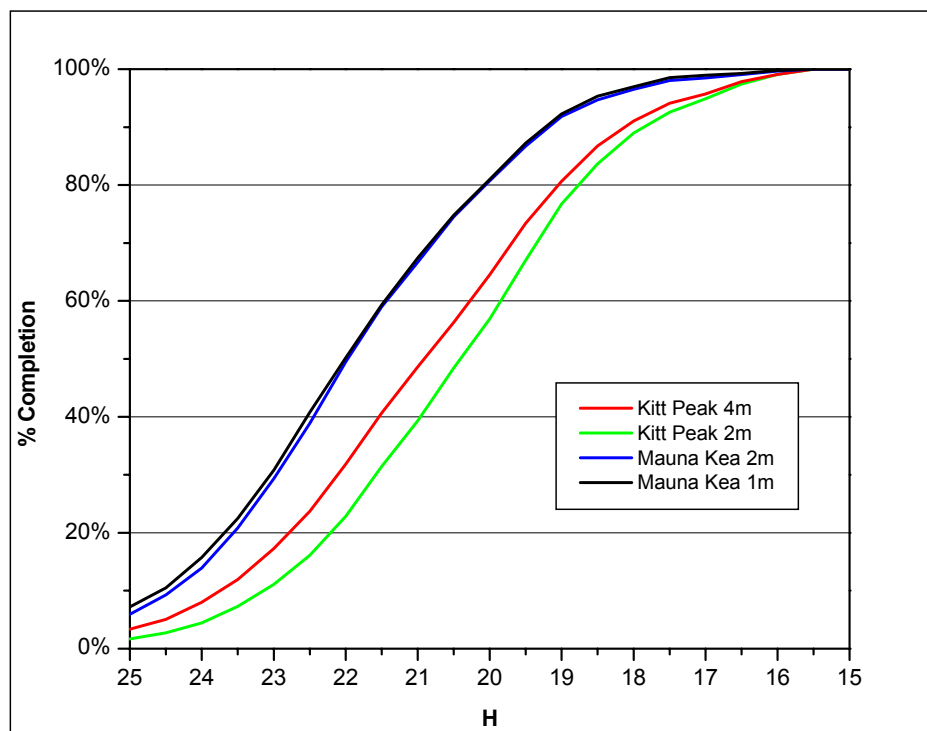
Figure 6-8. Comparison of (a) cataloging capability and (b) warning efficiency of 1m, 2m, 4m, and 8m ground-based systems, with both large format and small format CCDs shown for comparison.

6.3.2.2 Mauna Kea versus Kitt Peak

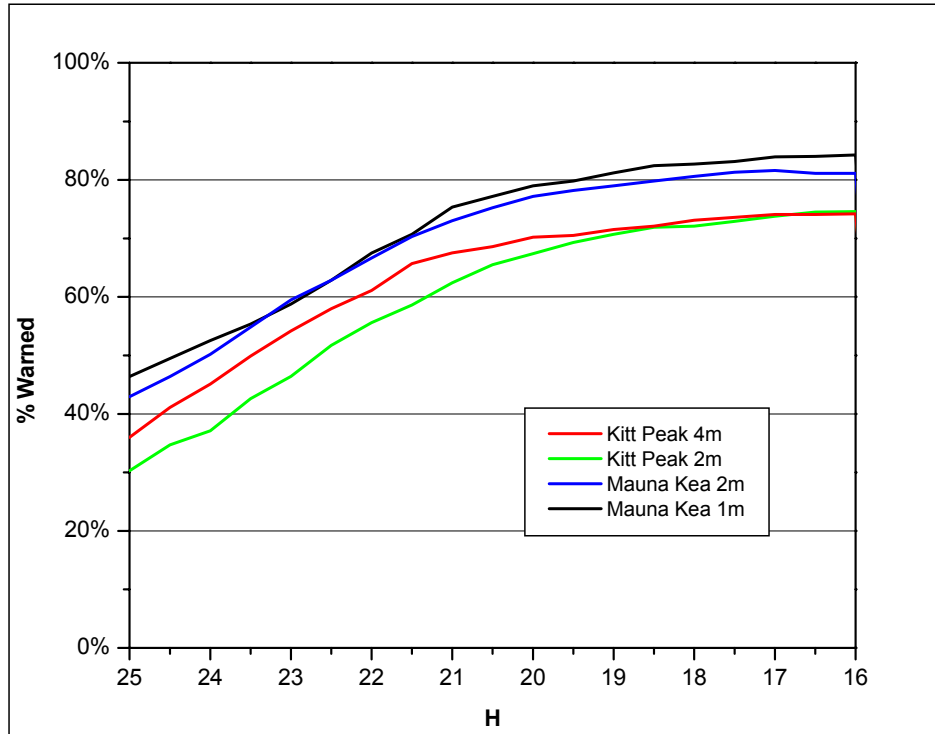
Mauna Kea is acknowledged as a premier site in the United States for locating a ground-based search system. The majority of the current asteroid search systems are located in the desert Southwest. It is assumed in some cost models that building in Hawaii is more costly than building in the Southwest. For this reason, consideration was given to locating a system in the desert Southwest with the logic that it may be possible to build a larger diameter telescope in the Southwest for a comparable amount of money as a smaller system in Hawaii.

There were two assumptions driving the performance results for this comparison. The seeing for Mauna Kea is assumed to be 0.6 arcsec while the seeing for Kitt Peak is assumed to be 0.9 arcsec. Both of these numbers are supported by reported experimental data. The percentage of nights lost to poor weather for the two sites is estimated to be 25% loss year round for Mauna Kea, and 20%, 50%, 20%, and 23% for spring, summer, fall, and winter, respectively, for Kitt Peak. The Mauna Kea numbers were estimated from general observer experience, and the Kitt Peak numbers were estimated from LINEAR's experience elsewhere in the Southwest.

Figure 6-9 shows the performance of a 2m and 4m system in the Southwest and a 1m and 2m system in Hawaii. The figure shows that the conditions are sufficiently inferior in the Southwest versus Hawaii as to negate the larger optics. The primary discriminator in this comparison is the telescope availability (i.e., the notorious Southwest Summer monsoon season takes a toll).



(a) Cataloging capability.



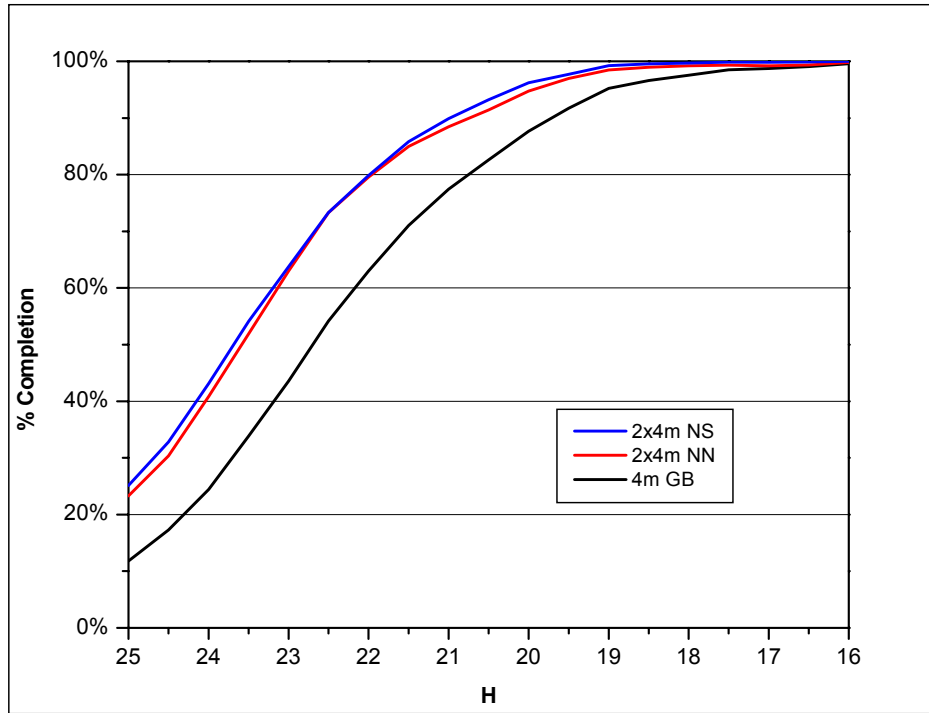
(b) Warning capability.

Figure 6-9. Comparison of (a) cataloging capability and (b) warning efficiency at Mauna Kea versus Kitt Peak.

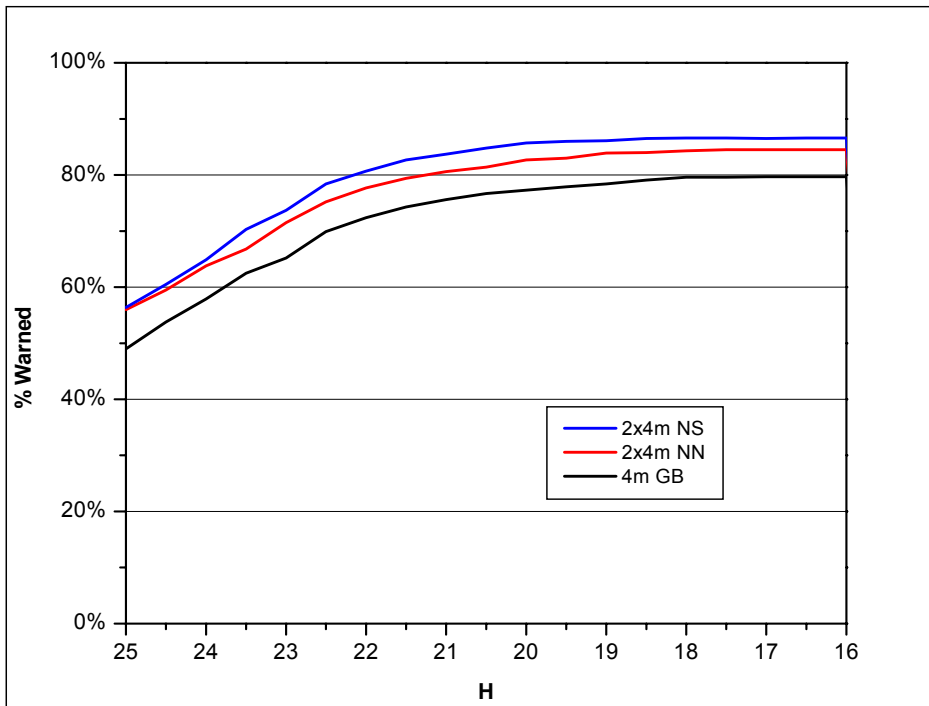
6.3.2.3 Dual Systems

The cases of two 2m telescopes and two 4m telescopes were considered. For each case, the possibility of collocating the systems at Mauna Kea were compared to the possibility of locating one system at Mauna Kea and one system in Chile. Total sky accessible to a dual hemisphere system is appealing – especially for warning. However, collocated systems are easier to coordinate, given that they experience the same weather patterns, and are less expensive to operate.

Figures 6-10(a) and (b) show the cataloging and warning capabilities of the 4 cases: collocated 2m and 4m systems in Mauna Kea and dual hemisphere 2m and 4m systems. Operating from two hemispheres has only a slight cataloging advantage over the course of 10 years, but a definite warning advantage. A single 4m system is also shown on the plot for reference. Both of the dual 4m systems provide a significant improvement over the single system.



(a) Cataloging capability.



(b) Warning capability.

Figure 6-10. Comparison of (a) cataloging capability and (b) warning efficiency for two 4m systems collocated in the northern hemisphere (2x4m NN), two 4m systems located one in each hemisphere (2x4m NS), and a single 4m system.

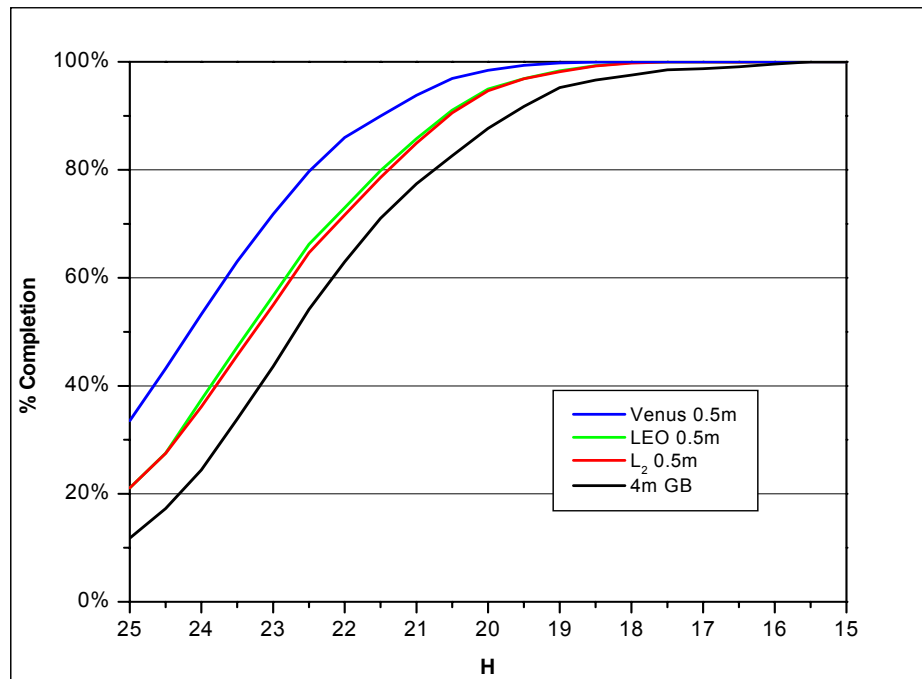
6.3.3 Space-Based Systems

Three general orbits and three different telescopes were compared, resulting in nine cases. The orbits are a low-Earth orbit (LEO), Sun-synchronous, at approximately 900 km; an L_2 orbit which is a satellite at the Earth's second Lagrange point 1.5×10^6 km from Earth at opposition; and a heliocentric orbit at about 0.7 AU modeled as a satellite at Venus's L_2 point. The last orbit is typically referred to as a Venus-trailing orbit or Venus-like orbit. For each orbit, telescopes of 0.5m, 1m, and 2m were modeled and assessed for cataloging and warning capability.

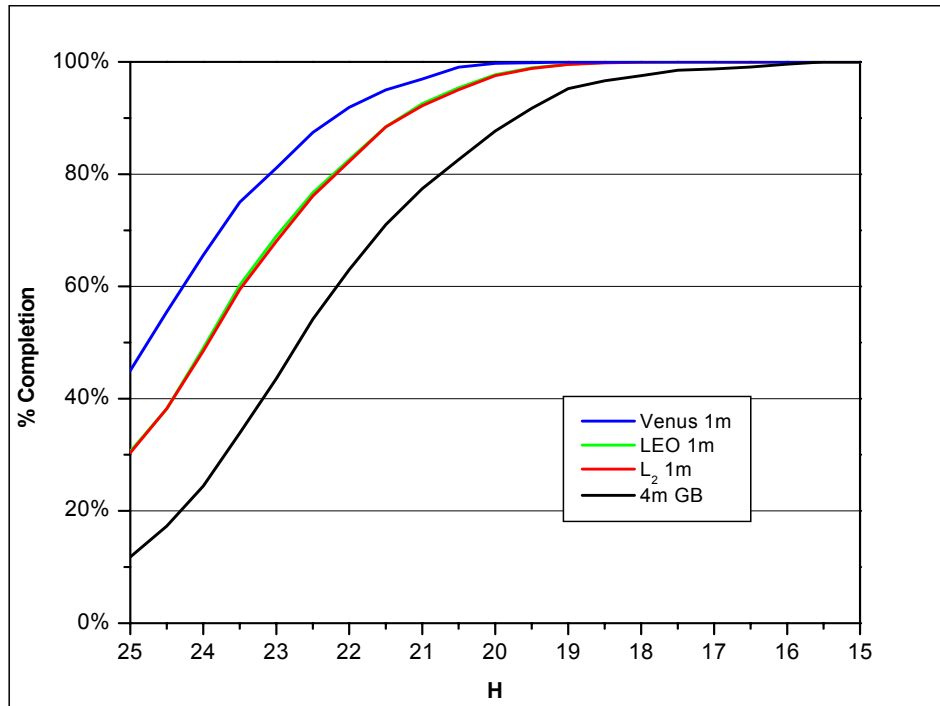
The space-based designs all offer a significant coverage advantage over the ground-based designs because of the 24-hour-a-day availability. There are no weather outages and no daylight hours to avoid. The same cataloging requirement of 2 detections in 7 days and 3 detections in 21 days applies to the space-based and ground-based systems, although no special effort was made to tune the space-based search patterns to an optimal cadence. All of the space-based systems have sufficient sky coverage to negate the need for special search strategies such as the near-Sun regions used for the ground-based systems.

6.3.3.1 Cataloging

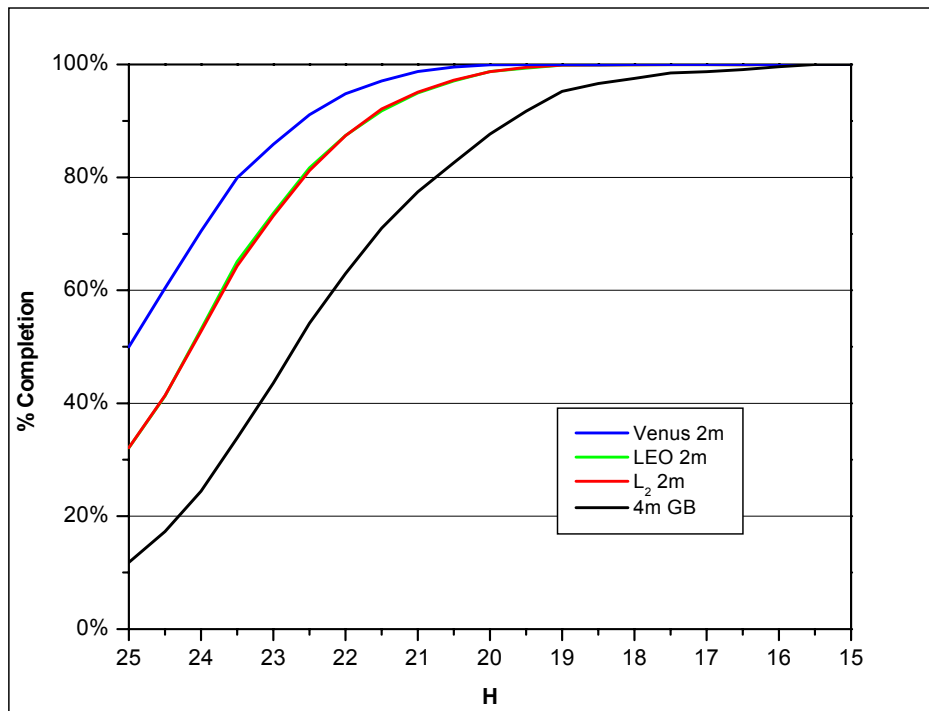
Figures 6-11(a), (b), and (c) show the cataloging capabilities of the different orbits for the 0.5m, 1m, and 2m systems, respectively. For a performance comparison, the 4m ground system is also included on the plots. Note there is no significant difference in the cataloging capability for the LEO and L_2 systems, while the system with the Venus-like orbit provides superior cataloging. That system benefits significantly from its phase-angle advantage.



(a) 0.5m space-based systems.



(b) 1m space-based systems.

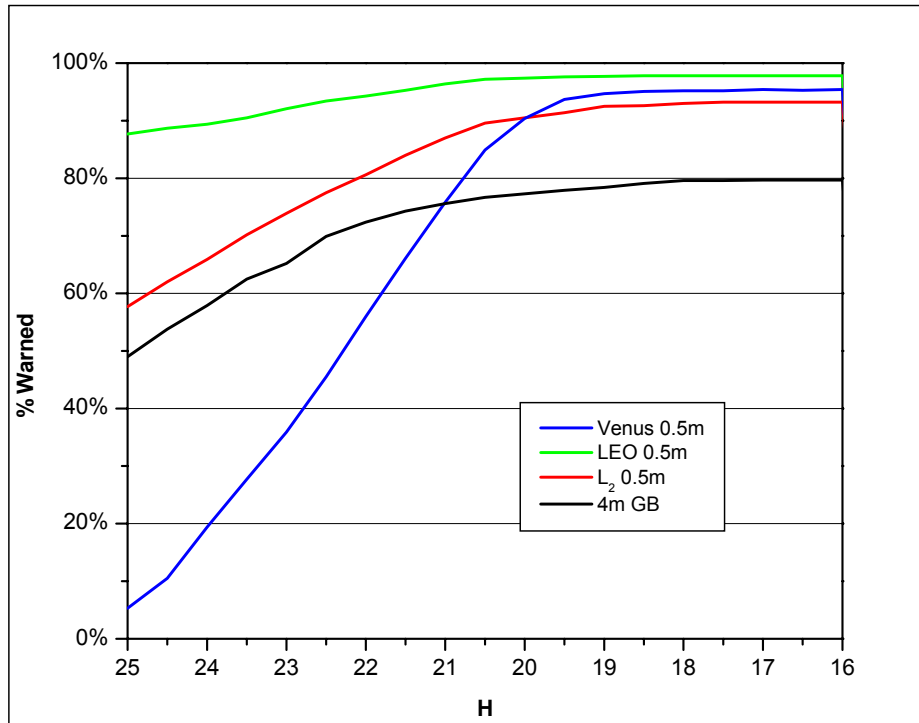


(c) 2m space-based systems.

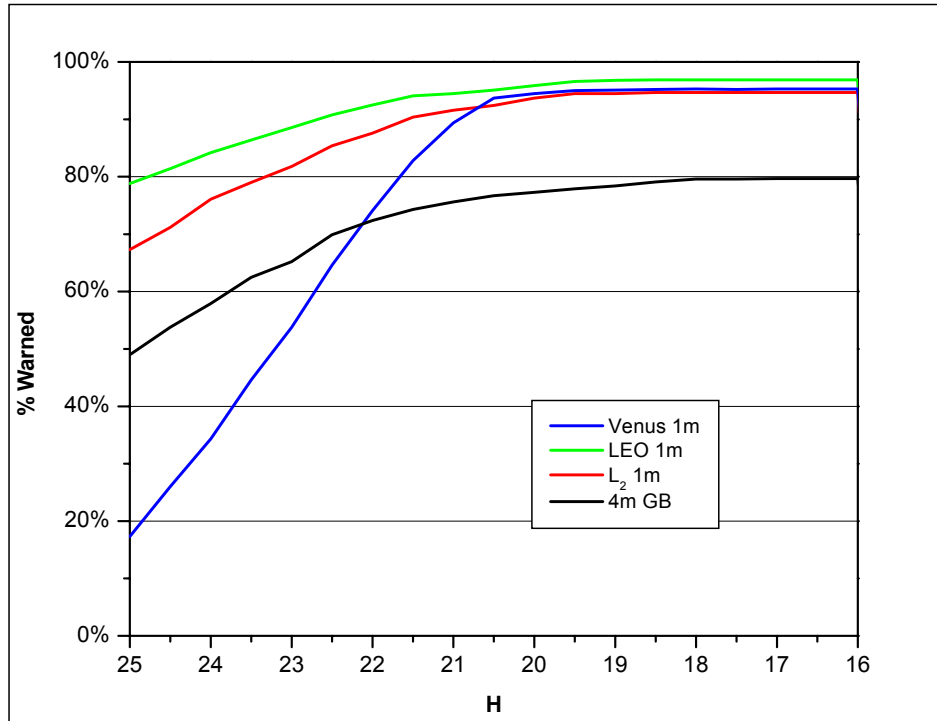
Figure 6-11. The cataloging capability of (a) 0.5m, (b) 1m, and (c) 2m space-based systems are shown for systems in orbits that are Venus-trailing, LEO, and at L₂. A 4m ground-based (GB) system is shown for reference.

6.3.3.2 Warning

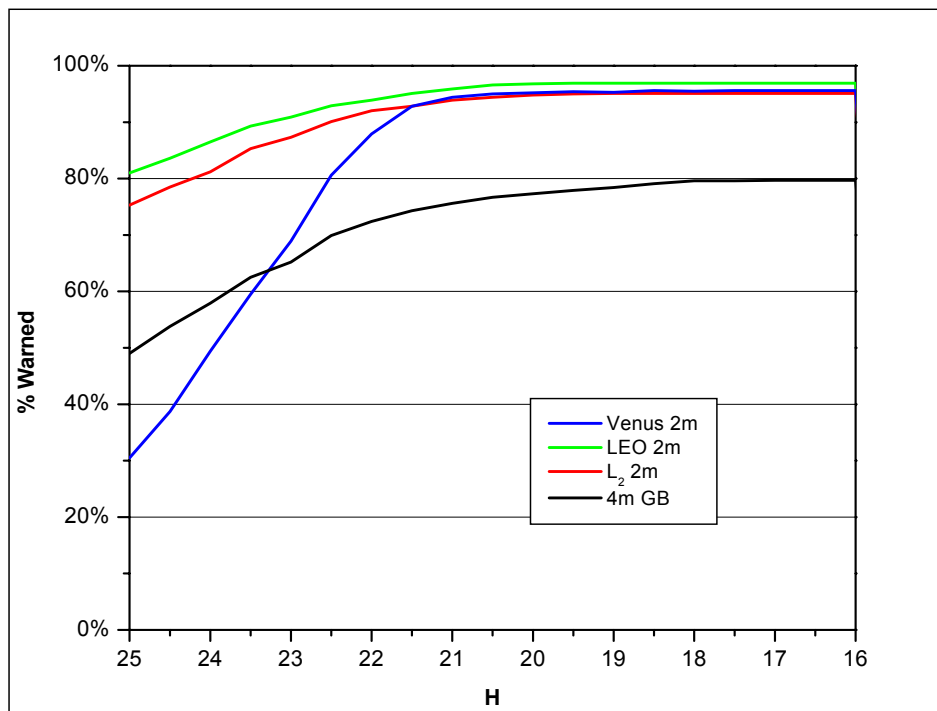
Figures 6-12(a), (b), and (c) depict the warning efficiency of the different orbits for the 0.5m, 1m, and 2m systems, respectively. Again, the 4m ground-based system is added to the charts as a reference. While the LEO and L₂ systems had similar cataloging capabilities, the LEO system is a better warning system than the L₂ system due to its proximity to Earth. The Venus-trailing system is an inferior warning system, primarily because of its great distance from Earth and the fact that it is on the opposite side of the Sun at times.



(a) 0.5m space-based systems.



(b) 1m space-based systems



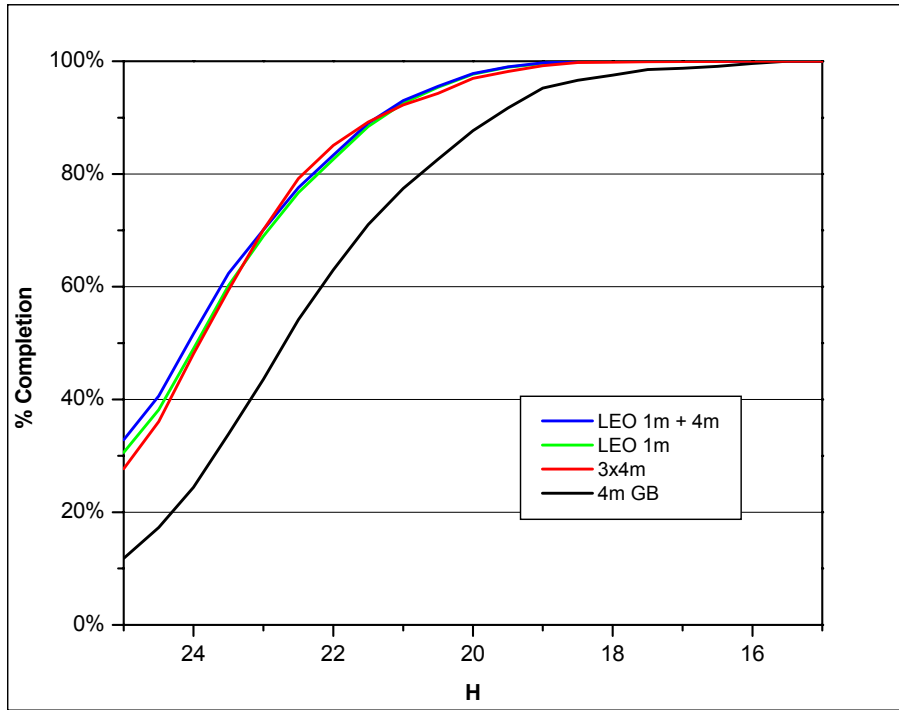
(c) 2m space-based systems

Figure 6-12. Warning efficiency of (a) 0.5m, (b) 1m, and (c) 2m space-based systems. A comparison is made for orbits that are Venus-trailing, in LEO, and at L2. A 4m ground-based system is shown for reference.

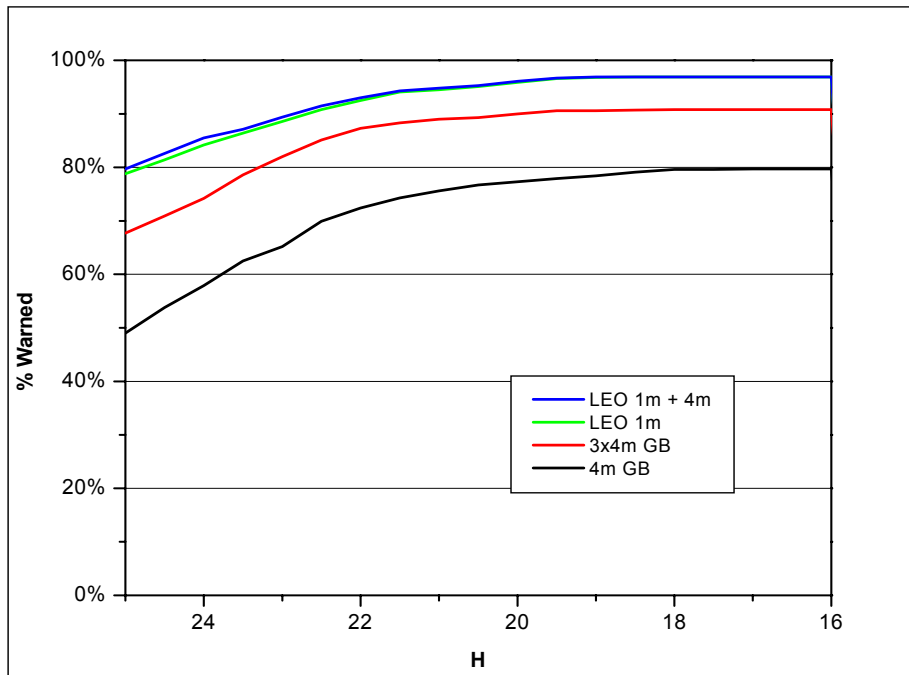
6.3.4 Networks

A number of networked systems were considered including purely ground-based networks along with ground-based and space-based combinations. The best performing ground-based system is a 4m telescope. A network of three 4m systems was simulated. Two telescopes were assumed to be collocated at Mauna Kea, and a third telescope was located in the Southern hemisphere in Chile. The search patterns for the three systems were coordinated and optimized to the cataloging cadence. The performance of the three 4m ground-based systems was similar to a single 1m LEO system. This is shown in Figures 6-13(a) and (b) along with a 4m ground-based system added to the 1m LEO system. Not surprisingly, the 4m does not significantly enhance the performance of the system. The 1m LEO system and the 4m ground-based system have similar strengths so the more capable of the two systems dominates.

The Venus-trailing system has superb cataloging capability but marginal warning efficiency. Both the 0.5m and 1m Venus-trailing systems were networked with a 4m ground-based system. The addition of the 4m ground-based system does not add significantly to the cataloging capability, but significantly enhances the warning capability of the system. Figures 6-14(a) and (b) show the efficiency curves for these Venus-trailing systems.

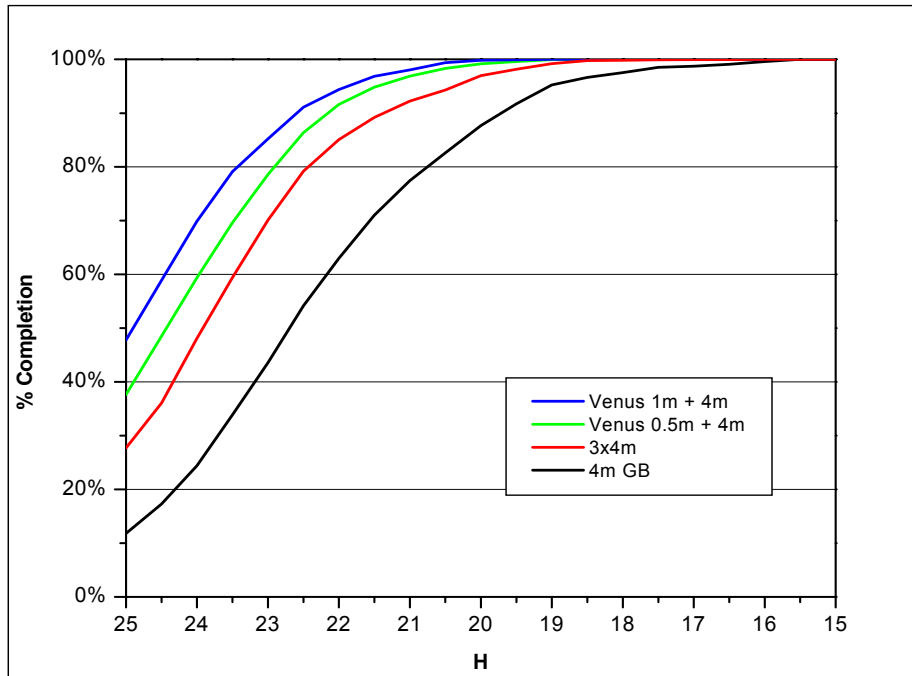


(a) Cataloging

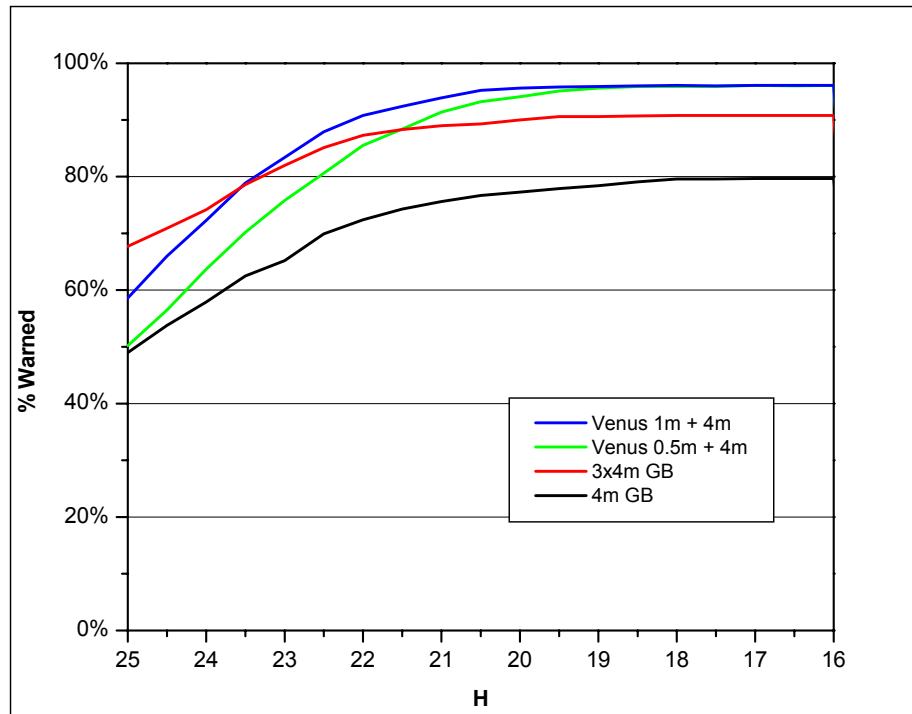


(b) Warning

Figure 6-13. Comparison of (a) cataloging capability and (b) warning efficiency for a ground-based network of three 4m systems, and a network of a single 4m ground-based system combined with a 1m LEO space-based system. A single 1m LEO space-based systems and a single 4m ground-based system is also shown for comparison.



(a) Cataloging



(b) Warning

Figure 6-14. Comparison of (a) cataloging capability and (b) warning efficiency for a ground-based network of three 4m systems, and networks of a single 4m ground-based system combined with a 0.5m or a 1m Venus-trailing space-based system. A single 4m ground-based system is also shown for comparison.

7 SYSTEM COST ESTIMATION

One of the factors involved in determining the most appropriate means of detecting NEOs is the cost of the observatory. In particular, one needs to compare the cost of a particular observing technology or strategy against the associated benefits. Space-based observatories incur greater development costs, but provide a much better resolution and can be operated 24 hours a day regardless of weather. Ground-based observatories, on the other hand, are typically less expensive and allow for easier maintenance and upgrades, but observation is limited to nighttime operations and is subject to weather and atmospheric distortion.

The goal of this section is to address the question posed in the Science Definition Team charter: What would it cost? Cost estimates are presented for both ground-based and space-based observatories. Additional cost estimates are given for multiple ground-based systems as well as combined ground- and space-based systems.

The cost estimates presented here include development, construction and operation of the facility. In estimating the cost of a space-based observatory, several parametric estimating tools exist which provide cost information organized in a work breakdown structure. In the case of ground-based observatories, however, no general parametric cost estimating tools were found within the community. Therefore, the cost estimate in this case is based on analogy with similar technologies and observatories as well as rules of thumb based on related technology development trends.

7.1 Ground-Based Observatory

As stated above, no general cost estimating tools are available to predict the costs associated with designing, constructing and operating a ground-based telescope. However, there are rules of thumb, based on previous completed projects and technology trends, which can yield reasonable estimates of telescope construction costs. Furthermore, parametric models can be constructed to estimate instrument cost based on the focal plane array area and number of channels. The cost of required software can be estimated using commercial packages such as COCOMO (CONstructive COSt MODEL) and the operations can be modeled via rules of thumb and data from previous operational programs. Thus, the cost of a ground-based observatory is broken down into the telescope structure (including telescope optics and facility), instrument (including CCD imager, electronics, cryostat and camera housing), software and operations.

7.1.1 Telescope Development and Construction

The telescope development and construction can be broken down into the development of the facility and the design and development of the telescope optics. The elements included in each of these sub-categories are summarized as follows:

- Facility
 - project management and engineering (including technical salaries)
 - site development (leveling, generators, roads, etc.)
 - transportation of mirrors and equipment to the site
 - dome (control room building, base of dome, top of dome, etc.)
 - altitude-azimuth control system
 - instrument mount
 - cranes and rigging for erecting enclosure
- Optics
 - telescope structure (body, mount)
 - optics support and control (and mirror moving container, if necessary)
 - optics (primary, secondary, tertiary mirrors)
 - mirror coating/aluminizing

In estimating the cost of the optics component, the general rule is to scale the cost as an exponential growth rate using the aperture as the independent variable, i.e.

$$\text{Optics Cost} = \alpha D^\gamma$$

where γ is the exponential growth rate of the cost, D is the aperture diameter in meters and α is a constant. This relationship between cost and aperture has been cited by several authors including Schmidt-Kaler and Rucks (1997, and references therein) and Stepp, et al. (2002). The approximation appears to work best for apertures within the range of 1 to 10 meters. The Cost Estimating Relationship, or CER, tends to over-estimate the cost beyond this range and in cases in which cost reduction techniques (such as light-weighting or segmenting of the mirror) have been employed.

In the current study, the aperture diameters under consideration are 1, 2, 4 and 8 meters with no segmentation or light-weighting of the mirrors. The cost estimating relationship should provide a good estimate of the cost in this range. Based on data obtained from recent existing programs, a CER for the optics component is determined to be

$$\text{Optics Cost (FY03 \$K)} = 2000D^{1.3}.$$

The facility cost is approximated by a linear relationship with aperture diameter D as the independent variable. The CER is

$$\text{Facility Cost} = \beta D + \tau$$

where β and τ are constants. Based on available data, an appropriate CER for the facility is

$$\text{Facility Cost (FY03 \$K)} = 2500D + 2000.$$

Figure 7-1 shows the combined facilities and optics cost for existing programs (as reported) and the predicted costs obtained by combining the CERs for optics and facilities. The scatter in the data from the existing systems is primarily a result of differing reporting practices. Also, some

of the “Actuals” data shown on this plot were obtained from program web sites and journals. In such cases, it is difficult to determine what is included in these costs. For these reasons, the only Actuals data used in constructing the above CERs were obtained from reliable sources and available in a predefined breakdown structure.

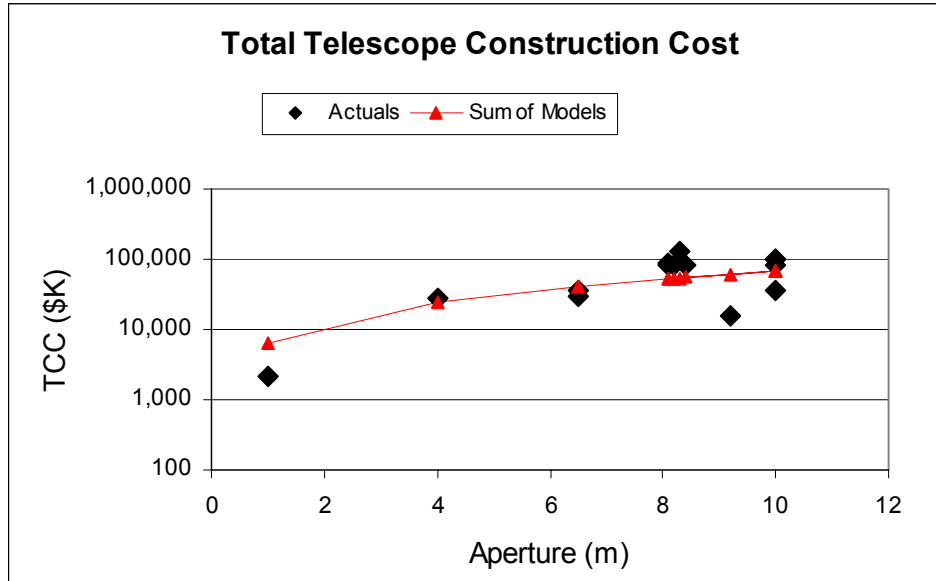


Figure 7-1. Telescope Construction Cost – Actual versus CER

The cost information used to construct the optics and facility CERs constitutes a limited set of data. However, the use of an exponential model describing the cost of a ground-based telescope optical system has proven to be a useful tool for systems with apertures between 1 and 10 meters. As Figure 7-1 shows, the optics and facilities CERs given above provide a reasonable approximation to the cost of several recent telescope projects. For the four aperture diameters under consideration, the corresponding costs are summarized in Table 7-1.

Table 7-1. Telescope Construction Cost (TCC)

Aperture (m)	Total Construction Cost (\$M)
1	6.50
2	11.92
4	24.13
8	51.86

7.1.2 Instrument Design and Development

The cost of the instrument, including the CCD, electronics and the cryostat and camera housing were estimated using CERs developed at MIT Lincoln Lab. The instrument cost is broken down as follows:

CCD imagers: Unpackaged scientific grade back illuminated Si CCD imagers

$$C_{CCD}(\$M) = 13A_{Focal\ Plane}$$

where $A_{Focal\ Plane}$ is the area of the focal plane given in m^2 .

Electronics: Analog front end, signal conditioning, video chain, analog to digital conversion, multiplexing, data formatting and mechanical packaging of the electronics boards

$$C_{Elec}(\$M) = 0.01(\# channels).$$

Cryostat/Camera-Housing: Focal plane assembly, CCD packaging, dewar window, cooling head, internal cabling

$$C_{Cryo}(\$M) = 2.5 A_{Focal\ Plane}.$$

The total instrument cost is the sum of the CCD, electronics and cryostat/camera housing costs, i.e

$$C_{Instr}(\$M) = C_{CCD} + C_{Elec} + C_{Cryo}.$$

The cost of a shutter (not included in the above CERs) is estimated to be \$150k based on data from proposed and existing programs. The instruments under consideration for the ground-based observatory, and their associated costs, are summarized in Table 7-2.

Table 7-2. Instrument Parameters

Parameter	#1	#2
Pixel width (microns)	10	10
# pixels	36K x 24K	18K x 12K
Basis CCD	CCID-34	CCID-34
Basis CCD pixel #	6k x 3k	6k x 3k
Basis CCD FP area (mm)	60 x 30	60 x 30
# basis CCDs for tiling	48	12
FP area (mm)	360 x 240	180 x 120
# ports/basis CCD	4	4
Total # ports	192	48
Readout time (s)	1.5	1.5
Average solar quantum efficiency	0.66	
QE variation (% rms)	0.3	
Dark current (e/pixel/s)	5	
Dark current variation (% rms)	2	
Data rate (MHz)	2	
Readout noise at 2 MHz (e/pixel rms)	5	
Well capacity (e/pixel)	200k	
Average solar quantum efficiency	0.66	
Instrument Cost (\$M)	3.41	0.97

7.1.3 Observatory Operations

The operations budget for a ground-based telescope includes observing time as well as the maintenance of the facility, optics and instrument. This includes the periodic replacement of failed components. No budget is included for upgrades of original components. This is generally not included as part of the acquisition cost. Furthermore, since the FROSST simulations do not account for improved performance over time, the cost associated with explicit system improvements has been omitted from the current estimate. Over the lifetime of the observatory, however, failed components will be replaced with newer, upgraded components. The cost of these upgraded replacements is included in the operations budget.

The telescope operations costs are estimated using rules of thumb and are based on data from existing programs. This estimate includes allocation for labor hours, hardware replacement as well as the integration and commissioning of replacement components that are not identical to the original (failed) components. The CER for the yearly operations cost, C_{Ops} , is:

$$C_{Ops} = 0.649D + 0.065(TCC)$$

where D is the aperture diameter in meters. In this equation, the first term represents the labor hours based on facility size and historical data. The second term describes the increase in operations costs as the aperture, and thus the instrumentation, becomes larger. The total cost for operations is given in Table 7-3.

Table 7-3. Operations and Upgrades Costs

Aperture (m)	Annual Operations Cost (\$M)
1	1.07
2	2.07
4	4.16
8	8.56

7.1.4 Software

Finally, the cost of software for the ground-based observatory was estimated using COCOMO, the CONstructive COst MOdel, and is based primarily on the number of Source Lines of Code (SLOC). The SLOC estimates are derived from existing programs. Table 7-4 summarizes the required software.

COCOMO assumptions include a total of 332,000 SLOC and a cost of \$200k/year for a full time software developer. Using these assumptions, the level of effort and estimated cost of the software development for the ground-based observatory is as described in Table 7-5.

Table 7-4. Software SLOC by Module

Software Module	SLOC
Operations, e.g., telescope control, operator interface, scheduling	200,000
Data Processing, e.g., data acquisition, image processing, detection algorithms	27,000
Data Management, e.g., archiving, database management, data submission scripts	5,000
Orbit-fitting software	100,000

Table 7-5. Software Costs and Level of Effort

	Units	1m	2m	4m	8m
Cost	FY03 \$M	5.1	6.5	6.5	7.6
Effort	Person-Months	305	390	390	455
Schedule	Months	20	22.1	22.1	23.5
Productivity	SLOC/FTE/Month	1087	851	851	730
Instructions	\$/SLOC	15.3	19.6	19.6	22.8
Staff	FTEs	15.2	17.7	17.7	19.3

In addition to the development cost, it is estimated that software maintenance will require the equivalent of one FTE per year at \$200k/year.

7.1.5 Ground-Based Observatory Cost Roll-up

The cost roll-up for the ground-based systems is presented in Table 7-6. Four separate apertures are considered along with two separate focal plane array configurations. The smaller imager (12K x 18K) is not considered in combination with the large (8m) aperture telescope. The third column shows the combination of the telescope construction cost (TCC), the cost of the imager and the required software development cost. The total cost presented for each configuration is the cumulative total for a program consisting of design and development, 10 years of operations and a 25% cost reserve.

Table 7-6. Ground-Based Observatory Cost Roll-Up with Contingency

Aperture (m)	CCD Imager	TCC + CCD + Software (\$M)	Annual Cost: Operations + Software Maintenance	10-year Subtotal (\$M)	Total including 25% Reserve (\$M)
1	24 x 36	15.01	1.27	27.72	34.65
2	"	21.83	2.27	44.56	55.70
4	"	34.03	4.36	77.67	97.08
8	"	62.87	8.76	150.47	188.09
1	18 x 12	12.56	1.27	25.28	31.60
2	"	19.39	2.27	42.12	52.64
4	"	31.59	4.36	75.22	94.03

7.2 Space-Based Observatory

In the case of a space-based observatory, cost estimates are generated for three separate mission scenarios: a Sun-synchronous LEO orbiter, an observatory in a Halo orbit about the Sun-Earth L₂ libration point and a spacecraft in a heliocentric orbit at 0.7 AU. The estimates for these space-based observatories are broken down into instrument (telescope), spacecraft bus, mission operations, communications (for example, the Deep Space Network or a commercial alternative) and launch vehicle cost.

The NASA/Air Force Cost Model (NAFCOM) is used in estimating the cost of the spacecraft bus and the instrument. NAFCOM provides cost estimates for hardware development broken down by subsystem. Input parameters vary from subsystem to subsystem. Inputs common to all subsystems included subsystem weight, percent new design, year of technology as well as various complexity drivers describing aspects of the development team, funding availability, risk management strategy and integration complexity that affect the overall cost. The CERs in NAFCOM are based on historical data from over 90 missions. In addition to hardware development, NAFCOM generates estimates for the cost of integration and test, ground support equipment, system engineering, program management and launch operations (launch plus 30 days).

The cost of mission operations for a space-based observatory is estimated using the NASA Space Operations Cost Model (SOCM). SOCM covers all post-launch mission operations and data analysis tasks for planetary and Earth orbiting missions. However, the cost for communications services, such as the Deep Space Network or similar services, are not included in SOCM and must be estimated separately based on the rates associated with the selected service provider. The estimated cost of the launch vehicle is taken from launch vehicle provider quotes. Finally, the individual cost components described above are rolled-up into a complete estimate.

7.2.1 Space-Based Instruments

The instruments under consideration are all telescopes operating in the visible range. Three variations on the telescope have been examined and costed. The candidate instruments have apertures of 0.5 m, 1.0 m and 2.0 m. Some general assumptions made in estimating the cost of the instrument in NAFCOM are summarized in Table 7-7.

Table 7-7. General Instrument Parameters

Technology year (launch year)	2008
Development time	36 months
Percent new design	80%

Mass input to NAFCOM, specific to each of these instruments, is outlined in Table 7-8.

Table 7-8. System-Specific Cost Model Input

	#1	#2	#3
Aperture (m)	0.5	1.0	2.0
Mass (kg)	130	340	1065

The resulting NAFCOM estimates for the 3 candidate instruments are summarized in Table 7-9.

Table 7-9. Space-Based Instrument Cost Summary

	#1	#2	#3
Aperture (m)	0.5	1.0	2.0
Cost (FY03 \$M)	20.0	36.0	72.6

7.2.2 Spacecraft Bus

The spacecraft bus configuration and subsystem detail depends on the choice of orbit. The three scenarios presented are: a Sun-synchronous LEO orbiter, an observatory in a Halo orbit about the Sun-Earth L₂ libration point and a spacecraft in a heliocentric orbit at 0.7 AU. The spacecraft subsystems most affected by the choice of orbit are on-board propulsion, communications, guidance and control and on-board processing. The choice of launch vehicle is also dependent on the operational orbit of the spacecraft.

Details of the three spacecraft are given in Section 4.2. NAFCOM uses this spacecraft subsystem detail to generate subsystem costs. System integration and program level costs are then generated as wrap factors, i.e. each subsystem contributes a certain percentage to the overall integration and program level costs. Since the NAFCOM CERs are strongly influenced by weight, the subsystem mass breakdown for each of the three mission scenarios described in Section 4.2.3 is repeated in Table 7-10. The spacecraft bus cost (in FY03 \$M), broken down by

subsystem as well as system integration elements, is presented in Table 7-11 for each of the three scenarios.

Table 7-10. Spacecraft Mass Breakdown for Three Mission Scenarios

Subsystem Mass (kg)	LEO	L₂	0.7 AU
Propulsion System (Dry)	0	26	26
Bus Electronics (Integrated avionics)	43	43	43
Power System (Solar arrays, Battery, Electronics)	44	44	48
RF/Comm (Amps, Switches, Antennas)	12	22	33
Guidance & Control Devices	24	22	22
Thermal	12	12	12
Harness	24	26	26
Fuel	0	60	60
Structure (@10% of wet mass)	49.9	59.5	61
Total Mass (kg)	208.9	314.5	331

Table 7-11. Spacecraft Bus Cost Summary

Spacecraft	LEO	L₂	0.7AU
Observatory Spacecraft	68.3	77.7	101.7
<i>Spacecraft Bus (LEO)</i>	<i>42.0</i>	<i>48.0</i>	<i>63.0</i>
Structures & Mechanisms	3.3	3.6	3.6
Thermal Control	1.8	1.8	1.8
Reaction Control Subsystem	0.0	1.4	1.4
Electrical Power and Distribution	1.2	1.2	1.3
Command, Control & Data Handling	30.7	35.3	50.2
Attitude Determination & Control	5.0	4.7	4.7
<i>Spacecraft System Integration</i>	<i>26.3</i>	<i>29.7</i>	<i>38.7</i>
Integration, Assembly and Checkout (IACO)	4.5	5.1	6.7
System Test Operations (STO)	1.1	1.2	1.5
Ground Support Equipment (GSE)	3.9	4.5	5.8
System Engineering & Integration (SE&I)	7.3	8.3	10.8
Program Management (PM)	6.8	7.5	9.8
Launch and Orbital Operations Supports (LOOS)	2.7	3.1	4.1

7.2.3 Operations and Ground Tracking

The operations cost for each of the three mission scenarios is generated using the NASA Spacecraft Operations Cost Model (SOCM). Inputs to SOCM include the length of operation, operating orbit, type of observations (survey or targeted), tracking network, acceptable level of risk as well as several inputs describing the operations strategy and spacecraft power and data margins. In the current analysis, we assume a 10-year operational lifetime performing survey observations with a minimal amount of risk assumed.

In the case of the LEO system, the tracking network is the Universal Space Network. The data are transmitted through three 10-minute downlinks per day. It is assumed that the Operations Center is operated 24 hours to monitor the transmissions for complete and uncorrupted data downlink. The LEO operations cost is based on this three-shift assumption. However, as the operations team becomes more experienced and efficient, the operations may become more automated and the required operator hours may drop down to one shift per day.

The Earth-Sun L₂ system uses the DSN 34m antenna for tracking and data downlink. In this case, the data are downlinked once per day over a period of 4.2 hours. Only one shift is required in the operations center. Finally, the heliocentric orbit spacecraft at 0.7 AU also uses the DSN 34m antenna for tracking and data downlink. The data are transmitted in a single 8-hour contact per day. Table 7-12 summarizes the cost of operations and ground tracking for the three space-based scenarios over 10 years of operation.

Table 7-12. 10-year Operations and Ground Track Cost Summary

	LEO FY03 \$K	L₂ FY03 \$K	0.7 AU FY03 \$K
Mission Planning and Integration	454.30	856.20	889.80
Command/Uplink Management	3,117.90	1,963.70	2,041.00
Mission Control and Operations	3,444.90	2,177.30	2,263.70
Data Capture	1,877.10	1,247.30	1,302.10
Pos/Loc Planning and Analysis	194.40	121.80	126.50
S/C Planning and Analysis	387.90	253.40	264.20
Science Planning and Analysis	1,647.60	3,282.50	3,422.20
Science Data Processing	3,580.80	6,762.40	7,019.40
Long-Term Archives	1,269.70	2,475.30	2,576.10
System Engineering, Integration and Test	1,297.20	2,441.50	2,536.80
Computer and Communications Support	1,833.00	1,148.90	1,193.60
Science Investigations	521.80	1,034.10	1,077.70
Management	210.60	401.50	417.60
<i>Project Direct Total</i>	<i>19,837.20</i>	<i>24,165.90</i>	<i>25,130.50</i>
Ground Network	5,300.00	23,230.00	40,200.00
Total Ops & Ground Network	25,137.20	47,395.90	65,330.50

7.2.4 Space-Based Observatory Cost Roll-up

The final element in the cost roll-up for the space-based candidate observatories is the cost of a launch vehicle. As described in Section 4.2.3, each of the three spacecraft can be launched on a Delta II. The potential missions and the corresponding Delta II models are shown in Table 7-13. The cost of a Delta II launch vehicle is also shown.

Table 7-14 shows the cost roll-up of the complete spacecraft (including bus and instrument), 10 years of operations (including ground network usage) and Delta II launch vehicle. The totals are in FY03 millions of dollars. Note that these totals do not include any cost reserve to cover unexpected growth or complexity.

Table 7-13. Mission/Delta II Correlations

Mission	Delta II Model #	Delta II Cost (FY03 \$M)
LEO	7320-10	56
Earth-Sun L ₂	7425-10	62
Heliocentric 0.7 AU	7926-10	69

Table 7-14. Total Space-Based Observatory Cost without Reserves

	Spacecraft + Instrument + Operations	Launch Vehicle	Total \$M (FY03)
LEO			
0.50m VIS Telescope	117.4	56	173.4
1.00m VIS Telescope	133.4	56	189.4
2.00m VIS Telescope	170.0	56	226.0
L₂			
0.50m VIS Telescope	149.1	62	211.1
1.00m VIS Telescope	165.1	62	227.1
2.00m VIS Telescope	201.7	62	263.7
0.7 AU			
0.50m VIS Telescope	191.0	69	260.0
1.00m VIS Telescope	207.0	69	276.0
2.00m VIS Telescope	243.6	69	312.6

At this level of development, a 25% reserve on all costs (except launch vehicle) is not uncommon. Adding a 25% reserve to the cost of each of the systems shown in Table 7-14 yields the results in Table 7-15.

Table 7-15. Total Space-Based Observatory Cost with Reserves

	Spacecraft + Instrument + Operations	25% Reserve	Launch Vehicle	Total \$M (FY03)
LEO				
0.50m VIS Telescope	117.4	29.4	56	202.8
1.00m VIS Telescope	133.4	33.4	56	222.8
2.00m VIS Telescope	170.0	42.5	56	268.5
L₂				
0.50m VIS Telescope	149.1	37.3	62	248.4
1.00m VIS Telescope	165.1	41.3	62	268.4
2.00m VIS Telescope	201.7	50.4	62	314.1
0.7 AU				
0.50m VIS Telescope	191.0	47.8	69	307.8
1.00m VIS Telescope	207.0	51.8	69	327.8
2.00m VIS Telescope	243.6	60.9	69	373.5

7.3 Multiple Ground-Based and Combined Ground-Based and Space-Based Systems

A network of multiple observing locations can offer several advantages over a single ground- or space-based telescope. Such a network may include multiple collocated or non-collocated ground telescopes or a combination of ground-based and spaced-based observatories. Advantages to such networked systems were discussed in Section 6. In this section, the cost of developing and operating a network of observatories is presented.

7.3.1 Ground-Based Network of Observatories

The cost of developing and operating multiple ground-based observatories was estimated by applying appropriate learning curves and eliminating cost elements that are redundant. The learning curve is defined as follows: Given the cost of a Theoretical First Unit (*TFU*) and a learning curve slope *S*, the cost of *n* units is

$$C_n = TFU(n^{[1-\ln(100/S)/\ln(2)]}).$$

Note that a learning curve of 100% implies there is no cost savings for multiple systems.

Separate learning curves are defined for design and construction of the facility, development and manufacture of the optics, development and manufacture of the CCD and operations costs. These learning curves are based on experience with previous programs and are summarized in Table 7-16.

Table 7-16. Learning Curves

Cost Element	Learning Curve (%)
Facility	80
Optics	100
CCD	90
Operations	80

Software development costs are also reduced for multiple aperture systems. Software that is developed for a given aperture size can be re-used at another location with only minimal changes. Thus, in the case of multiple observatories with common aperture, software development (and maintenance) costs are only incurred once.

Another factor affecting the cost of networked systems is the relative location of the facilities. Collocated systems can share more of the facilities and maintenance costs than non-collocated systems.

The multiple aperture systems under consideration are:

- Two 1m telescopes – collocated
- Two 2m telescopes – collocated
- Two 1m telescopes – non-collocated
- Two 2m telescopes – non-collocated
- Two 4m telescopes – collocated
- Two 4m telescopes – non-collocated
- Three 4m telescopes – 2 collocated and 1 remote

Each of these telescopes uses the 18K x 12K pixel CCD. After applying the learning curves and all appropriate discounts, the costs for multiple aperture system are summarized in Table 7-17.

Table 7-17. Costs for Multiple Aperture Systems

Aperture	Quantity	Collocated?	Acquisition Cost (\$M FY03)	Annual Operating Cost (\$M FY03)	Years of Operation	Total Cost including 25% reserve (\$M FY03)
1m	2	Yes	18.04	1.91	10	46.47
2m	2	Yes	29.29	3.52	10	80.56
1m	2	No	19.84	2.34	10	54.08
2m	2	No	32.09	4.35	10	94.42
4m	2	Yes	51.69	6.86	10	150.37
4m	2	No	56.49	8.53	10	177.19
4m	3	1 remote	76.53	11.02	10	233.46

7.3.2 Mixed Ground- Based and Space-Based Observatories

Since ground-based and space-based observations each offer unique advantages, the combination of the two should bring together the cataloging benefits and rapid results of the space-based systems (particularly the 0.7 AU Venus-trailing observatory) and the high warning efficiency achieved from Earth. The mixed-base systems under consideration are:

- a 1m Venus-trailing telescope and a 4m ground-based telescope
- a 0.5m Venus-trailing telescope and a 4m ground-based telescope
- a 1m LEO telescope and a 4m ground-based telescope

In estimating the cost of the combined space/ground systems, there is little overlap between the operations and no learning curve benefits since the three configurations above employ no duplicates. The total cost is the sum of the cost for each system. The only cost that is not duplicated is the cost of the orbit-fitting software. It is assumed that the data from both observatories will be forwarded to a central Science Operations Center for this step of the data processing. Thus, the cost of the combined space/ground systems is summarized in Table 7-18.

Table 7-18. Costs for Combined Space/Ground Systems

Space/Ground Combination	Acquisition Cost (\$M FY03)	Annual Operating Cost (\$M FY03)	Years of Operation	Launch Vehicle (\$M FY03)	Total Cost including 25% reserve (\$M FY03)
1m Venus-trailing + 4m ground	169.29	10.9	10	69	416.8
.5m Venus-trailing + 4m ground	153.29	10.9	10	69	396.8
1m LEO + 4m ground	135.89	6.9	10	56	311.8

7.4 Summary

The cost estimates presented in this section demonstrate that the space-based observatories are all significantly more expensive than their ground-based counterparts. They also carry with them an inherent risk and are less maintainable than comparable ground-based systems. Space-based systems do, however, offer significant advantages, particularly in the cataloging of NEOs. The question arises: What is “comparable” when comparing the cost of these two types of observatories? To answer this, it is necessary to assess the cost of a given system (or combination of systems) as a function of the benefit that can be derived. This is the focus of the next section.

8 COST / BENEFIT CONCLUSIONS

8.1 Approach

The purpose of a Cost Benefit Analysis (CBA) is to support better decision-making and ensure that resources are effectively allocated to support the proposed mission. The analysis should be commensurate with the size, complexity and cost of the proposed project, and be supported by a management decision as to the level of analysis necessary. The results of the analysis should demonstrate that the chosen alternative is the most cost-effective within the context of budgetary and political considerations.

The Team performed a type of CBA called Benefit-Cost Analysis (BCA), a systematic, quantitative method of assessing the life cycle costs and benefits of competing alternative approaches. The standard criterion for justifying a project is that the benefits exceed the costs over the life cycle of the project. The competing alternative with the greatest net benefit (benefits minus costs) is a primary candidate for selection. The approach used is broken down into eleven steps, as outlined below.

STEP 1 - DETERMINE/DEFINE PROJECT OBJECTIVES

In August of 2002, NASA initiated the formation of a Science Definition Team with a charter to develop an understanding of the threat posed by near-Earth objects smaller than one kilometer and to assess methods of providing warnings of potential impacts. The Team was instructed to provide recommendations to NASA and to outline an executable approach to addressing any recommendations made.

Providing authoritative answers to the questions posed for the Team (see Section 1) requires an understanding of the relationships between the costs of implementing a search effort for smaller asteroids and the benefits accrued. Thus, the study process was constructed along the lines of a cost benefit analysis as shown in Figure 1-1.

STEP 2 - DOCUMENT CURRENT PROCESS

The current process must be thoroughly documented because it is the baseline for nearly all decisions regarding new alternatives. The cost of the current system provides the baseline for the BCA and must include all elements.

For the purposes of this study, the baseline will be the current LINEAR system. LINEAR detects more than 95% of all NEOs detected by all the current surveys and can be considered a reasonable model for the current capability. While the current systems are always evolving and improving, and it is almost certain that the baseline capability in 2008 and beyond will exceed the current baseline, without more knowledge of the predicted improvements, it is not feasible to simulate an enhanced baseline. Therefore, this study has determined the 2003 LINEAR capability as the minimum baseline capability that will exist in 2008 and throughout the duration of the simulation period.

STEP 3 - ESTIMATE FUTURE REQUIREMENTS

In order to map the cost benefit potential of each search technology, a series of technically realizable search systems were defined by the Team. Driven largely by the diameter of the primary optics, these systems covered the range of capability considered reasonable by the Team. The design methodology for each of the systems and their expected performance with respect to search rate and detection sensitivity are described in Section 4.

STEP 4 - COLLECT COST DATA

This is one of the most difficult steps in a BCA, but also one of the most important. The quality of the analysis is only as good as the quality of the cost data. Historical data can be used to estimate future purchase price of hardware, software, and services. Also, the cost of current systems can be used to price similar alternatives. In some cases, data may not be available to provide an adequate cost estimate. In that situation, the best alternative is to use the judgment and experience of the BCA team members to estimate costs.

In collecting data for the cost of a space-based observatory, several parametric estimating tools exist which provide cost information organized in a work breakdown structure and divided into recurring and non-recurring cost. In the case of ground-based observatories, however, no uniformly accepted cost data were found within the community. The data collection processes for the space-based and ground-based observatories are discussed in Section 7.

STEP 5 - CHOOSE AT LEAST THREE ALTERNATIVES

In addition to the baseline, a total of 28 alternatives were analyzed. Ground-based system alternatives (Table 8-1) with a variety of primary optics apertures (Ap), Field of View (FOV), and geographic locations were considered. In addition, space-based system alternatives (Table 8-2) with a variety of primary optics apertures and orbits were considered. Finally, networks of space-based and ground-based systems (Table 8-3) were considered. For example, in Table 8-1, the first entry for Mauna Kea “MK_LCCD1m” denotes the Mauna Kea observatory, a large CCD and a 1m aperture. In Table 8-3, the first entry “LEO1m_4m” denotes a 1m aperture telescope in low-Earth orbit together with a ground-based telescope with an aperture of 4 meters.

STEP 6 - DOCUMENT BCA ASSUMPTIONS

The BCA analysis uses the results of the Population Estimates (Section 2), Risk and Hazard Assessment (Section 3), Candidate Technologies and Systems (Section 4), Search Strategy (Section 5), Simulation Description and Results (Section 6), and System Cost Estimation (Section 7). The assumptions used in each of these analyses are justified and documented in their respective sections of this report.

STEP 7 - ESTIMATE COSTS

Life Cycle cost estimates were done for each of the competing alternatives. The details of the cost estimating process are included in Section 7.

Table 8-1. Ground-Based System Alternatives

Location	FOV	Aperture	Ground Based Systems
Current LINEAR			LINEAR
Mauna Kea	Large	1m	MK_LCCD1m
		2m	MK_LCCD2m
		4m	MK_LCCD4m
		8m	MK_LCCD8m
	Small	1m	MK_SCCD1m
		2m	MK_SCCD2m
4m		MK_SCCD4m	
Kitt Peak	Small	2m	KP_SCCD2m
		4m	KP_SCCD4m
Two at Mauna Kea	Small	1m	DualNN_SCCD1m
		2m	DualNN_SCCD2m
		4m	DualNN_SCCD4m
Mauna Kea and Chile	Small	1m	DualNS_SCCD1m
		2m	DualNS_SCCD2m
		4m	DualNS_SCCD4m
Mauna Kea and Chile	Small	4m	3_4m

Table 8-2. Space-Based System Alternatives

Orbit	Aperture	Space Based Systems
LEO	0.5m	LEO_50cm
	1m	LEO_1m
	2m	LEO_2m
L ₂	0.5m	L2_50cm
	1m	L2_1m
	2m	L2_2m
Venus	0.5m	Venus_50cm
	1m	Venus_1m
	2m	Venus_2m

Table 8-3. Joint System Alternatives

Location	FOV/Orbit	Aperture	Joint Systems
Mauna Kea	Large/LEO	4m/1m	LEO1m_4m
Mauna Kea	Large/Venus	4m/50cm	Venus50cm_4m
Mauna Kea	Large/Venus	4m/1m	Venus1m_4m

STEP 8 - ESTIMATE BENEFITS

The benefits provided by a given search system need to be measured relative to the system costs. The costs of a given system are governed by the construction and operational expenses, which can be estimated in a relatively straightforward manner, while the benefit side of the equation is

much more challenging for several reasons. Most importantly, the benefits provided by a system cannot be described in strictly financial terms due to the potential for casualties and to various political and emotional considerations that are relevant to the problem. Furthermore the benefit depends directly upon estimates of the hazard posed by NEOs, and these estimates are plagued by large uncertainties.

The direct benefit of a search program has two sources, cataloging and warning. “Cataloging” refers to the idea that the statistical impact risk is only posed by the undiscovered component of the NEO population. Therefore, by discovering and cataloging NEOs, and by verifying that none will impact within the next century, we reduce the potential risk to life and property on Earth. If an object is actually discovered on a threatening trajectory, there will presumably be many years, even decades, in which to execute a plan to deflect or disrupt the impactor. Hence, the cataloging approach enables the complete mitigation of future impacts, saving both population and infrastructure.

The term “warning” describes a situation where an impactor is first detected and recognized some days to months before the event. This “warning period” would afford civil authorities an opportunity to take actions that would mitigate the impact effects, but there would be insufficient time to avert the collision. In such a scenario the warning benefit is largely comprised of casualties avoided through the evacuation of affected areas. Major infrastructure would not be saved, although, time permitting, some portion of the physical infrastructure could also be removed to a safe distance.

To further describe the methodology used in this report some terms need to be defined. The “completeness” C describes the fraction of objects in a given size range, or bin, that have been discovered and cataloged; its complement is the “incompleteness” C' ($C' = 1 - C$). As a survey progresses, C steadily increases until all objects in the size bin have been discovered. Meanwhile, as the survey operates, it has a known likelihood of serendipitously detecting an impactor on its final approach to collision. This likelihood, which we term the “warning efficiency” W , varies with impactor size. The completeness and warning efficiency are largely controlled by the search equipment and strategy. The annual impact hazard to infrastructure (h_I) and to the population (h_P) for each size bin is dependent upon the impact flux and the resulting damage, which is measured in terms of either dollars or population affected.

Canavan (1995) defines the losses from impacts with global effects as an interruption in Earth’s gross product for a 20 year period due to damages and evacuation of large regions. Using global population data obtained from the U.S. Bureau of the Census, International Data Base (2003), and global Gross Domestic Product (GDP) data contained in “A Case Study: Gross Domestic Product - December 2002” written by The National Council on Economic Education (2002), we derived the global and U.S. values for the annual impact hazard to infrastructure h_I where:

$$h_I = (20 \text{ years}) * (\text{GDP} / \text{Population}).$$

In assigning a value to the annual impact hazard to the population h_P we chose an approach based on societal willingness to pay (WTP) for mortality risk reductions. In this approach, specific people whose lives are saved cannot be identified. Instead, “statistical lives” are saved, and the

associated cost is referred to as the value of a statistical life (VSL). The VSL should be thought of as a convenient way to summarize the value of small reductions in mortality risks. It is not meant to be applied to the value of saving the life of an identified person (i.e., the value of changing the risk of mortality from one to zero). Based on previous research done by the U.S. Environmental Protection Agency (Kenkel, 2000) a reasonable estimate of the U.S. VSL has a mean of \$4.8 million with a confidence interval of plus or minus \$3.2 million (in 1990 dollars), or \$6.96 million +/- \$4.6 million (in 2003 dollars). To determine the global VSL we assumed that one's WTP varies in proportion to income, and so one could scale from the U.S. VSL to a global VSL by taking the ratios of incomes/person in the U.S. and the world (World Bank Group, 2003). The results yield a global VSL of \$1.6 million +/- \$1.1 million (in 2003 dollars).

The warning benefit only applies to the undiscovered component of the population, and so the annual warning benefit is derived from the product of warning efficiency W , incompleteness C' and annual population hazard h_p for each size bin under consideration

$$B_W = W * C' * h_p.$$

Since C' decreases over the course of the search program, the annual warning benefit diminishes accordingly. Of course, if the program is terminated at the end of the planned operation period the warning benefit would cease to accrue. If the incompleteness were small enough this may be an acceptable outcome since the warning benefit may be very small relative to the operations costs.

The benefit from cataloging has a very different character because the statistical hazard has been permanently reduced by the cataloging process and thus the benefit continues to accrue after the survey ends. Another important difference is that the hazards to both population and infrastructure are mitigated. The annual cataloging benefit is:

$$B_{CAT} = C * (h_p + h_I).$$

It is important to baseline the cataloging benefit against the benefit of doing nothing, since ongoing surveys have already reached a substantial level of completeness in the larger size ranges. While a candidate survey is operational, C increases each year and so B_{CAT} increases during the survey period. At the end of the survey the annual benefit is constant and accrues each year for an indefinite period; however, the present value of benefits that accrue in the distant future is much smaller than the value of such benefits accruing in the near future. In this report we will accumulate “net present value” of the cataloging benefit gained during the survey operation and for up to 100 years afterwards.

STEP 9 - DISCOUNT COSTS AND BENEFITS

After the costs and benefits for each year of the system life cycle have been estimated, they must be converted to a common unit of measurement to properly compare competing alternatives. That is accomplished by discounting future dollar values, thus transforming future benefits and costs to their “present value”. For the purposes of this study, the team developed a tool using Microsoft Excel (Table 8-4) to provide rapid discounting of costs and benefits to FY2003\$M.

Table 8-4. Net Present Value (NPV) Tool

		Assumptions		2003		2008		2003		2008		2003		2008		2003		2008		2003		2008	
		current year =		(same as or earlier than 1st year of operation)		(assume full year of ops)		(same as or earlier than 1st year of operation)		(assume full year of ops)		(same as or earlier than 1st year of operation)		(assume full year of ops)		(same as or earlier than 1st year of operation)		(assume full year of ops)		(same as or earlier than 1st year of operation)		(assume full year of ops)	
		1st year of operation =		Global Average value = \$1,600 (FY2003\$M)		Global Average value = \$1,600 (FY2003\$M)		WGD/P-20/W pop = \$0.098 (FY2003\$M)		WGD/P-20/W pop = \$0.098 (FY2003\$M)		Inflation rate =		Inflation rate =		acquisition cost (\$M) =		acquisition cost (\$M) =		h_p Value		h_p Value	
		population impact hazard/person (\$M) =		18.762 (FY2003\$M)		18.762 (FY2003\$M)		2.8%		2.8%		Global		Global		Global		Global		Global		Global	
		infrastructure impact hazard/person (\$M) =		1.589		1.589		1.589		1.589		Global		Global		Global		Global		Global		Global	
		yearly ops costs (\$M) =		1.589		1.589		1.589		1.589		Global		Global		Global		Global		Global		Global	
Phase	Year	Inflation	(RYSM)	Benefit	Benefit	Benefit	Benefit	Benefit	Benefit	Benefit	Benefit	Benefit	(FY03\$M)	Benefit	Benefit	Benefit	Benefit	Benefit	Benefit	Benefit	Benefit	Benefit	Benefit
Fund	2003	1.000	1.9	-1.9	-1.9	-1.9	-1.9	-1.9	-1.9	-1.9	-1.9	-1.9	1.9	-1.9	-1.9	-1.9	-1.9	-1.9	-1.9	-1.9	-1.9	-1.9	-1.9
Fund	2004	1.029	3.9	-3.9	-3.9	-3.9	-3.9	-3.9	-3.9	-3.9	-3.9	-3.9	3.8	-3.8	-3.8	-3.8	-3.8	-3.8	-3.8	-3.8	-3.8	-3.8	-3.8
Fund	2005	1.059	6.0	-6.0	-6.0	-6.0	-6.0	-6.0	-6.0	-6.0	-6.0	-6.0	5.6	-5.6	-5.6	-5.6	-5.6	-5.6	-5.6	-5.6	-5.6	-5.6	-5.6
Fund	2006	1.090	6.1	-6.1	-6.1	-6.1	-6.1	-6.1	-6.1	-6.1	-6.1	-6.1	5.6	-5.6	-5.6	-5.6	-5.6	-5.6	-5.6	-5.6	-5.6	-5.6	-5.6
Fund	2007	1.121	2.1	-2.1	-2.1	-2.1	-2.1	-2.1	-2.1	-2.1	-2.1	-2.1	1.9	-1.9	-1.9	-1.9	-1.9	-1.9	-1.9	-1.9	-1.9	-1.9	-1.9
Ops	2008	1.154	1.8	93.4	198	113.2	111.4	91.5	118.1	120.0	118.1	209.6	1.6	81.0	17.2	98.1	96.6	77.8	96.6	77.8	96.6	77.8	96.6
Ops	2009	1.187	1.9	86.6	33.3	120.0	118.1	118.1	124.7	128.7	124.7	209.6	1.6	73.0	28.1	101.1	99.5	177.3	99.5	177.3	99.5	177.3	99.5
Ops	2010	1.222	1.9	80.8	45.9	126.7	124.7	124.7	130.9	136.9	130.9	334.3	1.6	66.1	37.5	103.7	102.1	279.4	102.1	279.4	102.1	279.4	102.1
Ops	2011	1.257	2.0	76.6	56.3	132.9	130.9	130.9	136.6	142.4	136.6	465.2	1.6	60.9	44.8	105.7	104.1	383.5	104.1	383.5	104.1	383.5	104.1
Ops	2012	1.293	2.1	74.0	64.7	138.7	136.6	136.6	142.4	148.5	142.4	601.8	1.6	57.2	50.0	107.2	105.6	489.1	105.6	489.1	105.6	489.1	105.6
Ops	2013	1.331	2.1	71.7	72.8	144.5	142.4	142.4	148.5	154.3	148.5	744.2	1.6	53.9	54.7	108.6	107.0	596.1	107.0	596.1	107.0	596.1	107.0
Ops	2014	1.370	2.2	69.3	81.4	150.7	148.5	148.5	154.3	160.2	154.3	892.7	1.6	50.6	59.4	110.0	108.4	704.6	108.4	704.6	108.4	704.6	108.4
Ops	2015	1.409	2.2	67.8	88.7	156.5	154.3	154.3	160.2	166.3	1,047.0	1,047.0	1.6	48.1	63.0	111.1	109.5	814.0	109.5	814.0	109.5	814.0	109.5
Ops	2016	1.450	2.3	66.4	96.1	162.5	160.2	160.2	166.3	172.1	1,207.1	1,207.1	1.6	45.8	66.2	112.1	110.5	924.5	110.5	924.5	110.5	924.5	110.5
Ops	2017	1.492	2.4	65.0	103.7	168.7	166.3	166.3	172.1	178.2	1,373.5	1,373.5	1.6	43.5	69.5	113.1	111.5	1,036.0	111.5	1,036.0	111.5	1,036.0	111.5
Ops	2018	1.535	2.4	63.5	106.7	168.7	166.3	166.3	172.1	178.2	1,548.2	1,548.2	1.6	43.5	69.5	113.1	111.5	1,036.0	111.5	1,036.0	111.5	1,036.0	111.5
Ops	2019	1.580	2.4	61.8	109.8	168.7	166.3	166.3	172.1	178.2	1,733.5	1,733.5	1.6	43.5	69.5	113.1	111.5	1,036.0	111.5	1,036.0	111.5	1,036.0	111.5
Ops	2020	1.626	2.4	60.1	109.8	168.7	166.3	166.3	172.1	178.2	1,928.0	1,928.0	1.6	43.5	69.5	113.1	111.5	1,036.0	111.5	1,036.0	111.5	1,036.0	111.5
Ops	2021	1.673	2.4	58.4	109.8	168.7	166.3	166.3	172.1	178.2	2,133.5	2,133.5	1.6	43.5	69.5	113.1	111.5	1,036.0	111.5	1,036.0	111.5	1,036.0	111.5
Ops	2022	1.721	2.4	56.7	109.8	168.7	166.3	166.3	172.1	178.2	2,348.0	2,348.0	1.6	43.5	69.5	113.1	111.5	1,036.0	111.5	1,036.0	111.5	1,036.0	111.5
Ops	2023	1.771	2.4	55.0	109.8	168.7	166.3	166.3	172.1	178.2	2,573.5	2,573.5	1.6	43.5	69.5	113.1	111.5	1,036.0	111.5	1,036.0	111.5	1,036.0	111.5
Ops	2024	1.823	2.4	53.3	109.8	168.7	166.3	166.3	172.1	178.2	2,818.0	2,818.0	1.6	43.5	69.5	113.1	111.5	1,036.0	111.5	1,036.0	111.5	1,036.0	111.5
Ops	2025	1.876	2.4	51.6	109.8	168.7	166.3	166.3	172.1	178.2	3,082.5	3,082.5	1.6	43.5	69.5	113.1	111.5	1,036.0	111.5	1,036.0	111.5	1,036.0	111.5
Ops	2026	1.930	2.4	49.9	109.8	168.7	166.3	166.3	172.1	178.2	3,367.0	3,367.0	1.6	43.5	69.5	113.1	111.5	1,036.0	111.5	1,036.0	111.5	1,036.0	111.5

STEP 10 - EVALUATE ALTERNATIVES

The results of the BCA are compared and ranked in Section 8.2 and Appendix 5.

STEP 11 - PERFORM SENSITIVITY ANALYSIS

The sensitivity analysis process required three steps: identification of input parameters with the greatest influence on the outcome, repetition of the cost analysis, and evaluation of the results. The input parameters with the greatest influence on the outcome are the values assigned to the annual impact hazard to infrastructure h_I and to the population h_P , the total hazard, and the inclusion or exclusion of the global hazard due to large impactors. The costs and benefits for each competing alternative, taking into account the sensitivity of the parameters with the greatest influence on the outcome, have been assigned dollar values and discounted. The results of these excursions are compared and ranked in Section 8.2 and Appendix 5.

8.2 Results and Conclusions of Cost Benefit Study

The results of the baseline case are presented in tabular format below. The quantities h_P and h_I are the hazard to population and the hazard to infrastructure values. The global averages for h_P and h_I are \$1.6 million per person and \$98 thousand per person, respectively. The corresponding US averages for h_P and h_I are \$6.96 million per person and \$734 thousand per person, respectively. In Table 8-5, for various search systems under consideration, the columns give the system cost in millions of FY03 dollars. This cost includes the acquisition costs plus 10 years of operations. The “break even (BE)” year is the year that the candidate system’s total benefit is greater than or equal to the system costs. “ROI 10 years” is the return on investment after 10 years of operations. This is a multiplicative factor so that the total benefit after 10 years would be the “Cost” multiplied by “ROI 10 years”. “Sub-Gbl Haz Ret” is the percent of the sub-global hazard retired after 10 years. This column is blank for those cases in Appendix 5 that include the global hazard. “ROI 20 Yrs” and “ROI 100 Yrs” are the returns on investment after 20 and 100 years, respectively. In Appendix 5, Table 8-5 is repeated along with several other cases that provide results for the Global and US values for h_P and h_I , for the minimum, nominal, and maximum hazards, and for cases that include and exclude the global hazard. The bottom line from these analyses presented in Table 8-5 and Appendix 5, is that, for all but a few of the “minimum” hazard cases considered, the hazard reduction, or benefit derived from the search, is reached after the first year. The cost benefit analysis confirmed that, based solely upon cost considerations, all the explored options are viable. The next section summarizes the comparisons between these options in terms of costs and the efficiency with which they can meet the stated goal.

Table 8-5. Global h_p & h_l value, Nominal Hazard, Global Hazard Included

	Cost FY03\$M	BE Year	ROI 10 Yrs	Sub-Gbl Haz Ret	ROI 20 Yrs	ROI 100 Yrs
--- Ground Based Systems ---						
LINEAR	\$12.5	2008	181.0	---	259.9	891.1
MK_LCCD1m	\$34.7	2008	119.0	---	209.7	935.5
MK_LCCD2m	\$55.7	2008	73.0	---	128.7	574.8
MK_LCCD4m	\$97.1	2008	43.6	---	80.5	375.3
MK_LCCD8m	\$188.1	2008	20.1	---	37.6	177.1
MK_SCCD1m	\$31.6	2008	131.1	---	233.5	1053.4
MK_SCCD2m	\$52.6	2008	77.2	---	137.2	617.5
MK_SCCD4m	\$94.0	2008	44.3	---	81.7	380.7
KP_SCCD2m	\$52.6	2008	65.6	---	102.1	393.9
KP_SCCD4m	\$94.0	2008	38.7	---	63.1	257.9
DualNN_SCCD1m	\$46.5	2008	91.2	---	165.3	758.3
DualNN_SCCD2m	\$80.6	2008	52.9	---	97.9	458.2
DualNN_SCCD4m	\$150.4	2008	29.5	---	56.9	276.7
DualNS_SCCD1m	\$54.1	2008	80.1	---	135.7	580.2
DualNS_SCCD2m	\$94.4	2008	46.4	---	86.2	404.9
DualNS_SCCD4m	\$177.2	2008	25.2	---	49.2	241.0
3_4m	\$233.5	2008	19.4	---	38.1	188.1
--- Space Based Systems ---						
LEO_50cm	\$202.8	2008	22.8	---	42.9	204.0
LEO_1m	\$222.8	2008	20.7	---	40.3	197.2
LEO_2m	\$268.5	2008	17.1	---	33.8	167.4
L2_50cm	\$248.4	2008	17.6	---	33.9	164.2
L2_1m	\$268.4	2008	16.8	---	33.0	162.9
L2_2m	\$314.1	2008	14.4	---	28.7	142.9
Venus_50cm	\$307.8	2008	13.5	---	28.0	143.7
Venus_1m	\$327.8	2008	13.3	---	27.5	140.9
Venus_2m	\$373.5	2008	11.9	---	24.5	125.9
--- Joint Systems ---						
LEO1m_4m	\$311.8	2008	14.5	---	28.6	141.5
Venus50cm_4m	\$396.8	2008	11.0	---	22.6	115.4
Venus1m_4m	\$416.8	2008	10.6	---	22.0	112.5

Cost for LINEAR represents 10 years of operations only

9 SYSTEM COMPARISONS AND SUMMARY OF STUDY RESULTS

9.1 Establishing A Realistic Goal

The goal of the current NEO search systems is the discovery, by the end of 2008, of 90% of the near-Earth objects larger than one kilometer since it is collisions with these large objects that can cause global consequences. The Team concluded that a realistic goal for the next generation of search surveys would be to ***construct a search system that is capable of retiring 90% of the risk posed by collisions with asteroids whose diameters are less than one kilometer.*** At the same time, such a system would substantially eliminate the remaining global risk due to the potentially hazardous objects (PHOs) that will remain undiscovered by the current search efforts. Current surveys use the number of discovered near-Earth asteroids as a success metric. However, since these objects have perihelion distances out to 1.3 AU, many of them do not pose a real threat to Earth until their orbits can evolve, over thousands of years, into the region of the Earth's neighborhood at 1 AU. Hence, the Team considered only potentially hazardous objects (PHOs), or asteroids and short-period comets that can currently approach the Earth's orbit to within 0.05 AU (7.5 million km).

Using realistic estimates of the near-Earth object population and a risk analysis that considered both land-based and water-based impactors, the Team determined that to retire 90% of the remaining risk due to sub-kilometer impactors would require the next generation of searches to find and catalog 90% of those PHOs that are larger than 140 meters in diameter (Figure 9-1). Such a search would eliminate 90% of the hazard due to sub-global impact consequences. Such systems would also discover and catalog about 50% of the PHOs down to the size of 50 meters, and would have a substantial probability of providing short-term warning from a previously undiscovered impactor of that size by detecting it shortly before impact. Tunguska-sized PHOs (about 50 meters in diameter) are just at the limit where a rocky body would be expected to cause a significant air blast in the Earth's atmosphere, whereas rocky PHOs about 140 meters and larger would be expected to punch completely through the Earth's atmosphere, causing a cratering event on the Earth's surface (Hills and Goda, 1993).

The above goal is quite robust to the uncertainty bounds for the sub-global hazard that were established by the Team's analysis. Figure 9-2 displays the cumulative sub-global hazard as a function of object diameter. The three curves correspond to the minimum, nominal and maximum levels of hazard viewed as credible by the Team. For example, in the nominal case, 93% of the sub-global hazard is associated with objects larger than 110m in diameter. The small separations between the curves indicate that the result is relatively insensitive to the total hazard over the entire credible range of uncertainties.

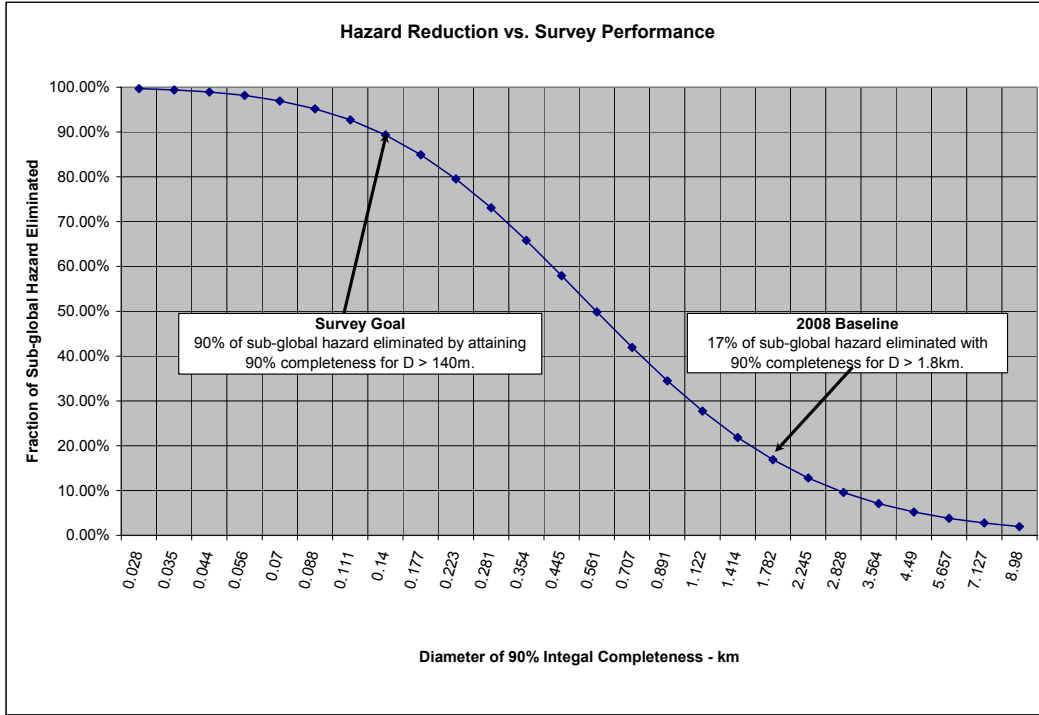


Figure 9-1. Fraction of hazard eliminated from impactors causing sub-global effects (i.e., local damage only) as a function of survey completeness.

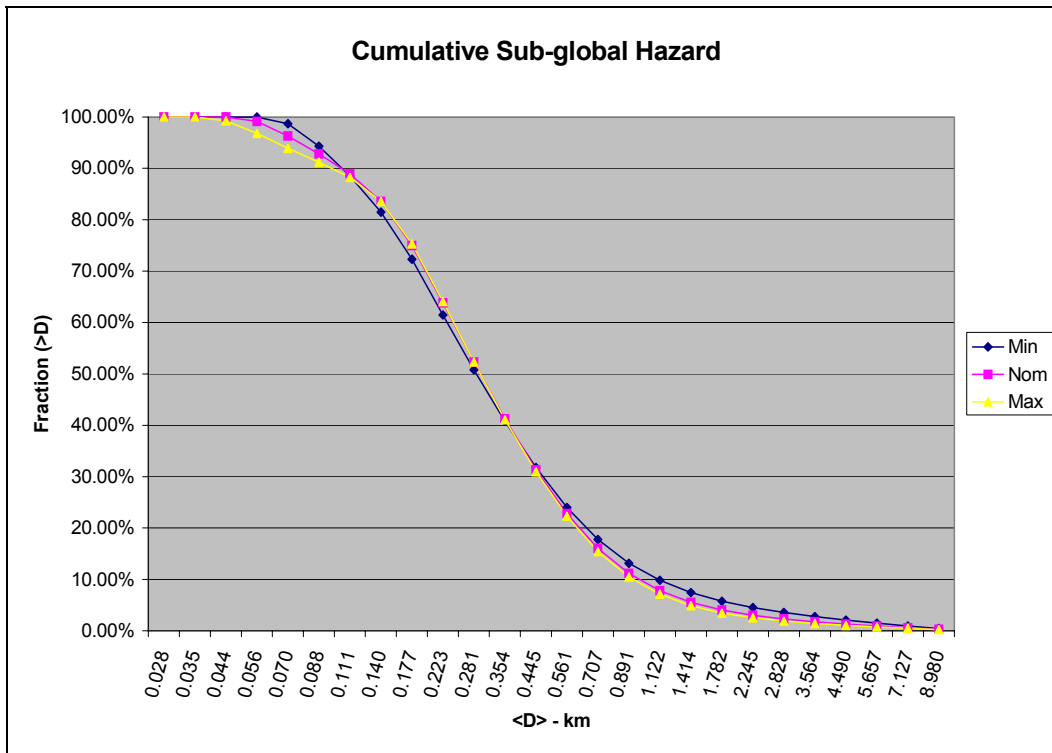


Figure 9-2. Fraction of the sub-global hazard arising from objects larger than a given size for the minimum, nominal and maximum hazard models.

9.2 Performance Overview For Systems Designed To Meet The Goal

Cataloging and Warning Efficiency: The analyses conducted by the Team included search telescopes located at ground-based sites, space-based platforms, and combination networks of both ground-based and space-based systems. From our analyses, we determined that, for a particular limiting magnitude, the search system that covers the most sky per day is the most efficient system for discovering and cataloging new PHOs. Not surprisingly, the rate at which a particular telescope can discover PHOs is highest in the first year and decreases in subsequent years (see Figure 6-7). Once discovered and cataloged, a PHO's motion can be extrapolated into the future to assess the likelihood that it could make an Earth threatening encounter. At that point, a PHO is not considered a threat (and requires no warning) since subsequent observations will either rule out an Earth impact or, if not, a mitigation campaign could presumably prevent the impact. Warning is the ability to detect an impactor during its final orbital period and we assume that the benefits due to warning (e.g., timely evacuation) are only relevant for those objects that are not yet cataloged.

Ground-Based Systems: For ground-based systems, telescopes with apertures of 4 and 8 meters using the large format CCD detectors had roughly comparable performance and, in fact, the 4-meter telescope with the smaller format CCD did nearly as well (see Figure 6-8(a)). Telescope location is important for cataloging efficiency and our simulations showed that the superior astronomical seeing and clear weather on Mauna Kea allowed a one meter aperture search telescope to out perform 2- and 4-meter telescopes located in the southwestern U.S. (See Figure 6-9.) Dual ground-based systems were studied to assess the benefit of collocating two similar telescopes (to increase sky coverage) and placing similar systems in the northern and southern hemispheres. From Figures 6-10a and 6-10b, it is clear that while the north/south placement of telescopes provides a modest cataloging improvement over collocated northern telescopes, the real advantage of the north/south system comes from the increased warning efficiency.

Not surprisingly, the conclusions put forward by various studies will depend critically upon the assumptions made. In this report, we have adopted simulation assumptions for ground-based search systems that are based upon currently employed, successful techniques and technology. It should be noted that there are ongoing studies that make more ambitious assumptions of performance and search methodology. These studies include four 1.8-meter telescopes collocated in Hawaii (Pan-STARRS) and a single mirror 8.4-meter telescope (LSST) proposed by the National Optical Astronomy Observatory. Very large focal plane detectors are being planned to provide a net 5.8 square degree coverage per image, and sky-subtraction rather than repeatedly imaging the same region to detect an object's motion, is being assumed. Sky-subtraction differences a recently imaged star field with an archived version of the same field to note any newly arrived (i.e., moving) objects. More ambitious orbital linkage protocols and operating at lower signal-to-noise ratios are also assumed. These study reports are not yet complete, so it is not possible to make detailed quantitative comparisons. However, preliminary work suggests they will claim substantially greater search efficiency than the ground-based systems considered herein. The reason for this difference is that these systems plan on using ambitious optical and camera designs and optimized sky coverage strategies that have not yet been fully tested, whereas we decided to provide estimates based upon proven methods and

readily achievable technologies. Nevertheless, if these next-generation surveys can perform as advertised, they further strengthen the cost/benefit of ground-based survey systems over what is reported here.

Space-Based Systems and Combined Ground- and Space-Based Systems: Telescopes in Venus-like orbits at 0.7 AU have several advantages over their ground-based counterparts: they can cover more sky, they have short orbital periods that allow them to observe objects near perihelion missed by ground-based surveys, and the objects themselves are brighter due to fuller phases (smaller phase angles) and smaller heliocentric distances. For these reasons, these systems are very efficient in terms of cataloging PHOs. All of the space-based systems that we considered were more efficient in cataloging PHOs than a single ground-based search system (see Figure 6-11). Search telescopes of equal aperture sizes located at low-Earth orbit (LEO) and at the second Lagrange point (L_2) had comparable cataloging efficiencies and, because of their proximity to Earth, each had a better warning efficiency than comparable systems in Venus-like orbits. The cataloging efficiency, and particularly the warning efficiency, of the systems in Venus-like orbits could be improved by adding a ground-based system (see Figures 6-13(a) and 6-13(b)).

Cost/Benefit Ratios: From Table 8-5 and the Tables in Appendix 5, it is noted that, for all the nominal and maximum hazard models under consideration, the benefits derived from all the search systems match or exceed their costs within the first year of operation. That is, the “break even” year for the systems assumed to begin in 2008 is the very same year. This is true whether or not one considers the global hazards from the larger PHOs. For a few of the minimum hazard cases in Appendix 5, this break even year can be one or two years after the initiation of the survey. As is evident from these charts, the cost/benefit ratios for any of the systems considered, whether they are for 10, 20 or 100 years, are extremely favorable. Some systems are more efficient than others, some are less expensive, some do (and do not) reach the stated goal in 10 years, but all of them have extremely high returns on investment.

9.3 Space-Based Systems Verses Ground-Based System Performance

A number of ground-based, space-based, and networked systems are capable of meeting the goal of retiring 90% of the risk from sub-kilometer sized PHOs. Space-based systems and mixed space-based/ground-based systems will generally accomplish the goal more quickly than single or multiple ground-based search systems but this increased efficiency, and hence shorter completion time, can come at a higher cost. In general, the mixed space- and ground-based systems do not have as attractive a cost/benefit ratio as either the space-based or ground-based systems alone. In a mixed system, the more capable space-based system will dominate the results and the addition of the ground-based system brings little extra cataloging capability for the extra cost. If a decision is made to meet the above goal with the next generation of PHO searches within ten years, and if one accepts the experience-based assumptions that went into the simulations, then the only option is to use space-based systems. However, some large aperture, wide field-of-view, ground-based systems can achieve the goal in less than 20 years. In addition, ground-based systems can be repaired, upgraded and provided with improved capability as the search continues so that they have far longer useful lifetimes than space-based systems.

9.4 Time And Expense Required To Complete The Survey Goal

Depending upon the time or expense constraints assumed, there are a number of options available for meeting the stated goal to retire 90% of the sub-global hazard. For a ten-year survey interval constraint, Figure 9-3 plots the cost of the systems versus the fraction of the sub global risk remaining at the end of the 10-year interval. Figure 9-4 plots the costs for various systems versus the number of survey years required to meet the goal. In both plots, the most attractive systems (i.e., lowest cost, highest efficiency) would be nearest the plot origin. Each plotted point is labeled with the system characteristics. For example, the point in the upper left of Figure 9.3 is a 1-meter telescope in a Venus-like orbit together with a 4-meter ground-based telescope. MK, KP, NN, NS, NNS refer, respectively, to Mauna Kea, Kitt Peak, North-North, North-South, and two collocated northern telescopes together with a single southern hemisphere telescope. There are large uncertainties in both the horizontal and vertical placement of these points, so that systems that appear close to one another on these plots should be considered comparable.

It is evident from these two plots that if one insists upon meeting the stated goal within 10 years, then only the 1- and 2-meter aperture systems in Venus-like orbits will provide the cataloging efficiency to accomplish this goal. On the other hand, Figure 9-4 shows that there are some less costly space- and ground-based options available if more than 10 years are allowed to meet the goal. For cataloging PHOs, the addition of a ground-based telescope in conjunction with a space-based system is not cost effective. Telescopes at LEO are as efficient, but less expensive, than comparable systems located at the L_2 Lagrange point. For cataloging PHOs using ground-based systems, the superiority of the Mauna Kea sites to those in the American southwest is evident as is the relatively small improvement gained by placing similar telescopes in the northern and southern hemispheres versus collocating both telescopes. Despite the numerous options explored here, there are likely to be some cost effective systems that have not been considered. This report offers only a preliminary assessment of some of the possibilities. When the time and cost constraints are well understood for the next generation of PHO search surveys, a future detailed cost/benefit study will need to define a particular, optimal system that meets the requirements.

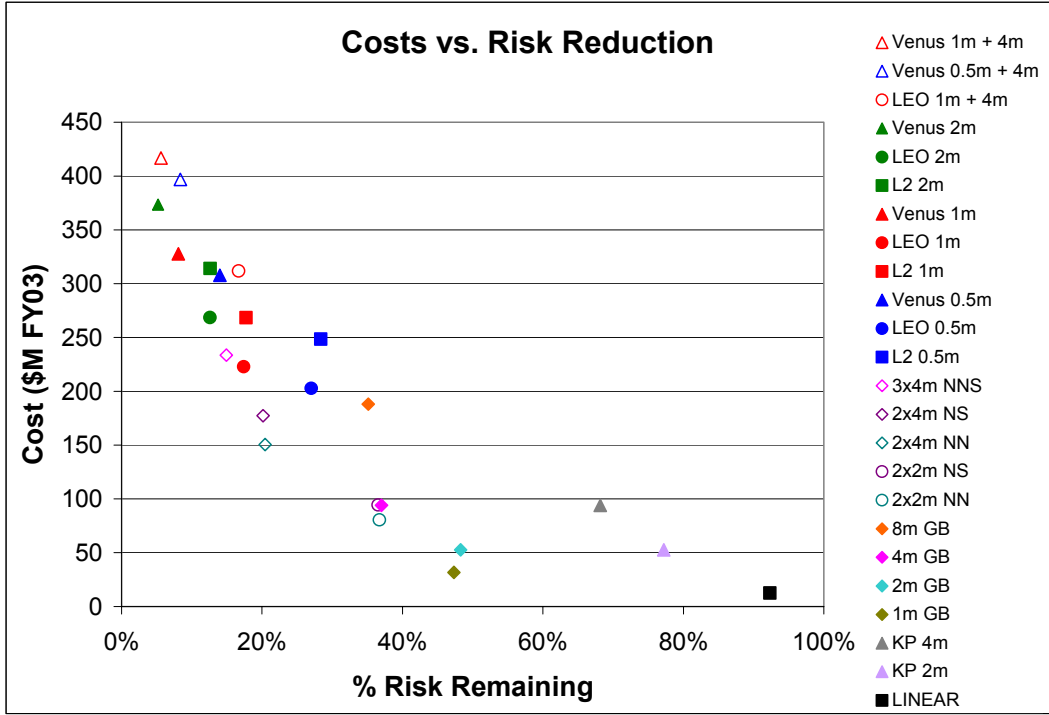


Figure 9-3. For various ground-based, space-based, and combined search systems, the system cost is plotted versus the % of the sub-global risk remaining after a 10-year survey.

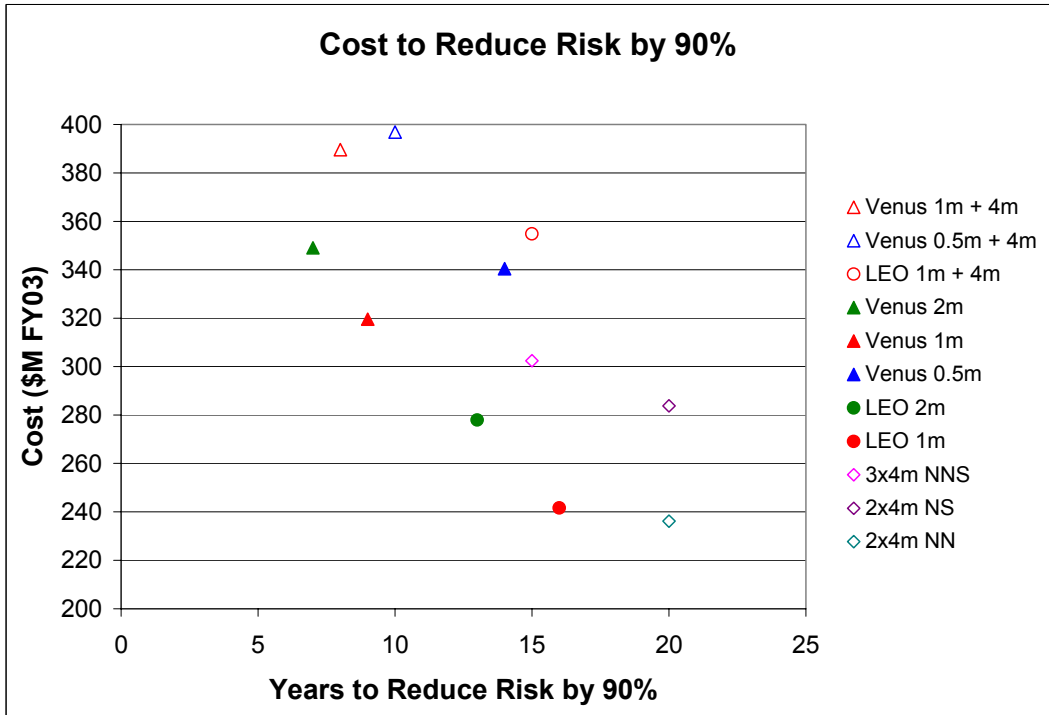


Figure 9-4. The cost of various space-based and ground-based search systems are plotted against the number of search years required to reduce by 90% the sub-global risk from impacts by sub-kilometer sized objects.

10 RESPONSES TO THE CHARTER QUESTIONS

1. What are the smallest objects for which the search should be optimized?

In the view of the Team, future goals related to searching for potential Earth impacting objects should be stated explicitly in terms of the statistical risk eliminated (or characterized). The recommended goal is to eliminate 90% of the statistical hazard related to sub-kilometer objects. These are objects (almost entirely asteroids) that will not cause global environmental effects, but may cause considerable local or regional damage. The analysis of the Team indicates that a catalog 90% complete to a diameter of 140 meters will satisfy this recommendation.

2. Should comets be included in anyway in the survey?

Earth-threatening, long-period comets present a vexing problem since their returns cannot be predicted long in advance. They would likely be discovered only a few months prior to a potentially catastrophic collision with Earth. Their velocities, and hence impact energies, would be relatively high and the warning time could be very short. However, in Sections 2.5, 2.6 and 3.5, the case is made that comets represent only about 1% of the hazard from near-Earth asteroids. The frequency with which long-period comets (of any size) closely approach the Earth is roughly one-hundredth the frequency with which sub-kilometer NEAs closely approach the Earth. For an impacting comet and NEA of equal sizes, the comet's impact velocity would be a factor of about 2 larger than an impacting NEA (factor of 4 in energy), but the density of the NEA would be expected to be nearly a factor of four larger so the energies of both impactors would be comparable. For those very rare, large NEOs (>5 km) that would be expected to cause major global extinction events, the number of cometary impact events may be nearly comparable to the number of impacts from near-Earth asteroids. However, for the far more frequent impacts by smaller objects, near-Earth asteroids completely dominate the impact hazard.

At least for the next generation of NEO surveys, the limited amount of resources available for near-Earth object searches would be better spent on finding and cataloging Earth-threatening near-Earth asteroids. The same system would also discover the far less plentiful near-Earth, short-period comets and, in addition, provide an advance warning system for threatening long-period comets.

3. What is technically possible?

Current technology offers NEO detection and cataloging capability several orders of magnitude more capable than the current operating systems. The question of performance achieved for NEO search is generally not technically driven, but is resource driven. This report outlines a variety of search system examples, spanning a factor of ~100 in search capability, all of which are quite possible using current technology. Specifically, as shown by the analysis presented in this report, it is quite possible to construct a NEO search and cataloging system, that, when operated over a period of 7-20 years, allows a catalog 90% complete to 140-meter diameter. Such systems, depending on which implementation is chosen, could in addition provide 60-90% effective warning for impacts of NEOs as small as those capable of causing significant air blasts (about 50 meters in diameter).

4. How would the expanded search be done?

There are a number of cost/benefit effective options for executing an expanded search that would vastly reduce the risk posed by potential NEO impacts. The Team identified a series of specific ground-based, space-based and mixed ground/space-based systems that could accomplish the next generation of search. The choice of specific systems will depend on the time allowed for the search and the resources available. Generally, space-based systems are more effective than ground-based systems when generating a catalog complete to a specified level. In addition, space-based systems can have more effective warning capabilities. However, the advantages of space-based systems come at an increased cost.

5. What would it cost?

Depending on the time allocated to accomplish the search, the Team identified systems that could achieve a 90% complete catalog for potentially hazardous objects (PHOs) 140 meters and larger, with costs ranging between \$236M and \$397 M. All of these systems have risk reduction benefits which vastly exceed the costs of system acquisition and operation.

6. How long would the search take?

A period of 7-20 years is sufficient to generate a catalog 90% complete down to 140 meters in diameter, which would eliminate 90% of the risk for sub-kilometer objects. The specific interval depends on the choice of search technology and the investment allocated. The most rapid method to reaching the recommended goal identified by the Team was to launch a 1-2 meter aperture telescope into a Venus-trailing orbit. Such systems could accomplish the goal in less than ten years. Generally, ground-based systems will take longer to reach the goal. For example a network of 3 ground-based 4-meter telescopes dedicated to searching for PHOs could accomplish the goal in 15 years.

7. Is there a transition size above which one catalogs all the objects, and below which the design is simply to provide warning?

Analysis conducted by the Team indicates that, if sufficient time and resources are allocated, a substantially complete catalog of PHOs with sizes down to the significant air blast limit (about 50 meters) could be constructed. Below this limit, there is relatively little direct damage caused by the object. Over the 7-20 year interval (starting in 2008) during which the next generation search would be accomplished, the Team suggests that cataloging is the preferred approach down to approximately the 140-meter diameter level and that the search systems would naturally provide 60-90% effective warning down to the 50-meter diameter level.

Recommendations

The Team has developed the following recommendations as a result of the analysis undertaken through this Science Definition Team effort:

Recommendation 1 – Future goals related to searching for potential Earth-impacting objects should be stated explicitly in terms of the statistical risk eliminated (or characterized) and should be firmly based on cost/benefit analysis.

This recommendation recognizes that searching for potential Earth impacting objects is of interest primarily to eliminate the statistical risk associated with the hazard of impacts. The “average” rate of destruction due to impacts is large enough to be of great concern. However, the event rate is low. Thus, a search to determine if there are potentially hazardous objects (PHOs) likely to impact the Earth within the next few hundred years is prudent. Such a search should be executed in a way that eliminates the maximum amount of statistical risk per dollar of investment.

Recommendation 2 – Develop and operate a NEO search program with the goal of discovering and cataloging the potentially hazardous objects sufficiently to eliminate 90% of the risk associated with the sub-kilometer members of this population.

The above goal is sufficient to reduce the average casualty rate from about 300 per year to less than 30 per year. Any such search would find essentially all of the larger objects remaining undiscovered after 2008, thus eliminating the global risk from these larger objects. Over a period of 7-20 years, there are a number of system approaches that are capable of meeting this search metric, with quite good cost/benefit ratios.

Recommendation 3 – Release a NASA Announcement of Opportunity (AO) to allow system implementers to recommend a specific approach to satisfying the goal stated in Recommendation 2.

Based upon our analysis, the Team is convinced that there are a number of credible, current technology/system approaches that can satisfy the goal stated in Recommendation 2. The various approaches will have different characteristics with respect to the expense and time required to meet the goal. The Team relied on engineering judgment and system simulations to assess the expected capabilities of the various systems and approaches considered. While the Team considers the analysis results to be well-grounded by current operational experience, and thus, a reasonable estimate of expected performance, the Team did not conduct analysis at the detailed system design level for any of the systems considered. The next natural step in the process of considering a follow-on to the current Spaceguard program would be to issue a NASA Announcement of Opportunity (AO) as a vehicle for collecting search system estimates of cost, schedule and the most effective approaches for satisfying the recommended goal. The AO should be specific with respect to NASA’s position on the trade between cost and time to completion of the goal.

REFERENCES

- Ben-Henahem, A. 1975. Source Parameters of the Siberian Explosion of June 30, 1908, from Analysis and Synthesis of Signals at Four Stations. *Phys. Earth Planet. Inter.* 11, 1-35.
- Bland, P.A. and N.A. Artemieva, 2003. Efficient Disruption of Small Asteroids by Earth's Atmosphere. *Nature*, v. 424, 288-291.
- Boslough, M. B. E. and D. A. Crawford, 1997. Shoemaker-Levy 9 and Plume-Forming Collisions on Earth. Near-Earth Objects, the United Nations International Conference: Proceedings of the International Conference held April 24-26, 1995, in New York, NY. Edited by John L. Remo, 1997. *Annals of the New York Academy of Sciences*, v. 822, 236-282.
- Bottke, W. F., R. Jedicke, A. Morbidelli, J.-M. Petit and B. Gladman, 2000. Understanding the Distribution of Near-Earth Asteroids. *Science*, v. 288, 2190-2194.
- Bottke, W. F., A. Morbidelli, R. Jedicke, J. Petit, H. F. Levison, P. Michel, and T. S. Metcalfe 2002a. Debaised Orbital and Absolute Magnitude Distribution of the Near-Earth Objects. *Icarus* 156, 399-433.
- Bottke, W. F., D. Vokrouhlicky, D. P. Rubincam, and M. Broz, 2002b. The Effect of Yarkovsky Thermal Forces on the Dynamical Evolution of Asteroids and Meteoroids. In *Asteroids III* (W.F. Bottke, A. Cellino, P. Paolicchi, and R.P. Binzel, Eds), U. of Arizona Press, Tucson, 395-408.
- Bowell, E., 2003. Personal communication.
- Bowell, E.; B. Hapke, D. Domingue, K. Lumme, J. Peltoniemi, and A. Harris, 1989. Application of Photometric Models to Asteroids (Appendix: The IAU Two-Parameter Magnitude System for Asteroids). In *Asteroids II* (R.P. Binzel, T. Gehrels, and M. Matthews, Eds.), U. of Arizona Press, Tucson, 549-556.
- Brown, P., R.E. Spalding, D.O. ReVelle, E. Tagliaferri, and S.P. Worden, 2002. The Flux of Small Near-Earth Object Colliding with the Earth. *Nature*, v. 420, 294-296.
- Canavan, G. H., 1995, Cost and Benefit of Near-Earth Object Defences, Proceedings of the Planetary Defence Workshop, Lawrence Livermore National Laboratories, CONF-9505266, 273-298.
- Carusi, A., L. Kresak, E. Perozzi, and G. B. Valsecchi, 1987. High-order Librations of Halley-type Comets. *Astron. Astrophys.* v.187, 899.
- Chesley, S. R. and T.B. Spahr, 2003. Earth Impactors: Orbital Characteristics and Warning Times. In *Mitigation of Hazardous Impacts Due to Asteroids and Comets*, Cambridge Univ. Press (in press).

- Chesley, S.R. and S.N. Ward, 2003. A Quantitative Assessment of the Human and Economic Hazard from Impact-generated Tsunami, submitted to *Environmental Hazards*.
- Chyba, C. F., P. J. Thomas, and K. J. Zahnle, 1993. The 1908 Tunguska Explosion - Atmospheric Disruption of a Stony Asteroid. *Nature*, v. 361, 40-44.
- D'Abramo, G., A. W. Harris, A. Boattini, S. C. Werner, and G. B. Valsecchi, 2001. A Simple Probabilistic Model to Estimate the Population of near-Earth Asteroids. *Icarus*, v. 153, 214-217.
- Duncan, M., T. Quinn and S. Tremaine, 1987. The Formation and Extent of the Solar System Comet Cloud. *Astron. J.* v. 94, 1330-1338.
- Duncan, M., T. Quinn, and S. Tremaine, 1988. The Origin of Short-period Comets. *Astrophysical Journal Letters*, v. 328, L69 – L73.
- Duncan, M.J. and H.F. Levison, 1997. A Scattered Comet Disk and the Origin of Jupiter Family Comets. *Science*, v. 276, 1670-1672
- Everhart, E., 1967. Intrinsic Distributions of Cometary Perihelia and Magnitudes, *Astronomical Journal*, v. 72, 1002-1011.
- Farinella, P., L. Foschini, C. Froeschle, R. Gonczi, T. J. Jopek, G. Longo, and P. Michel, 2001. Probable Asteroidal Origin of the Tunguska Cosmic Body. *Astronomy and Astrophysics*, v. 377, 1081-1097.
- Gladman, B.J., F. Migliorini, A. Morbidelli, V. Zappala, P. Michel, A. Cellino, C. Froeschle, H.F. Levison, M. Bailey and M. Duncan, 1997. Dynamical Lifetimes of Objects Injected into Asteroid Belt Resonances. *Science*, v. 277, 197-201.
- Harris, A.W., 2002. A New Estimate of the Population of Small NEAs. *Bulletin of the American Astronomical Society*, #34, 835.
- Hills, J.G. and M.P. Goda, 1993. The Fragmentation of Small Asteroids in the Atmosphere, *Astronomical J.*, v. 105, 1114-1144.
- Ivezic, Z. and 32 colleagues, 2001. Solar System Objects Observed in the Sloan Digital Sky Survey Commissioning Data. *Astronomical Journal*, v. 122, 2749-2784.
- Jedicke, R., 1996. Detection of Near-Earth Asteroids Based upon Their Rates of Motion. *Astron. J.* v. 111, 970.
- Jedicke, R. and T.S. Metcalfe, 1998. The Orbital and Absolute Magnitude Distributions of Main Belt Asteroids. *Icarus*, v. 131, 245-260.

- Jedicke, R., J. Larsen, and T. Spahr, 2002. Observational Selection Effects in Asteroid Surveys. In *Asteroids III* (W.F. Bottke, A. Cellino, P. Paolicchi, and R.P. Binzel, Eds), U. of Arizona Press, Tucson, 71-87.
- Jedicke, R., A. Morbidelli, J.-M. Petit, T. Spahr, and W.F. Bottke, 2003. Earth and Space-based NEO Survey Simulations: Prospects for Achieving the Spaceguard Goal. *Icarus*, v. 161, 17-33.
- Jet Propulsion Laboratory, Near Earth Object Program website, <http://neo.jpl.nasa.gov>, retrieved August 7, 2003.
- Kenkel, D., 2000, Using Estimates of the Value of a Statistical Life in Evaluating Regulatory Effects, <http://www.ers.usda.gov/publications/mp1570/mp1570d.pdf>, retrieved July 16, 2003.
- Kresak, L., 1979. Dynamical Interrelations Among Comets and Asteroids. In *Asteroids* (T. Gehrels, Ed.), U. of Arizona Press, Tucson, 289-309.
- Krinov, E. L., 1963. The Tunguska and Sikhote-Alin Meteorites. In *the Moon, Meteorites, and Comets* (eds. B. M. Middlehurst and G. P. Kuiper). U. of Chicago, Chicago, IL, 208-243.
- Lambour, R., E. Rork, and E. Pearce. 2003. Modeling the Sky Background and Its Impact on Electro-Optic Sensors. MIT Lincoln Laboratory, in press.
- Levison, H.F., 1996. Comet Taxonomy. In *Completing the Inventory of the Solar System*. (T. W. Rettig and J. M. Hahn, Eds.) ASP Conf. Series 107, 173-191.
- Lamy, P., I. Toth, Y.R. Fernandez, H.A. Weaver, 2003. The Sizes, Shapes, Albedos, and Colors of Cometary Nuclei. In *Comets II*, U. of Arizona Press (in press).
- Levison, H.F. and M.J. Duncan, 1994. The Long-term Dynamical Behavior of Short-period Comets. *Icarus*, v. 108, 18-36.
- Levison, H.F. and M.J. Duncan, 1997. From the Kuiper Belt to Jupiter-family Comets: The Spatial Distribution of Ecliptic Comets. *Icarus*, v. 127, 13-32.
- Levison, H.F., L. Dones, and M.J. Duncan, 2001. The Origin of Halley-Type Comets: Probing the Inner Oort Cloud. *Astron. J.*, v. 121, 2253-2267.
- Levison, H.F., A. Morbidelli, L. Dones, R. Jedicke, P.A. Wiegert, and W.F. Bottke, 2002. The Mass Disruption of Oort Cloud Comets. *Science*, v. 296, 2212-2215. [For a detailed treatment, see <http://www.boulder.swri.edu/~hal/PDF/disrupt.pdf>]
- Magnier, E. and D. Jewett, 2003, Personal communication.
- Marsden, B.G., 1992. To Hit or Not to Hit. Proceedings, Near-Earth Objects Interception Workshop. (G.H. Canavan, J.C. Solem, J.D.G. Rather, eds.). Los Alamos National Laboratory, Los Alamos, NM. 67-71.

- Marsden, B.G. and Steel, D.I., 1994. Warning Times and Impact Probabilities for Long-period Comets. In, *Hazards Due to Comets and Asteroids* (T. Gehrels, ed.). U. of Arizona press, 221-239.
- Melosh, H.J., 2003. Impact-generated Tsunamis: An Over-rated Hazard. *Lunar & Planetary Science XXXIV*, 2013.
- Michel, P., F. Migliorini, A. Morbidelli and V. Zappala, 2000. The Population of Mars-crossers: Classification and Dynamical Evolution. *Icarus*, v. 145, 332-347.
- Migliorini, F., P. Michel, A. Morbidelli, D. Nesvorny and V. Zappala, 1998. Origin of Earth-crossing Asteroids: a Quantitative Simulation. *Science*, v. 281, 2022-2024.
- Morbidelli, A. and D. Nesvorny, 1999. Numerous Weak Resonances Drive Asteroids Toward Terrestrial Planets Orbits. *Icarus*, v. 139, 295-308.
- Morbidelli, A., 2001. *Modern Celestial Mechanics: Aspects of Solar System Dynamics*. Gordon and Breach, London, U.K., in press.
- Morbidelli, A., R. Jedicke, W.F. Bottke, P. Michel, and E.F. Tedesco, 2002a. From Magnitudes to Diameters: The Albedo Distribution of Near Earth Objects and the Earth Collision Hazard. *Icarus* 158, 329-342.
- Morbidelli, A., W. F. Bottke, Ch Froeschle, and P. Michel. 2002b. Origin and Evolution of Near-Earth Objects. In *Asteroids III* (W.F. Bottke, A. Cellino, P. Paolicchi, and R.P. Binzel, Eds), U. of Arizona Press, Tucson, 409-422.
- Morrison, D., 1992. *The Spaceguard Survey: Report of the NASA International Near-Earth-Object Detection Workshop*. NASA, Washington, D.C.
- National Center for Geographic Information and Analysis (NCGIA), <http://www.ciesin.org/datasets/gpw/globldem.doc.html>, retrieved August 7, 2003.
- National Council on Economic Education (NCEE), 2002. A Case Study: Gross Domestic Product - December 2002, <http://www.econedlink.org/lessons/index.cfm?lesson=EM225>, retrieved July 16, 2003.
- Nesvorny, D., S. Ferraz-Mello, M. Holman, A. Morbidelli, 2002. Regular and Chaotic Dynamics in the Mean Motion Resonances: Implications for the Structure and Evolution of the Main Belt. In *Asteroids III* (W. F. Bottke, A. Cellino, P. Paolicchi, and R.P. Binzel, Eds), U. of Arizona Press, Tucson, 379-394.
- Öpik, E.J., 1951. Collisional Probabilities with the Planets and the Distribution of Interplanetary Matter. *Proceedings, Royal Irish Academy*, v. 54, 165-199.

- Öpik, E.J., 1976. *Interplanetary Encounters*. Elsevier, Amsterdam, The Netherlands.
- Rabinowitz, D.L., 1994. The Size and Shape of the Near-Earth Asteroid Belt. *Icarus*, v.111, 364-377.
- Rabinowitz, D.L., E. Bowell, E. M. Shoemaker, and K. Muinonen, 1994. The Population of Earth-crossing Asteroids. In *Hazards Due To Comets and Asteroids* (T. Gerhels, Ed), U. of Arizona Press, Tucson, 285-312.
- Rabinowitz, D.L., E. Helin, K. Lawrence, and S. Pravdo, 2000. A Reduced Estimate of the Number of Kilometre-sized Near-Earth Asteroids. *Nature*, v. 403, 165-166.
- Rhodes, R., 1986. *The Making of the Atomic Bomb*. Simon & Schuster.
- Rickman, H., L. Kamel, M.C. Festou, and C. Froeschlé, 1987. Estimates of Masses, Volumes and Densities of Short-period Comet Nuclei. Symposium on the Diversity and Similarity of Comets, ESA SP-278 edited by E.J. Rolfe and B. Battrick, 471-481.
- Roach, F.E. and Janet L. Gordon, 1973. *The Light of the Night Sky*, D. Rediel Publishing Company, Dordecht, Holland.
- Schmidt-Kaler, T. and P. Rucks, 1997. Telescope Costs and Cost Reduction, SPIE v. 2871, 635-640.
- Sekanina, Z., 1983. The Tunguska Event - No Cometary Signature in Evidence. *Astronomical Journal*, v. 88, 1382-1413.
- Sekanina, Z. and D.K. Yeomans, 1984. Close Encounters and Collisions of Comets with the Earth. *Astronomical Journal*, v. 89, 154-161.
- Shoemaker, E.M. 1983. Asteroid and Comet Bombardment of the Earth. *Annual Review of Earth and Planetary Sciences*, v. 11, 461-494.
- Shoemaker, E.M., 1995. Report of the Near-Earth Objects Survey Working Group. NASA Office of Space Science, Solar System Exploration Office.
- Shoemaker, E.M. and R.F. Wolfe, 1982. Cratering Time Scales for the Galilean Satellites. In, *Satellites of Jupiter* (David Morrison, Ed.). U. of Arizona Press, 275-339.
- Shoemaker, E.M., R.S. Wolfe, and C.S. Shoemaker, 1990. Asteroid and Comet Flux in the Neighborhood of Earth. In, *Global Catastrophes in Earth History* (V.L. Sharpton and P.D. Ward, Eds.). Geological Society of America, Special Paper 247, 155-170.
- Stepp, L., L. Daggert and P. Gillett, 2002, Estimating the Costs of Extremely Large Telescopes, Paper and Presentation Submitted to the SPIE Conference, Waikoloa, HI, August 22 - 28, 2002.

Paper and presentation, http://www.aura-nio.noao.edu/documentation/SPIE_Paper.html, retrieved May 14, 2002.

Stuart, J.S., 2001. A Near-Earth Asteroid Population Estimate from the LINEAR Survey. *Science*, v. 294, 1691-1693.

Stuart, J.S., 2003. Observation Constraints on the Number, Albedos, Sizes, and Impact Hazards of the Near-Earth Asteroids. MIT Ph.D. thesis.

Toon, O.B., K. Zahnle, D. Morrison, R.P. Turco, and C. Covey, 1997. Environmental Perturbations Caused by the Impacts of Asteroids and Comets. *Reviews of Geophysics*, v. 35, 41-78.

United States Bureau of the Census, International Database website, <http://www.census.gov/ipc/www/worldpop.html>, retrieved July 16, 2003.

Van Dorn, W.G., B. LeMehaute, L.-S. Hwang, 1968. *Handbook of Explosion-generated Water Waves. Vol. 1 – State of the Art*. Tetra Tech, Pasadena, CA.

Vasilyev, N. V., 1998. The Tunguska Meteorite Problem Today. *Planetary and Space Science*, v. 46, 129-150.

Ward, S.N., and E. Aspaugh, 2000. Asteroid Impact Tsunami: A Probabilistic Hazard Assessment. *Icarus*, v. 145, 64-78.

Weissman, P.R., 1997. Long-period Comets and the Oort Cloud. In, Near-Earth Objects: The United Nations International Conference (J.L. Remo, Ed.). *Annals of the New York Academy of Sciences*, v. 822, 67-95.

Weissman, P.R., 1990. The Cometary Impactor Flux at Earth. In *Global Catastrophes in Earth History*. (V. L. Sharpton and P. D. Ward, Eds). 171-180. Geo. Soc. Am. Special Paper 247.

Weissman, P.R., W.F. Bottke, and H. Levison, 2002. Evolution of Comets into Asteroids. In *Asteroids III* (W.F. Bottke, A. Cellino, P. Paolicchi, R. Binzel, Eds.) U. of Arizona Press, Tucson, 669-686.

Weissman, P.R. and S.C. Lowry, 2003. The Size Distribution of Jupiter-family Cometary Nuclei. LPSC 34 (abstract), in press.

Werner, S.C., A.W. Harris, G. Neukum, and B.A. Ivanov, 2002. NOTE: The Near-Earth Asteroid Size-Frequency Distribution: A Snapshot of the Lunar Impactor Size-Frequency Distribution. *Icarus*, v. 156, 287-290.

Wetherill, G.W., 1979. Steady State Populations of Apollo-Amor Objects. *Icarus*, v. 37, 96-112.

Whiteley, R.J. and D.J. Tholen, 1998. *Icarus*, v. 136, Issue 1, 154-167.

Wiegert, P. and S. Tremaine, 1999. The Evolution of Long-period Comets. *Icarus*, v. 137, 84-121.

Williams, G. V. and T. B. Spahr, 2003. Personal communication.

Wisdom, J., 1983. Chaotic Behavior and the Origin of the 3/1 Kirkwood Gap. *Icarus*, v. 56, 51-74.

World Bank Group, 2003. <http://www.worldbank.org/depweb/english/modules/economic/gnp>, retrieved July 16, 2003.

**APPENDIX 1 - 1998 Statement before Subcommittee on Space and
Aeronautics**

**Statement of
Dr. Carl Pilcher
Science Director, Solar System Exploration
Office of Space Science
National Aeronautics and Space Administration
Before the
Subcommittee on Space and Aeronautics
Committee on Science
House of Representative
May 21, 1998**

Mr. Chairman and Members of the Subcommittee:

I am pleased to have this opportunity to appear before the Subcommittee today to discuss NASA's current efforts and future plans to inventory and characterize the population of Near Earth Objects (NEOs).

Background

This Committee has been a leader in focusing attention on the importance of cataloging and characterizing Earth-approaching asteroids and comets. In 1992, the Committee on Science directed that NASA sponsor two workshop studies, the NEO Detection Workshop, which was chaired by NASA, and the NEO Interception Workshop, which was chaired by the Department of Energy. In March 1993, the Science Committee held a hearing to review the results of these two workshops. In 1995, at the Committee's request, NASA conducted a follow-up study which was chaired by the late Dr. Gene Shoemaker. Each of these studies stressed the importance of characterizing and cataloging NEOs with diameters larger than 1 km within the next decade. We have taken steps to put us on a path to achieving this goal. I am here today to tell you about those steps, as well as to bring you up to date on the rich program of space missions to NEOs and related objects.

The NEO population is derived from a variety of scientifically interesting sources including planetesimal fragments and some Kuiper belt objects. Indeed, the Office of Space Science Strategic Plan includes as a specific goal "...to complete the inventory and characterize a sample of Near Earth Objects down to 1 km diameter". While the threat of a catastrophic collision is statistically small, NASA has a vigorous program of exploration of NEOs planned, including both asteroids and comets.

There has been much recent discussion about the potential threat posed by NEOs, but NASA has long been interested in them from a scientific standpoint. NEO investigations have had to compete for support against a number of other compelling science programs; funding selection

criteria were based principally on scientific merit. This approach has led to the detection of over 400 NEOs, including more than 100 objects larger than 1 km and to a rapid advancement of the technologies necessary for NEO detection. In fact, this research effort has demonstrated that we can inventory the NEO population in a reasonable time, about a decade, with an achievable increase in funding from recent levels.

A little less than a year ago, NASA initiated a study of its existing NEO research to determine how well we were doing in terms of reaching our goal of inventorying the population of NEOs larger than 1 km and characterizing a sample of them. While we have made some impressive strides, it became apparent that the funding levels resulting from scientific competitive review (\$1-1.5 M per year) was not sufficient to accomplish our goal. The detection of new NEOs in 1997, the last year for which we have statistics, is barely 10% of the rate needed to achieve the goal suggested in the Shoemaker report (detection of 90% of the NEO population larger than 1 km within a decade). In simple terms, we need to survey about 20,000 square degrees of sky a month for NEOs to a limiting brightness of approximately 20th magnitude to accomplish the inventory. To understand what this means, note that 20,000 square degrees is about half the sky and that magnitudes are a measure of apparent brightness—a 6th magnitude object is at the limit of detection for the human eye and 20th magnitude is almost 100,000 times fainter.

I would now like to describe briefly the existing search programs, NASA's plans to improve them, and some promising new research programs which we are considering. I will also comment on our joint activities with the Air Force Space Command. All of these efforts are directed toward increasing the rate of discovery of NEOs in order to reach our goal.

Status of Ongoing Search Programs

NASA's ground-based NEO program comprises three parts: Spacewatch, the Near-Earth Asteroid Tracking (NEAT) program, and the Lowell Near Earth Asteroid Survey (LONEOS).

Spacewatch

Spacewatch is a program at the University of Arizona, led by Dr. Tom Gehrels, which has done much of the pioneering work in the field of NEO detection. This group is responsible for more NEO discoveries than any other. The current Spacewatch Program searches 200 square degrees of sky per month to a depth of 21st magnitude. This year NASA is funding a new state-of-the-art focal plane camera for Spacewatch, which will lead to an 8-fold increase in the area of sky that they search each month (to 1600 square degrees per month). We hope in the future to assist them in their efforts to bring their new 1.8m telescope on line. This telescope will enable them to detect even fainter NEOs.

NEAT

NEAT is a program headed by Dr. Eleanor Helin at the Jet Propulsion Laboratory. NEAT uses a specialized camera, which is based on a 4096x4096 CCD array for use on the 1m GEODSS (Ground-based Electro-Optical Deep Space Surveillance) telescope, operated by United States Air Force Space Command (USAFSC) on Haleakala, Maui, Hawaii. This group is currently

limited by the number of nights per month on which they can observe the sky using the GEODSS system. They are presently observing six nights per month on one of the seven GEODSS telescopes. With recent improvements they are now able to search 800 square degrees per night (4800 square degrees per month) to about 20th magnitude. We have funded the construction of 2 more cameras, which we hope to install on two other GEODSS telescopes. This increase in the level of effort for NEO detection is being discussed in the NASA-USAFSC Partnership Council co-chaired by NASA Administrator Daniel Goldin and AFSC Commander Gen. Howell Estes. It is in principle possible to scan 21,000 square degrees a month with three cameras and full access to three of the GEODSS telescopes. It is important to note that the GEODSS system includes one southern hemisphere site.

While we certainly hope to increase our surveying ability using the GEODSS system, we are aware that it has other vital missions. NASA's FY 1999 budget request includes sufficient funding for the construction of four more NEAT cameras, which will enable us to equip all seven GEODSS telescopes. The final application of the funds will depend on the demonstration that the NEAT camera can support the existing mission of the GEODSS system as well as the search for NEOs. This matter is currently being reviewed by the Partnership Council on NEOs.

LONEOS

LONEOS is led by Dr. Ted Bowell at Lowell Observatory in Flagstaff, Arizona. This group has great potential (capability to observe 4,300 square degrees a month down to 20th magnitude); however, they have not yet reached this level of performance. We are funding an augmentation to buy a second focal plane CCD and to support additional software development in order to allow them to reach their performance objective.

NEW Search Programs

The increased interest in the search for NEOs has led to several recent proposals from new groups:

Catalina NEO Survey

We are supporting a new search program at the University of Arizona, which is headed by Mr. Steven Larson, to refurbish an existing telescope on Mount Lemon. When fully operational, this system will survey 8,000 square degrees of sky per month to a depth of 19th magnitude. This program will be fully operational within a year.

LINEAR

NASA is evaluating a proposal for support of a very promising search program from the MIT Lincoln Labs. This effort called LINEAR (Lincoln Near Earth Asteroid Research program) uses a state-of-the-art camera which was developed as a possible prototype for the next generation GEODSS detector. They are proposing to use a 1m telescope at their Experimental Test Site near Socorro, New Mexico, to survey 10,000 square degrees down to 21st magnitude each month.

With coordination of these different observational programs, NASA believes it is possible to obtain the level of sky coverage to the appropriate limiting magnitude required to complete the survey. NASA has already committed over \$3M this year, much of it to fund improvements to focal plane detectors, software, and electronics. NASA is committed to funding both existing and new search programs at, at least, the FY1998 level. We believe this is close to the level required to achieve our objective.

Space-Bases Missions Relevant to our Understanding of NEOs

The study of the physical characteristics of NEOs is a major focus of both ground-based research and space missions. The ground-based work includes NASA-supported radar imaging of NEOs utilizing the Arecibo Radio Telescope and spectroscopy of NEOs from optical/IR telescopes to determine their composition.

Several NASA missions will travel to asteroids and/or comets to provide us with exciting new scientific insights about these objects at the same time this information is valuable for any future effort to respond to an impact threat. Over the next decade NASA will invest approximately \$1B in these missions. Missions in flight or in development are:

1. **NEAR**, which will reach the near-Earth object Eros in January, 1999, orbit for one year to measure its surface and interior properties, and then land on Eros.
2. **CONTOUR**, which will fly by a set of three short-period comets and make the first detailed comparative study of cometary nuclei.
3. **STARDUST**, which will return a sample from the coma of short-period comet in 2006.
4. **ROSETTA**, is a European Space Agency (ESA) mission to comet P/Wirtanen. NASA is providing three ROSETTA orbiter instruments and support to eight U.S. co-investigators on other orbiter instruments.

Missions soon to enter development are:

1. **MUSES-C/N** with Japan to deploy a US-provided micro-rover on the surface of an NEO and to return a sample of the asteroid to Earth in 2006.
2. **DS-4/Championion** to land on a comet, measure its composition, test sampling and sample-return technologies for small bodies, and perhaps even return a sample.
3. **Pluto/Kuiper Belt Express** to survey one or more Kuiper belt objects before deflection into the inner solar system.

Concluding Remarks

The issues and challenges posed by NEOs are inherently international, and any comprehensive approach to addressing them must be international as well. Central areas of concern include coordination among NEO observers and orbit calculators around the globe and public notification should an object posing a significant hazard to Earth be discovered. NASA has begun discussing, with the international community, convening an international workshop to address these issues. The workshop will likely be held during the first half of 1999. The goal of this workshop will be to develop international procedures and lines of communication to ensure

that the best available accurate information about any potentially hazardous object is assembled and disseminated to the public in the shortest possible time.

To facilitate coordination among NASA-supported researchers, other agencies and scientists, and the international community, NASA is establishing an NEO Program Office. This Office will coordinate ground-based observations, ensure that calculated orbital elements for NEOs are based on the best available data and support NASA Headquarters in the continuing development of strategies for the exploration and characterization of NEOs. In the unlikely event that a potentially hazardous object is detected, the Office would coordinate the notification of both the observing community and the public of any Potentially Hazardous Asteroids discovered.

NASA is committed to achieving the goal of detecting and cataloging 90% of NEOs larger than 1 km in diameter within 10 years, and to characterizing a sample of these objects. We are developing and building instruments, and developing partnerships -- particularly with the Air Force -- which should lead to the necessary detection and cataloging capability being in place in 1-2 years. This capability will also allow us to detect and characterize many NEOs smaller than 1 km.

In summary, NASA's obligation and commitment is to ensure that we have the information necessary to understand the hazards posed by NEOs.

APPENDIX 2 - Study Charter

A Study to Determine the Feasibility of Extending the Search for NEOs to Smaller Limiting Diameters

Introduction

The Solar System Exploration Division (SSED) of the National Aeronautics and Space Administration (NASA) is currently working to discover all the Near Earth Objects (NEOs) with diameters larger than 1 km and to obtain good orbital information for them. Our metric for the current program is to discover 90% of the NEOs with diameters larger than 1 km and to obtain good orbital information for them by December 31, 2008. There has been an increasing interest by the public and by the Congress as to the wisdom of extending the current effort to objects smaller than one kilometer. The following study is being undertaken to determine:

1. What are the smallest objects for which the search should be optimized?
2. Should comets be included in any way in the survey?
3. What is technically possible?
4. How would the expanded search be done?
5. What would it cost?
6. How long would the search take?
7. Is there a transition size above which one catalogs all the objects, and below which the design is simply to provide warning?

It should be emphasized that NASA's current goal for NEO detection has not changed. However we believe that this study represents a prudent step. Finally, we must stress that NASA is a space agency. Space-based solutions are to be included. If the suggested solution to the extended search leads to a requirement for construction of large new ground-based facilities, the results may be forwarded to the National Science Foundation for their consideration.

Need for the Study

It might, at first, be thought that a simple extrapolation of the performance of present archetype ground based facilities would be all that is required. However, both the difficulty of detecting an object and the number to be detected increase dramatically with decreasing diameter. Current ground-based search efforts with 1m class telescopes do well to survey an appreciable portion of the night sky in one lunation to 20.5 magnitude. A simple extrapolation of the current ground-based effort to 100 m diameter objects would require searching the night sky each lunation to 25.5 magnitude. At some point as one goes from detection of objects with a diameters of 1 km down to smaller sizes (100 m or less), it will become impossible to perform such a search from the ground.

In addition, present models of the increase in the number of objects with decreasing object diameter suggest that there may be more than 100,000 objects with diameters greater or equal to 100m. Thus astrometric follow-up needed to obtain predictive orbits of small objects may prove prohibitive. Thus it may be that a dual approach—cataloging large NEOs and obtaining good

orbits for them and establishing an early warning system for recently discovered small objects to allow for a timely response on the ground—will be required.

Ground-based searches have used the visible portion of the spectrum, not only because of the need to work through the atmosphere of the Earth, but also because large-format infrared detector arrays have lagged the developments in the visible. If space-based detection systems are considered, the IR region of the spectrum may be superior. The issue must be examined.

Approach

The SSED director will select a Science and Definition Team (SDT) composed of 10 to 12 Scientists and Engineers including those currently leading NEO search teams, those who model the NEO population, and those with technical expertise in the design and operation of ground-based and space-based survey telescopes, including the areas of visible and IR large detector arrays, to address the questions above and to provide a non-advocate technical report to the Director of the SSED. NASA's Langley Research Center will provide logistical and technical support. The duration of the study is expected to be 9 months. The Minor Planets Program scientist will be an *ex officio* member of the SDT.

The team will be encouraged to document any joint uses of these facilities or the data that would be useful for other scientific studies

Liason with Our Sister Executive Branch Departments

The Department of Defense (DoD) may have the expertise relevant to the subject. An example of this would be the Space-Based Visible (SBV) sensor on the Midcourse Space Experiment (MSX) satellite. In addition, other elements of the Government may have some ancillary interest in the results of such a search effort (which might detect other classes of moving objects not germane to NASA's focused objectives). Because of these factors, DoD will be informed of the study in the event that DoD should wish to suggest possible team members or to participate in some other manner.

Expected Product

The agency looks forward to a technical report that may include recommendations that answer all the questions above together with a presentation to the Director of the SSED and other interested parties as required.

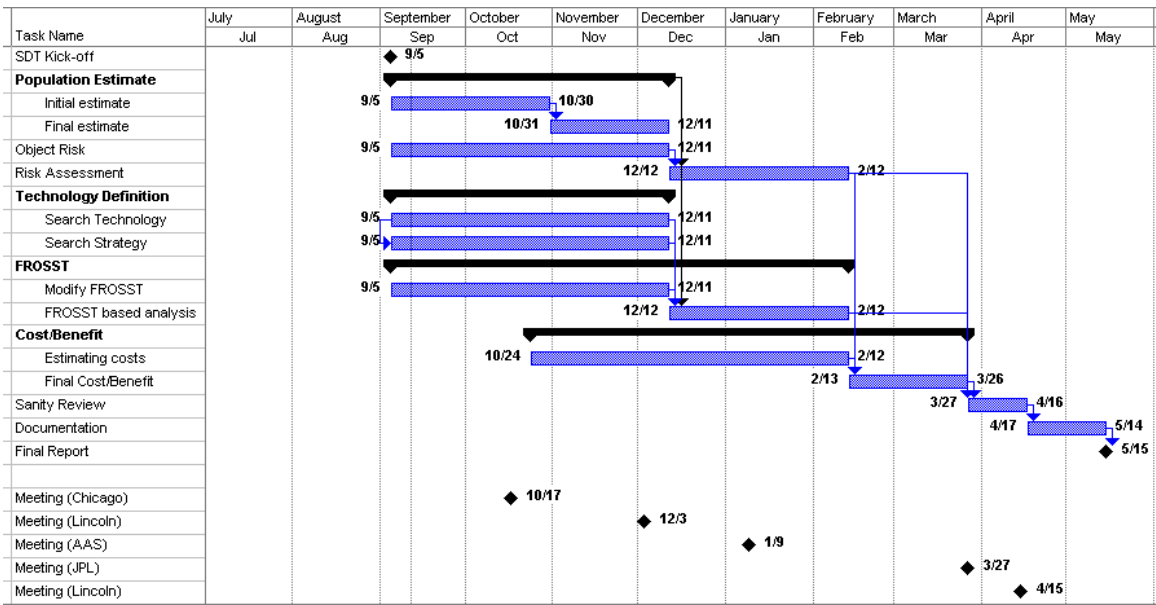


Figure A2-1. Project Schedule

APPENDIX 3 - Optimal Search Sensor Design

This appendix provides the analytical basis for the design of a telescope system optimized for search of broad areas of the sky. The costs involved in fabricating such systems are not addressed here.

Signal to Noise

In a sky-limited observation of a point source, the signal to noise is given by

$$\frac{S}{N} = \frac{I_* t A \Delta \nu}{\sqrt{I_s (\Delta \theta)^2 t A \Delta \nu}} = \left(\frac{I_*}{\Delta \theta} \right) \sqrt{\frac{t A \Delta \nu}{I_s}} \quad (1)$$

where I_* (phot/s/m²/Hz) is the photon flux density, t is the integration time, A is the collecting area, $\Delta \nu$ is the filter bandwidth, I_s (phot/s/m²/Hz/sr) is the sky surface brightness, $\Delta \theta$ is the angular size of the region used to do the photometry.

The collecting area of the telescope is just

$$A = \frac{\pi d^2}{4} \quad (2)$$

where D is the telescope diameter. Substituting, you get (for all else equal)

$$\frac{S}{N} \propto \frac{D}{\Delta \theta}. \quad (3)$$

For example, a 2m telescope with $\Delta \theta = 0.6''$ (where $''$ denotes arcsec) seeing is equivalent to a 4m with $\Delta \theta = 1.2''$ seeing. This is why the selection of the site on the basis of the seeing is such a big deal. In wide-field, ground-based imaging, where there is no real possibility of making adaptive optics corrections to the point spread function (PSF), image quality is of prime importance.

Ground-Based Case

Equation (3) shows that $\Delta \theta$ is crucial and is not at all a free parameter of the telescope design. How should $\Delta \theta$ be selected?

If $\Delta \theta$ is too large (compared to the PSF delivered by the optical system), you will indeed capture all the light under the PSF; but you will also grab all the light from the background sky. For example, if $\Delta \theta = 2''$, and I_s corresponds to 21 mag per sq. arcsec, then every measurement of a star or asteroid within the 2'' box will have to compete with $21 - 5 \log(2) = 19.5$ magnitude of sky. It is hard to win that way. On the other had, if $\Delta \theta$ is too small (compared to the PSF

delivered by the optical system), then sensitivity will suffer because the photometry will exclude some fraction of the light from the PSF.

The dividing line between “not too big” and “not too small” is Nyquist, or nearly Nyquist, sample the image. This means about 2 resolution elements per PSF full width half maximum (FWHM), and you could reasonably set $\Delta\theta = \text{seeing FWHM}$ when doing the photometry.

Metrics

A useful metric is “how long will it take to survey the whole sky to a given limiting magnitude?” This time is

$$T = \frac{4\pi}{\Omega} t \quad (4)$$

where t is the time required on each field to reach the desired S/N and Ω is the solid angle viewed per field.

For ground-based observations, we just saw that

$$\frac{S}{N} \propto \sqrt{At} \quad (5)$$

assuming all else is constant (i.e., same filter, seeing, sky brightness, etc) so that the time required to reach a given S/N on a given object scales like

$$t \propto \frac{1}{A}. \quad (6)$$

Then Eq (4) gives

$$T \propto \frac{4\pi}{\Omega} \frac{1}{A}. \quad (7)$$

So, $A\Omega$ is a suitable metric. If comparing systems on the ground with different seeing (e.g., Palomar compared with CTIO), it is easy to see that

$$T \propto \frac{4\pi}{\Omega} \frac{(\Delta\theta)^2}{A} \quad (8)$$

so the relevant metric would be $\frac{A\Omega}{(\Delta\theta)^2}$, and so on.

Some examples: (assume same seeing for each)

Keck, $D = 10\text{-m}$, $\Omega = 6 \times 8 \text{ arcmin}$, $A\Omega = 1 \text{ m}^2 \text{ deg}^2$.

CFHT, $D = 3.6\text{-m}$, $\Omega = 1 \text{ deg}^2$, $A\Omega = 10 \text{ m}^2 \text{ deg}^2$.

Pan Starrs, $D = 3.6\text{-m}$, $\Omega = 7 \text{ deg}^2$, $A\Omega = 70 \text{ m}^2 \text{ deg}^2$.

LSST nominal, $D = 3.6\text{-m}$, $\Omega = 7 \text{ deg}^2$, $A\Omega = 220 \text{ m}^2 \text{ deg}^2$.

CFHT, a smaller telescope than Keck, is 10 times more powerful as a survey telescope. LSST could be 200 times more powerful.

Space Case – Stars

In space, the PSF can be as small as the diffraction limited size

$$\theta_{diff} \approx \frac{\lambda}{D}. \quad (9)$$

For example, $D = 2\text{-m}$, $\lambda = 5000 \text{ \AA}$, $\theta_{diff} = 0.05''$.

More realistically, the jitter of the pointing direction, θ_{jitter} , will determine the PSF in most long integrations. Then, the signal to noise relations are the same except that $\Delta\theta \rightarrow \theta_{jitter}$.

$$\frac{S}{N} = \left(\frac{I_*}{\theta_{jitter}} \right) \sqrt{\frac{tA\Delta\nu}{I_S}} \quad (10)$$

or

$$\frac{S}{N} \propto \left(\frac{I_*}{\theta_{jitter}} \right) \sqrt{tA} \quad (11)$$

and the relevant metric is just $A\Omega$ again (or $A\Omega / (\theta_{jitter})^2$ if designs with different θ_{jitter} are compared).

Moving Objects

The analysis, so far, assumes that the objects we are searching for do not move out of a pixel over the time that we are integrating. Of course, since asteroids move, they will eventually move out of a single pixel; if we continue to integrate, only noise will accrue in the pixel, severely reducing detection performance.

A reasonable way to deal with trailing is to limit the integration time so that the trail length is less than, or comparable to, the natural scale offered by the telescope. For image size (seeing or, in space, jitter stability), $\Delta\theta$, this means limiting the exposure to

$$t \leq \frac{\Delta\theta}{V} \quad (12)$$

where V (arcseconds/sec) is the rate of motion of the fastest objects in which we are interested. Then the need to reach a particular depth within the time given by Eq. (12) determines how large a telescope is needed.

The time needed to cover the whole sky with a system in which the integration time is trail-limited is

$$T \propto \frac{4\pi}{\Omega} t \propto \frac{4\pi}{\Omega} \frac{\Delta\theta}{V} \quad (13)$$

and so, for objects with a given maximum allowable speed V the figure of merit is $\frac{\Omega}{\Delta\theta}$, where $\Delta\theta$ is the image quality delivered by the atmosphere (for a ground-based telescope) or the diffraction or jitter in space. But the total number of pixels is

$$N_p = \frac{\Omega}{(\Delta\theta)^2} \quad (14)$$

so the figure of merit can also be written

$$\frac{\Omega}{\Delta\theta} = N_p \Delta\theta \propto N_p \quad (15)$$

since $\Delta\theta$ is fixed. A trail-limited design has a diameter that is determined by using Eq. (12) for the integration time substituted into Eq. (1) for the S/N. The larger is V , the shorter is t , and the larger will be the required telescope diameter, scaling like $A \propto V$, or $D \propto V^{1/2}$, all else being equal. With the diameter D so fixed, the largest number of pixels optimizes the design.

This means that the most powerful survey instruments for the trail-limited case will be those with the largest diameters and the largest numbers of pixels.

The Main Points

1. Focal plane scale is not, in general, a free parameter. Each telescope provides a “natural scale”, whether it is the seeing scale (for a ground-based design) or the diffraction or jitter scale (in space).
2. Using pixel sizes much larger than the natural scale is equivalent to loss of sensitivity, no better than cutting the mirror aperture. Designs with non-optimal sampling of the focal plane must be explicitly justified.

APPENDIX 4 - Some Caveats on Predicting the Frequency of Tunguska-Type Events

Introduction

On the morning of June 30th, 1908, a powerful explosion blasted trees over an area greater than 2000 square kilometers in a remote region of central Siberia near the Podkamennaya Tunguska river basin (e.g., Vasilyev 1998). Although speculation about the cause of this event has gone on for nearly a century, the consensus of most experts is that the so-called Tunguska event was produced by the disruption of a small stony asteroid that entered Earth's atmosphere at hypersonic velocities (Chyba et al. 1993; Farinella et al. 2001). Additional details about the event, such as the entry trajectory and velocity of the bolide or the height and yield of the explosion, however, are still debated by numerous investigators around the world. The answers are important because scientists, policy experts, and the public need to know whether Tunguska-sized impactors pose a significant danger to human life on Earth.

In this essay, we briefly re-examine the Tunguska blast and raise some questions about particular aspects of the event that, to our knowledge, have yet to be satisfactorily modeled. It is unclear to our team whether more refined simulations of the Tunguska event would lead to results that are similar or highly discordant with previous work. For this reason alone, we believe that a renewed exploration of the Tunguska event in the near future is warranted.

The Tunguska Event: A Plume-Forming Impact

Many new insights into the nature of the Tunguska event over the last decade have come not from work on terrestrial impacts but from studies of what happened when the fragments of comet Shoemaker-Levy-9 (SL9) slammed into Jupiter in 1994. Computer simulations of the SL9 impact events, which are constrained by numerous ground- and space-based observations, provide a good template for understanding the Tunguska event. Boslough and Crawford (1997) claim that the atmospheric disruption of bolides from both SL9 and Tunguska can be characterized as “plume-forming” impacts, which they break down into three general, sometimes overlapping phases:

Entry phase. When a bolide penetrates a planetary atmosphere, it encounters gases at high speed that both slow it down and heat it up. A “bow shock” develops in front of the bolide where atmospheric gases are compressed and heated. Some of this energy is radiated to the bolide, causing ablation (i.e., melting and vaporization that removes material off the bolide's surface) and deformation. The rest of the energy is deposited along the long column created by the bolide's passage; much of the bolide's kinetic energy is lost in this manner. In some cases, aerodynamic stresses may overcome the bolide's tensile strength and cause it to catastrophically disrupt within seconds of entering the atmosphere. Airblast shock waves produced by this sequence of events may, in some cases, reflect off the surface (if one exists) and mimic the destruction produced by a nuclear weapon.

Fireball phase. The events taking place during the entry phase produce a hot mixture of bolide material and atmospheric gas called a fireball that is ballistically shot upward by the impact. Since it is incandescent, it radiates away energy in visible and near infrared wavelengths. Buoyant forces cause the fireball to rise because it is less dense than the surrounding atmosphere, creating an effect that is not unlike the characteristic “mushroom cloud” seen in nuclear explosions. Unlike a nuclear blast, however, the fireball's energy expands most easily along the low-density high sound speed entry column that was created by the bolide's passage. This phase can last several tens of seconds to minutes.

Plume phase. The expanding fireball (and associated debris) rushes back out the entry column, ultimately reaching altitudes of many hundreds of km above the top of the atmosphere. After ~10 minutes of cooling and contracting at these heights, however, the plume splashes back onto the planet's upper atmosphere, releasing additional energy as it collapses and impacts.

Modeling the Tunguska Event

Based on the experienced gleaned from SL9 modeling work, it is clear that models of the Tunguska event should account for all three phases of a plume-forming event. Only then should the results be compared with available constraints such as: (i) seismographic data, (ii) barographic data, (iii) measurements of fallen trees, and (iv) eyewitness accounts (e.g., Farinella et al. 2001). As we will describe below, however, most previous attempts to model Tunguska data have used simple (but potentially problematic) approximations to estimate various constraints, which may or may not lead to reasonable results.

Two widely accepted estimates of the Tunguska event's energy yield and height come from the work of Ben-Menahem (1975), who compared Tunguska blast seismograms taken at four different stations to modern seismograms of Russian and Chinese nuclear airblast tests, and Shoemaker (1983), who performed a comparable analysis by comparing barometric overpressure records to U.S. nuclear airblast information. Assuming that Tunguska can be treated as a point-source blast, they estimated Tunguska's yield to be 10-15 MT and the altitude of the bolide's break-up to be 8-9 km. If their calculations are accurate, we estimate, using the NEO impact model described in Section 3, and NEO albedo model of Morbidelli et al. (2002a), that the interval between Tunguska-like events on Earth should be once every 600-1000 years. These results are surprising, given that (i) the real Tunguska occurred less than 100 years ago, and (ii) the population estimate used by our NEO model is somewhat “optimistic” about the number of Tunguska projectiles residing in the NEO population. Still, we recognize that we are dealing with statistics of small numbers and low probability events do occur from time to time.

A potential problem with these results, however, is the assumption that Tunguska can be considered a point-source blast much like the detonation of a nuclear bomb. As described by Boslough and Crawford (1997), plume-forming events like Tunguska or SL9 may be more analogous to explosive line charges, with the bolide's kinetic energy deposited along the entry column in both the entry and fireball phases. Moreover, Boslough and Crawford's (preliminary) runs indicate that that plume-forming events may lead to (i) enhanced energy coupling and momentum to the ground and (ii) acoustic signatures that are different from nuclear blast data. If true, Tunguska-like events may very well come from 3-4 MT plume-forming events rather than

12.5 MT blasts. Hence, Ben-Menahem (1975) and Shoemaker (1983) may have overestimated the bolide size needed to produce Tunguska-like effects. An interesting (and potentially compelling) aspect to this problem is that the interval between 3 MT plume-forming impacts on Earth is ~250 years, a more reasonable match to the 1908 Tunguska event than the predicted interval of 600-1000 years expected for 10-15 MT events.

A constraint that could provide a “tie-breaker” between point-source and plume-forming model results is the Tunguska tree-fall data. Estimates suggest that 2150 +/- 50 square kilometers of conifer forests were blasted by the airburst, enough to make some suggest that explosive yield of the Tunguska event may have been greater than 10 MT (see various references listed in Sekanina 1983 and Boslough and Crawford 1997). A possible problem with this estimate, however, is that topography may play an important yet essentially unexplored role in focusing or deflecting energy from the airblast. The Tunguska region is covered with hills, many having slopes of 15-20 degrees or greater. These features should be natural concentrators (or baffles) for blast wave energy, enough to significantly change the outcome away from our expectations based on flat topography (e.g., Krinov 1963). Note that topography differences explain why the city of Hiroshima, with bowl-like surroundings, sustained considerable more destruction from a 15 kiloton (KT) nuclear airblast than the city of Nagasaki, with hilly terrain, sustained from a 21 KT airblast (e.g., Rhodes 1995). Until topography is accounted for in models of Tunguska damage, the explosive yield of the airblast will remain uncertain.

Conclusions

Modeling the Tunguska event using numerical codes is challenging, enough that it may require the use of sophisticated hydrocodes that can track several different factors: ablation and disruption of the bolide, the formation and evolution of a fireball and plume, the energy and momentum coupled into the atmosphere by plume-forming impacts, and the effect of impact-derived shock waves on a surface with realistic topography. No group has yet attempted to model all these features simultaneously. Until this is done, it will remain an open question as to whether we are correctly interpreting constraints from the Tunguska event. Interestingly, the best modeling effort of the Tunguska event to date suggests we may be significantly overestimating the explosive yield (Boslough and Crawford 1997). If true, Tunguska events may present a more serious hazard to human life than described in this report.

APPENDIX 5 - Cost/Benefit Analysis Cases

Table 8-5 is repeated (Table A5-1) along with several other cases that provide results for the Global and US values for h_p and h_i , for the minimum, nominal, and maximum hazards, and for cases that include and exclude the global hazard. The explanation of the various entries in these tables is described in Section 8.2.

Table A5-1. Baseline (Global h_p & h_i value, Nominal Hazard, Global Hazard Included)

	Cost FY03\$M	BE Year	ROI 10 Yrs	Sub-Gbl Haz Ret	ROI 20 Yrs	ROI 100 Yrs
--- Ground Based Systems ---						
LINEAR	\$12.5	2008	181.0	---	259.9	891.1
MK_LCCD1m	\$34.7	2008	119.0	---	209.7	935.5
MK_LCCD2m	\$55.7	2008	73.0	---	128.7	574.8
MK_LCCD4m	\$97.1	2008	43.6	---	80.5	375.3
MK_LCCD8m	\$188.1	2008	20.1	---	37.6	177.1
MK_SCCD1m	\$31.6	2008	131.1	---	233.5	1053.4
MK_SCCD2m	\$52.6	2008	77.2	---	137.2	617.5
MK_SCCD4m	\$94.0	2008	44.3	---	81.7	380.7
KP_SCCD2m	\$52.6	2008	65.6	---	102.1	393.9
KP_SCCD4m	\$94.0	2008	38.7	---	63.1	257.9
DualNN_SCCD1m	\$46.5	2008	91.2	---	165.3	758.3
DualNN_SCCD2m	\$80.6	2008	52.9	---	97.9	458.2
DualNN_SCCD4m	\$150.4	2008	29.5	---	56.9	276.7
DualNS_SCCD1m	\$54.1	2008	80.1	---	135.7	580.2
DualNS_SCCD2m	\$94.4	2008	46.4	---	86.2	404.9
DualNS_SCCD4m	\$177.2	2008	25.2	---	49.2	241.0
3_4m	\$233.5	2008	19.4	---	38.1	188.1
--- Space Based Systems ---						
LEO_50cm	\$202.8	2008	22.8	---	42.9	204.0
LEO_1m	\$222.8	2008	20.7	---	40.3	197.2
LEO_2m	\$268.5	2008	17.1	---	33.8	167.4
L2_50cm	\$248.4	2008	17.6	---	33.9	164.2
L2_1m	\$268.4	2008	16.8	---	33.0	162.9
L2_2m	\$314.1	2008	14.4	---	28.7	142.9
Venus_50cm	\$307.8	2008	13.5	---	28.0	143.7
Venus_1m	\$327.8	2008	13.3	---	27.5	140.9
Venus_2m	\$373.5	2008	11.9	---	24.5	125.9
--- Joint Systems ---						
LEO1m_4m	\$311.8	2008	14.5	---	28.6	141.5
Venus50cm_4m	\$396.8	2008	11.0	---	22.6	115.4
Venus1m_4m	\$416.8	2008	10.6	---	22.0	112.5

Cost for LINEAR represents 10 years of operations only

Table A5 -2. (Global h_p & h_I value, Minimum Hazard, Global Hazard Included)

	Cost FY03\$M	BE Year	ROI 10 Yrs	Sub-Gbl Haz Ret	ROI 20 Yrs	ROI 100 Yrs
--- Ground Based Systems ---						
LINEAR	\$12.5	2008	38.1	---	47.3	121.3
MK_LCCD1m	\$34.7	2008	29.9	---	50.0	210.4
MK_LCCD2m	\$55.7	2008	18.1	---	30.7	131.1
MK_LCCD4m	\$97.1	2008	10.8	---	19.7	91.4
MK_LCCD8m	\$188.1	2009	4.4	---	8.6	41.5
MK_SCCD1m	\$31.6	2008	33.1	---	56.3	241.8
MK_SCCD2m	\$52.6	2008	19.2	---	32.8	141.7
MK_SCCD4m	\$94.0	2008	10.9	---	19.9	92.0
KP_SCCD2m	\$52.6	2008	15.7	---	22.7	78.5
KP_SCCD4m	\$94.0	2008	9.2	---	14.3	54.9
DualNN_SCCD1m	\$46.5	2008	23.0	---	40.4	179.5
DualNN_SCCD2m	\$80.6	2008	13.2	---	24.1	111.6
DualNN_SCCD4m	\$150.4	2008	7.2	---	14.3	71.4
DualNS_SCCD1m	\$54.1	2008	20.5	---	33.3	135.4
DualNS_SCCD2m	\$94.4	2008	11.5	---	21.1	97.6
DualNS_SCCD4m	\$177.2	2008	6.1	---	12.2	61.6
3_4m	\$233.5	2008	4.5	---	9.4	48.6
--- Space Based Systems ---						
LEO_50cm	\$202.8	2009	5.5	---	10.5	50.9
LEO_1m	\$222.8	2009	4.9	---	10.0	50.9
LEO_2m	\$268.5	2009	3.9	---	8.4	43.6
L2_50cm	\$248.4	2009	4.0	---	8.1	40.6
L2_1m	\$268.4	2009	3.8	---	8.0	41.8
L2_2m	\$314.1	2010	3.2	---	7.0	37.1
Venus_50cm	\$307.8	2010	2.8	---	6.6	37.0
Venus_1m	\$327.8	2010	2.9	---	6.7	37.1
Venus_2m	\$373.5	2010	2.5	---	5.9	33.3
--- Joint Systems ---						
LEO1m_4m	\$311.8	2009	3.2	---	6.9	36.4
Venus50cm_4m	\$396.8	2010	2.3	---	5.4	30.1
Venus1m_4m	\$416.8	2010	2.2	---	5.2	29.7

Cost for LINEAR represents 10 years of operations only

Table A5-3. (Global h_p & h_l value, Maximum Hazard, Global Hazard Included)

	Cost FY03\$M	BE Year	ROI 10 Yrs	Sub-Gbl Haz Ret	ROI 20 Yrs	ROI 100 Yrs
--- Ground Based Systems ---						
LINEAR	\$12.5	2008	818.8	---	1277.4	4945.8
MK_LCCD1m	\$34.7	2008	480.6	---	894.1	4201.8
MK_LCCD2m	\$55.7	2008	295.8	---	550.0	2583.6
MK_LCCD4m	\$97.1	2008	175.4	---	334.1	1603.3
MK_LCCD8m	\$188.1	2008	84.7	---	162.3	783.1
MK_SCCD1m	\$31.6	2008	528.2	---	987.8	4664.6
MK_SCCD2m	\$52.6	2008	312.9	---	583.6	2749.8
MK_SCCD4m	\$94.0	2008	179.0	---	340.5	1632.1
KP_SCCD2m	\$52.6	2008	273.1	---	458.7	1943.5
KP_SCCD4m	\$94.0	2008	159.8	---	277.7	1220.4
DualNN_SCCD1m	\$46.5	2008	365.9	---	693.1	3311.0
DualNN_SCCD2m	\$80.6	2008	212.2	---	405.9	1955.1
DualNN_SCCD4m	\$150.4	2008	117.5	---	229.6	1126.3
DualNS_SCCD1m	\$54.1	2008	317.5	---	572.6	2613.3
DualNS_SCCD2m	\$94.4	2008	184.8	---	354.8	1714.4
DualNS_SCCD4m	\$177.2	2008	100.5	---	197.6	973.9
3_4m	\$233.5	2008	77.2	---	152.0	750.4
--- Space Based Systems ---						
LEO_50cm	\$202.8	2008	89.8	---	173.2	840.1
LEO_1m	\$222.8	2008	81.8	---	160.3	788.3
LEO_2m	\$268.5	2008	67.9	---	133.9	661.6
L2_50cm	\$248.4	2008	71.4	---	139.1	680.8
L2_1m	\$268.4	2008	67.2	---	132.3	653.0
L2_2m	\$314.1	2008	57.7	---	114.1	565.2
Venus_50cm	\$307.8	2008	56.4	---	113.8	572.9
Venus_1m	\$327.8	2008	54.3	---	109.4	549.9
Venus_2m	\$373.5	2008	48.1	---	96.9	487.1
--- Joint Systems ---						
LEO1m_4m	\$311.8	2008	58.2	---	114.5	564.6
Venus50cm_4m	\$396.8	2008	45.1	---	90.4	452.3
Venus1m_4m	\$416.8	2008	43.3	---	86.9	436.0

Cost for LINEAR represents 10 years of operations only

Table A5-4. (Global h_p & h_l value, Minimum Hazard, Global Hazard Excluded)

	Cost FY03\$M	BE Year	ROI 10 Yrs	Sub-Gbl Haz Ret	ROI 20 Yrs	ROI 100 Yrs
--- Ground Based Systems ---						
LINEAR	\$12.5	2008	35.3	23.0%	43.1	104.8
MK_LCCD1m	\$34.7	2008	28.5	57.8%	47.3	197.3
MK_LCCD2m	\$55.7	2008	17.3	58.3%	29.1	123.6
MK_LCCD4m	\$97.1	2008	10.3	69.0%	18.8	87.0
MK_LCCD8m	\$188.1	2009	4.2	63.3%	8.1	39.5
MK_SCCD1m	\$31.6	2008	31.6	60.2%	53.3	227.4
MK_SCCD2m	\$52.6	2008	18.3	59.3%	31.1	133.6
MK_SCCD4m	\$94.0	2008	10.4	67.6%	18.9	87.5
KP_SCCD2m	\$52.6	2008	14.9	38.2%	21.3	72.8
KP_SCCD4m	\$94.0	2008	8.7	45.1%	13.5	51.7
DualNN_SCCD1m	\$46.5	2008	22.0	64.9%	38.4	169.7
DualNN_SCCD2m	\$80.6	2008	12.6	69.5%	22.9	105.9
DualNN_SCCD4m	\$150.4	2008	6.9	81.6%	13.7	68.3
DualNS_SCCD1m	\$54.1	2008	19.6	58.1%	31.7	128.5
DualNS_SCCD2m	\$94.4	2008	11.0	70.5%	20.0	92.2
DualNS_SCCD4m	\$177.2	2008	5.8	82.6%	11.7	58.8
3_4m	\$233.5	2008	4.3	85.7%	9.0	46.4
--- Space Based Systems ---						
LEO_50cm	\$202.8	2009	5.2	78.2%	10.0	48.4
LEO_1m	\$222.8	2009	4.7	85.4%	9.6	48.6
LEO_2m	\$268.5	2009	3.8	88.3%	8.0	41.8
L2_50cm	\$248.4	2009	3.8	77.2%	7.6	38.5
L2_1m	\$268.4	2009	3.6	85.0%	7.7	39.9
L2_2m	\$314.1	2010	3.0	88.2%	6.6	35.5
Venus_50cm	\$307.8	2010	2.7	87.2%	6.3	35.3
Venus_1m	\$327.8	2010	2.7	92.1%	6.4	35.5
Venus_2m	\$373.5	2010	2.4	94.2%	5.7	32.0
--- Joint Systems ---						
LEO1m_4m	\$311.8	2009	3.1	86.0%	6.6	34.8
Venus50cm_4m	\$396.8	2010	2.1	90.9%	5.1	28.8
Venus1m_4m	\$416.8	2010	2.1	93.9%	5.0	28.5

Cost for LINEAR represents 10 years of operations only

Table A5-5. (Global h_p & h_I value, Nominal Hazard, Global Hazard Excluded)

	Cost FY03\$M	BE Year	ROI 10 Yrs	Sub-Gbl Haz Ret	ROI 20 Yrs	ROI 100 Yrs
--- Ground Based Systems ---						
LINEAR	\$12.5	2008	96.0	22.1%	117.1	285.9
MK_LCCD1m	\$34.7	2008	77.1	58.3%	127.8	533.0
MK_LCCD2m	\$55.7	2008	47.4	58.8%	79.3	334.4
MK_LCCD4m	\$97.1	2008	28.8	69.3%	51.5	233.6
MK_LCCD8m	\$188.1	2008	12.8	63.7%	23.3	107.4
MK_SCCD1m	\$31.6	2008	85.3	60.6%	143.9	612.3
MK_SCCD2m	\$52.6	2008	50.2	59.8%	84.7	360.9
MK_SCCD4m	\$94.0	2008	29.0	68.0%	52.0	235.4
KP_SCCD2m	\$52.6	2008	41.2	38.2%	58.8	199.4
KP_SCCD4m	\$94.0	2008	24.8	45.3%	37.7	141.4
DualNN_SCCD1m	\$46.5	2008	59.8	65.3%	103.9	456.0
DualNN_SCCD2m	\$80.6	2008	34.8	69.7%	62.5	283.6
DualNN_SCCD4m	\$150.4	2008	19.7	81.6%	37.8	182.2
DualNS_SCCD1m	\$54.1	2008	53.5	58.5%	86.1	347.3
DualNS_SCCD2m	\$94.4	2008	30.7	70.8%	54.8	247.4
DualNS_SCCD4m	\$177.2	2008	16.8	82.6%	32.4	157.0
3_4m	\$233.5	2008	13.0	85.6%	25.3	124.1
--- Space Based Systems ---						
LEO_50cm	\$202.8	2008	15.4	78.4%	28.1	130.1
LEO_1m	\$222.8	2008	13.9	85.4%	26.8	130.0
LEO_2m	\$268.5	2008	11.5	88.2%	22.6	111.7
L2_50cm	\$248.4	2008	11.6	77.5%	21.9	103.9
L2_1m	\$268.4	2008	11.2	85.1%	21.9	107.1
L2_2m	\$314.1	2008	9.6	88.1%	19.1	95.2
Venus_50cm	\$307.8	2008	8.7	87.3%	18.3	94.9
Venus_1m	\$327.8	2008	8.8	92.0%	18.4	95.1
Venus_2m	\$373.5	2008	7.9	94.0%	16.5	85.7
--- Joint Systems ---						
LEO1m_4m	\$311.8	2008	9.7	86.0%	19.0	93.4
Venus50cm_4m	\$396.8	2008	7.3	90.8%	15.1	77.5
Venus1m_4m	\$416.8	2008	7.0	93.7%	14.8	76.5

Cost for LINEAR represents 10 years of operations only

Table A5-6. (Global h_p & h_l value, Maximum Hazard, Global Hazard Excluded)

	Cost FY03\$M	BE Year	ROI 10 Yrs	Sub-Gbl Haz Ret	ROI 20 Yrs	ROI 100 Yrs
--- Ground Based Systems ---						
LINEAR	\$12.5	2008	192.6	21.7%	235.0	574.0
MK_LCCD1m	\$34.7	2008	155.1	57.9%	256.4	1066.3
MK_LCCD2m	\$55.7	2008	95.7	58.4%	159.4	669.4
MK_LCCD4m	\$97.1	2008	58.4	68.7%	103.7	466.1
MK_LCCD8m	\$188.1	2008	26.5	63.1%	47.4	215.1
MK_SCCD1m	\$31.6	2008	171.5	60.1%	288.4	1223.7
MK_SCCD2m	\$52.6	2008	101.1	59.4%	170.1	722.0
MK_SCCD4m	\$94.0	2008	58.9	67.5%	104.6	470.0
KP_SCCD2m	\$52.6	2008	83.2	37.8%	118.5	400.9
KP_SCCD4m	\$94.0	2008	50.4	44.9%	76.4	284.0
DualNN_SCCD1m	\$46.5	2008	120.5	64.8%	208.3	910.6
DualNN_SCCD2m	\$80.6	2008	70.5	69.1%	125.4	565.3
DualNN_SCCD4m	\$150.4	2008	40.3	80.8%	76.1	362.8
DualNS_SCCD1m	\$54.1	2008	107.8	58.1%	173.1	695.0
DualNS_SCCD2m	\$94.4	2008	62.3	70.2%	110.2	493.5
DualNS_SCCD4m	\$177.2	2008	34.6	81.9%	65.5	312.8
3_4m	\$233.5	2008	26.9	84.7%	51.3	247.1
--- Space Based Systems ---						
LEO_50cm	\$202.8	2008	31.8	77.7%	57.2	259.7
LEO_1m	\$222.8	2008	28.9	84.5%	54.5	259.1
LEO_2m	\$268.5	2008	24.0	87.2%	46.1	222.5
L2_50cm	\$248.4	2008	24.2	76.8%	44.6	207.7
L2_1m	\$268.4	2008	23.4	84.3%	44.5	213.7
L2_2m	\$314.1	2008	20.2	87.3%	39.1	189.9
Venus_50cm	\$307.8	2008	18.2	86.5%	37.2	189.5
Venus_1m	\$327.8	2008	18.4	91.2%	37.4	189.8
Venus_2m	\$373.5	2008	16.6	93.2%	33.7	171.1
--- Joint Systems ---						
LEO1m_4m	\$311.8	2008	20.4	85.2%	38.9	186.5
Venus50cm_4m	\$396.8	2008	15.5	90.0%	31.0	154.9
Venus1m_4m	\$416.8	2008	15.0	92.8%	30.4	152.8

Cost for LINEAR represents 10 years of operations only

Table A5-7. (US h_p & h_l value, Minimum Hazard, Global Hazard Included)

	Cost FY03\$M	BE Year	ROI 10 Yrs	Sub-Gbl Haz Ret	ROI 20 Yrs	ROI 100 Yrs
--- Ground Based Systems ---						
LINEAR	\$12.5	2008	170.0	---	211.8	546.7
MK_LCCD1m	\$34.7	2008	135.9	---	226.8	953.9
MK_LCCD2m	\$55.7	2008	83.9	---	140.7	595.4
MK_LCCD4m	\$97.1	2008	51.4	---	91.9	416.6
MK_LCCD8m	\$188.1	2008	23.2	---	41.9	191.2
MK_SCCD1m	\$31.6	2008	150.4	---	255.4	1095.8
MK_SCCD2m	\$52.6	2008	88.7	---	150.4	643.5
MK_SCCD4m	\$94.0	2008	51.8	---	92.7	419.2
KP_SCCD2m	\$52.6	2008	72.5	---	104.1	357.1
KP_SCCD4m	\$94.0	2008	44.0	---	67.0	251.0
DualNN_SCCD1m	\$46.5	2008	105.9	---	184.6	814.7
DualNN_SCCD2m	\$80.6	2008	62.1	---	111.6	508.0
DualNN_SCCD4m	\$150.4	2008	35.6	---	68.0	326.7
DualNS_SCCD1m	\$54.1	2008	94.1	---	152.0	614.6
DualNS_SCCD2m	\$94.4	2008	54.9	---	98.2	444.7
DualNS_SCCD4m	\$177.2	2008	30.6	---	58.5	282.3
3_4m	\$233.5	2008	23.7	---	45.9	223.5
--- Space Based Systems ---						
LEO_50cm	\$202.8	2008	27.9	---	50.8	233.8
LEO_1m	\$222.8	2008	25.4	---	48.6	233.7
LEO_2m	\$268.5	2008	21.2	---	41.2	201.0
L2_50cm	\$248.4	2008	21.3	---	39.7	186.9
L2_1m	\$268.4	2008	20.6	---	39.7	192.7
L2_2m	\$314.1	2008	17.8	---	34.9	171.4
Venus_50cm	\$307.8	2008	16.2	---	33.4	170.9
Venus_1m	\$327.8	2008	16.4	---	33.6	171.3
Venus_2m	\$373.5	2008	14.8	---	30.3	154.5
--- Joint Systems ---						
LEO1m_4m	\$311.8	2008	17.9	---	34.6	168.2
Venus50cm_4m	\$396.8	2008	13.7	---	27.7	139.8
Venus1m_4m	\$416.8	2008	13.3	---	27.2	138.0

Cost for LINEAR represents 10 years of operations only

Table A5-8. (US h_p & h value, Nominal Hazard, Global Hazard Included)

	Cost FY03\$M	BE Year	ROI 10 Yrs	Sub-Gbl Haz Ret	ROI 20 Yrs	ROI 100 Yrs
--- Ground Based Systems ---						
LINEAR	\$12.5	2008	799.3	---	1156.8	4016.4
MK_LCCD1m	\$34.7	2008	533.6	---	944.6	4232.7
MK_LCCD2m	\$55.7	2008	328.6	---	581.1	2601.7
MK_LCCD4m	\$97.1	2008	198.5	---	365.5	1701.1
MK_LCCD8m	\$188.1	2008	93.4	---	172.4	804.4
MK_SCCD1m	\$31.6	2008	587.8	---	1052.0	4765.9
MK_SCCD2m	\$52.6	2008	347.6	---	619.5	2795.0
MK_SCCD4m	\$94.0	2008	201.5	---	370.8	1725.5
KP_SCCD2m	\$52.6	2008	293.5	---	458.7	1780.6
KP_SCCD4m	\$94.0	2008	175.1	---	285.4	1167.9
DualNN_SCCD1m	\$46.5	2008	410.6	---	746.4	3432.7
DualNN_SCCD2m	\$80.6	2008	239.9	---	443.9	2076.1
DualNN_SCCD4m	\$150.4	2008	135.8	---	260.2	1255.6
DualNS_SCCD1m	\$54.1	2008	359.5	---	611.2	2625.2
DualNS_SCCD2m	\$94.4	2008	211.1	---	391.5	1835.3
DualNS_SCCD4m	\$177.2	2008	116.8	---	225.4	1094.3
3_4m	\$233.5	2008	90.5	---	175.5	854.9
--- Space Based Systems ---						
LEO_50cm	\$202.8	2008	105.5	---	196.7	926.3
LEO_1m	\$222.8	2008	96.4	---	185.2	896.1
LEO_2m	\$268.5	2008	80.4	---	156.1	761.5
L2_50cm	\$248.4	2008	82.5	---	156.3	746.6
L2_1m	\$268.4	2008	78.9	---	152.5	740.9
L2_2m	\$314.1	2008	68.2	---	132.9	650.3
Venus_50cm	\$307.8	2008	64.5	---	130.0	654.2
Venus_1m	\$327.8	2008	63.7	---	127.9	641.6
Venus_2m	\$373.5	2008	57.0	---	114.4	573.5
--- Joint Systems ---						
LEO1m_4m	\$311.8	2008	68.7	---	132.6	643.8
Venus50cm_4m	\$396.8	2008	53.3	---	105.8	525.9
Venus1m_4m	\$416.8	2008	51.5	---	102.8	513.0

Cost for LINEAR represents 10 years of operations only

Table A5-9. (US h_p & h_l value, Maximum Hazard, Global Hazard Included)

	Cost FY03\$M	BE Year	ROI 10 Yrs	Sub-Gbl Haz Ret	ROI 20 Yrs	ROI 100 Yrs
--- Ground Based Systems ---						
LINEAR	\$12.5	2008	3614.4	---	5691.7	22310.2
MK_LCCD1m	\$34.7	2008	2155.0	---	4028.1	19012.9
MK_LCCD2m	\$55.7	2008	1327.2	---	2478.7	11691.3
MK_LCCD4m	\$97.1	2008	791.0	---	1509.8	7259.5
MK_LCCD8m	\$188.1	2008	383.8	---	735.3	3547.6
MK_SCCD1m	\$31.6	2008	2368.6	---	4450.7	21107.6
MK_SCCD2m	\$52.6	2008	1403.8	---	2630.5	12443.6
MK_SCCD4m	\$94.0	2008	807.0	---	1538.4	7389.8
KP_SCCD2m	\$52.6	2008	1215.8	---	2056.6	8782.8
KP_SCCD4m	\$94.0	2008	714.7	---	1248.5	5519.0
DualNN_SCCD1m	\$46.5	2008	1644.5	---	3127.0	14986.6
DualNN_SCCD2m	\$80.6	2008	956.4	---	1833.7	8852.0
DualNN_SCCD4m	\$150.4	2008	532.6	---	1040.4	5102.6
DualNS_SCCD1m	\$54.1	2008	1421.8	---	2577.4	11822.2
DualNS_SCCD2m	\$94.4	2008	833.7	---	1603.6	7763.1
DualNS_SCCD4m	\$177.2	2008	456.5	---	896.1	4412.9
3_4m	\$233.5	2008	351.4	---	690.3	3401.2
--- Space Based Systems ---						
LEO_50cm	\$202.8	2008	407.6	---	785.2	3806.4
LEO_1m	\$222.8	2008	372.0	---	727.7	3572.7
LEO_2m	\$268.5	2008	309.9	---	608.7	2999.1
L2_50cm	\$248.4	2008	324.8	---	631.5	3085.5
L2_1m	\$268.4	2008	306.6	---	601.4	2960.2
L2_2m	\$314.1	2008	263.9	---	519.4	2562.9
Venus_50cm	\$307.8	2008	258.0	---	518.0	2597.8
Venus_1m	\$327.8	2008	248.8	---	498.3	2494.0
Venus_2m	\$373.5	2008	221.0	---	441.9	2209.5
--- Joint Systems ---						
LEO1m_4m	\$311.8	2008	265.9	---	520.8	2560.1
Venus50cm_4m	\$396.8	2008	207.2	---	412.1	2051.7
Venus1m_4m	\$416.8	2008	199.1	---	396.8	1978.1

Cost for LINEAR represents 10 years of operations only

Table A5-10. (US h_P & h_I value, Minimum Hazard, Global Hazard Excluded)

	Cost FY03\$M	BE Year	ROI 10 Yrs	Sub-Gbl Haz Ret	ROI 20 Yrs	ROI 100 Yrs
--- Ground Based Systems ---						
LINEAR	\$12.5	2008	157.9	23.0%	192.8	472.6
MK_LCCD1m	\$34.7	2008	129.7	57.8%	214.6	894.2
MK_LCCD2m	\$55.7	2008	80.1	58.3%	133.6	561.5
MK_LCCD4m	\$97.1	2008	49.2	69.0%	87.8	396.7
MK_LCCD8m	\$188.1	2008	22.2	63.3%	40.0	182.2
MK_SCCD1m	\$31.6	2008	143.5	60.2%	242.0	1030.3
MK_SCCD2m	\$52.6	2008	84.7	59.3%	142.7	606.8
MK_SCCD4m	\$94.0	2008	49.6	67.6%	88.4	399.1
KP_SCCD2m	\$52.6	2008	68.9	38.2%	98.1	331.4
KP_SCCD4m	\$94.0	2008	42.0	45.1%	63.6	236.6
DualNN_SCCD1m	\$46.5	2008	101.2	64.9%	175.5	770.2
DualNN_SCCD2m	\$80.6	2008	59.4	69.5%	106.4	482.3
DualNN_SCCD4m	\$150.4	2008	34.1	81.6%	65.1	312.7
DualNS_SCCD1m	\$54.1	2008	90.2	58.1%	145.0	583.6
DualNS_SCCD2m	\$94.4	2008	52.5	70.5%	93.3	420.4
DualNS_SCCD4m	\$177.2	2008	29.3	82.6%	56.0	269.4
3_4m	\$233.5	2008	22.7	85.7%	44.0	213.7
--- Space Based Systems ---						
LEO_50cm	\$202.8	2008	26.7	78.2%	48.5	222.5
LEO_1m	\$222.8	2008	24.4	85.4%	46.5	223.4
LEO_2m	\$268.5	2008	20.3	88.3%	39.5	192.5
L2_50cm	\$248.4	2008	20.3	77.2%	37.8	177.7
L2_1m	\$268.4	2008	19.7	85.0%	38.0	184.2
L2_2m	\$314.1	2008	17.1	88.2%	33.4	164.1
Venus_50cm	\$307.8	2008	15.5	87.2%	31.9	163.4
Venus_1m	\$327.8	2008	15.7	92.1%	32.2	164.3
Venus_2m	\$373.5	2008	14.2	94.2%	29.1	148.3
--- Joint Systems ---						
LEO1m_4m	\$311.8	2008	17.2	86.0%	33.2	160.8
Venus50cm_4m	\$396.8	2008	13.1	90.9%	26.6	134.0
Venus1m_4m	\$416.8	2008	12.8	93.9%	26.1	132.5

Cost for LINEAR represents 10 years of operations only

Table A5-11. (US h_p & h_I value, Nominal Hazard, Global Hazard Excluded)

	Cost FY03\$M	BE Year	ROI 10 Yrs	Sub-Gbl Haz Ret	ROI 20 Yrs	ROI 100 Yrs
--- Ground Based Systems ---						
LINEAR	\$12.5	2008	423.0	22.1%	518.6	1283.2
MK_LCCD1m	\$34.7	2008	345.3	58.3%	574.7	2410.3
MK_LCCD2m	\$55.7	2008	213.7	58.8%	358.2	1513.8
MK_LCCD4m	\$97.1	2008	131.5	69.3%	234.6	1059.6
MK_LCCD8m	\$188.1	2008	60.3	63.7%	107.9	489.0
MK_SCCD1m	\$31.6	2008	381.9	60.6%	647.1	2769.2
MK_SCCD2m	\$52.6	2008	225.9	59.8%	382.3	1633.8
MK_SCCD4m	\$94.0	2008	132.7	68.0%	236.5	1067.6
KP_SCCD2m	\$52.6	2008	184.5	38.2%	264.2	901.4
KP_SCCD4m	\$94.0	2008	112.7	45.3%	171.4	641.0
DualNN_SCCD1m	\$46.5	2008	269.3	65.3%	468.8	2064.3
DualNN_SCCD2m	\$80.6	2008	158.5	69.7%	283.7	1285.7
DualNN_SCCD4m	\$150.4	2008	91.6	81.6%	173.4	828.0
DualNS_SCCD1m	\$54.1	2008	240.0	58.5%	387.9	1571.2
DualNS_SCCD2m	\$94.4	2008	140.1	70.8%	249.2	1121.8
DualNS_SCCD4m	\$177.2	2008	78.8	82.6%	149.3	713.9
3_4m	\$233.5	2008	61.5	85.6%	117.4	564.9
--- Space Based Systems ---						
LEO_50cm	\$202.8	2008	72.1	78.4%	129.9	591.7
LEO_1m	\$222.8	2008	65.9	85.4%	124.3	591.5
LEO_2m	\$268.5	2008	55.1	88.2%	105.5	508.8
L2_50cm	\$248.4	2008	55.3	77.5%	101.8	473.5
L2_1m	\$268.4	2008	53.6	85.1%	101.9	488.1
L2_2m	\$314.1	2008	46.6	88.1%	89.7	434.3
Venus_50cm	\$307.8	2008	42.5	87.3%	85.9	433.3
Venus_1m	\$327.8	2008	43.0	92.0%	86.4	434.2
Venus_2m	\$373.5	2008	38.8	94.0%	78.0	391.4
--- Joint Systems ---						
LEO1m_4m	\$311.8	2008	47.0	86.0%	89.1	426.2
Venus50cm_4m	\$396.8	2008	36.2	90.8%	71.5	354.5
Venus1m_4m	\$416.8	2008	35.2	93.7%	70.2	349.8

Cost for LINEAR represents 10 years of operations only

Table A5-12. (US h_p & h_l value, Maximum Hazard, Global Hazard Excluded)

	Cost FY03\$M	BE Year	ROI 10 Yrs	Sub-Gbl Haz Ret	ROI 20 Yrs	ROI 100 Yrs
--- Ground Based Systems ---						
LINEAR	\$12.5	2008	845.3	21.7%	1037.3	2573.3
MK_LCCD1m	\$34.7	2008	690.8	57.9%	1149.4	4818.6
MK_LCCD2m	\$55.7	2008	427.6	58.4%	716.4	3026.6
MK_LCCD4m	\$97.1	2008	263.3	68.7%	468.5	2110.5
MK_LCCD8m	\$188.1	2008	121.4	63.1%	216.3	975.5
MK_SCCD1m	\$31.6	2008	764.0	60.1%	1293.6	5530.5
MK_SCCD2m	\$52.6	2008	451.8	59.4%	764.4	3264.7
MK_SCCD4m	\$94.0	2008	265.7	67.5%	472.6	2127.8
KP_SCCD2m	\$52.6	2008	369.3	37.8%	529.2	1808.6
KP_SCCD4m	\$94.0	2008	225.9	44.9%	343.4	1283.9
DualNN_SCCD1m	\$46.5	2008	538.9	64.8%	936.6	4118.4
DualNN_SCCD2m	\$80.6	2008	317.2	69.1%	566.2	2558.7
DualNN_SCCD4m	\$150.4	2008	183.7	80.8%	346.0	1644.8
DualNS_SCCD1m	\$54.1	2008	480.7	58.1%	776.2	3140.6
DualNS_SCCD2m	\$94.4	2008	280.8	70.2%	497.8	2234.2
DualNS_SCCD4m	\$177.2	2008	158.1	81.9%	298.2	1418.6
3_4m	\$233.5	2008	123.8	84.7%	234.6	1121.3
--- Space Based Systems ---						
LEO_50cm	\$202.8	2008	145.4	77.7%	260.1	1177.5
LEO_1m	\$222.8	2008	132.8	84.5%	248.6	1175.7
LEO_2m	\$268.5	2008	111.2	87.2%	211.1	1010.3
L2_50cm	\$248.4	2008	111.4	76.8%	203.8	942.9
L2_1m	\$268.4	2008	108.1	84.3%	204.0	970.6
L2_2m	\$314.1	2008	94.1	87.3%	179.6	862.8
Venus_50cm	\$307.8	2008	85.3	86.5%	171.5	861.2
Venus_1m	\$327.8	2008	86.3	91.2%	172.6	862.9
Venus_2m	\$373.5	2008	78.2	93.2%	155.9	778.0
--- Joint Systems ---						
LEO1m_4m	\$311.8	2008	94.9	85.2%	178.5	847.4
Venus50cm_4m	\$396.8	2008	73.0	90.0%	143.2	704.4
Venus1m_4m	\$416.8	2008	71.2	92.8%	140.5	695.3

Cost for LINEAR represents 10 years of operations only